JAERI-M
85-100

DATA COMPILATION FOR PARTICLE IMPACT DESORPTION II

July 1985

Takashi OSHIYAMA*, Siro NAGAI, Kunio OZAWA
and Fujio TAKEUTCHI**

日 本 原 子 力 研 究 所
Japan Atomic Energy Research Institute

JAERI-Mレポートは，日本原子力研究所が不定期に公刊している研究報告書です。
入手の問合わせは，日本原子力研究所技術情報部情報資料課（〒319-11 茨城県那珂郡東海村）あて，お申しこしください。なお，このほかに財団法人原子力弘済会資料センター（〒319-11 茨城県那珂郡東海村日本原子力研究所内）で複写による実費頒布をおこなっております。

JAERI-M reports are issued irregularly.
Inquiries about availability of the reports should be addressed to Information Division Department of Technical Information, Japan Atomic Energy Research Institute, Tokaimura, Naka-gun, Ibaraki-ken 319-11, Japan.

© Japan Atomic Energy Research Institute, 1985

編集兼発行　日本原子力研究所
印　　刷　日青工業株式会社

JAERI-M 85-100

Data Compilation for Particle-Impact Desorption II

Takashi OSHIYAMA*, Siro NAGAI, Kunio OZAWA and Fujio TAKEUTCHI**

Research Committee on A & M Data,
Tokai Research Establishment, JAERI

(Received June 21, 1985)

The particle impact desorption is one of the elementary processes of hydrogen recycling in controlled thermonuclear fusion reactors. We have surveyed the literature concerning the ion impact desorption and photon stimulated desorption published through the end of 1984 and compiled the data on the desorption cross sections and yields with the aid of a computer. This report presents the results of the compilation in graphs and tables as functions of incident energy, surface temperature and surface coverage.

Keywords: Data Compilation, Plasma-Wall Interaction, Ion Impact Desorption, Photon Stimulated Desorption, Desorption Cross Section, Desorption Yield, Literature

---

This report was prepared as an account of work by the sub-working group for data-banking of particle-material interaction in the research committee of A & M Data of JAERI.

* Department of Physics, Kyoto Sangyo University, Kyoto
** Institute of Computer Sciences, Kyoto Sangyo University, Kyoto

粒子衝撃脱離に関するデータ収集と評価 II

日本原子力研究所・原子分子データ研究委員会
押山　孝*・永井　士郎・小沢　国夫・竹内富士雄**

（1985年6月21日受理）

粒子衝撃による固体表面からの気体，不純物の脱着は核融合炉におけるプラズマ壁相互作用の重要な素過程のひとつであり，脱着に関するデータの収集が要請されている。本報告書は，1958年から1984年までに公刊されたイオン衝撃，フォトン衝撃に関するデータの収集と評価を行った結果をまとめたものである。収集されたデータは入射エネルギー，固体表面温度，吸着ガスの種類，吸着量などの関数として，グラフ及び数値表にまとめてある。

本報告書は，原子分子データ収集評価専門部会，粒子－物質相互作用データワーキンググループにより行われた成果である。

* 京都産業大学　理学部
** 京都産業大学　計算機科学研究所

CONTENTS

1. Introduction 1

2. Definitions of Desorption Cross Sections and Yields 3

3. Ion Impact Desorption 5
3.1 Theoretical Considerations 5
3.2 Experimental Methods 7

4. Photon Stimulated Desorption 12
4.1 Theoretical Considerations 12
4.2 Experimental Methods 13

5. Experimental Data 16

5.1 Experimental Data of IID 16
5.1.1 Tables 16
5.1.2 Graphs and Data Lists for Desorption Cross Sections 23
5.1.3 Graphs and Data Lists for Desorption Yields 91
5.1.4 Data Lists for Miscellaneous Data 169

5.2 Experimental Data of PSD 177
5.2.1 Tables 177
5.2.2 Graphs and Data Lists for Desorption Cross sections 183
5.2.3 Graphs and Data Lists for Desorption Yields 186
5.2.4 Data Lists for Miscellaneous Data 249

6. Conclusions 258

Appendix 260

References 269

目　　次

1. まえがき …… 1
2. 脱着断面積と脱着収率 …… 3
3. イオン衝撃脱離 …… 5
3.1 理論的考察 …… 5
3.2 実験方法 …… 7
4. フォトン衝撃脱離 …… 12
4.1 理論的考察 …… 12
4.2 実験方法 …… 13
5. 実験データ …… 16
5.1 イオン衝撃脱離のデータ …… 16
5.1.1 表 …… 16
5.1.2 脱着断面積の各種パラメータ依存に関するグラフと数値表 …… 23
5.1.3 脱着収率の各種パラメータ依存に関するグラフと数値表 …… 91
5.1.4 雑多なデータに関する数値表 …… 169
5.2 フォトン衝撃脱離のデータ …… 177
5.2.1 表 …… 177
5.2.2 脱着断面積の入射エネルギー依存に関するグラフと数値表 …… 183
5.2.3 脱着収率の各種パラメータ依存に関するグラフと数値表 …… 186
5.2.4 雑多なデータに関する数値表 …… 249
6. 結　論 …… 258
付　録 …… 260
文　献 …… 269

1. Introduction

The surface of the wall in controlled thermonuclear fusion reactors is usually covered with adsorbates. When the wall is bombarded by particles and radiation diffusing across the confining magnetic field, these absorbates are released as ions, neutral atoms and molecules. The released particles enter the plasma region as the well-known sources of impurities and plasma particles. Study of this process, which is called desorption, is therefore important for estimation of both hydrogen recycling and impurity influx. The compilation of desorption data on various adsorbate-substrate combinations is needed not only to understand the mechanism underlain but also to present available data in response to the request from practical users.

According to the species of incident particles, the desorption can often be classified into three processes. These are ion-impact desorption (IID), electron-stimulated desorption (ESD) and photon-stimulated desorptin (PSD). Typical cross sections and yields for IID are at least one or two orders of magnitude larger than those for ESD and PSD. The impurity or hydorgen isotope influx due to desorption processes can be estimated with the known desorption cross section and the expected particle flux to the wall. The assessed impurity influxes from deuterium ion impact desorption from stainless steel wall [1] are about two orders of magnitude larger than those expected from either electron or photon induced desorption. Therefore, IID plays most important role in the desorption relevant to plasma-surface interactions.

In this report, we present the results of data compilation for the desorption cross sections and yields of both IID and PSD. The results of the data compilation on ESD were already published in a previous M report of JAERI [2]. A survey has been made of the literature published from 1958 through 1984. These data are classified according to different adsorbate-substrate combination and shown in figures and tables as functions of the incident energy, surface coverage or exposure, and surface temperature. An attempt to represent the compiled data with a certain type of function is carried out by the least-square

method. Some examples of curve fittings for IID are presented in the Appendix. The compiled data are stored in the FACOM system of JAERI. The references, from which the data are adopted, are listed at the end of this report.

References for section 1

1) K.L. Wilson: J. Nucl. Mater. 103/104 (1981) 453.
2) T. Oshiyama, S. Nagai, K. Ozawa and F. Takeutchi: JAERI - M, 84 - 093 (1984).

2. Definitions of Desorption Cross Section and Yield [1)]

There are two quantities to describe particle-impact desorption quantitatively. One is desorption yield which is the number of desorbed particles per incident particle, i.e. ion, electron and photon. Another is desorption cross section, which shows the strength of interaction involved. Using the surface coverage N (adsorbates/cm^2), the desorption cross section σ (cm^2) is defined as follows,

$$-\frac{dN}{dt} = i \sigma N \quad , \qquad (1)$$

where i is incident flux (incident particles/sec/cm^2). Equation (1) suggests the value of σ is obtained from measurements which monitor the surface composition. On the other hand, the desorption yield is measured by mass spectrometric analysis of the desorbed particles. The signal I of the desorbed particles is given by

$$I \propto i \sigma N \quad . \qquad (2)$$

Thus the desorption yield Y(=I/i) can be related to the desorption cross section and coverage,

$$Y \propto \sigma N \quad . \qquad (3)$$

It is noted that the desorption cross section shows the strength of the interaction involved, regardless of the coverage, whereas the desorption yield depends on the coverage as well as the strength of the interaction. Therefore, the desorption yields decrease as the surface becomes cleaner. Care must be taken that these equations (1),(2),(3)

hold only when the surface coverage of adsorbates is monolayer or less. Some of the compiled data show that the desorption yield is not directly proportional to coverage for the surfaces with multiple layers and coadsorption of several gases.

Reference for section 2

1) E. Taglauer: Nucl. Fusion, Special Issue, "Data Compendium for Plasma-Surface Interactions" edited by R.A. Langley et al. (IAEA, Vienna 1984), P43 - 54.

3. Ion Impact Desorption (IID)

3.1 Theoretical Considerations

The first detailed attempt [1] to study desorption of adsorbed nitorgen atom, which was chemisorbed on a polycrystalline tungsten surface, was measured with an ion gauge and/or a residual gas analyzer. The yield of nitrogen atom due to Ar^+ ion impact was found to be quite large at low energies of Ar^+ ions. The threshold energies were small despite the high surface binding energy of nitrogen. These results were not consistent with what had been usually observed for materials with high sublimination energy. Winters and Sigmund [2] proposed a model which consists of a series of binary elastic collisions involving bombarding ions, tungsten and nitrogen target atoms. The desorption can occur independently from the following processes.

(I) A primary ion induces desorption of nitrogen atom, either directly or after being reflected by tungsten atoms at the surface. (Direct-knock-off contribution)

(II) A primary ion, which is backscattered by tungsten atoms below the surface, may knock off nitrogen atoms on its way out. (Reflected-ion contribution)

(III) A primary ion causes a sputtered flux of tungsten atoms, which may knock off nitrogen atoms on their way out. (Sputtered-atom contribution)

They analytically calculated the desorption yield assuming a power potential for interactions between primary ions and target atoms. It was found that adsorbed nitrogen atoms were desorbed primarily as a consequence of direct knock-on collisions with primary and reflected ions. In other words, the contributions from mechanisms (I) and (II) dominate in the energy range investigated. Their estimates also showed that mechanism (III) is significant at high energies and for heavy ions.

Desorption cross section depends on a number of parameters, such as mass, energy and angle of incidence of primary ions, crystallographic orientation of the surface, surface temperatures, and surface binding energy of the adsorbates etc. Some of the parameter dependences have been qualitatively discussed according to the model mentioned above [3,4]. The desorption cross section generally increases for heavier incident particles. This corresponds to the mass dependence of the collision cross sections in the model. Besides this general trend, there is no simple relation between the desorption cross section and the mass.

Due to the energy dependence of the collision cross section, contributions from mechanisms (I) and (II) decrease with increasing energy. On the other hand, contribution from (III) increases. The yields of the sputtered particles are small for light and low energy ions. Therefore, the desorption cross section should decrease with increasing energy according to the model. This corresponds to the experimental data on desorption of oxygen from Ni [5] and Mo [6] substrates by He^+ ions. The increase of the desorption cross section with incident energy suggests a substantial contribution from sputtered atoms. There are many cases [5,6,7] of this example.

The angular dependences of desorption cross section were found for desorption of S from Ni by Ne^+ [8] and O from Si by He^+ [9]. Each showed a maximum around 75 ^{o} from normal to the surface. The general behaviour can be attributed to the increase of sputtered yields and particle reflections with increasing angle from normal.

The desorption of O from various metal surfaces was measured in order to investigate the dependence on surface binding energies [10]. The desorption cross section was found to be inversely propotional to binding energy. This provides as a support for applying a collisional sputtering theory to the case of IID. Several calculations [4,8] of desorption cross section have been done on the basis of the model of Winters and Sigmund. In comparison with experimental data, reasonable agreements have been obtained. However, more detailed comparisons between the calculated and experimental data show that the quantitative agreement is not satisfactory at all.

For simulations [4] of desorption, two computer codes have been used, which are called MORLAY and TRIM respectively. MORLAY code treats the surface and solid as a single-crystalline lattice. Then the position of adsorbates in the lattices can be previously determined and thermal vibrations can be also included. On the other hand, the whole of solid and surface is considered to be amorphous in TRIM code. The general dependence of desorption cross section on incident energy is similar in two codes and also similar to analytical calculations based on the model of Winters and Sigmund. Quantitative agreement with experimental data depends on the choice of parameters such as binding energies.

3.2 Experimental methods

In a desorption experiment, the desorption cross sections and yields are measured for a certain adsorbate-substrate combination in a UHV system. The main parts of the system are an ion source, a sample manipulator, and a detector. Scattered and sputtered ions are energy- and/or mass- analyzed with QMS or magnetic analyzer. Photons due to ion bombardment are detected with an optical monochromator, of which the optical axis is usually parallel to the speciemen surface and perpendicular to the projectile beams. The system can be combined with other surface analytical methods such as Auger electron spectroscopy (AES) and low energy electron diffraction (LEED). Adsorbate gases are admitted from a nozzle pointed toward the surface. Impurities such as As, Se and C can be brought to the solid surface simply by heating the solid. Ambient residual gases such as O_2, H_2O and CO also are adsorbed on the solid surface. Most experiments were performed in a static situation, [3] where a surface is bombarded after evacuation of the surface which has been exposed to a gas to a dosage. In this case, the desorption cross sections and yields are easily obtained from the relations of eqs. (1) and (3). Another case is a dynamical situation [3] where a surface is bombarded in a gas atmosphere at a constant pressure. The surface coverage is an equilibrium one due to desorption and adsorption. In principle there is some difference between dynamical and

static experiments since in the former case the surface may be changed due to the formation of damage, occurrence of chemical reactions. This can result in different adsorption sites with different binding energies. So differences in the magnitude of desorption cross section in both cases are possible but they have not yet been clearly demonstrated experimentally. In the dynamical case, a contribution of gas adsorption should be considered. That is, the rate of arrival of gas atoms or molecules at the surface should be added in the right hand side of eq. (1). However, the desorption experiments in the dynamical case are very rare so far.

If a solid surface is bombarded by ions in the KeV range, various processes occur at or near the surface of the solid owing to energy transfer and electronic interaction between incident ions and surface atoms. Consequently atomic and molecular particles, electrons and photons are emitted from the surface. The primary ions are backscattered as ions, metastables or neutrals. Since ions with low energy interact mainly with the top atomic layers because of their low penetration depth, they are well suited to probe the physical properties of a surface. Ion scattering spectroscopy (ISS) [3,11,12] can yield informations about surface composition during a desorption experiment. The analyzing beam can be stimultaneously used to induce desorption. For the analysis of energy of backscattered ions the binary collision model can be applied. The backscattered intensity depends on the coverage of adsorbates, neutralization probability and scattering cross section. The scattering cross section can be approximately derived from interaction potentials between primary ions and target atoms. Neutralization may depend on the chemical state of adsorbate atom and hence on a condition of the whole surface. In the desorption experiments, it is assumed that neutralization probability is constant for each atomic mass on the surface, independent of surface coverage. It was also found that ISS signal is not always linear to coverage near or above one monolayer. Under some conditions, the signal does not increase with coverage but even decrease. The linear relation, however, has been shown to hold for a number of adsorbate-substrate systems except for a few examples such as Be on W [11]. It should be pointed out that a linear relation between coverage and ISS signal cannot be true in

general without experimental proof. Since ISS signal is used as monitoring the surface composition, the desorbed species are not detected directly in ISS so that no direct information about the state of the desorbed particles, e.g. charge or molecular state is obtained. In addition, this method cannot distinguish whether the particles leave the surface into the vaccum or those are buried into the bulk by recoil implantation.

Secondary Ion Mass Spectrometry (SIMS) [13] has rapidly become a widely used technique for surface and bulk analysis. Compared with other surface analysis techniques as AES, SIMS has some unique advantages in detection of all elements including hydrogen and extremely high sensitivity for many elements. As a result of ion impact, atomic and molecular particles are emitted from the surface. They may be in a neutral or charged state, depending on the chemical environment before emission as well as the atomic number of the emitted atom. The emitted secondary ion species and their intensities depend on the surface structure and coverage. The width of the secondary ion energy distributions reflects the strength of a chemisorption state. The signal of mass-analyzed secondary ion is proportional to primary current, surface coverage and sputtering yield. Therfore, SIMS signal can also be used for measuring the desorption cross section, which is suggested from eqs. (1) and (2).

Impact of energetic ions on surface gives rise to photon emission from excited sputtered atoms or from projectiles reflected by the surface. This is called ion-induced photon (IIP) [14,15]. It is well known that the photon emissions depend strongly on the surface composition, i.e. they are very sensitive to the presence of adsorbates. The photon yield from sputtered atoms was measured as a function of surface coverge, which was monitored by the ISS signal of backscattered ions [14]. The photon yield was found to increase linearly with coverages. This means that the photon yield can also be used for analysis of desorption. The mechanisms which produce excited sputtered particle are not quite clear but discussed using thermodynamic, band structure and bond breaking models. On the other hand, a small fraction of incident ions is backscattered as excited atoms and gives rise to emission of Doppler broadened spectral lines [16]. Detailed analysis of

the line shape provides information on the distribution in speed and direction of the backscattered species. It is also well known that the emission intensity is very sensitive to the presence of adsorbates, i.e. it is very much enhanced when a surface with adsorbates is bombarded, as compared to the clean surface. A linear dependence of the emission intensity on surface coverages is found. This linear correlation observed in IIP as well as ISS and SIMS suggests that either of these techniques can be used substitutionally for measurement of desorption cross sections.

References for section 3

1) H.F. Winters: J. Vac. Sci. & Technol. 8 (1971) 17.
2) H.F. Winters and P. Sigmund: J. Appl. Phys. 45 (1974) 4760.
3) E. Taglauer, W. Heiland and J. Onsagaard: Nucl. Instrum. & Methods 168 (1980) 571.
4) E. Taglauer: Nucl. Fusion, Special Issue "Data Compendium for Plasma-Surface Interactions" edited by R.A. Langley et al. (IAEA, Vienna, 1984) p 43.
5) E. Taglauer, G. Marin, W. Heiland and U. Beitat: Surf. Sci. 63 (1977) 507.
6) A. Sagara, K. Akaishi, K. Kamada and A. Miyahara: J. Nucl. Mat. 103/104 (1981) 357.
7) H. Windawi and J.R. Katzer: Surf. Sci. 75 (1978) L761.
8) E. Taglauer, U. Beitat, C. Marin and W. Heiland: J. Nucl. Mat. 63 (1976) 193.
9) J. Onsagaard, W. Heiland and U. E. Taglauer: Surf. Sci. 89 (1979) 112.
10) E. Taglauer, W. Heiland and U. Beitat: Surf. Sci. 89 (1979) 710.
11) E. Taglauer and W. Heiland: Appl. Phys. 9 (1976) 261.
12) E. Taglauer, G. Marin and W. Heiland: Appl. Phys. 13 (1977) 47.
13) K. Wittmaack: Surf. Sci. 89 (1979) 668.
14) R.J. MacDonald, E. Taglauer and W. Heiland: Appl. Surf. Sci. 5 (1980) 197.

15) E.O. Rausch, M.W. Murray, H. Inouye and E.W. Thomas: J. Appl. Phys. 48 (1977) 4347.

16) E.O. Rausch and E.W. Thomas: Nucl. Instrum. & Methods 149 (1978) 511.

4. Photon Stimulated Desorption

4.1 Theoretical Considerations

It has long been recongnized that the desorption of atoms from surfaces by photon impact is initiated by electronic excitations of the surface bond. This is an adaptation of the theory of gas-phase dissociation and called MGR model [3,4]. According to this model, the photon excites the electronic structure of the bonding configuration in a Franck-Condon excitation. Consequently, desorption occurs via a direct excitation to an antibonding state or via an adiabatic curve crossing to a state where the ion or neutral will have enough kinetic energy to escape. In this model, the excitations for gas-phase dissociation and surface desorption are identical, but the surface can recapture or reneutralize an excited atom, which dramatically reduces the overall dissociation yield from surfaces. Therefore processes that are strong in the gas-phase may be quenched on the surface. This model explains the following experimental results: (1) Absolute thresholds for neutrals lie in the energy region of valence band. (2) Desorption cross sections are considerably smaller than those for gas phase dissiociation and depend on different adsorbate states of the same species. (3) An isotope effect is observed for W(100) surfaces with H_2 and D_2.

However, it was found in 1978 that desorption from surfaces is not a simple extension of gas-phase bonding-antibonding excitation mediated by the presence of a surface. Knotek and Feibelman [5] reported that O^+ ions are desorbed from TiO_2 not due to excitation at the valence level but due to excitation of Ti (3p) core level and to a lesser extent O (2s) level. Both levels have little to do with bonding. Futhermore, the oxygen is desorbed as O^+ whereas it is nominally an O^{2-} ion on the surface. This result implies a large charge transfer prior to desorption. The MGR model predicted neither of these features. They proposed a new model of desorption based on Auger decay, which is called KF model. For ionic adsorbate systems, desorption spectra displayed fine structure at energies above the excitation threshold for the core level. This structure was shown to closely parallel the total yield of secondary electrons from the same surface. It was suggested

that the KF model applies to these systems. In covalent adsorbate systems, core ionization of adsorbate, not substrate, was found to be responsible for ion desorption. However, a desorption through shake-up excitations [6], in which departing photoelectrons excite other electrons, is also found in covalent systems. More data are necessary for detailed understanding of photon-stimulated desorption.

4.2 Experimental Methods [7,8]

In attempting to measure photodesorption, it was difficult to produce controlled beams of photons whose energy is sufficient to cause desorption without simultaneously causing thermal desorption. In addition [8], the yield from adsorbed gases on metals is very small or perhaps even zero. The average yields are always of the order of 10^{-8} molecules per photon, corresponding to the value of detection limit of apparatus. Therefore, instead of metals, experiments were often carried out on photodesorption from semiconductors such as ZnO, Al_2O_3 and stainless steel with chrome oxide surface due to high yields of the order of 10^{-3} molecules per photon. As photon sources, intense lines from a mercury lamp were used to induce desorption. Their photon energies cover the range from visible to far UV radiation. Most of the earlier works on photodesorption was concerned with the use of low energy photons.

Gas release from surfaces under X-rays irradiation is also important for the operation of accelerators, storage rings and nuclear fusion reactors. The surfaces of these instruments are exposed to photons with a broad energy spectrum ranging from a few eV to about 10 KeV. X-rays bremsstrahlung and synchrotron radiation are used with or without various filters as photon sources of desorption. Using various monochrometors, it is possible to obtain the photon with usable intensity and desired energy. Then a number of interesting results [2] on photodesorption, especially photon stimulated ionic desorption (PSID), have been reported using synchrotron orbital radiation. One of

them has suggested a new mechanism of PSD and put on an almost equal footing with ESD.

Measurement [9] of either the initial rate of pressure change or the total increment of pressure change with the known system parameters, i.e. pumping speed etc, gives the desorption yield. Photodesorption from semiconductors such as CdS and ZnO was also observed indirectly by monitoring changes in the electrical conductivity of the surface region [7]. However the standard method of photodesorption is a measurement of desorbed molecules by the mass spectrometers, i.e. magnetic sector mass spectrometer and quadrupole mass spectrometer. Desorbed positive ions are often detected with the time of flight method [10], using a spiraltron detector or a microchannel-plate assembly [11].
By reversing the polarities of the deflecting voltages in the cylindrical mirror analyser (CMA), the positively charged ions could readily be detected and energy-analyzed [12].

References for section 4

1) D. Menzel: J. Vac. Sci. Technol. 20 (1982) 538.
2) M.L. Knotek: Physica Scripta T6 (1983) 94.
3) D. Menzel and R. Gomer: J. Chem. Phys. 41 (1964) 3311.
4) P.A. Redhead: Can. J. Phys. 42 (1964) 886.
5) P.J. Feibelman and M.L. Knotek: Phys. Rev. B 18 (1978) 6531.
6) R. Jaeger, J. Stöhr, R. Treichler and K. Baberschke: Phys. Rev. Lett. 47 (1981) 1300.
7) D. Lichtman and Y. Shapira: CRC Crit. Rev. Solid State Mater. Sci. 8 (1978) 93.
8) M.J. Drinkwine, Y. Shapira and D. Lichtman: Adv. Chem. Ser. 158 (1976) 171.
9) R.O. Adams and E.E. Donaldson: J. Chem. Phys. 42 (1965) 770.
10) M.L. Knotek, V.O. Jones and V. Rehn: Phys. Rev. Lett. 43 (1979) 300.

11) R.Stockbauer, D.M. Hanson, S.A. Foldstrom and T.E. Madey: Phys. Rev. B 26 (1982) 1885.

12) D.P. Woodruff, P.D. Johnson, M.M. Traum, H.H. Farrell, N.V. Smith, R.L. Benbow and Z. Hurych: Surf. Sci. 104 (1981) 282.

5. Experimental Data

5.1 Experimental Data for IID

5.1.1 Tables

All the references on IID published through the end of 1984 are classified by the combination of adsorbate and solid, with which each reference is concerned. It follows that the compiled data are divided into 54 classes. The references belonging to each class are summarized in Table 1, where the references are shown by registered symbols. The registered symbols consist of the two sets of two figures and the abbreviation of the first author's name. The former set of two figures denotes the year of the publication in the 1900's and the latter set of two figures denotes the series number for an identical abbreviation of the authors. The first column in the table shows the substrates and the first line the adsorbates. The figure number of the graphs showing the data for each adsorbate-substrate combination is shown in Table 2. In this table, DL indicates the list of miscellaneous data in the section of 5.1.4.

TABLE 1 ADSORBATE/SUBSTRATE SYSTEMS IN IID

	H_2	D_2	N_2	O_2	CO	C	S	He	Ar	As,Se	R.G.
Be		84Ba04									
Si				80On01						80On01	
Ti	80Sa02			78Ta07 79Ta08 81Le01 84Su01 84Ta12	79Ta08 80Sa02						
Fe				81Le01							
Ni	81Be04 82Bo01	82Ba04		76Ta02 76Ta03 77Ta04 77Ta05 78Ta07 79Ta08 84Ta12	76Ta03 78Ta06 79Ta08 80Ma04 81Sa03		75Ta01 76Ta02 77Ta05 78Wi03 81Sa03 84Ta12				
Cu	73Er01	73Er01	75Er02	79De01 79Ta08 80Ta10 84Ta12	75Er02			75Er02	75Er02		78Ma03 79Ac01
Mo	81Sa03		82Wi05	77Ra01 78Ak01 78Ra02 79Sa01 81Sa03	79Sa01 80Sa02 81Sa03		81Sa03				

Rh				83Mo01	
Pd			78Ta07 79Ta08 84Ta12		
Ta			79Ta08 84Ta12		81Pe01
W	78Ta06 78Ta07 84Ta12	71Wi01 74Wi02 82Wi05 84Ta12	78Ta07 79Ta08 84Ta12		
Pt			79Ta08 84Ta12		

H_2O/Mo: 74Mc01, (Cl + C)/Ni : 81Pe02, H_2/(Ar + Cu): 75Er02, H_2/(Ni + Oxide): 82Bo01

TABLE 1 -CONTINUED

	H_2	D_2	N_2	O_2	CO	CO_2	H_2O	S	He	Ar,Kr	R.G.
SS	77Hi01	81Ba03 84Ba04	77Hi01		74Mc01 76Ma01 80Fa01	74Mc01	74Mc01	80Ba02	77Hi01	74Mc01	74Ca01 74Mc01 77Ma02 78Ma03 79Ac01
TiC				84Su01							
Inco. Alloy											77Ma02 78Ma03 79Ac01
Ti-Alloy											79Ac01
Al-Alloy											79Ac01

CH_4/SS: 74Mc01, Organic samples/Mylar: 84Ne01, Organic samples/Au: 84Ni01

TABLE 2 FIGURE NUMBER OF GRAPHS AND DATA LIST (DL)

	H_2	D_2	N_2	O_2	CO	C	S	He	Ar	As,Se	R.G.
Be		DL									
Si				fig.29						DL	
Ti	DL			fig.15 fig.31	DL						
Fe				fig.14 DL							
Ni	DL	DL		fig.20 fig.31 DL	fig.4 fig.5 fig.27 DL		fig.22 fig.23 fig.24 fig.25 fig.30 DL				
Cu	fig.44	fig.45	fig.54	fig.16 fig.17 fig.31 DL	fig.52			fig.51 fig.55	fig.51		fig.57
Mo	fig.10 DL		fig.12	fig.18 fig.19 DL	fig.2 fig.3 DL		fig.21				
Rh					fig.6						

Pd			fig.31	
Ta			fig.31	fig.8
W	fig.11 DL	fig.13 fig.34 fig.35	fig.31	
Pt			fig.31	

H_2O/Mo:DL, (Cl + C)/Ni:fig.1, H_2/(Ar + Cu):fig.53, H_2/(Ni + Oxide):DL

TABLE 2 -CONTINUED

	H_2	D_2	N_2	O_2	CO	CO_2	H_2O	S	He	Ar,Xe	R.G.
SS	fig.46 fig.47 fig.48 DL	fig.9 fig.28 fig.32 DL	fig.50		fig.7 DL	DL	fig.33 DL	fig.26	fig.49	DL	fig.36 fig.37 fig.38 fig.39 fig.40 fig.60 DL
TiC				DL							
Inco. Alloy											fig.58 fig.59
Ti-Alloy											fig.61
Al-Alloy											fig.56

CH_4/SS: DL, Organic samples/Mylar: figs.41-43, Organic samples/Au: figs.62-65

5.1.2 Graphs and Data Lists for Desorption Cross Section

The desorption cross sections for various adsorbate-substrate combinations are shown in Figs. 1 - 26 as a function of incident ion energy. Figures 27 - 30 show the dependence on incident angle from the surface normal. Figure 31 shows the dependence on the surface binding energy. It can be seen from the complied data that the desorption cross sections range from 10^{-17} cm^2 to 10^{-14} cm^2 and depend on projectile mass, i.e. the desorption cross sections increase for heavior particle due to larger scattering cross sections.

The energy dependence of the desorption cross sections has a few remarkable features in the observed energy range. For heavior ions, the desorption cross section increases or remains relatively constant with increasing energy. For light ions such as H^+ and He^+ ions, however, the desorption cross section is found to decrease with increasing energy. There are some exceptional cases shown in Figs. 7, 16 and 17. In Fig. 7 the desorption cross section shows a minimum in the energy region 150 - 350 eV. On the other hand, the desorption cross sections have a maximum near 3 KeV in Figs. 16 and 17. The threshold energies for desorption are not clear. The dependence of the desorption cross section on surface crystallographic structure is also found in Figs. 18 and 24.

Note on Graphs

E_i : incident ion energy

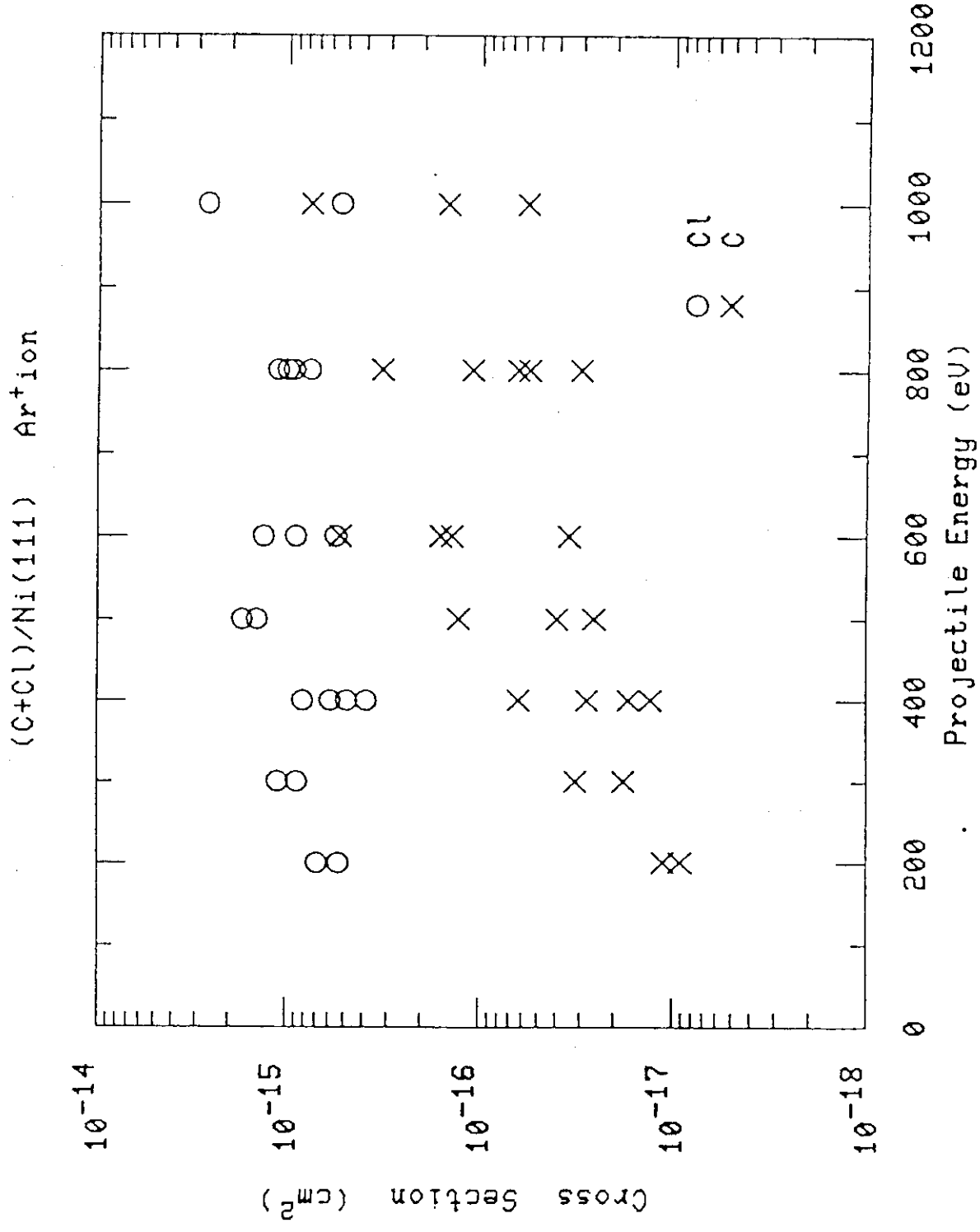

Fig. 1 Desorption cross section as a function of incident energy

DATA LIST

Substrate	Incident ion species	Incident energy (eV)	Incident angle from normal (deg.)	Method	Desorption cross section (cm**2)	Ref.	Remark
Ni(111)	Ar+	0.200E+03	60	AES	0.532E-15	81Pe02	*1)
Ni(111)	Ar+	0.200E+03	60	AES	0.686E-15	81Pe02	*1)
Ni(111)	Ar+	0.300E+03	60	AES	0.876E-15	81Pe02	*1)
Ni(111)	Ar+	0.300E+03	60	AES	0.110E-14	81Pe02	*1)
Ni(111)	Ar+	0.400E+03	60	AES	0.384E-15	81Pe02	*1)
Ni(111)	Ar+	0.400E+03	60	AES	0.484E-15	81Pe02	*1)
Ni(111)	Ar+	0.400E+03	60	AES	0.587E-15	81Pe02	*1)
Ni(111)	Ar+	0.400E+03	60	AES	0.815E-15	81Pe02	*1)
Ni(111)	Ar+	0.500E+03	60	AES	0.141E-14	81Pe02	*1)
Ni(111)	Ar+	0.500E+03	60	AES	0.169E-14	81Pe02	*1)
Ni(111)	Ar+	0.600E+03	60	AES	0.554E-15	81Pe02	*1)
Ni(111)	Ar+	0.600E+03	60	AES	0.889E-15	81Pe02	*1)
Ni(111)	Ar+	0.600E+03	60	AES	0.131E-14	81Pe02	*1)
Ni(111)	Ar+	0.800E+03	60	AES	0.761E-15	81Pe02	*1)
Ni(111)	Ar+	0.800E+03	60	AES	0.924E-15	81Pe02	*1)
Ni(111)	Ar+	0.800E+03	60	AES	0.994E-15	81Pe02	*1)
Ni(111)	Ar+	0.800E+03	60	AES	0.111E-14	81Pe02	*1)
Ni(111)	Ar+	0.100E+04	60	AES	0.531E-15	81Pe02	*1)
Ni(111)	Ar+	0.100E+04	60	AES	0.265E-14	81Pe02	*1)
Ni(111)	Ar+	0.200E+03	60	AES	0.919E-17	81Pe02	*2)
Ni(111)	Ar+	0.200E+03	60	AES	0.112E-16	81Pe02	*2)
Ni(111)	Ar+	0.300E+03	60	AES	0.179E-16	81Pe02	*2)
Ni(111)	Ar+	0.300E+03	60	AES	0.317E-16	81Pe02	*2)
Ni(111)	Ar+	0.400E+03	60	AES	0.130E-16	81Pe02	*2)
Ni(111)	Ar+	0.400E+03	60	AES	0.169E-16	81Pe02	*2)
Ni(111)	Ar+	0.400E+03	60	AES	0.277E-16	81Pe02	*2)
Ni(111)	Ar+	0.400E+03	60	AES	0.626E-16	81Pe02	*2)
Ni(111)	Ar+	0.500E+03	60	AES	0.257E-16	81Pe02	*2)
Ni(111)	Ar+	0.500E+03	60	AES	0.397E-16	81Pe02	*2)
Ni(111)	Ar+	0.500E+03	60	AES	0.128E-15	81Pe02	*2)
Ni(111)	Ar+	0.600E+03	60	AES	0.343E-16	81Pe02	*2)
Ni(111)	Ar+	0.600E+03	60	AES	0.139E-15	81Pe02	*2)
Ni(111)	Ar+	0.600E+03	60	AES	0.159E-15	81Pe02	*2)
Ni(111)	Ar+	0.600E+03	60	AES	0.527E-15	81Pe02	*2)
Ni(111)	Ar+	0.800E+03	60	AES	0.300E-16	81Pe02	*2)
Ni(111)	Ar+	0.800E+03	60	AES	0.557E-16	81Pe02	*2)
Ni(111)	Ar+	0.800E+03	60	AES	0.638E-16	81Pe02	*2)
Ni(111)	Ar+	0.800E+03	60	AES	0.110E-15	81Pe02	*2)
Ni(111)	Ar+	0.800E+03	60	AES	0.323E-15	81Pe02	*2)
Ni(111)	Ar+	0.100E+04	60	AES	0.573E-16	81Pe02	*2)
Ni(111)	Ar+	0.100E+04	60	AES	0.149E-15	81Pe02	*2)
Ni(111)	Ar+	0.100E+04	60	AES	0.762E-15	81Pe02	*2)

The sample was a Ni(111) ribbon. The carbon in the adlayer was coming from the residual gas atomosphere while the chlorine was a common surface contaminant in UHV systems.

*1)The desorption cross section was obtained from chlorine Auger signal.

*2)The desorption cross section was obtained from charbon Auger signal.

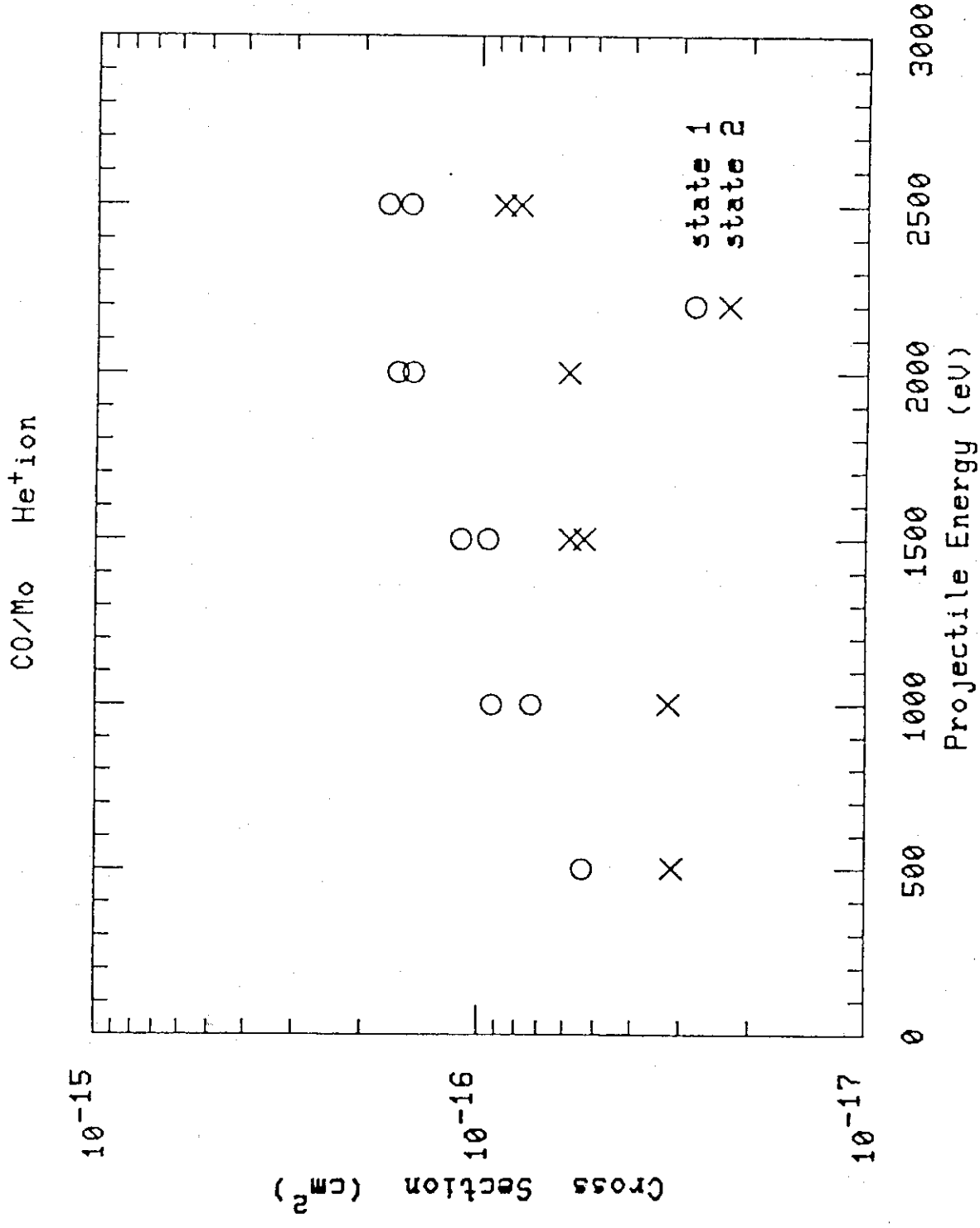

Fig. 2 Desorption cross section as a function of incident energy

DATA LIST

Substrate	Incident ion species	Incident energy (eV)	Incident angle from normal (deg.)	Method	Desorption cross section (cm**2)	Ref.	Remark
Mo	He+	0.500E+03	45	ISS	0.534E-16	79Sa01	*1)
Mo	He+	0.100E+04	45	ISS	0.921E-16	79Sa01	*1)
Mo	He+	0.100E+04	45	ISS	0.727E-16	79Sa01	*1)
Mo	He+	0.150E+04	45	ISS	0.111E-15	79Sa01	*1)
Mo	He+	0.150E+04	45	ISS	0.943E-16	79Sa01	*1)
Mo	He+	0.200E+04	45	ISS	0.163E-15	79Sa01	*1)
Mo	He+	0.200E+04	45	ISS	0.149E-15	79Sa01	*1)
Mo	He+	0.250E+04	45	ISS	0.173E-15	79Sa01	*1)
Mo	He+	0.250E+04	45	ISS	0.151E-15	79Sa01	*1)
Mo	He+	0.500E+03	45	ISS	0.313E-16	79Sa01	*2)
Mo	He+	0.100E+04	45	ISS	0.321E-16	79Sa01	*2)
Mo	He+	0.150E+04	45	ISS	0.579E-16	79Sa01	*2)
Mo	He+	0.150E+04	45	ISS	0.531E-16	79Sa01	*2)
Mo	He+	0.200E+04	45	ISS	0.586E-16	79Sa01	*2)
Mo	He+	0.250E+04	45	ISS	0.865E-16	79Sa01	*2)
Mo	He+	0.250E+04	45	ISS	0.785E-16	79Sa01	*2)

*1) Electron beam melted Mo sample, adsorption state 1
*2) Electron beam melted Mo sample, adsorption state 2

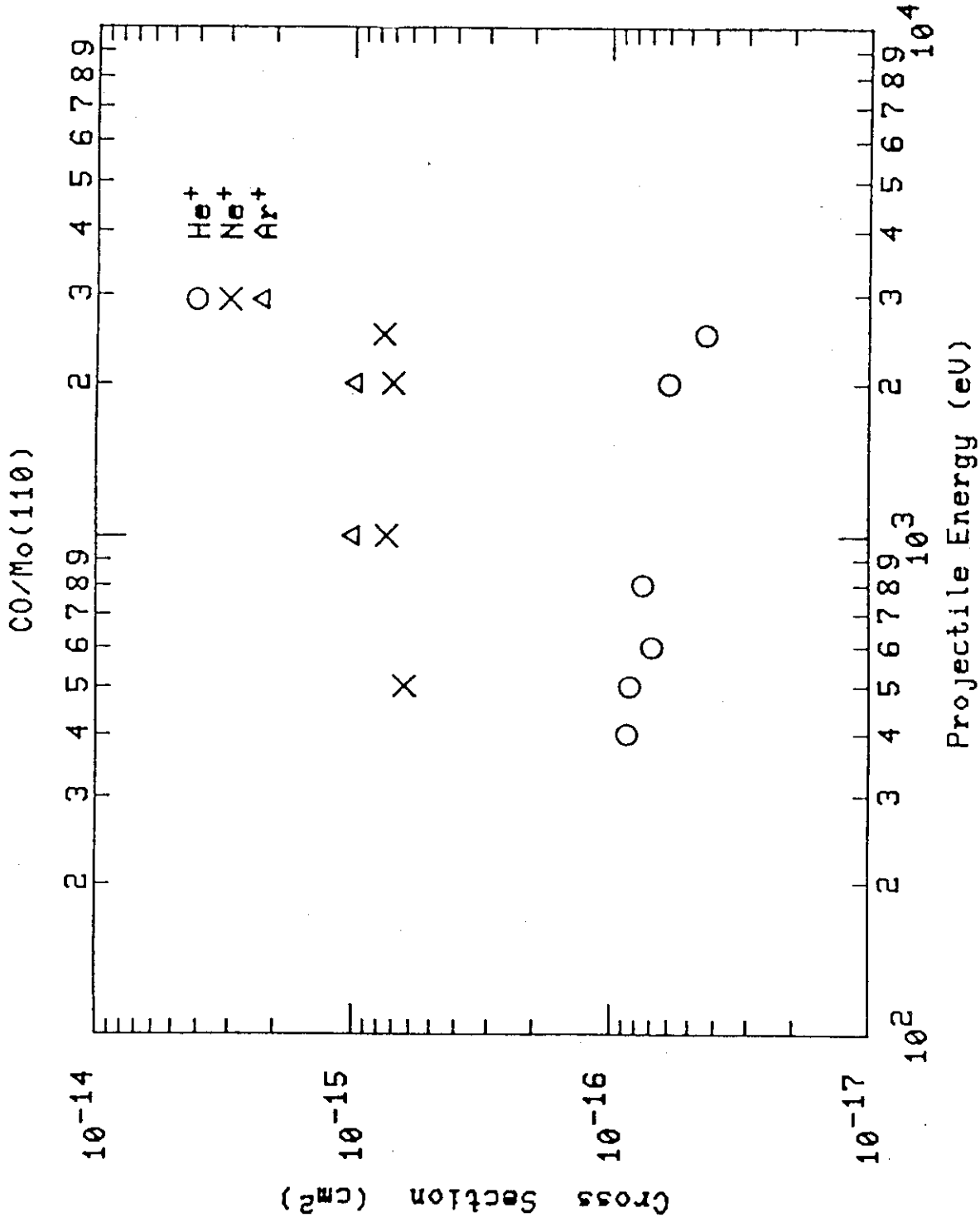

Fig. 3 Desorption cross section as a function of incident energy

DATA LIST

Substrate	Incident ion species	Incident energy (eV)	Incident angle from normal (deg.)	Method	Desorption cross section (cm**2)	Ref.
Mo(110)	He+	0.400E+03	45	ISS	0.856E-16	81Sa03
Mo(110)	He+	0.500E+03	45	ISS	0.835E-16	81Sa03
Mo(110)	He+	0.600E+03	45	ISS	0.687E-16	81Sa03
Mo(110)	He+	0.800E+03	45	ISS	0.746E-16	81Sa03
Mo(110)	He+	0.200E+04	45	ISS	0.596E-16	81Sa03
Mo(110)	He+	0.250E+04	45	ISS	0.430E-16	81Sa03
Mo(110)	Ne+	0.500E+03	45	ISS	0.629E-15	81Sa03
Mo(110)	Ne+	0.100E+04	45	ISS	0.740E-15	81Sa03
Mo(110)	Ne+	0.200E+04	45	ISS	0.701E-15	81Sa03
Mo(110)	Ne+	0.250E+04	45	ISS	0.762E-15	81Sa03
Mo(110)	Ar+	0.100E+04	45	ISS	0.993E-15	81Sa03
Mo(110)	Ar+	0.200E+04	45	ISS	0.976E-15	81Sa03

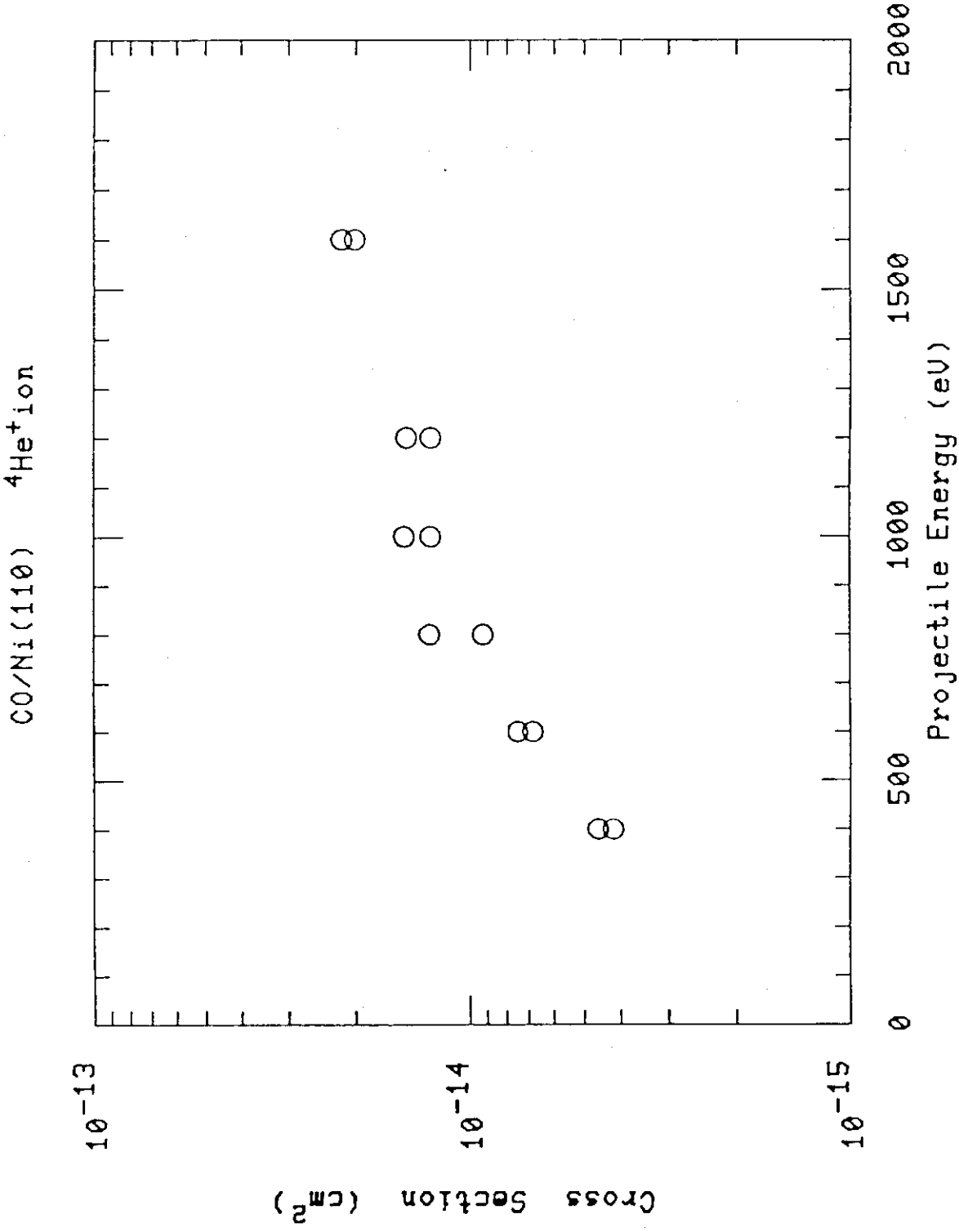

Fig. 4 Desorption cross section as a function of incident energy

DATA LIST

Substrate	Incident ion species	Incident energy (eV)	Incident angle from normal (deg.)	Method	Desorption cross section (cm**2)	Ref.	Remark
Ni(110)	4He+	0.400E+03	60	ISS	0.418E-14	78Ta06	*1)
Ni(110)	4He+	0.400E+03	60	ISS	0.458E-14	78Ta06	*2)
Ni(110)	4He+	0.600E+03	60	ISS	0.680E-14	78Ta06	*1)
Ni(110)	4He+	0.600E+03	60	ISS	0.746E-14	78Ta06	*2)
Ni(110)	4He+	0.800E+03	60	ISS	0.923E-14	78Ta06	*1)
Ni(110)	4He+	0.800E+03	60	ISS	0.128E-13	78Ta06	*2)
Ni(110)	4He+	0.100E+04	60	ISS	0.149E-13	78Ta06	*2)
Ni(110)	4He+	0.100E+04	60	ISS	0.127E-13	78Ta06	*1)
Ni(110)	4He+	0.120E+04	60	ISS	0.147E-13	78Ta06	*2)
Ni(110)	4He+	0.120E+04	60	ISS	0.127E-13	78Ta06	*1)
Ni(110)	4He+	0.160E+04	60	ISS	0.218E-13	78Ta06	*1)
Ni(110)	4He+	0.160E+04	60	ISS	0.201E-13	78Ta06	*2)

*1) The desorption measurements were carried out by monitoring the carbon peak in the 4He+ scattering spectrum.
*2) The desorption measurements were carried out by monitoring the oxygen peak in the 4He+ scattering spectrum.

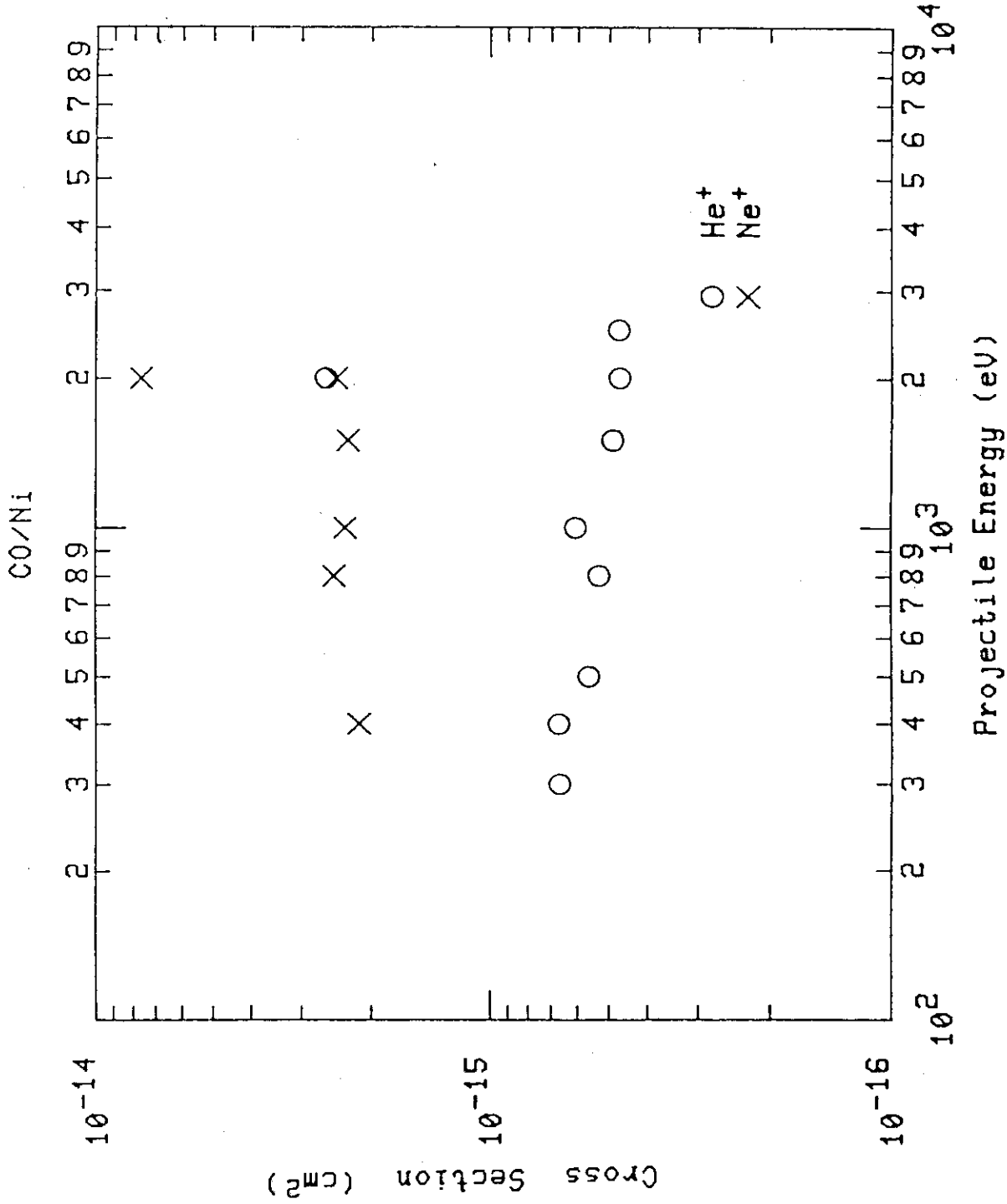

Fig. 5 Desorption cross section as a function of incident energy

DATA LIST

Substrate	Incident ion species	Incident energy (eV)	Incident angle from normal (deg.)	Method	Desorption cross section (cm**2)	Ref.
Ni poly	He+	0.300E+03	45	ISS	0.663E-15	81Sa03
Ni poly	He+	0.400E+03	45	ISS	0.666E-15	81Sa03
Ni poly	He+	0.500E+03	45	ISS	0.560E-15	81Sa03
Ni poly	He+	0.800E+03	45	ISS	0.528E-15	81Sa03
Ni poly	He+	0.100E+04	45	ISS	0.605E-15	81Sa03
Ni poly	He+	0.150E+04	45	ISS	0.488E-15	81Sa03
Ni poly	He+	0.200E+04	45	ISS	0.469E-15	81Sa03
Ni poly	He+	0.200E+04	45	IPP	0.260E-14	80Ma04
Ni poly	He+	0.250E+04	45	ISS	0.471E-15	81Sa03
Ni poly	Ne+	0.400E+03	45	ISS	0.215E-14	81Sa03
Ni poly	Ne+	0.800E+03	45	ISS	0.248E-14	81Sa03
Ni poly	Ne+	0.100E+04	45	ISS	0.233E-14	81Sa03
Ni poly	Ne+	0.150E+04	45	ISS	0.229E-14	81Sa03
Ni poly	Ne+	0.200E+04	45	ISS	0.245E-14	81Sa03
Ni poly	Ne+	0.200E+04	45	IPP	0.770E-14	80Ma04

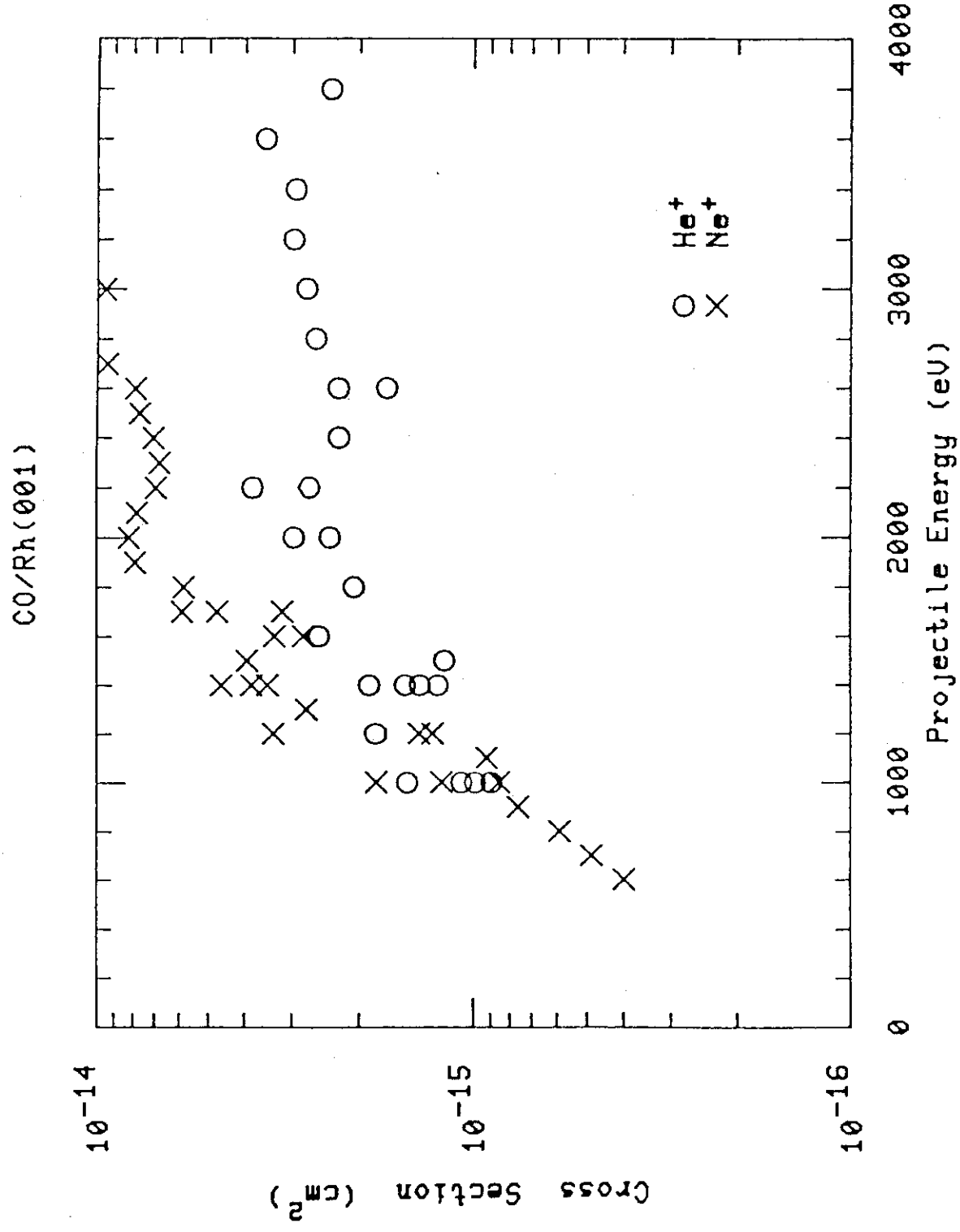

Fig. 6 Desorption cross section as a function of incident energy

DATA LIST

Substrate	Incident ion species	Incident energy (eV)	Incident angle from normal (deg.)	Method	Desorption cross section (cm**2)	Ref.
Rh(001)	He+	0.100E+04	60	ISS	0.894E-15	83Mo01
Rh(001)	He+	0.100E+04	60	ISS	0.986E-15	83Mo01
Rh(001)	He+	0.100E+04	60	ISS	0.107E-14	83Mo01
Rh(001)	He+	0.100E+04	60	ISS	0.149E-14	83Mo01
Rh(001)	He+	0.120E+04	60	ISS	0.181E-14	83Mo01
Rh(001)	He+	0.140E+04	60	ISS	0.124E-14	83Mo01
Rh(001)	He+	0.140E+04	60	ISS	0.138E-14	83Mo01
Rh(001)	He+	0.140E+04	60	ISS	0.151E-14	83Mo01
Rh(001)	He+	0.140E+04	60	ISS	0.188E-14	83Mo01
Rh(001)	He+	0.150E+04	60	ISS	0.119E-14	83Mo01
Rh(001)	He+	0.160E+04	60	ISS	0.254E-14	83Mo01
Rh(001)	He+	0.180E+04	60	ISS	0.206E-14	83Mo01
Rh(001)	He+	0.200E+04	60	ISS	0.238E-14	83Mo01
Rh(001)	He+	0.200E+04	60	ISS	0.296E-14	83Mo01
Rh(001)	He+	0.220E+04	60	ISS	0.270E-14	83Mo01
Rh(001)	He+	0.220E+04	60	ISS	0.381E-14	83Mo01
Rh(001)	He+	0.240E+04	60	ISS	0.226E-14	83Mo01
Rh(001)	He+	0.260E+04	60	ISS	0.169E-14	83Mo01
Rh(001)	He+	0.260E+04	60	ISS	0.227E-14	83Mo01
Rh(001)	He+	0.280E+04	60	ISS	0.260E-14	83Mo01
Rh(001)	He+	0.300E+04	60	ISS	0.275E-14	83Mo01
Rh(001)	He+	0.320E+04	60	ISS	0.297E-14	83Mo01
Rh(001)	He+	0.340E+04	60	ISS	0.294E-14	83Mo01
Rh(001)	He+	0.360E+04	60	ISS	0.353E-14	83Mo01
Rh(001)	He+	0.380E+04	60	ISS	0.238E-14	83Mo01
Rh(001)	Ne+	0.600E+03	60	ISS	0.398E-15	83Mo01
Rh(001)	Ne+	0.700E+03	60	ISS	0.484E-15	83Mo01
Rh(001)	Ne+	0.800E+03	60	ISS	0.588E-15	83Mo01
Rh(001)	Ne+	0.900E+03	60	ISS	0.758E-15	83Mo01
Rh(001)	Ne+	0.100E+04	60	ISS	0.852E-15	83Mo01
Rh(001)	Ne+	0.100E+04	60	ISS	0.121E-14	83Mo01
Rh(001)	Ne+	0.100E+04	60	ISS	0.180E-14	83Mo01
Rh(001)	Ne+	0.110E+04	60	ISS	0.920E-15	83Mo01
Rh(001)	Ne+	0.120E+04	60	ISS	0.128E-14	83Mo01
Rh(001)	Ne+	0.120E+04	60	ISS	0.139E-14	83Mo01
Rh(001)	Ne+	0.120E+04	60	ISS	0.336E-14	83Mo01
Rh(001)	Ne+	0.130E+04	60	ISS	0.275E-14	83Mo01
Rh(001)	Ne+	0.140E+04	60	ISS	0.348E-14	83Mo01
Rh(001)	Ne+	0.140E+04	60	ISS	0.384E-14	83Mo01
Rh(001)	Ne+	0.140E+04	60	ISS	0.463E-14	83Mo01
Rh(001)	Ne+	0.150E+04	60	ISS	0.395E-14	83Mo01
Rh(001)	Ne+	0.160E+04	60	ISS	0.280E-14	83Mo01

./..

Rh(001)	Ne+	0.160E+04	60	ISS	0.334E-14	83Mo01
Rh(001)	Ne+	0.170E+04	60	ISS	0.318E-14	83Mo01
Rh(001)	Ne+	0.170E+04	60	ISS	0.475E-14	83Mo01
Rh(001)	Ne+	0.170E+04	60	ISS	0.590E-14	83Mo01
Rh(001)	Ne+	0.180E+04	60	ISS	0.584E-14	83Mo01
Rh(001)	Ne+	0.190E+04	60	ISS	0.791E-14	83Mo01
Rh(001)	Ne+	0.200E+04	60	ISS	0.822E-14	83Mo01
Rh(001)	Ne+	0.210E+04	60	ISS	0.781E-14	83Mo01
Rh(001)	Ne+	0.220E+04	60	ISS	0.694E-14	83Mo01
Rh(001)	Ne+	0.230E+04	60	ISS	0.679E-14	83Mo01
Rh(001)	Ne+	0.240E+04	60	ISS	0.706E-14	83Mo01
Rh(001)	Ne+	0.250E+04	60	ISS	0.771E-14	83Mo01
Rh(001)	Ne+	0.260E+04	60	ISS	0.793E-14	83Mo01
Rh(001)	Ne+	0.270E+04	60	ISS	0.945E-14	83Mo01
Rh(001)	Ne+	0.300E+04	60	ISS	0.961E-14	83Mo01

The desorption cross sections measured for He+ were too high in comparison with Ne+ as well as in comparison with elastic models.

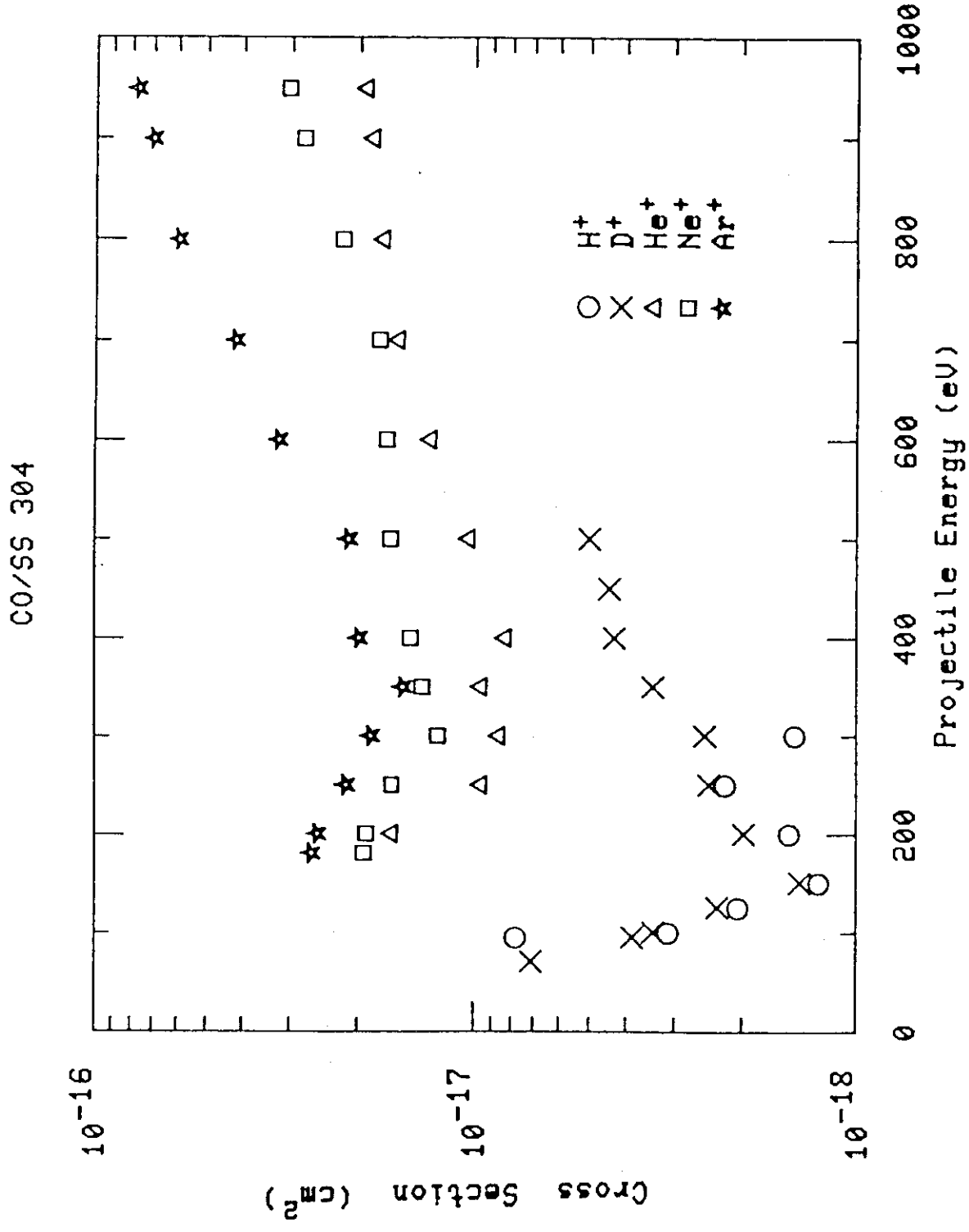

Fig. 7 Desorption cross section as a function of incident energy

DATA LIST

Substrate	Incident ion species	Incident energy (eV)	Incident angle from normal (deg.)	Method	Desorption cross section (cm**2)	Ref.
SS 304	H+	0.950E+02	0	MS	0.779E-17	80Fa01
SS 304	H+	0.100E+03	0	MS	0.311E-17	80Fa01
SS 304	H+	0.125E+03	0	MS	0.205E-17	80Fa01
SS 304	H+	0.150E+03	0	MS	0.126E-17	80Fa01
SS 304	H+	0.200E+03	0	MS	0.151E-17	80Fa01
SS 304	H+	0.250E+03	0	MS	0.222E-17	80Fa01
SS 304	H+	0.300E+03	0	MS	0.146E-17	80Fa01
SS 304	D+	0.700E+02	0	MS	0.709E-17	80Fa01
SS 304	D+	0.950E+02	0	MS	0.385E-17	80Fa01
SS 304	D+	0.100E+03	0	MS	0.339E-17	80Fa01
SS 304	D+	0.125E+03	0	MS	0.232E-17	80Fa01
SS 304	D+	0.150E+03	0	MS	0.141E-17	80Fa01
SS 304	D+	0.200E+03	0	MS	0.198E-17	80Fa01
SS 304	D+	0.250E+03	0	MS	0.244E-17	80Fa01
SS 304	D+	0.300E+03	0	MS	0.249E-17	80Fa01
SS 304	D+	0.350E+03	0	MS	0.339E-17	80Fa01
SS 304	D+	0.400E+03	0	MS	0.429E-17	80Fa01
SS 304	D+	0.450E+03	0	MS	0.442E-17	80Fa01
SS 304	D+	0.500E+03	0	MS	0.499E-17	80Fa01
SS 304	He+	0.200E+03	0	MS	0.163E-16	80Fa01
SS 304	He+	0.250E+03	0	MS	0.956E-17	80Fa01
SS 304	He+	0.300E+03	0	MS	0.857E-17	80Fa01
SS 304	He+	0.350E+03	0	MS	0.955E-17	80Fa01
SS 304	He+	0.400E+03	0	MS	0.826E-17	80Fa01
SS 304	He+	0.500E+03	0	MS	0.103E-16	80Fa01
SS 304	He+	0.600E+03	0	MS	0.130E-16	80Fa01
SS 304	He+	0.700E+03	0	MS	0.158E-16	80Fa01
SS 304	He+	0.800E+03	0	MS	0.173E-16	80Fa01
SS 304	He+	0.900E+03	0	MS	0.185E-16	80Fa01
SS 304	He+	0.950E+03	0	MS	0.193E-16	80Fa01
SS 304	Ne+	0.180E+03	0	MS	0.193E-16	80Fa01
SS 304	Ne+	0.200E+03	0	MS	0.190E-16	80Fa01
SS 304	Ne+	0.250E+03	0	MS	0.164E-16	80Fa01
SS 304	Ne+	0.300E+03	0	MS	0.124E-16	80Fa01
SS 304	Ne+	0.350E+03	0	MS	0.136E-16	80Fa01
SS 304	Ne+	0.400E+03	0	MS	0.146E-16	80Fa01
SS 304	Ne+	0.500E+03	0	MS	0.165E-16	80Fa01
SS 304	Ne+	0.600E+03	0	MS	0.169E-16	80Fa01
SS 304	Ne+	0.700E+03	0	MS	0.177E-16	80Fa01
SS 304	Ne+	0.800E+03	0	MS	0.220E-16	80Fa01
SS 304	Ne+	0.900E+03	0	MS	0.279E-16	80Fa01
SS 304	Ne+	0.950E+03	0	MS	0.306E-16	80Fa01

./..

SS 304	Ar+	0.180E+03	0	MS	0.263E-16	80Fa01
SS 304	Ar+	0.200E+03	0	MS	0.254E-16	80Fa01
SS 304	Ar+	0.250E+03	0	MS	0.215E-16	80Fa01
SS 304	Ar+	0.300E+03	0	MS	0.185E-16	80Fa01
SS 304	Ar+	0.350E+03	0	MS	0.153E-16	80Fa01
SS 304	Ar+	0.400E+03	0	MS	0.199E-16	80Fa01
SS 304	Ar+	0.500E+03	0	MS	0.212E-16	80Fa01
SS 304	Ar+	0.600E+03	0	MS	0.322E-16	80Fa01
SS 304	Ar+	0.700E+03	0	MS	0.419E-16	80Fa01
SS 304	Ar+	0.800E+03	0	MS	0.599E-16	80Fa01
SS 304	Ar+	0.900E+03	0	MS	0.706E-16	80Fa01
SS 304	Ar+	0.950E+03	0	MS	0.782E-16	80Fa01

SS : Stainless steel

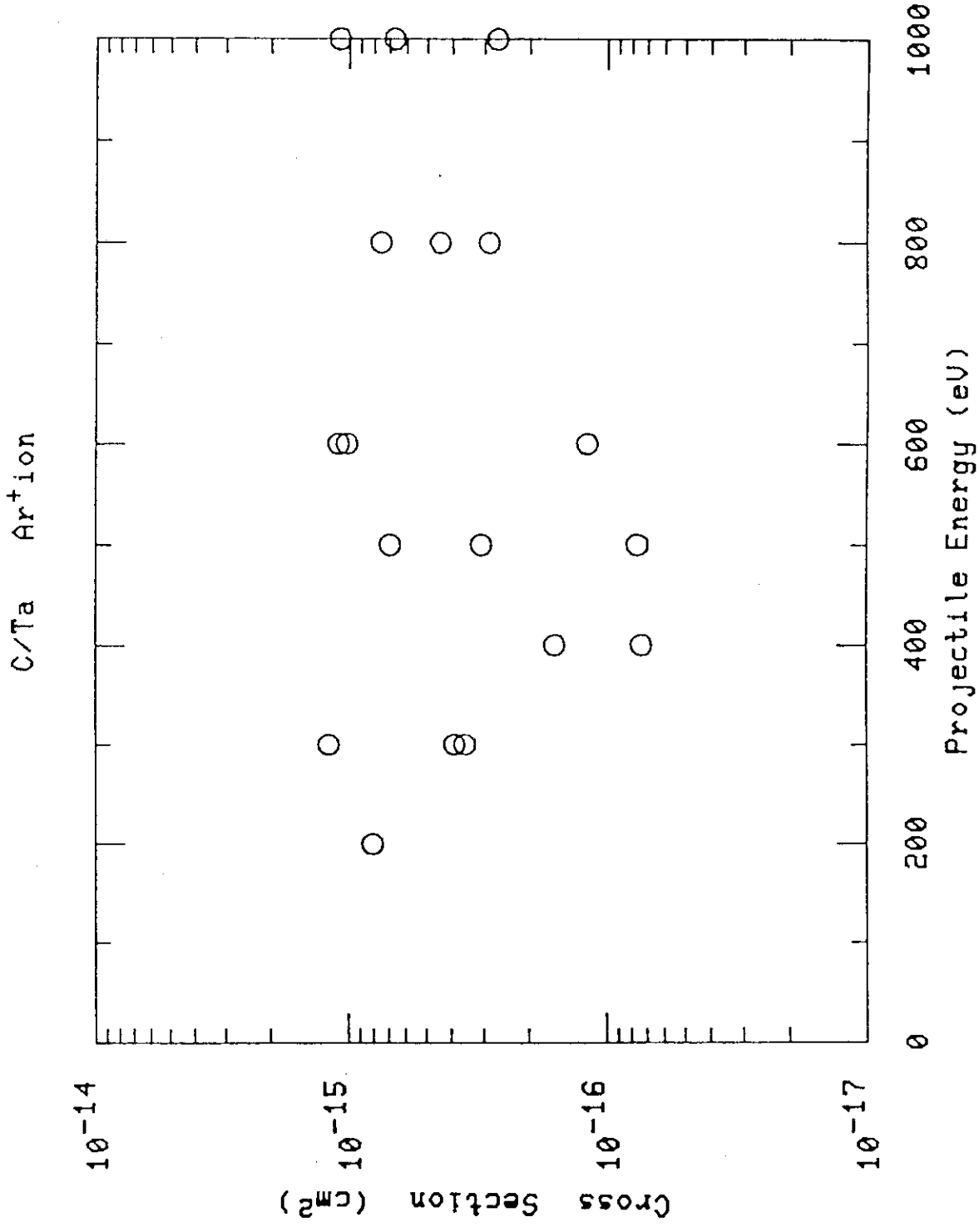

Fig. 8 Desorption cross section as a function of incident energy

DATA LIST

Substrate	Incident ion species	Incident energy (eV)	Incident angle from normal (deg.)	Method	Desorption cross section (cm**2)	Ref.
Ta sheet	Ar+	0.200E+03	60	AES	0.802E-15	81Pe01
Ta sheet	Ar+	0.300E+03	60	AES	0.355E-15	81Pe01
Ta sheet	Ar+	0.300E+03	60	AES	0.389E-15	81Pe01
Ta sheet	Ar+	0.300E+03	60	AES	0.119E-14	81Pe01
Ta sheet	Ar+	0.400E+03	60	AES	0.737E-16	81Pe01
Ta sheet	Ar+	0.400E+03	60	AES	0.160E-15	81Pe01
Ta sheet	Ar+	0.500E+03	60	AES	0.764E-16	81Pe01
Ta sheet	Ar+	0.500E+03	60	AES	0.307E-15	81Pe01
Ta sheet	Ar+	0.500E+03	60	AES	0.690E-15	81Pe01
Ta sheet	Ar+	0.600E+03	60	AES	0.119E-15	81Pe01
Ta sheet	Ar+	0.600E+03	60	AES	0.101E-14	81Pe01
Ta sheet	Ar+	0.600E+03	60	AES	0.109E-14	81Pe01
Ta sheet	Ar+	0.800E+03	60	AES	0.287E-15	81Pe01
Ta sheet	Ar+	0.800E+03	60	AES	0.446E-15	81Pe01
Ta sheet	Ar+	0.800E+03	60	AES	0.751E-15	81Pe01
Ta sheet	Ar+	0.100E+04	60	AES	0.267E-15	81Pe01
Ta sheet	Ar+	0.100E+04	60	AES	0.670E-15	81Pe01
Ta sheet	Ar+	0.100E+04	60	AES	0.109E-14	81Pe01

The scatter of the deta may be due to the surface roughness and the small change of carbon signal.

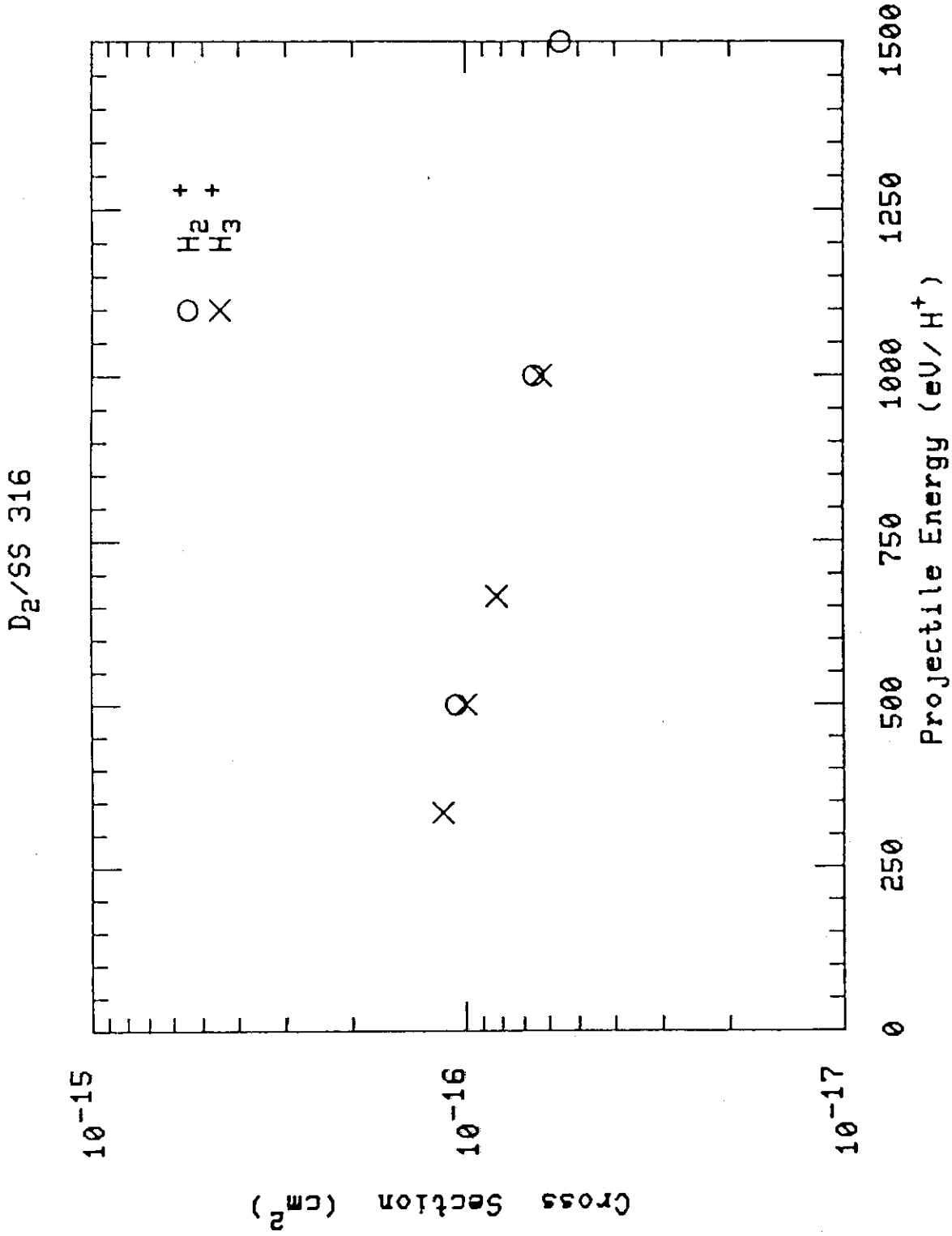

Fig. 9 Desorption cross section as a function of incident energy

DATA LIST

Substrate	Incident ion species	Incident energy per proton (eV)	Incident angle from normal (deg.)	Method	Desorption cross section (cm**2)	Ref.
SS 316	H2 +	0.500E+03	30	SIMS	0.106E-15	81Ba03
SS 316	H2 +	0.100E+04	30	SIMS	0.657E-16	81Ba03
SS 316	H2 +	0.150E+04	30	SIMS	0.556E-16	81Ba03
SS 316	H3 +	0.333E+03	30	SIMS	0.115E-15	81Ba03
SS 316	H3 +	0.500E+03	30	SIMS	0.997E-16	81Ba03
SS 316	H3 +	0.666E+03	30	SIMS	0.823E-16	81Ba03
SS 316	H3 +	0.100E+04	30	SIMS	0.627E-16	81Ba03

Desorbed species D- ion,
D2 exposure 3000 L
SS 316 : Stainless steel 316

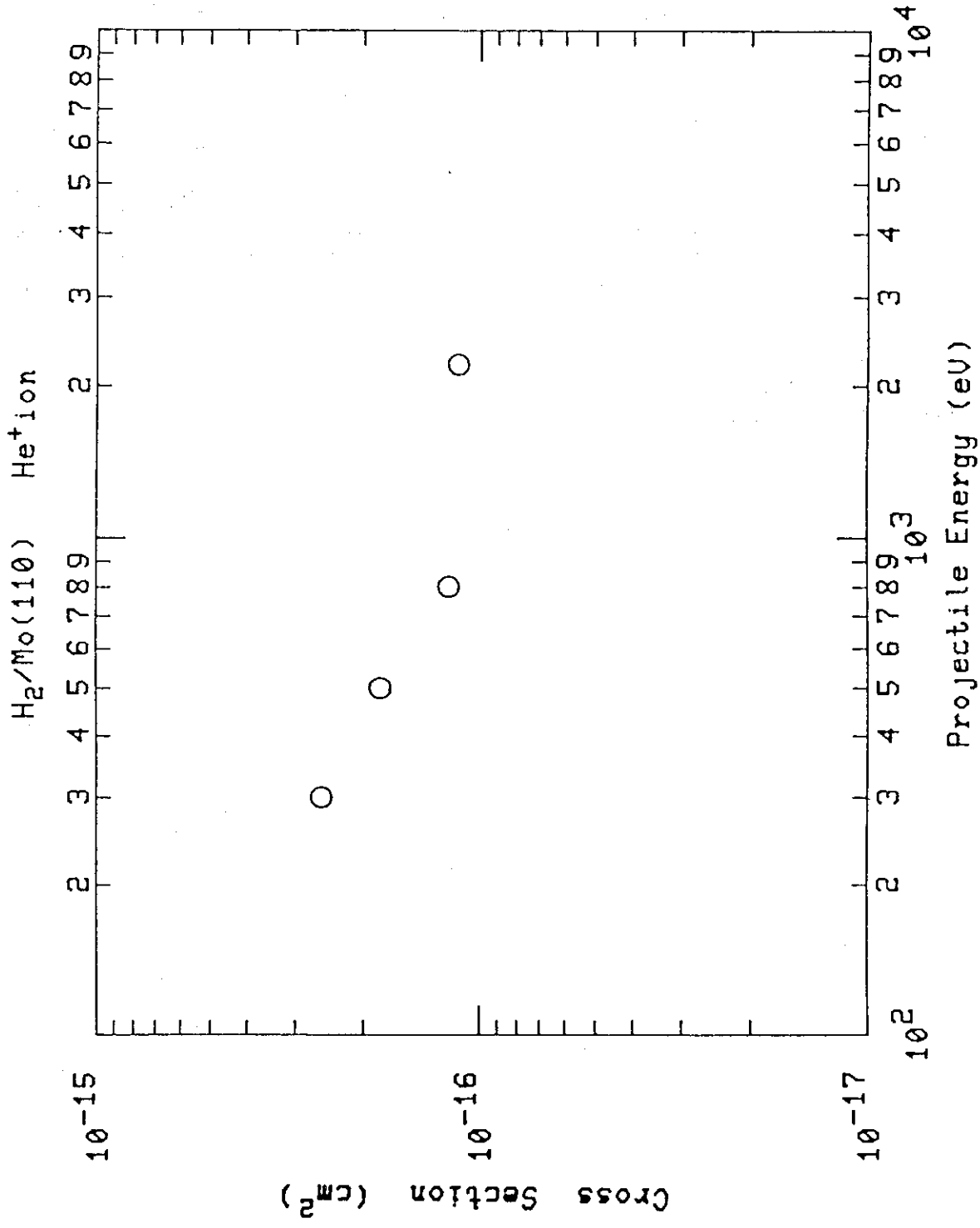

Fig.10 Desorption cross section as a function of incident energy

DATA LIST

Substrate	Incident ion species	Incident energy (eV)	Incident angle from normal (deg.)	Method	Desorption cross section (cm**2)	Ref.
Mo(110)	He+	0.300E+03	45	ISS	0.255E-15	81Sa03
Mo(110)	He+	0.500E+03	45	ISS	0.181E-15	81Sa03
Mo(110)	He+	0.800E+03	45	ISS	0.120E-15	81Sa03
Mo(110)	He+	0.220E+04	45	ISS	0.114E-15	81Sa03

The desorption measurements were carried out by monitoring the substrate-peak in the He+ scattering spectrum.

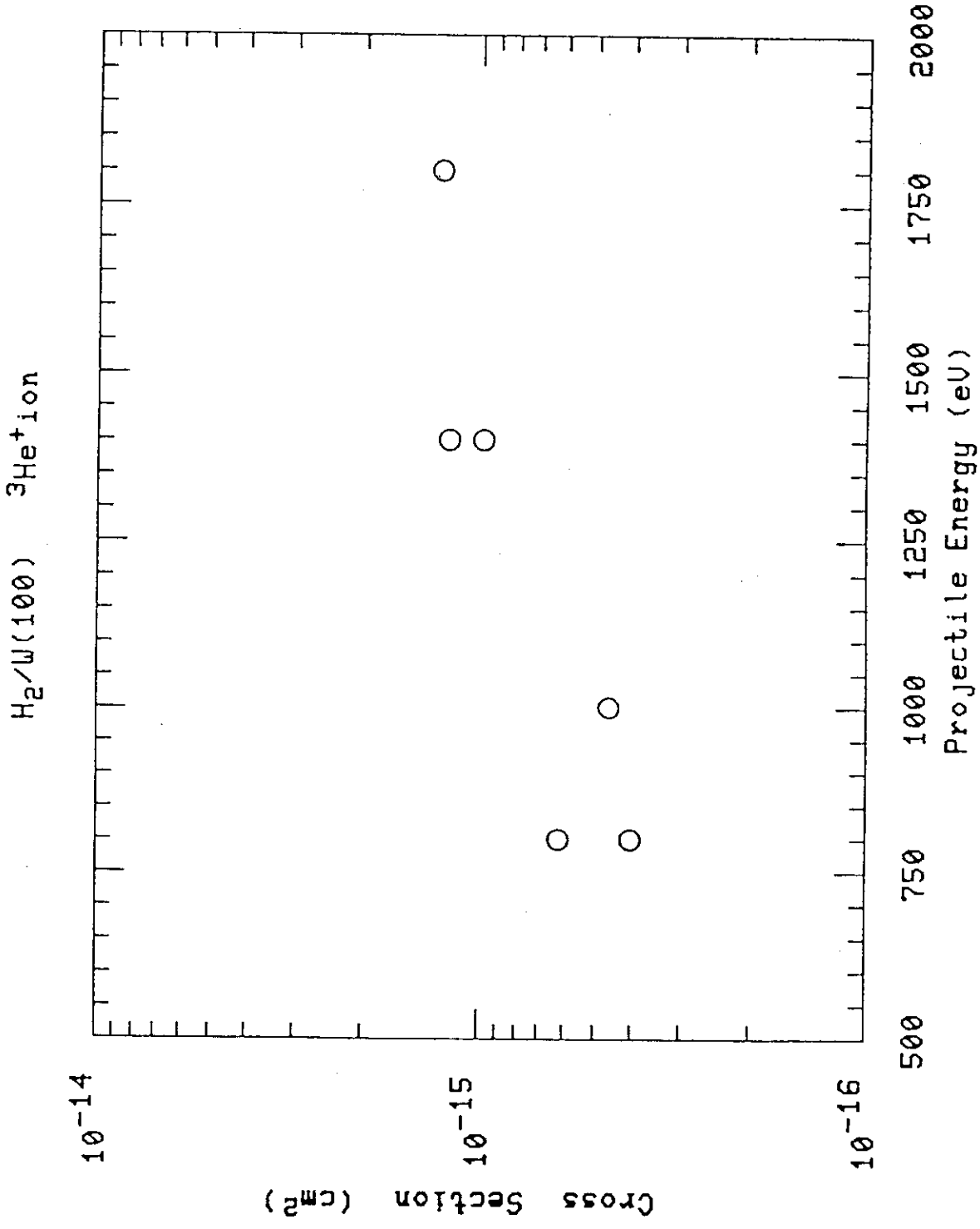

Fig.11 Desorption cross section as a function of incident energy

DATA LIST

Substrate	Incident ion species	Incident energy (eV)	Incident angle from normal (deg.)	Method	Desorption cross section (cm**2)	Ref.
W(100)	3He +	0.800E+03	60	ISS	0.617E-15	78Ta07
W(100)	3He +	0.800E+03	60	ISS	0.401E-15	78Ta07
W(100)	3He +	0.100E+04	60	ISS	0.458E-15	78Ta07
W(100)	3He +	0.140E+04	60	ISS	0.120E-14	78Ta07
W(100)	3He +	0.140E+04	60	ISS	0.979E-15	78Ta07
W(100)	3He +	0.180E+04	60	ISS	0.127E-14	78Ta07

The adsorption state of H2 molecules was in a dissociative state. The desorption measurements were carried out by monitoring the W-peak in the 3He+ scattering spectrum.

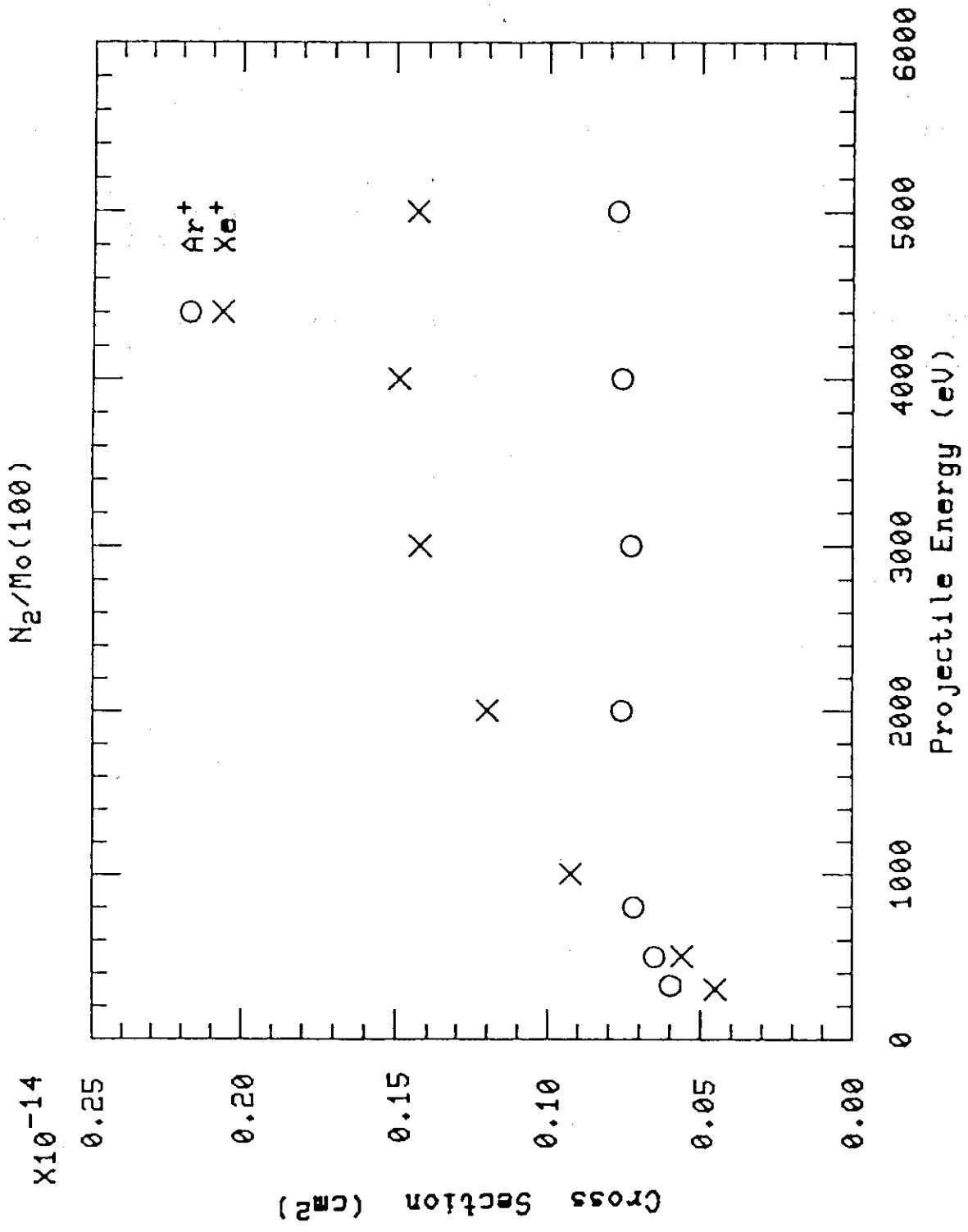

Fig.12 Desorption cross section as a function of incident energy

DATA LIST

Substrate	Incident ion species	Incident energy (eV)	Incident angle from normal (deg.)	Method	Desorption cross section (cm**2)	Ref.
Mo(100)	Ar+	0.325E+03	?	AES	0.598E-15	82Wi05
Mo(100)	Ar+	0.500E+03	?	AES	0.649E-15	82Wi05
Mo(100)	Ar+	0.800E+03	?	AES	0.717E-15	82Wi05
Mo(100)	Ar+	0.200E+04	?	AES	0.759E-15	82Wi05
Mo(100)	Ar+	0.300E+04	?	AES	0.728E-15	82Wi05
Mo(100)	Ar+	0.400E+04	?	AES	0.759E-15	82Wi05
Mo(100)	Ar+	0.500E+04	?	AES	0.773E-15	82Wi05
Mo(100)	Xe+	0.300E+03	?	AES	0.451E-15	82Wi05
Mo(100)	Xe+	0.500E+03	?	AES	0.560E-15	82Wi05
Mo(100)	Xe+	0.100E+04	?	AES	0.924E-15	82Wi05
Mo(100)	Xe+	0.200E+04	?	AES	0.120E-14	82Wi05
Mo(100)	Xe+	0.300E+04	?	AES	0.142E-14	82Wi05
Mo(100)	Xe+	0.400E+04	?	AES	0.149E-14	82Wi05
Mo(100)	Xe+	0.500E+04	?	AES	0.143E-14	82Wi05

The geometrical position of nitrogen atom was fourfold site and all measurements were taken at coverages below 6.0E+14 atoms/cm**2.

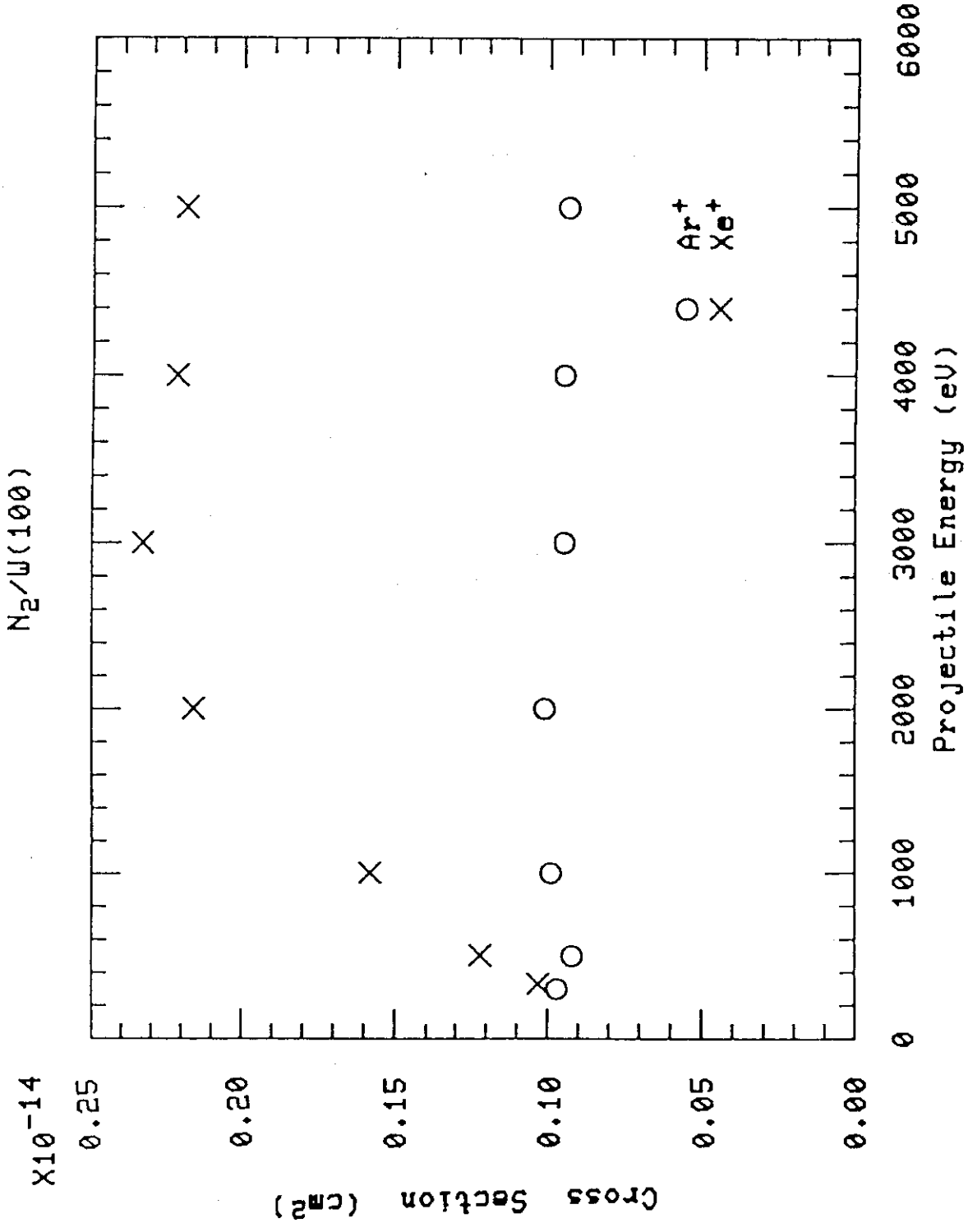

Fig.13 Desorption cross section as a function of incident energy

DATA LIST

Substrate	Incident ion species	Incident energy (eV)	Incident angle from normal (deg.)	Method	Desorption cross section (cm**2)	Ref.
W(100)	Ar+	0.300E+03	?	AES	0.970E-15	82Wi05
W(100)	Ar+	0.500E+03	?	AES	0.920E-15	82Wi05
W(100)	Ar+	0.100E+04	?	AES	0.989E-15	82Wi05
W(100)	Ar+	0.200E+04	?	AES	0.101E-14	82Wi05
W(100)	Ar+	0.300E+04	?	AES	0.949E-15	82Wi05
W(100)	Ar+	0.400E+04	?	AES	0.949E-15	82Wi05
W(100)	Ar+	0.500E+04	?	AES	0.937E-15	82Wi05
W(100)	Xe+	0.325E+03	?	AES	0.103E-14	82Wi05
W(100)	Xe+	0.500E+03	?	AES	0.122E-14	82Wi05
W(100)	Xe+	0.100E+04	?	AES	0.158E-14	82Wi05
W(100)	Xe+	0.200E+04	?	AES	0.216E-14	82Wi05
W(100)	Xe+	0.300E+04	?	AES	0.233E-14	82Wi05
W(100)	Xe+	0.400E+04	?	AES	0.222E-14	82Wi05
W(100)	Xe+	0.500E+04	?	AES	0.219E-14	82Wi05

The geometrical position of nitrogen atom was fourfold site and all measurements were taken at coverages below 6.0E+14 atoms/cm**2.

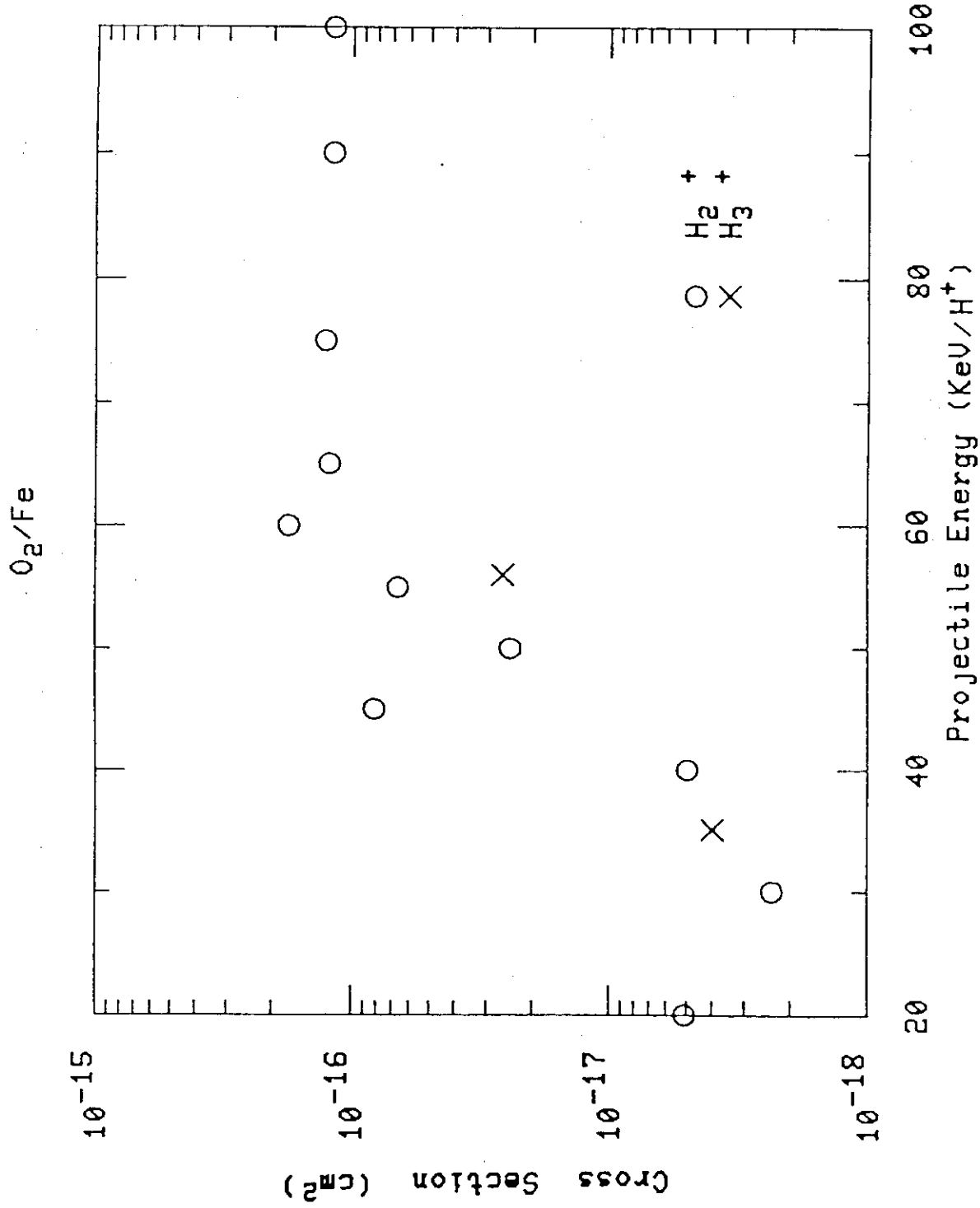

Fig.14 Desorption cross section as a function of incident energy

DATA LIST

Substrate	Incident ion species	Incident energy per proton (eV)	Incident angle from normal (deg.)	Method	Desorption cross section (cm**2)	Ref.
Fe poly	H2 +	0.200E+05	60	AES	0.507E-17	81Le01
Fe poly	H2 +	0.300E+05	60	AES	0.234E-17	81Le01
Fe poly	H2 +	0.400E+05	60	AES	0.494E-17	81Le01
Fe poly	H2 +	0.450E+05	60	AES	0.811E-16	81Le01
Fe poly	H2 +	0.500E+05	60	AES	0.243E-16	81Le01
Fe poly	H2 +	0.550E+05	60	AES	0.662E-16	81Le01
Fe poly	H2 +	0.600E+05	60	AES	0.173E-15	81Le01
Fe poly	H2 +	0.650E+05	60	AES	0.121E-15	81Le01
Fe poly	H2 +	0.750E+05	60	AES	0.125E-15	81Le01
Fe poly	H2 +	0.900E+05	60	AES	0.117E-15	81Le01
Fe poly	H2 +	0.100E+06	60	AES	0.118E-15	81Le01
Fe poly	H3 +	0.350E+05	60	AES	0.396E-17	81Le01
Fe poly	H3 +	0.560E+05	60	AES	0.259E-16	81Le01

About one monolayer of oxygen was adsorbed at RT.
At energies above 40KeV per H+ ions, the cross section showed a sharp rise,indicating onset of some new inelastic desorption mechanism.
O-KLL Auger signal

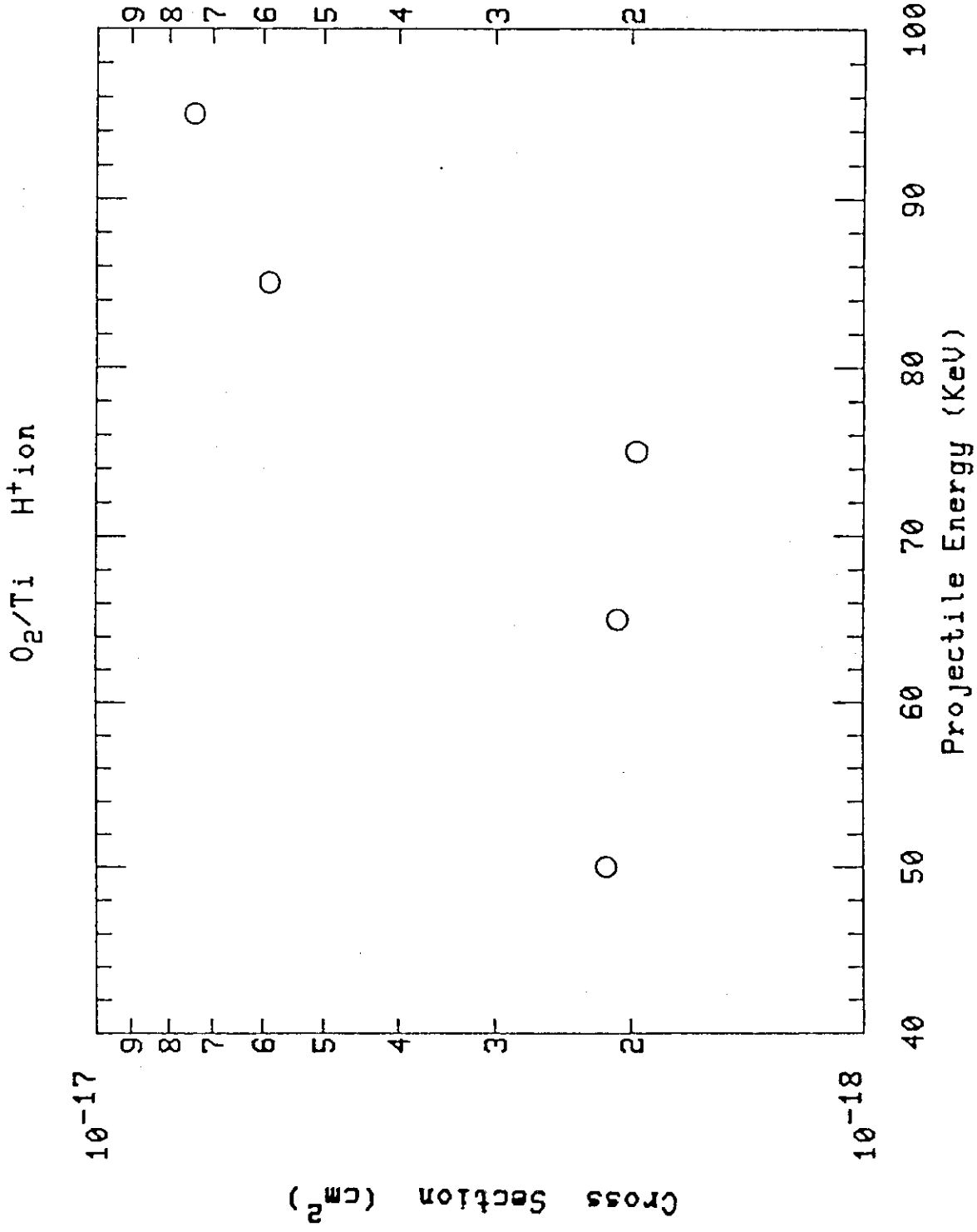

Fig.15 Desorption cross section as a function of incident energy

DATA LIST

Substrate	Incident ion species	Incident energy (eV)	Incident angle from normal (deg.)	Method	Desorption cross section (cm**2)	Ref.
Ti poly	H+	0.500E+05	60	AES	0.215E-17	81Le01
Ti poly	H+	0.650E+05	60	AES	0.208E-17	81Le01
Ti poly	H+	0.750E+05	60	AES	0.197E-17	81Le01
Ti poly	H+	0.850E+05	60	AES	0.588E-17	81Le01
Ti poly	H+	0.950E+05	60	AES	0.741E-17	81Le01

About one monolayer of oxygen was adsorbed at RT.
At energies above 80KeV per H+ ions, the cross section showed a sharp rise, indicating onset of some new inelastic desorption mechanism.
O-KLL Auger signal

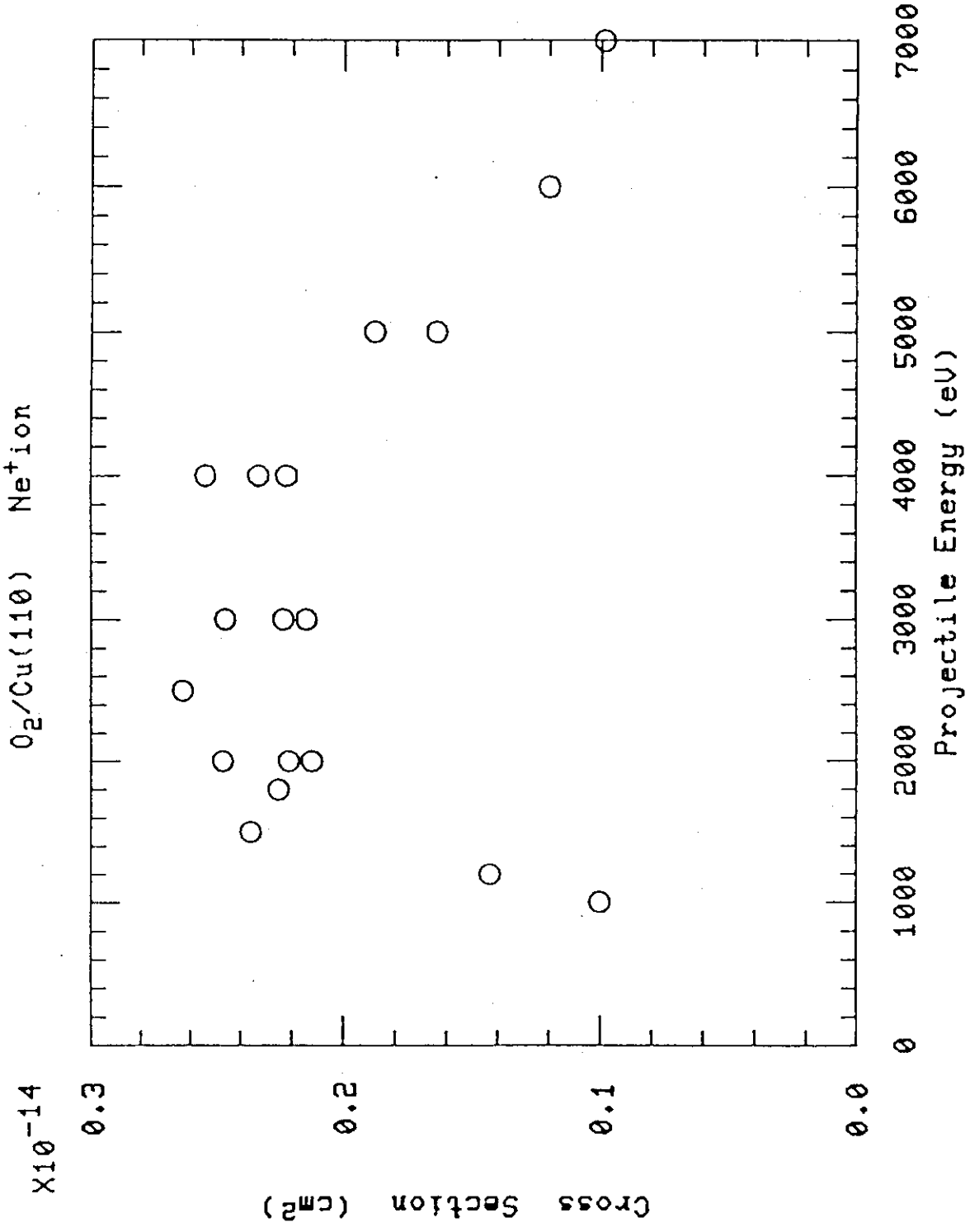

Fig.16 Desorption cross section as a function of incident energy

DATA LIST

Substrate	Incident ion species	Incident energy (eV)	Incident angle from normal (deg.)	Method	Desorption cross section (cm**2)	Ref.
Cu(110)	Ne+	0.100E+04	70	SIMS	0.100E-14	79De01
Cu(110)	Ne+	0.120E+04	70	SIMS	0.143E-14	79De01
Cu(110)	Ne+	0.150E+04	70	SIMS	0.236E-14	79De01
Cu(110)	Ne+	0.180E+04	70	SIMS	0.225E-14	79De01
Cu(110)	Ne+	0.200E+04	70	SIMS	0.212E-14	79De01
Cu(110)	Ne+	0.200E+04	70	SIMS	0.221E-14	79De01
Cu(110)	Ne+	0.200E+04	70	SIMS	0.247E-14	79De01
Cu(110)	Ne+	0.250E+04	70	SIMS	0.263E-14	79De01
Cu(110)	Ne+	0.300E+04	70	SIMS	0.214E-14	79De01
Cu(110)	Ne+	0.300E+04	70	SIMS	0.223E-14	79De01
Cu(110)	Ne+	0.300E+04	70	SIMS	0.246E-14	79De01
Cu(110)	Ne+	0.400E+04	70	SIMS	0.222E-14	79De01
Cu(110)	Ne+	0.400E+04	70	SIMS	0.233E-14	79De01
Cu(110)	Ne+	0.400E+04	70	SIMS	0.254E-14	79De01
Cu(110)	Ne+	0.500E+04	70	SIMS	0.164E-14	79De01
Cu(110)	Ne+	0.500E+04	70	SIMS	0.188E-14	79De01
Cu(110)	Ne+	0.600E+04	70	SIMS	0.120E-14	79De01
Cu(110)	Ne+	0.700E+04	70	SIMS	0.985E-15	79De01

Oxygen exposure 1000 L

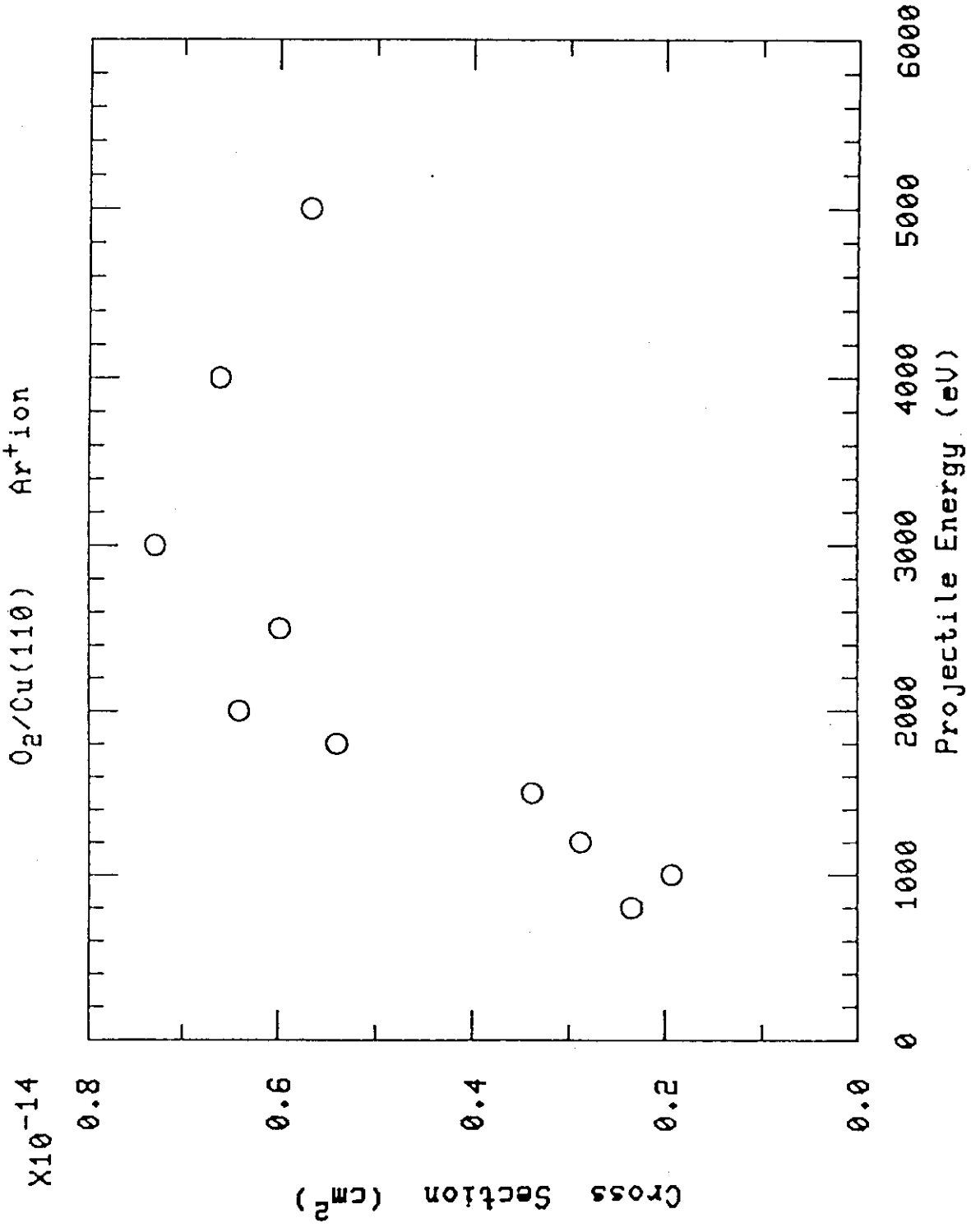

Fig.17 Desorption cross section as a function of incident energy

DATA LIST

Substrate	Incident ion species	Incident energy (eV)	Incident angle from normal (deg.)	Method	Desorption cross section (cm**2)	Ref.
Cu(110)	Ar+	0.800E+03	60	SIMS	0.235E-14	79De01
Cu(110)	Ar+	0.100E+04	60	SIMS	0.193E-14	79De01
Cu(110)	Ar+	0.120E+04	60	SIMS	0.288E-14	79De01
Cu(110)	Ar+	0.150E+04	60	SIMS	0.338E-14	79De01
Cu(110)	Ar+	0.180E+04	60	SIMS	0.539E-14	79De01
Cu(110)	Ar+	0.200E+04	60	SIMS	0.640E-14	79De01
Cu(110)	Ar+	0.250E+04	60	SIMS	0.598E-14	79De01
Cu(110)	Ar+	0.300E+04	60	SIMS	0.729E-14	79De01
Cu(110)	Ar+	0.400E+04	60	SIMS	0.661E-14	79De01
Cu(110)	Ar+	0.500E+04	60	SIMS	0.567E-14	79De01

Oxygen exposure 1000 L

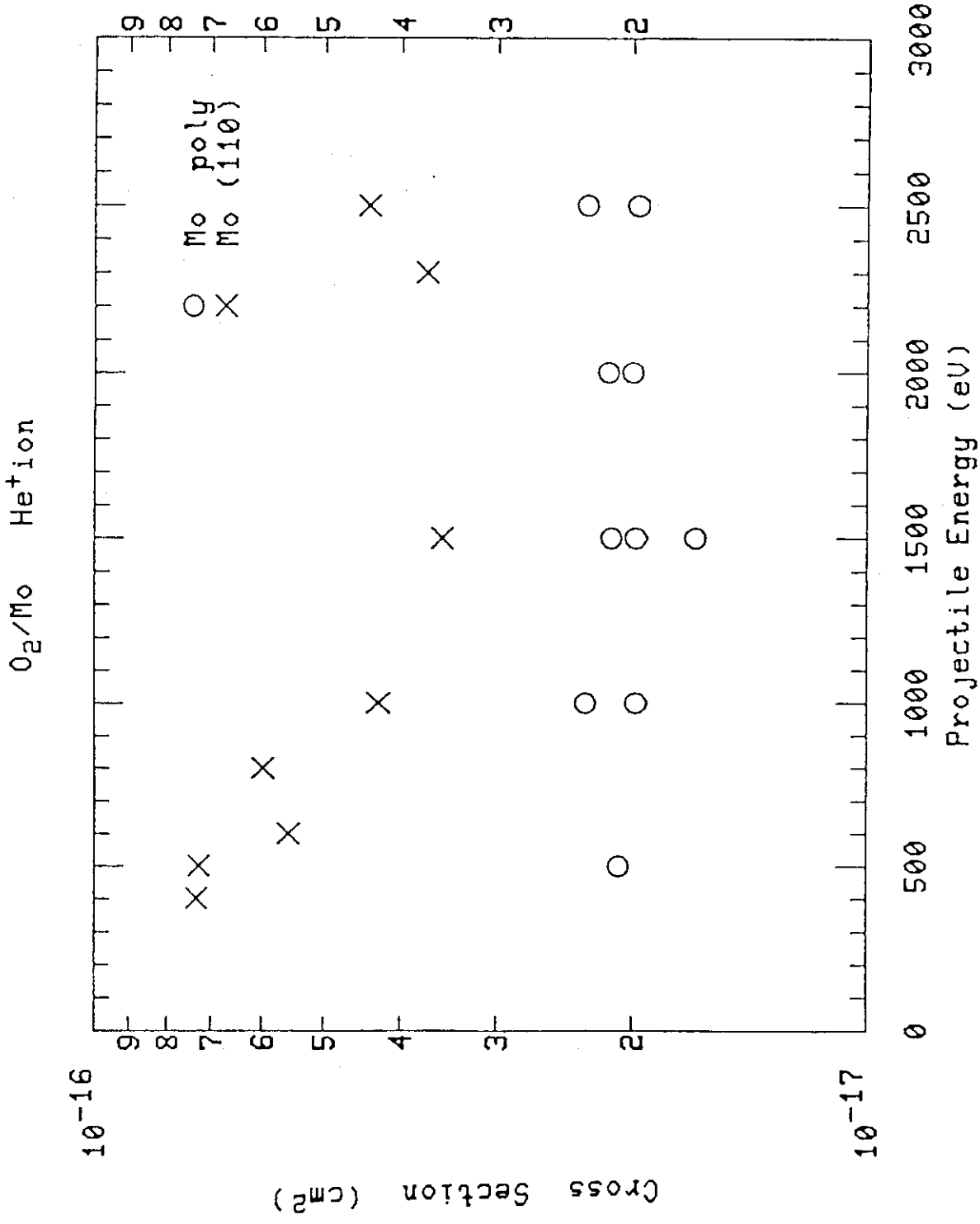

Fig.18 Desorption cross section as a function of incident energy

DATA LIST

Substrate	Incident ion species	Incident energy (eV)	Incident angle from normal (deg.)	Method	Desorption cross section (cm**2)	Ref.	Remark
Mo poly	He+	0.500E+03	45	ISS	0.208E-16	79Sa01	*1)
Mo poly	He+	0.100E+04	45	ISS	0.230E-16	79Sa01	*1)
Mo poly	He+	0.100E+04	45	ISS	0.198E-16	79Sa01	*1)
Mo poly	He+	0.150E+04	45	ISS	0.213E-16	79Sa01	*1)
Mo poly	He+	0.150E+04	45	ISS	0.198E-16	79Sa01	*1)
Mo poly	He+	0.150E+04	45	ISS	0.166E-16	79Sa01	*1)
Mo poly	He+	0.200E+04	45	ISS	0.215E-16	79Sa01	*1)
Mo poly	He+	0.200E+04	45	ISS	0.200E-16	79Sa01	*1)
Mo poly	He+	0.250E+04	45	ISS	0.229E-16	79Sa01	*1)
Mo poly	He+	0.250E+04	45	ISS	0.197E-16	79Sa01	*1)
Mo(110)	He+	0.400E+03	45	ISS	0.731E-16	81Sa03	*2)
Mo(110)	He+	0.500E+03	45	ISS	0.725E-16	81Sa03	*2)
Mo(110)	He+	0.600E+03	45	ISS	0.554E-16	81Sa03	*2)
Mo(110)	He+	0.800E+03	45	ISS	0.598E-16	81Sa03	*2)
Mo(110)	He+	0.100E+04	45	ISS	0.427E-16	81Sa03	*2)
Mo(110)	He+	0.150E+04	45	ISS	0.353E-16	81Sa03	*2)
Mo(110)	He+	0.230E+04	45	ISS	0.370E-16	81Sa03	*2)
Mo(110)	He+	0.250E+04	45	ISS	0.439E-16	81Sa03	*2)

*1) Cleaning processes of Mo sample were followed; 523K for 20 hours and pumped down to 3.0E-09 Pa ---> 623K for 4~5 hours at 1.0E-07 Pa ---> Ar+ ion bombardment ---> 723K for 1 hour

*2) 1300K ---> Ar+ and Ne+ ion bombardment

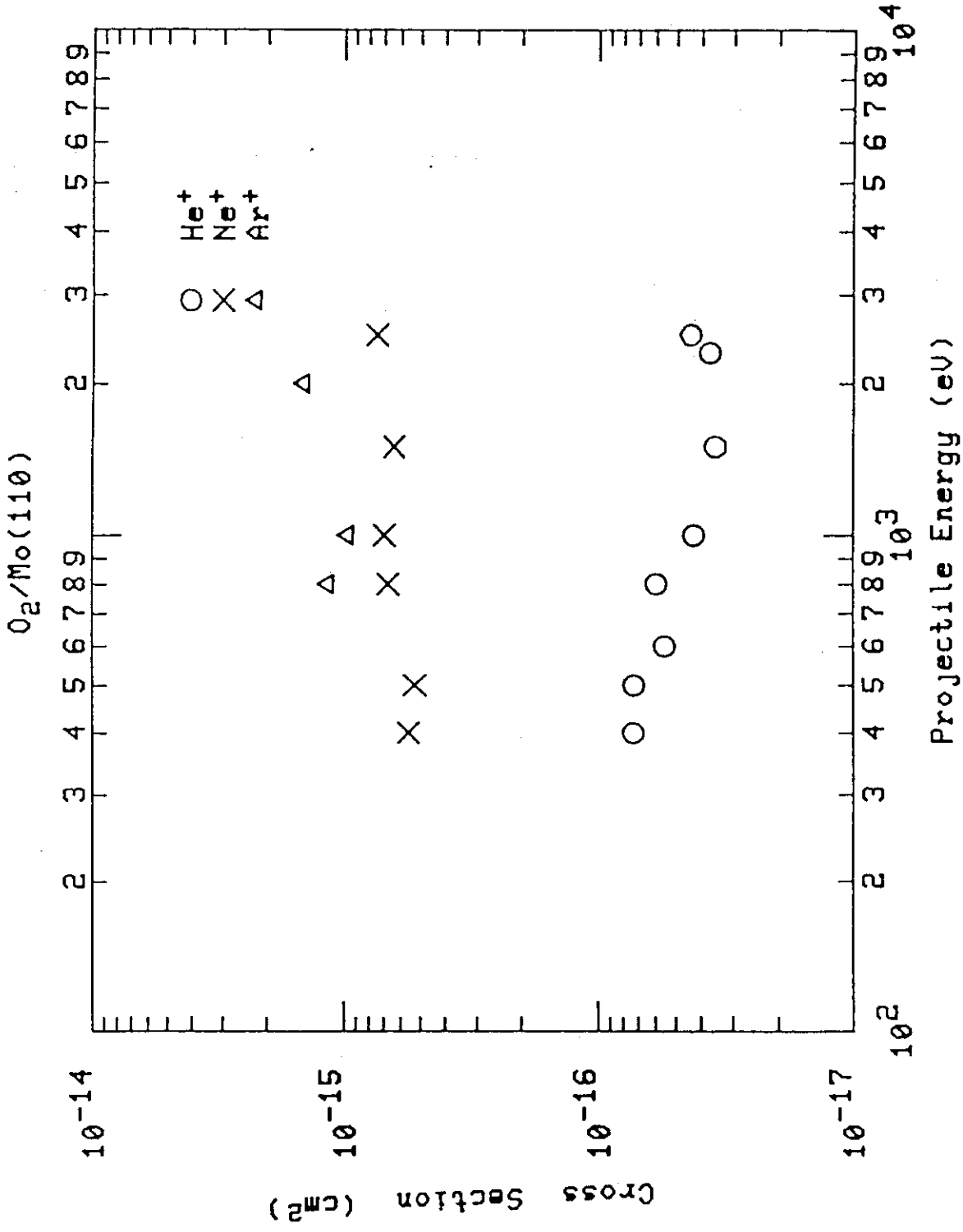

Fig.19 Desorption cross section as a function of incident energy

DATA LIST

Substrate	Incident ion species	Incident energy (eV)	Incident angle from normal (deg.)	Method	Desorption cross section (cm**2)	Ref.
Mo(110)	He+	0.400E+03	45	ISS	0.731E-16	81Sa03
Mo(110)	He+	0.500E+03	45	ISS	0.725E-16	81Sa03
Mo(110)	He+	0.600E+03	45	ISS	0.554E-16	81Sa03
Mo(110)	He+	0.800E+03	45	ISS	0.598E-16	81Sa03
Mo(110)	He+	0.100E+04	45	ISS	0.427E-16	81Sa03
Mo(110)	He+	0.150E+04	45	ISS	0.353E-16	81Sa03
Mo(110)	He+	0.230E+04	45	ISS	0.370E-16	81Sa03
Mo(110)	He+	0.250E+04	45	ISS	0.439E-16	81Sa03
Mo(110)	Ne+	0.400E+03	45	ISS	0.557E-15	81Sa03
Mo(110)	Ne+	0.500E+03	45	ISS	0.528E-15	81Sa03
Mo(110)	Ne+	0.800E+03	45	ISS	0.673E-15	81Sa03
Mo(110)	Ne+	0.100E+04	45	ISS	0.694E-15	81Sa03
Mo(110)	Ne+	0.150E+04	45	ISS	0.639E-15	81Sa03
Mo(110)	Ne+	0.250E+04	45	ISS	0.743E-15	81Sa03
Mo(110)	Ar+	0.800E+03	45	ISS	0.115E-14	81Sa03
Mo(110)	Ar+	0.100E+04	45	ISS	0.963E-15	81Sa03
Mo(110)	Ar+	0.200E+04	45	ISS	0.144E-14	81Sa03

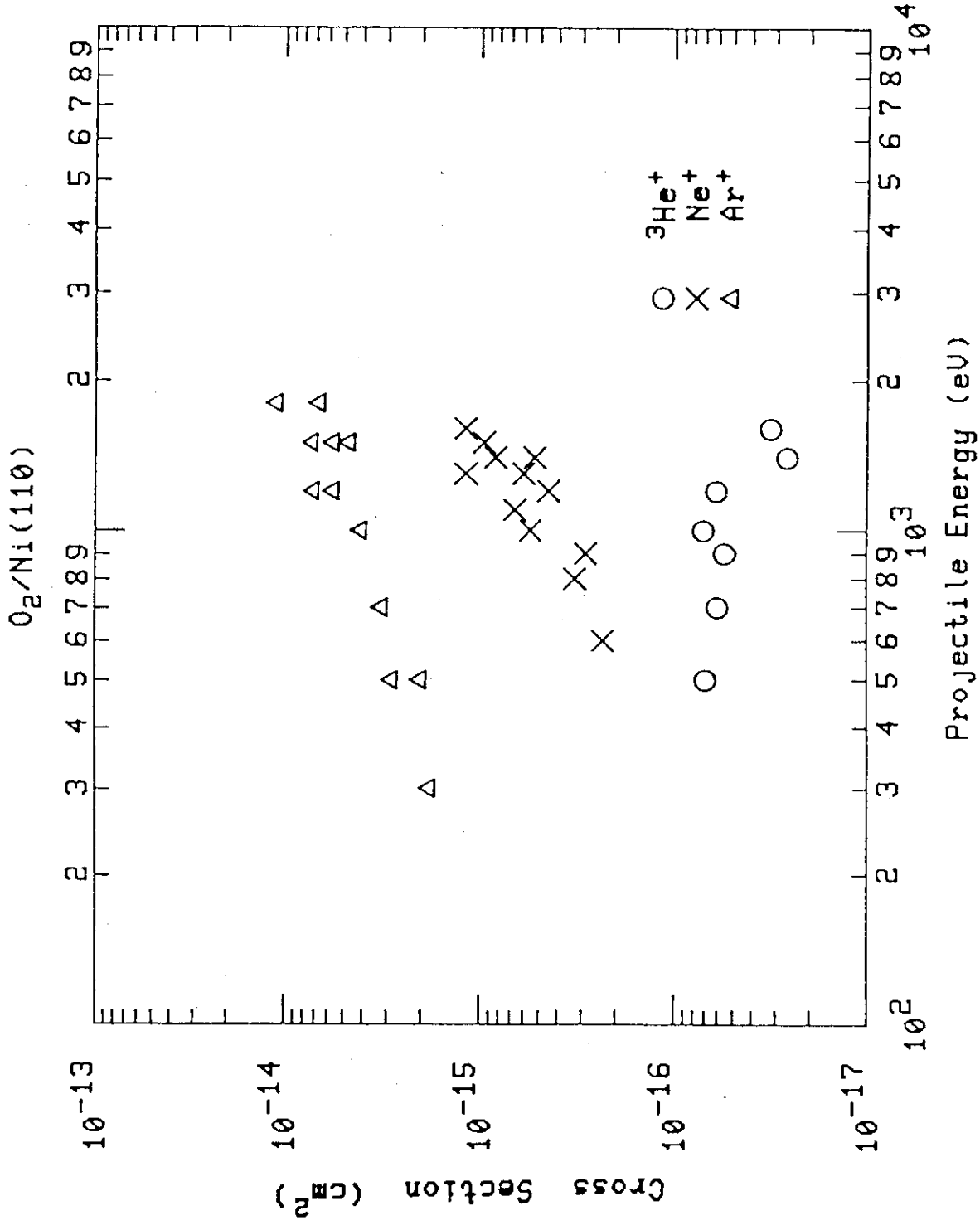

Fig.20 Desorption cross section as a function of incident energy

DATA LIST

Substrate	Incident ion species	Incident energy (eV)	Incident angle from normal (deg.)	Method	Desorption cross section (cm**2)	Ref.
Ni(110)	3He +	0.500E+03	30	ISS	0.690E-16	84Ta12
Ni(110)	3He +	0.700E+03	30	ISS	0.600E-16	84Ta12
Ni(110)	3He +	0.900E+03	30	ISS	0.551E-16	84Ta12
Ni(110)	3He +	0.100E+04	30	ISS	0.707E-16	84Ta12
Ni(110)	3He +	0.120E+04	30	ISS	0.606E-16	84Ta12
Ni(110)	3He +	0.140E+04	30	ISS	0.263E-16	84Ta12
Ni(110)	3He +	0.160E+04	30	ISS	0.320E-16	84Ta12
Ni(110)	Ne+	0.600E+03	30	ISS	0.233E-15	84Ta12
Ni(110)	Ne+	0.800E+03	30	ISS	0.324E-15	84Ta12
Ni(110)	Ne+	0.900E+03	30	ISS	0.285E-15	84Ta12
Ni(110)	Ne+	0.100E+04	30	ISS	0.555E-15	84Ta12
Ni(110)	Ne+	0.110E+04	30	ISS	0.663E-15	84Ta12
Ni(110)	Ne+	0.120E+04	30	ISS	0.443E-15	84Ta12
Ni(110)	Ne+	0.130E+04	30	ISS	0.593E-15	84Ta12
Ni(110)	Ne+	0.130E+04	30	ISS	0.119E-14	84Ta12
Ni(110)	Ne+	0.140E+04	30	ISS	0.523E-15	84Ta12
Ni(110)	Ne+	0.140E+04	30	ISS	0.827E-15	84Ta12
Ni(110)	Ne+	0.150E+04	30	ISS	0.949E-15	84Ta12
Ni(110)	Ne+	0.160E+04	30	ISS	0.118E-14	84Ta12
Ni(110)	Ar+	0.300E+03	30	ISS	0.181E-14	84Ta12
Ni(110)	Ar+	0.500E+03	30	ISS	0.281E-14	84Ta12
Ni(110)	Ar+	0.500E+03	30	ISS	0.201E-14	84Ta12
Ni(110)	Ar+	0.700E+03	30	ISS	0.318E-14	84Ta12
Ni(110)	Ar+	0.100E+04	30	ISS	0.408E-14	84Ta12
Ni(110)	Ar+	0.120E+04	30	ISS	0.714E-14	84Ta12
Ni(110)	Ar+	0.120E+04	30	ISS	0.563E-14	84Ta12
Ni(110)	Ar+	0.150E+04	30	ISS	0.723E-14	84Ta12
Ni(110)	Ar+	0.150E+04	30	ISS	0.562E-14	84Ta12
Ni(110)	Ar+	0.150E+04	30	ISS	0.468E-14	84Ta12
Ni(110)	Ar+	0.180E+04	30	ISS	0.110E-13	84Ta12
Ni(110)	Ar+	0.180E+04	30	ISS	0.664E-14	84Ta12

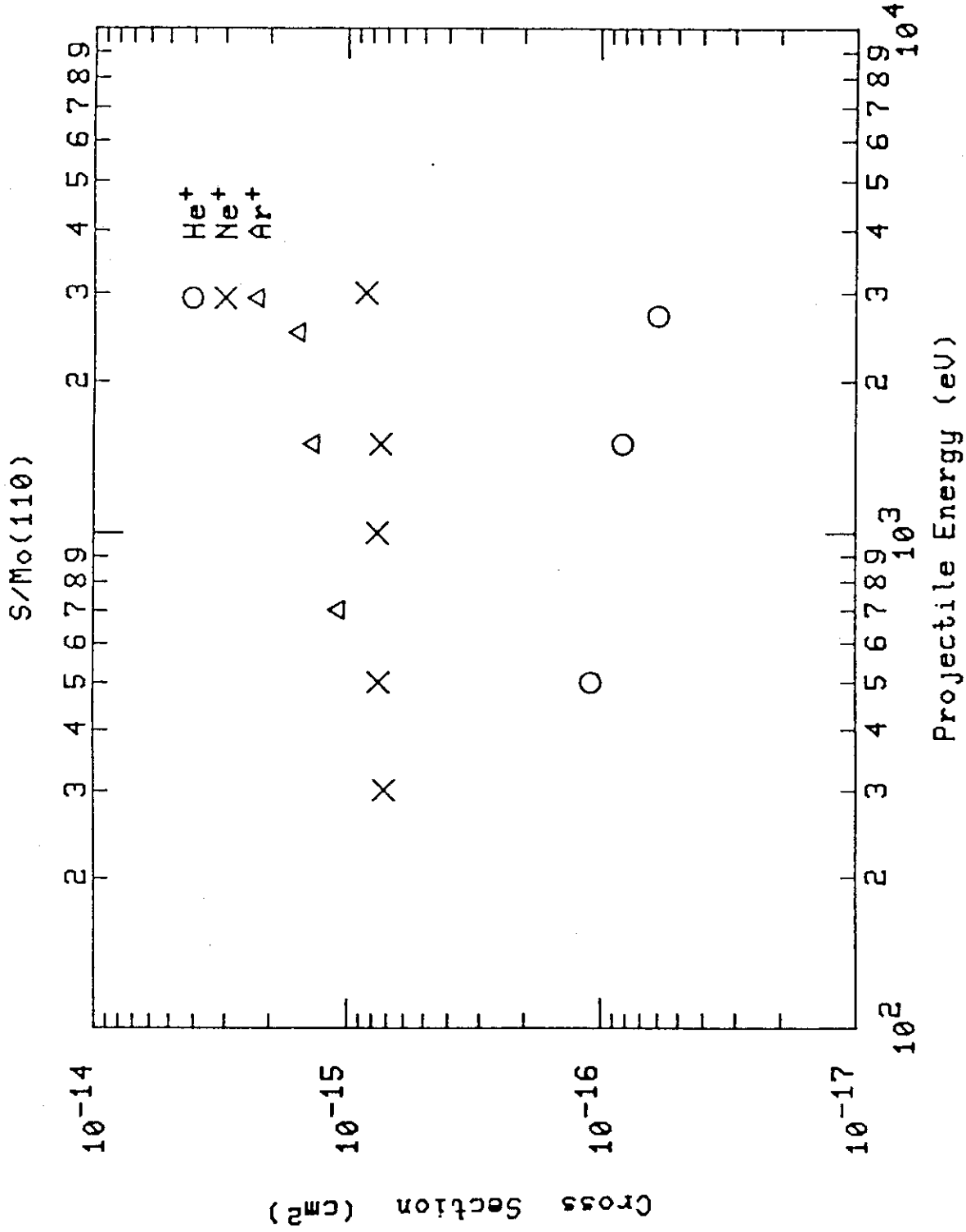

Fig.21 Desorption cross section as a function of incident energy

DATA LIST

Substrate	Incident ion species	Incident energy (eV)	Incident angle from normal (deg.)	Method	Desorption cross section (cm**2)	Ref.
Mo(110)	He+	0.500E+03	45	ISS	0.109E-15	81Sa03
Mo(110)	He+	0.150E+04	45	ISS	0.810E-16	81Sa03
Mo(110)	He+	0.270E+04	45	ISS	0.594E-16	81Sa03
Mo(110)	Ne+	0.300E+03	45	ISS	0.713E-15	81Sa03
Mo(110)	Ne+	0.500E+03	45	ISS	0.752E-15	81Sa03
Mo(110)	Ne+	0.100E+04	45	ISS	0.758E-15	81Sa03
Mo(110)	Ne+	0.150E+04	45	ISS	0.735E-15	81Sa03
Mo(110)	Ne+	0.300E+04	45	ISS	0.845E-15	81Sa03
Mo(110)	Ar+	0.700E+03	45	ISS	0.107E-14	81Sa03
Mo(110)	Ar+	0.150E+04	45	ISS	0.134E-14	81Sa03
Mo(110)	Ar+	0.250E+04	45	ISS	0.154E-14	81Sa03

S atoms were supplied to the surface from the bulk by the surface segregation when the Mo samples were heated up to 1300K for a few minutes.

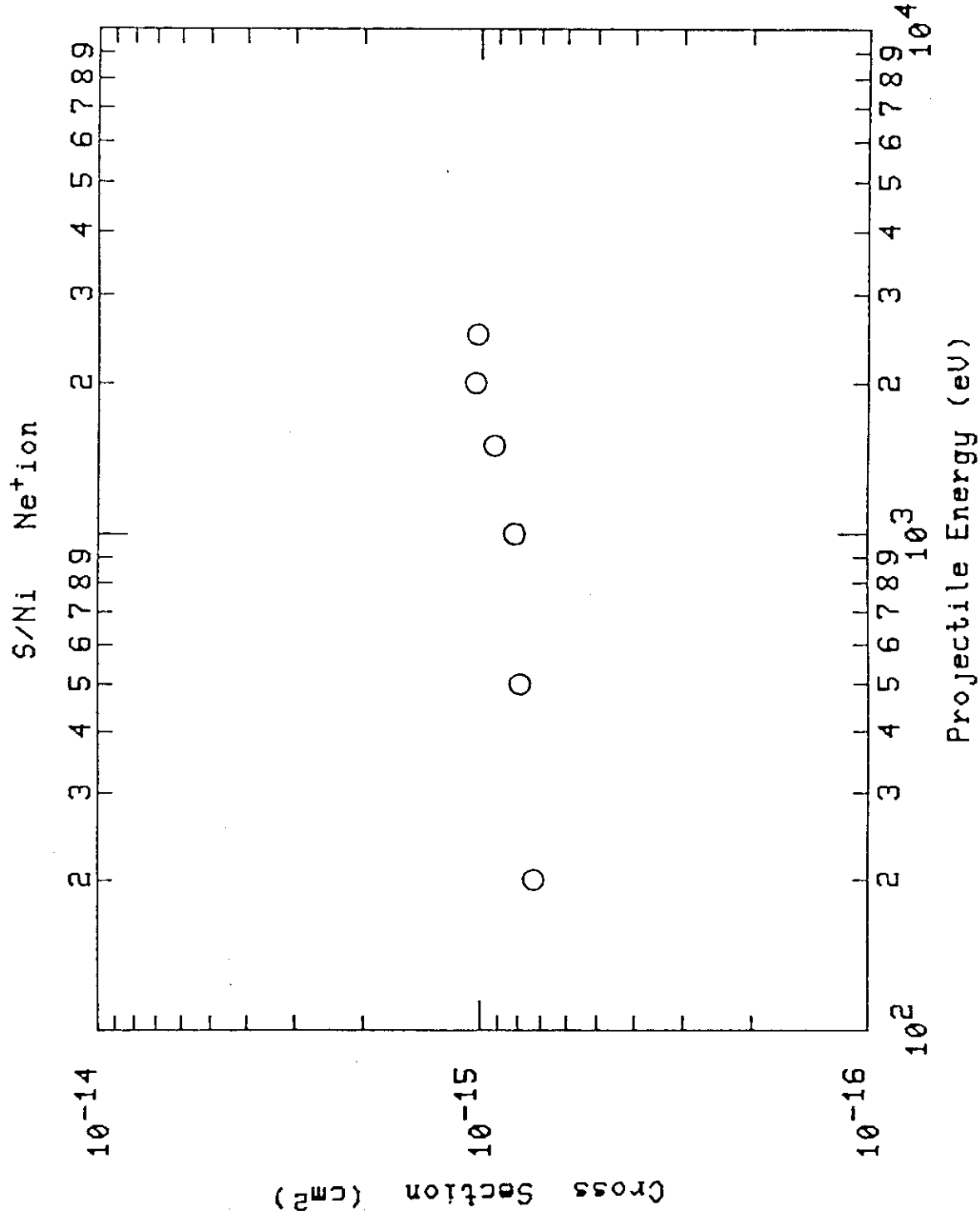

Fig.22 Desorption cross section as a function of incident energy

DATA LIST

Substrate	Incident ion species	Incident energy (eV)	Incident angle from normal (deg.)	Method	Desorption cross section (cm**2)	Ref.
Ni poly	Ne+	0.200E+03	45	ISS	0.727E-15	81Sa03
Ni poly	Ne+	0.500E+03	45	ISS	0.791E-15	81Sa03
Ni poly	Ne+	0.100E+04	45	ISS	0.819E-15	81Sa03
Ni poly	Ne+	0.150E+04	45	ISS	0.920E-15	81Sa03
Ni poly	Ne+	0.200E+04	45	ISS	0.103E-14	81Sa03
Ni poly	Ne+	0.250E+04	45	ISS	0.102E-14	81Sa03

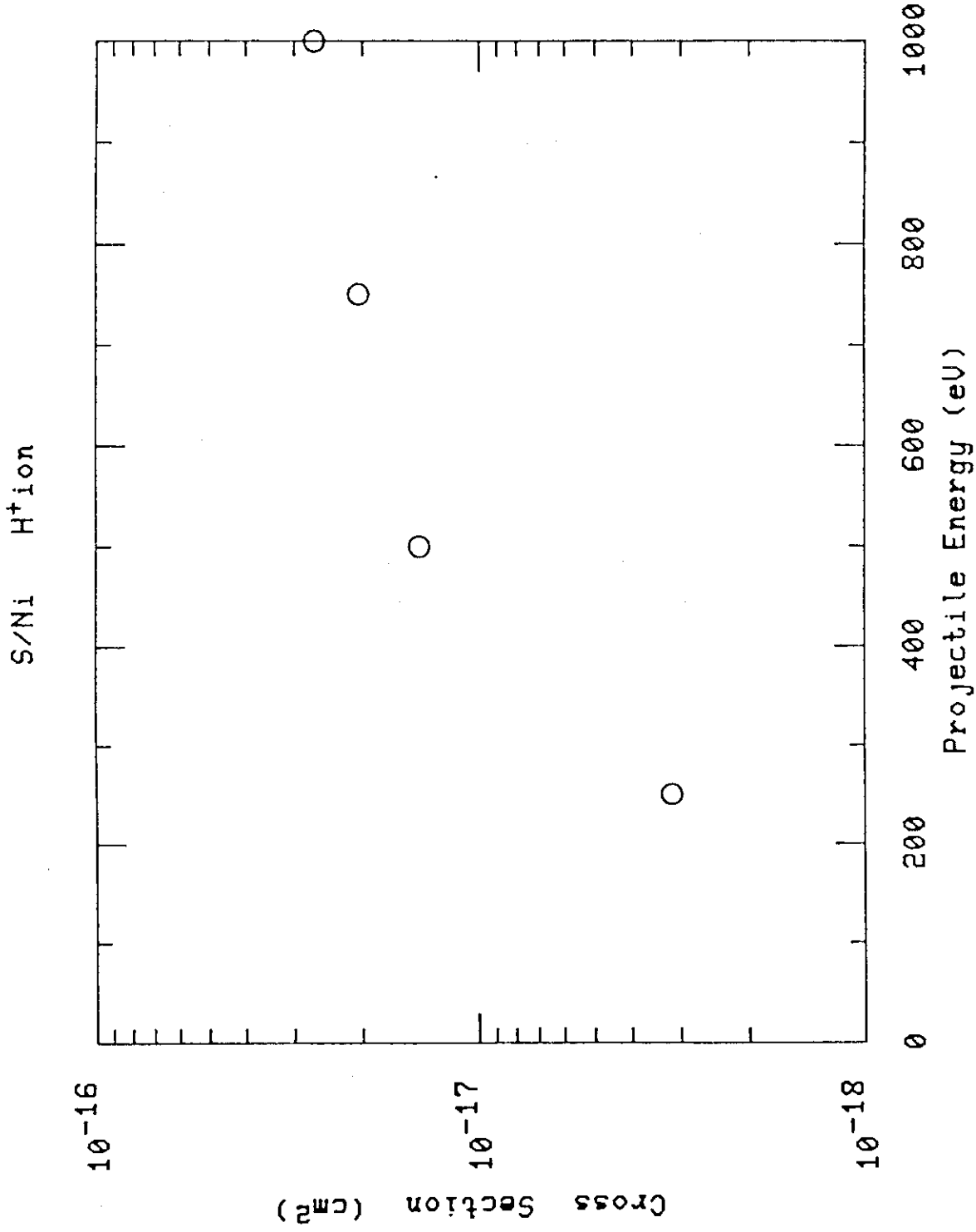

Fig.23 Desorption cross section as a function of incident energy

DATA LIST

Substrate	Incident ion species	Incident energy (eV)	Incident angle from normal (deg.)	Method	Desorption cross section (cm**2)	Ref.
Ni	H+	0.250E+03	30	AES	0.316E-17	78Wi03
Ni	H+	0.500E+03	30	AES	0.142E-16	78Wi03
Ni	H+	0.750E+03	30	AES	0.204E-16	78Wi03
Ni	H+	0.100E+04	30	AES	0.266E-16	78Wi03

Desorption measurements were carried out with sulfur coverages always greater than half a monolayer.
Auger peak S-L23MM

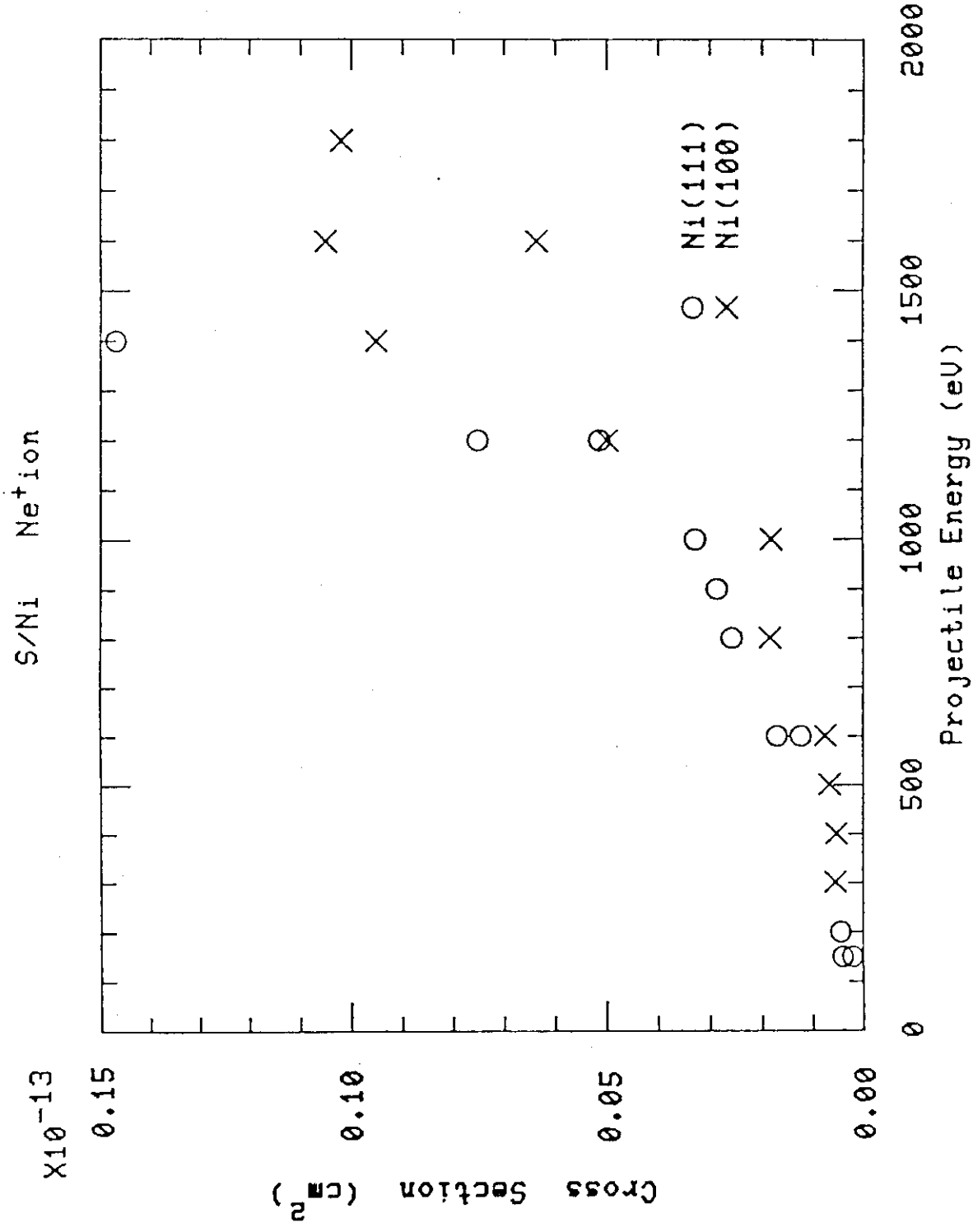

Fig.24 Desorption cross section as a function of incident energy

DATA LIST

Substrate	Incident ion species	Incident energy (eV)	Incident angle from normal (deg.)	Method	Desorption cross section (cm**2)	Ref.
Ni(111)	Ne+	0.150E+03	60	ISS	0.207E-15	76Ta02
Ni(111)	Ne+	0.150E+03	60	ISS	0.406E-15	76Ta02
Ni(111)	Ne+	0.200E+03	60	ISS	0.451E-15	76Ta02
Ni(111)	Ne+	0.600E+03	60	ISS	0.123E-14	76Ta02
Ni(111)	Ne+	0.600E+03	60	ISS	0.170E-14	76Ta02
Ni(111)	Ne+	0.800E+03	60	ISS	0.258E-14	76Ta02
Ni(111)	Ne+	0.900E+03	60	ISS	0.286E-14	76Ta02
Ni(111)	Ne+	0.100E+04	60	ISS	0.328E-14	76Ta02
Ni(111)	Ne+	0.120E+04	60	ISS	0.513E-14	76Ta02
Ni(111)	Ne+	0.120E+04	60	ISS	0.751E-14	76Ta02
Ni(111)	Ne+	0.140E+04	60	ISS	0.147E-13	76Ta02
Ni(100)	Ne+	0.300E+03	60	ISS	0.548E-15	76Ta02
Ni(100)	Ne+	0.400E+03	60	ISS	0.530E-15	76Ta02
Ni(100)	Ne+	0.500E+03	60	ISS	0.666E-15	76Ta02
Ni(100)	Ne+	0.600E+03	60	ISS	0.753E-15	76Ta02
Ni(100)	Ne+	0.800E+03	60	ISS	0.184E-14	76Ta02
Ni(100)	Ne+	0.100E+04	60	ISS	0.181E-14	76Ta02
Ni(100)	Ne+	0.120E+04	60	ISS	0.498E-14	76Ta02
Ni(100)	Ne+	0.140E+04	60	ISS	0.951E-14	76Ta02
Ni(100)	Ne+	0.160E+04	60	ISS	0.636E-14	76Ta02
Ni(100)	Ne+	0.160E+04	60	ISS	0.105E-13	76Ta02
Ni(100)	Ne+	0.180E+04	60	ISS	0.102E-13	76Ta02

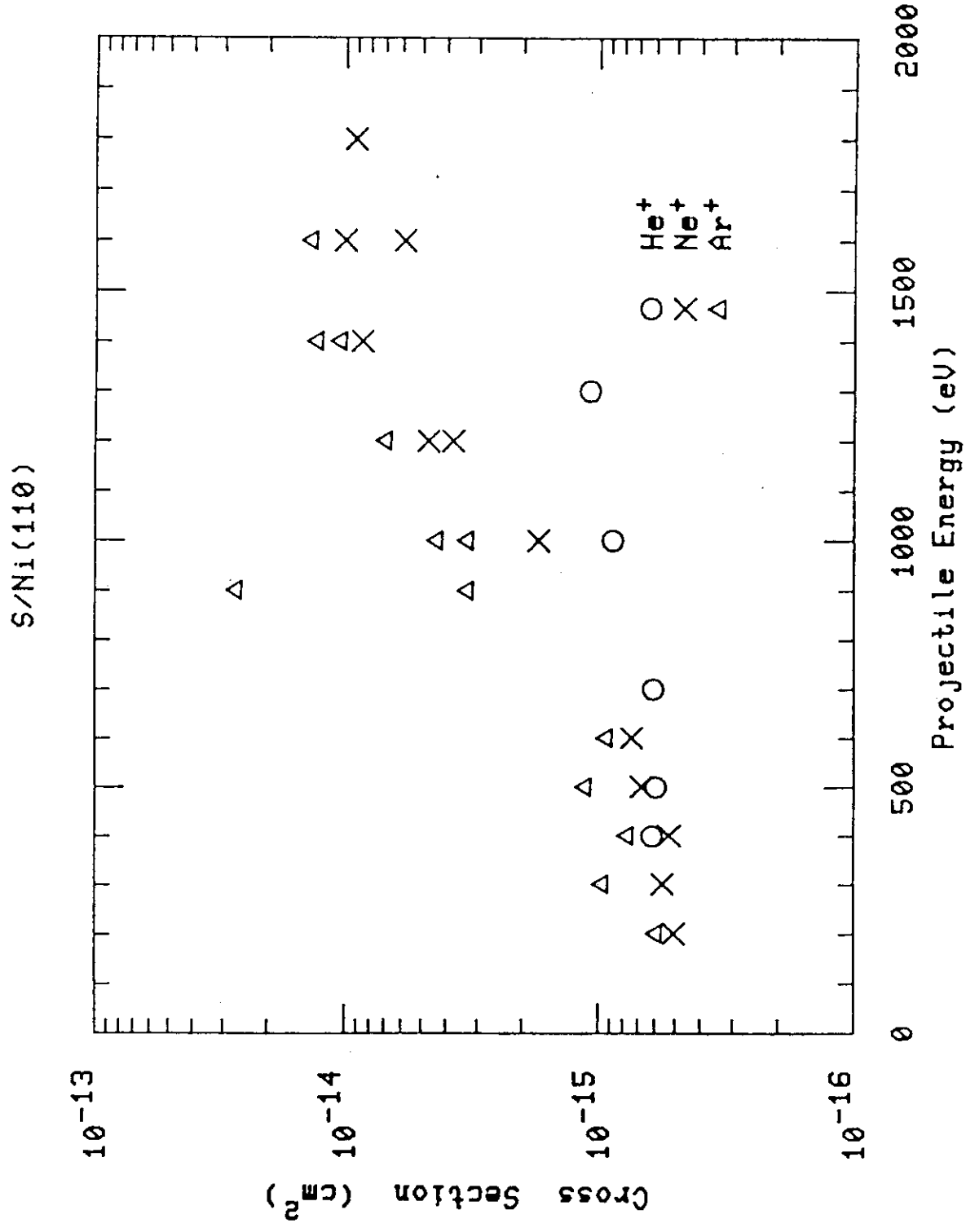

Fig.25 Desorption cross section as a function of incident energy

DATA LIST

Substrate	Incident ion species	Incident energy (eV)	Incident angle from normal (deg.)	Method	Desorption cross section (cm**2)	Ref.
Ni(110)	He+	0.400E+03	60	ISS	0.614E-15	76Ta02
Ni(110)	He+	0.500E+03	60	ISS	0.594E-15	76Ta02
Ni(110)	He+	0.700E+03	60	ISS	0.606E-15	76Ta02
Ni(110)	He+	0.100E+04	60	ISS	0.875E-15	76Ta02
Ni(110)	He+	0.130E+04	60	ISS	0.108E-14	76Ta02
Ni(110)	Ne+	0.200E+03	60	ISS	0.503E-15	76Ta02
Ni(110)	Ne+	0.300E+03	60	ISS	0.558E-15	76Ta02
Ni(110)	Ne+	0.400E+03	60	ISS	0.530E-15	76Ta02
Ni(110)	Ne+	0.500E+03	60	ISS	0.675E-15	76Ta02
Ni(110)	Ne+	0.600E+03	60	ISS	0.736E-15	76Ta02
Ni(110)	Ne+	0.100E+04	60	ISS	0.172E-14	76Ta02
Ni(110)	Ne+	0.120E+04	60	ISS	0.468E-14	76Ta02
Ni(110)	Ne+	0.120E+04	60	ISS	0.374E-14	76Ta02
Ni(110)	Ne+	0.140E+04	60	ISS	0.856E-14	76Ta02
Ni(110)	Ne+	0.160E+04	60	ISS	0.584E-14	76Ta02
Ni(110)	Ne+	0.160E+04	60	ISS	0.998E-14	76Ta02
Ni(110)	Ne+	0.180E+04	60	ISS	0.914E-14	76Ta02
Ni(110)	Ar+	0.200E+03	60	ISS	0.588E-15	76Ta02
Ni(110)	Ar+	0.300E+03	60	ISS	0.956E-15	76Ta02
Ni(110)	Ar+	0.400E+03	60	ISS	0.763E-15	76Ta02
Ni(110)	Ar+	0.500E+03	60	ISS	0.112E-14	76Ta02
Ni(110)	Ar+	0.600E+03	60	ISS	0.924E-15	76Ta02
Ni(110)	Ar+	0.900E+03	60	ISS	0.327E-14	76Ta02
Ni(110)	Ar+	0.900E+03	60	ISS	0.265E-13	76Ta02
Ni(110)	Ar+	0.100E+04	60	ISS	0.432E-14	76Ta02
Ni(110)	Ar+	0.100E+04	60	ISS	0.327E-14	76Ta02
Ni(110)	Ar+	0.120E+04	60	ISS	0.689E-14	76Ta02
Ni(110)	Ar+	0.140E+04	60	ISS	0.128E-13	76Ta02
Ni(110)	Ar+	0.140E+04	60	ISS	0.104E-13	76Ta02
Ni(110)	Ar+	0.160E+04	60	ISS	0.135E-13	76Ta02

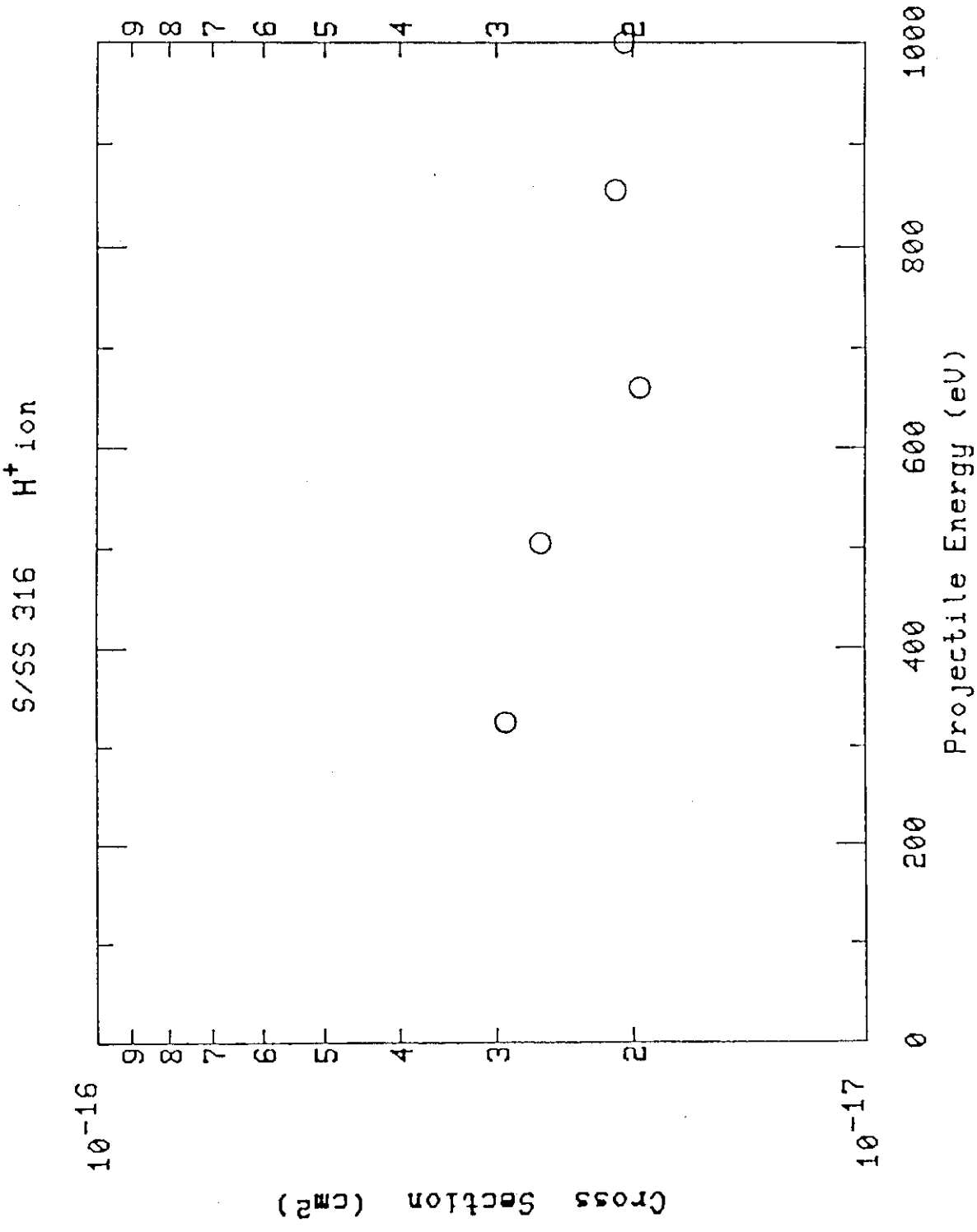

Fig.26 Desorption cross section as a function of incident energy

DATA LIST

Substrate	Incident ion species	Incident energy (eV)	Incident angle from normal (deg.)	Method	Desorption cross section (cm**2)	Ref.
SS 316	H+	0.325E+03	45	SIMS	0.292E-16	80Ba02
SS 316	H+	0.505E+03	45	SIMS	0.263E-16	80Ba02
SS 316	H+	0.660E+03	45	SIMS	0.196E-16	80Ba02
SS 316	H+	0.855E+03	45	SIMS	0.210E-16	80Ba02
SS 316	H+	0.100E+04	45	SIMS	0.205E-16	80Ba02

A sample was heated in vacuum (~1.0E-06 Pa) to 800K for 1.0E+03 sec to promote segregation of balk impurities (S atom, etc) to the sample surfaces.
Desorbed species S- ion
SS 316 : Stainless steel 316

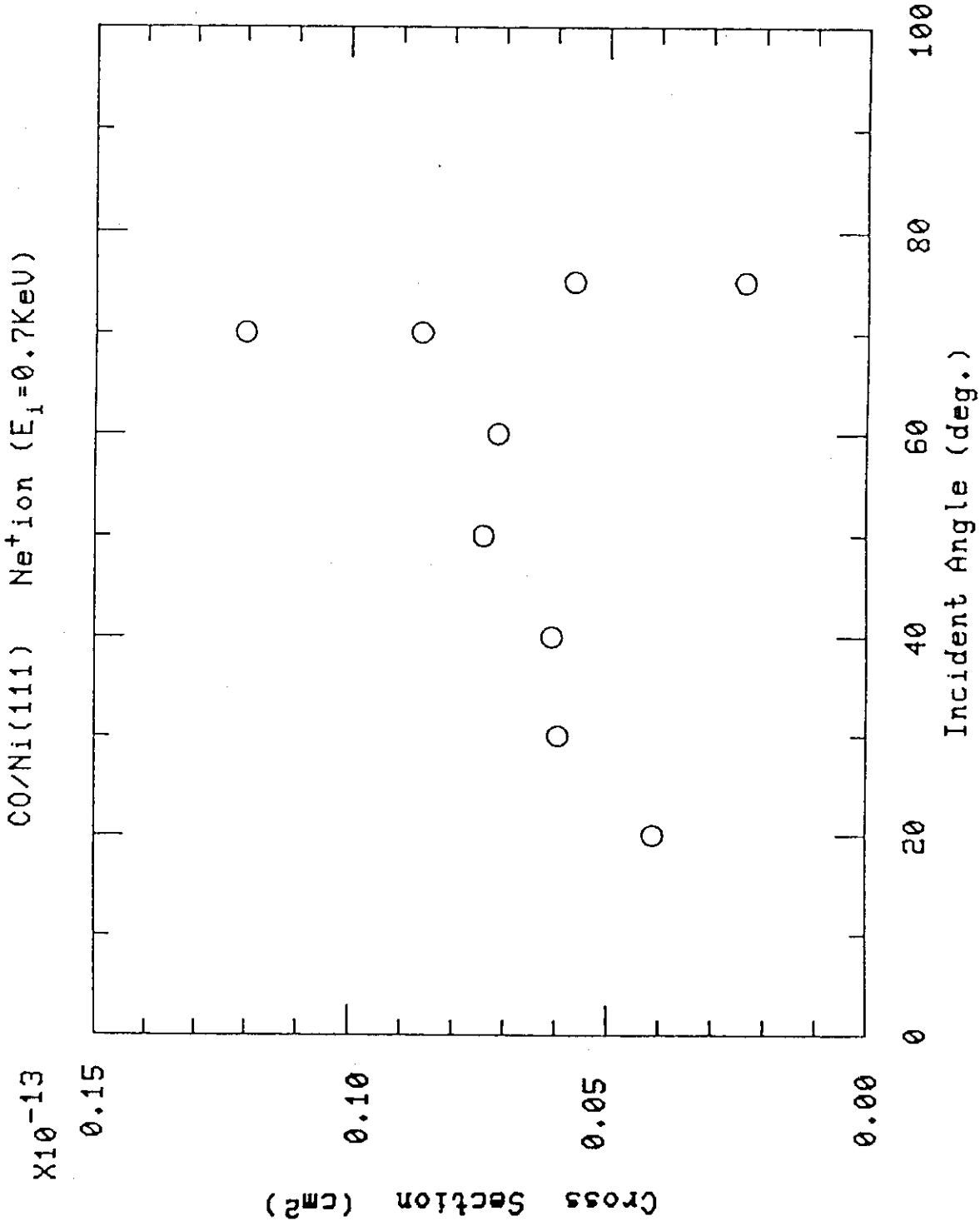

Fig.27 Desorption cross section as a function of incident angle

DATA LIST

Substrate	Incident ion species	Incident energy (eV)	Incident angle from normal (deg.)	Method	Desorption cross section (cm**2)	Ref.
Ni(111)	Ne+	0.700E+03	20	ISS	0.411E-14	78Ta06
Ni(111)	Ne+	0.700E+03	30	ISS	0.594E-14	78Ta06
Ni(111)	Ne+	0.700E+03	40	ISS	0.606E-14	78Ta06
Ni(111)	Ne+	0.700E+03	50	ISS	0.738E-14	78Ta06
Ni(111)	Ne+	0.700E+03	60	ISS	0.711E-14	78Ta06
Ni(111)	Ne+	0.700E+03	70	ISS	0.120E-13	78Ta06
Ni(111)	Ne+	0.700E+03	70	ISS	0.860E-14	78Ta06
Ni(111)	Ne+	0.700E+03	75	ISS	0.565E-14	78Ta06
Ni(111)	Ne+	0.700E+03	75	ISS	0.238E-14	78Ta06

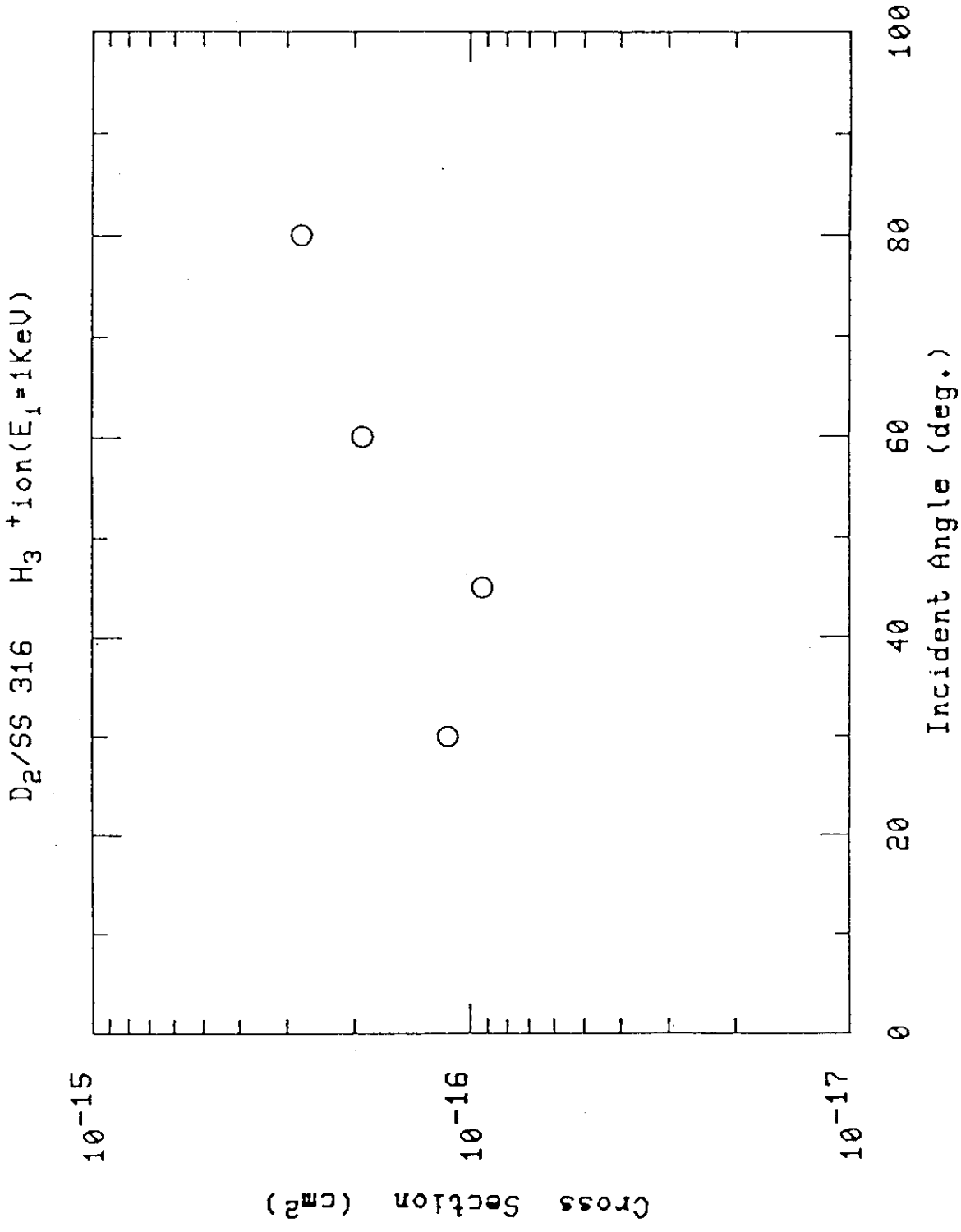

Fig.28 Desorption cross section as a function of incident angle

DATA LIST

Substrate	Incident ion species	Incident energy (eV)	Incident angle from normal (deg.)	Method	Desorption cross section (cm**2)	Ref.
SS 316	H3 +	0.100E+04	30	SIMS	0.114E-15	81Ba03
SS 316	H3 +	0.100E+04	45	SIMS	0.925E-16	81Ba03
SS 316	H3 +	0.100E+04	60	SIMS	0.190E-15	81Ba03
SS 316	H3 +	0.100E+04	80	SIMS	0.275E-15	81Ba03

Desorbed species D- ion,
D2 exposure 3000 L
SS 316 : Stainless steel 316

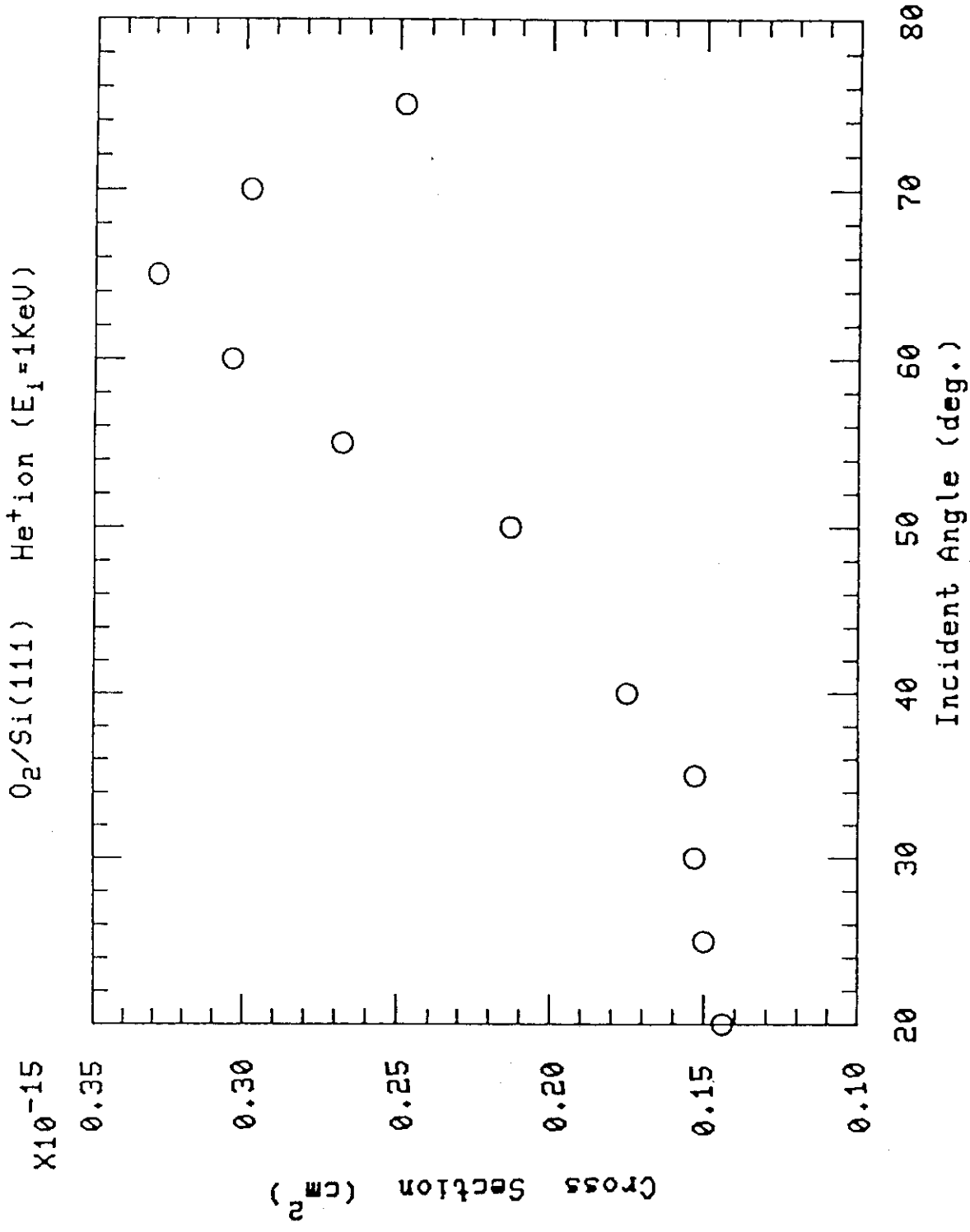

Fig.29 Desorption cross section as a function of incident angle

DATA LIST

Substrate	Incident ion species	Incident energy (eV)	Incident angle from normal (deg.)	Method	Desorption cross section (cm**2)	Ref.
Si(111)	He+	0.100E+04	20	ISS	0.144E-15	80On01
Si(111)	He+	0.100E+04	25	ISS	0.150E-15	80On01
Si(111)	He+	0.100E+04	30	ISS	0.153E-15	80On01
Si(111)	He+	0.100E+04	35	ISS	0.153E-15	80On01
Si(111)	He+	0.100E+04	40	ISS	0.175E-15	80On01
Si(111)	He+	0.100E+04	50	ISS	0.213E-15	80On01
Si(111)	He+	0.100E+04	55	ISS	0.268E-15	80On01
Si(111)	He+	0.100E+04	60	ISS	0.304E-15	80On01
Si(111)	He+	0.100E+04	65	ISS	0.329E-15	80On01
Si(111)	He+	0.100E+04	70	ISS	0.298E-15	80On01
Si(111)	He+	0.100E+04	75	ISS	0.248E-15	80On01

The desorption measurements were carried out by monitoring the oxygen peak in the He+ scattering spectrum as a function of time.

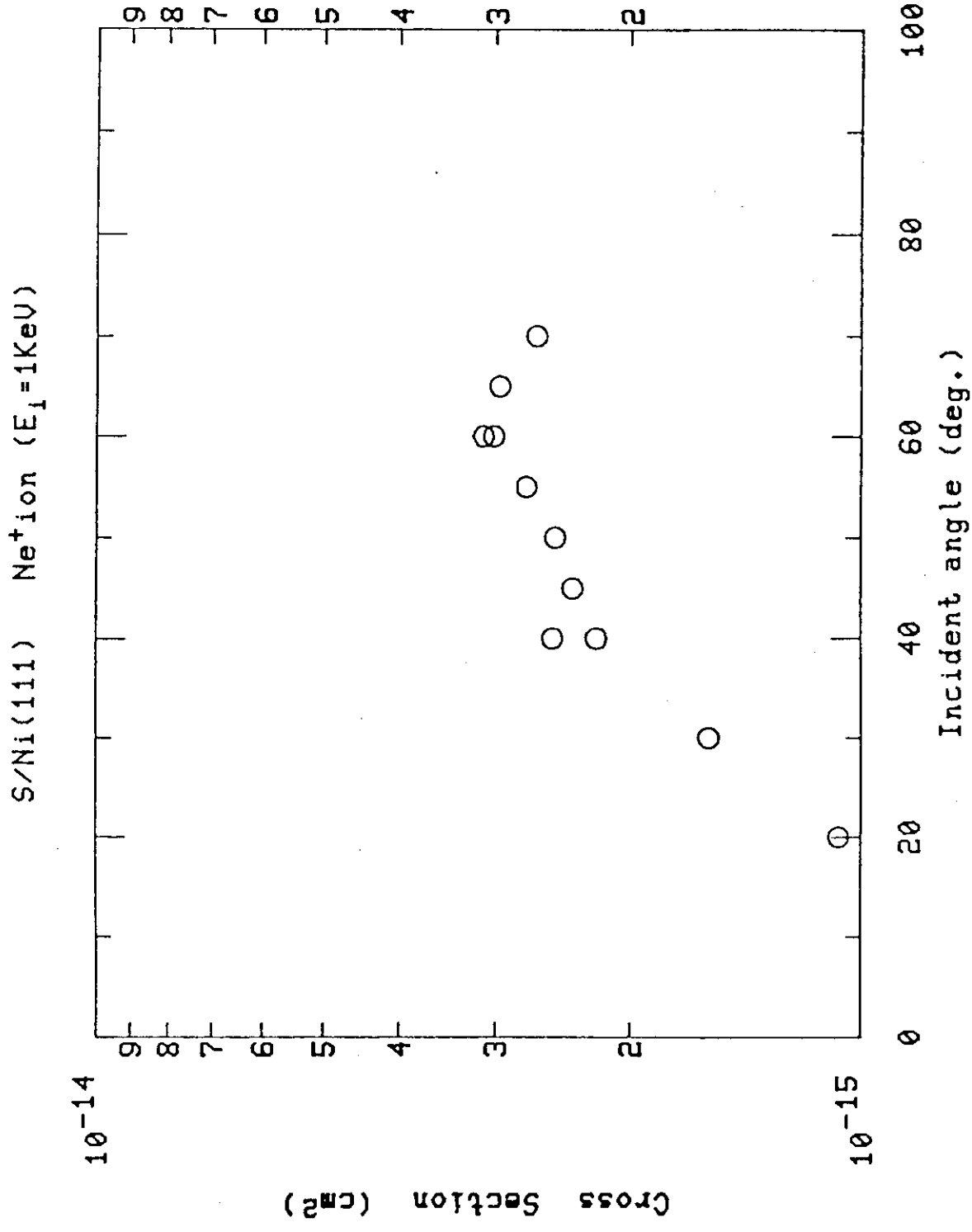

Fig.30 Desorption cross section as a function of incident angle

DATA LIST

Substrate	Incident ion species	Incident energy (eV)	Incident angle from normal (deg.)	Method	Desorption cross section (cm**2)	Ref.
Ni(111)	Ne+	0.100E+04	20	ISS	0.107E-14	76Ta02
Ni(111)	Ne+	0.100E+04	30	ISS	0.158E-14	76Ta02
Ni(111)	Ne+	0.100E+04	40	ISS	0.221E-14	76Ta02
Ni(111)	Ne+	0.100E+04	40	ISS	0.252E-14	76Ta02
Ni(111)	Ne+	0.100E+04	45	ISS	0.237E-14	76Ta02
Ni(111)	Ne+	0.100E+04	50	ISS	0.250E-14	76Ta02
Ni(111)	Ne+	0.100E+04	55	ISS	0.273E-14	76Ta02
Ni(111)	Ne+	0.100E+04	60	ISS	0.301E-14	76Ta02
Ni(111)	Ne+	0.100E+04	60	ISS	0.311E-14	76Ta02
Ni(111)	Ne+	0.100E+04	65	ISS	0.296E-14	76Ta02
Ni(111)	Ne+	0.100E+04	70	ISS	0.265E-14	76Ta02

Surface coverage of sulfur atoms was below 1 monolayer.

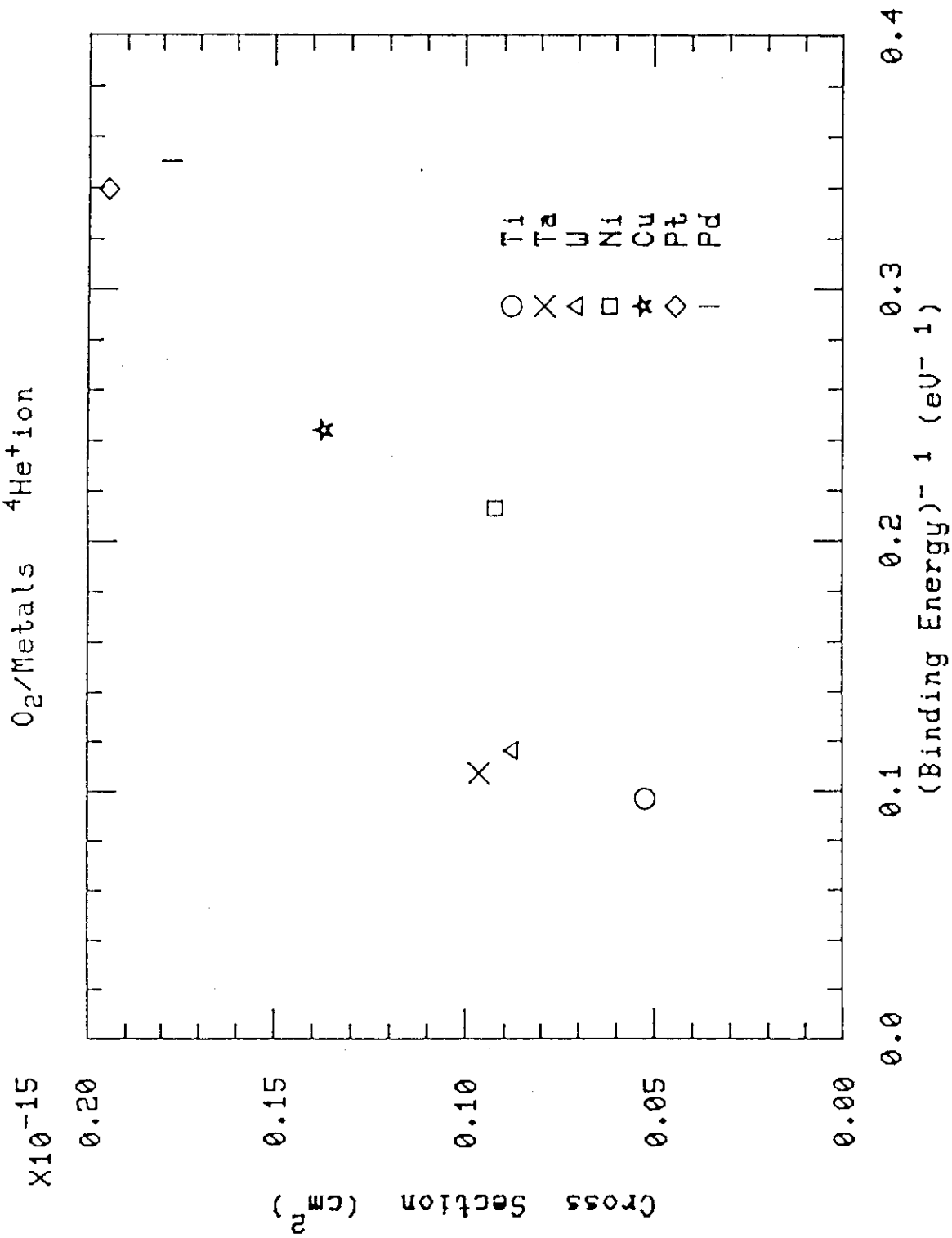

Fig.31 Desorption cross section as a function of surface binding energy

DATA LIST

Substrate	Incident ion species	Incident energy (eV)	Incident angle from normal (deg.)	Method	Desorption cross section (cm**2)	Ref.	Remark
Ti	4He+	0.500E+03	30	ISS	0.523E-16	84Ta12	*1)
Ta	4He+	0.500E+03	30	ISS	0.962E-16	84Ta12	*2)
W	4He+	0.500E+03	30	ISS	0.873E-16	84Ta12	*3)
Ni	4He+	0.500E+03	30	ISS	0.921E-16	84Ta12	*4)
Cu	4He+	0.500E+03	30	ISS	0.137E-15	84Ta12	*5)
Pt	4He+	0.500E+03	30	ISS	0.195E-15	84Ta12	*6)
Pd	4He+	0.500E+03	30	ISS	0.178E-15	84Ta12	*7)

Oxygen is known to adsorb dissociatively on most metals.
*1) Surface binding energy 10.3eV
*2) Surface binding energy 9.3eV
*3) Surface binding energy 8.6eV
*4) Surface binding energy 4.7eV
*5) Surface binding energy 4.1eV
*6) Surface binding energy 2.9eV
*7) Surface binding energy 2.8eV

5.1.3 Graphs and Data Lists for Desorption Yields

The desorption yields are shown in Figs. 32 - 43 as a function of incident energy. The desorption yields are much larger than corresponding sputtering yields, particularly for low energies and light primary ions. The energy dependence of desorption yields is similar to that of desorption cross sections. For organic samples, the desorption yields are found to decrease in the range from 7 MeV to 45 MeV (see Figs. 41 - 43).

The dependence of desorption yields on surface coverages is shown in Figs. 44 - 50. The exposure dependence is also shown in Figs.51 - 54. In general, the desorption yield increases with surface coverage and has a maximum at about one monolayers. Above one monolayer, it falls off. The dependence on incident energy and incident ion species is also shown in graphs.

Figure 55 shows the dependence of surface temperatures up to 4.5 K. Figs. 56 - 61 show the bakeout temperature dependence of desorption yields due to K^+ ion impact. In general, the desorption yields decrease with increasing temperatures. Especially, the desorption yields are linear with bakeout temperature on a logarithmic scale. The yields are also dependent on the desorbed species.

Figures 62 - 65 show the desorption yield from organic samples. The dependence on incident angle and ion species are shown in Figs. 62 -64. The dependence on charge state of incident oxygen ions are also shown in Fig.65.

Note on Graphs

E_i : incident ion energy

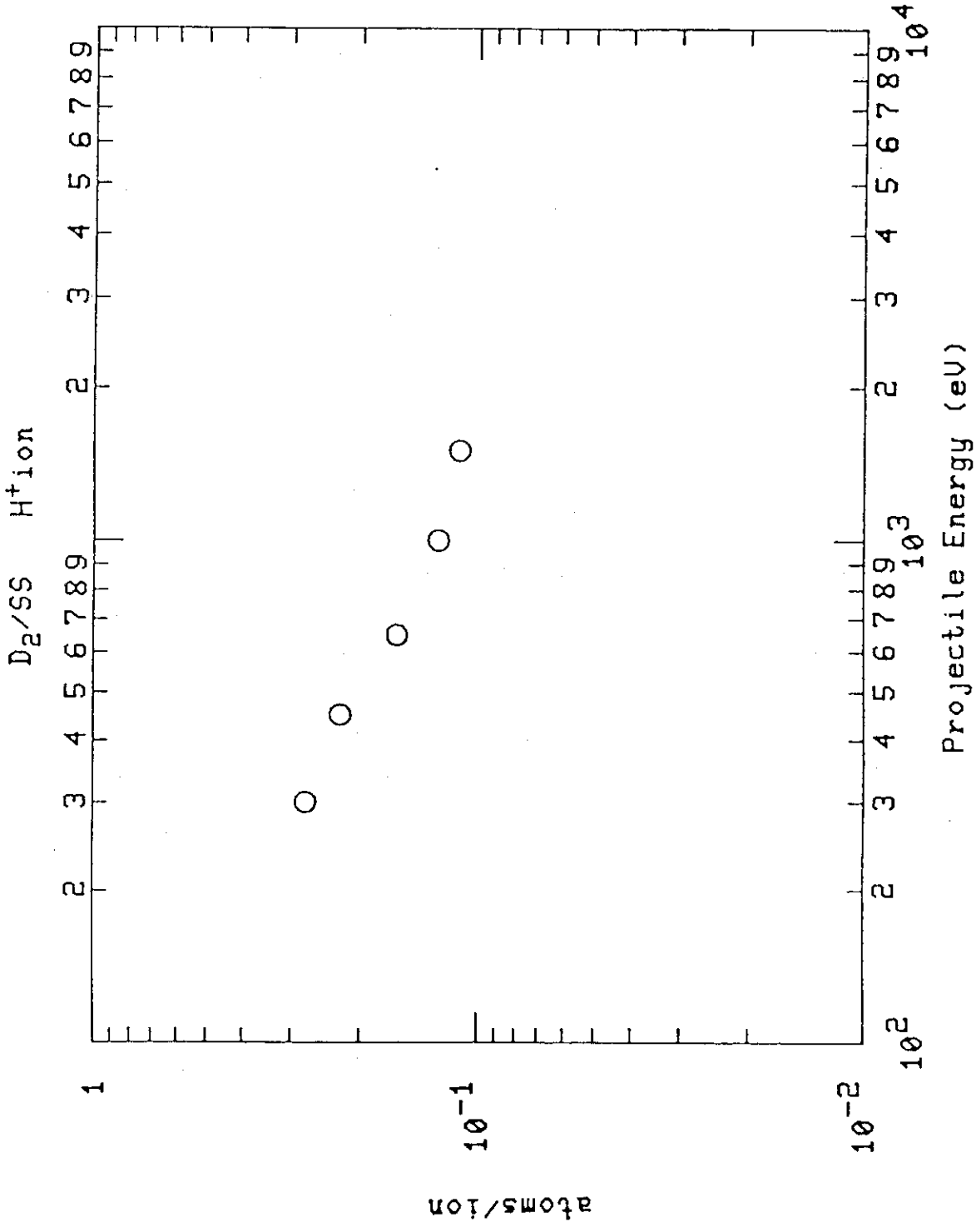

Fig.32 Desorption efficiency as a function of incident energy

DATA LIST

Substrate	Incident ion species	Incident energy (eV)	Incident angle from normal (deg.)	Method	Atoms per incident ion	Ref.
SS	H+	0.300E+03	30	SIMS	0.275E+00	84Ba05
SS	H+	0.450E+03	30	SIMS	0.224E+00	84Ba05
SS	H+	0.650E+03	30	SIMS	0.161E+00	84Ba05
SS	H+	0.100E+04	30	SIMS	0.126E+00	84Ba05
SS	H+	0.150E+04	30	SIMS	0.111E+00	84Ba05

Surface coverage 2.5E+15 (atoms/cm**2)
SS : Stainless steel

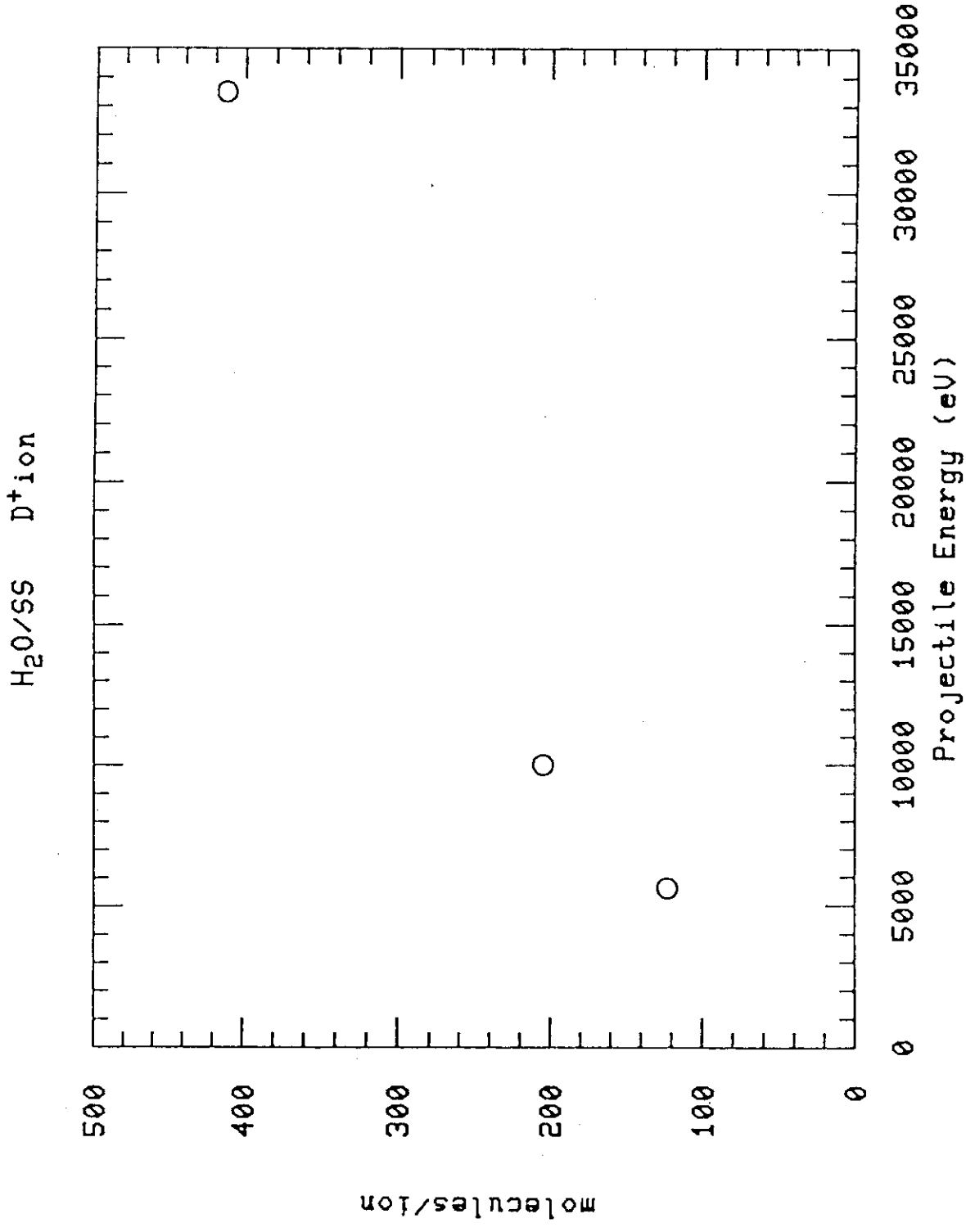

Fig.33 Desorption efficiency as a function of incident energy

DATA LIST

Substrate	Incident ion species	Incident energy (eV)	Incident angle from normal (deg.)	Method	Molecules per incident ion	Ref.
SS	D+	0.560E+04	0	MS	0.123E+03	74Mc01
SS	D+	0.100E+05	0	MS	0.205E+03	74Mc01
SS	D+	0.335E+05	0	MS	0.413E+03	74Mc01

Surface coverage 1.0E+18~1.0E+19 (molecules/cm**2)
SS : Stainless steeel

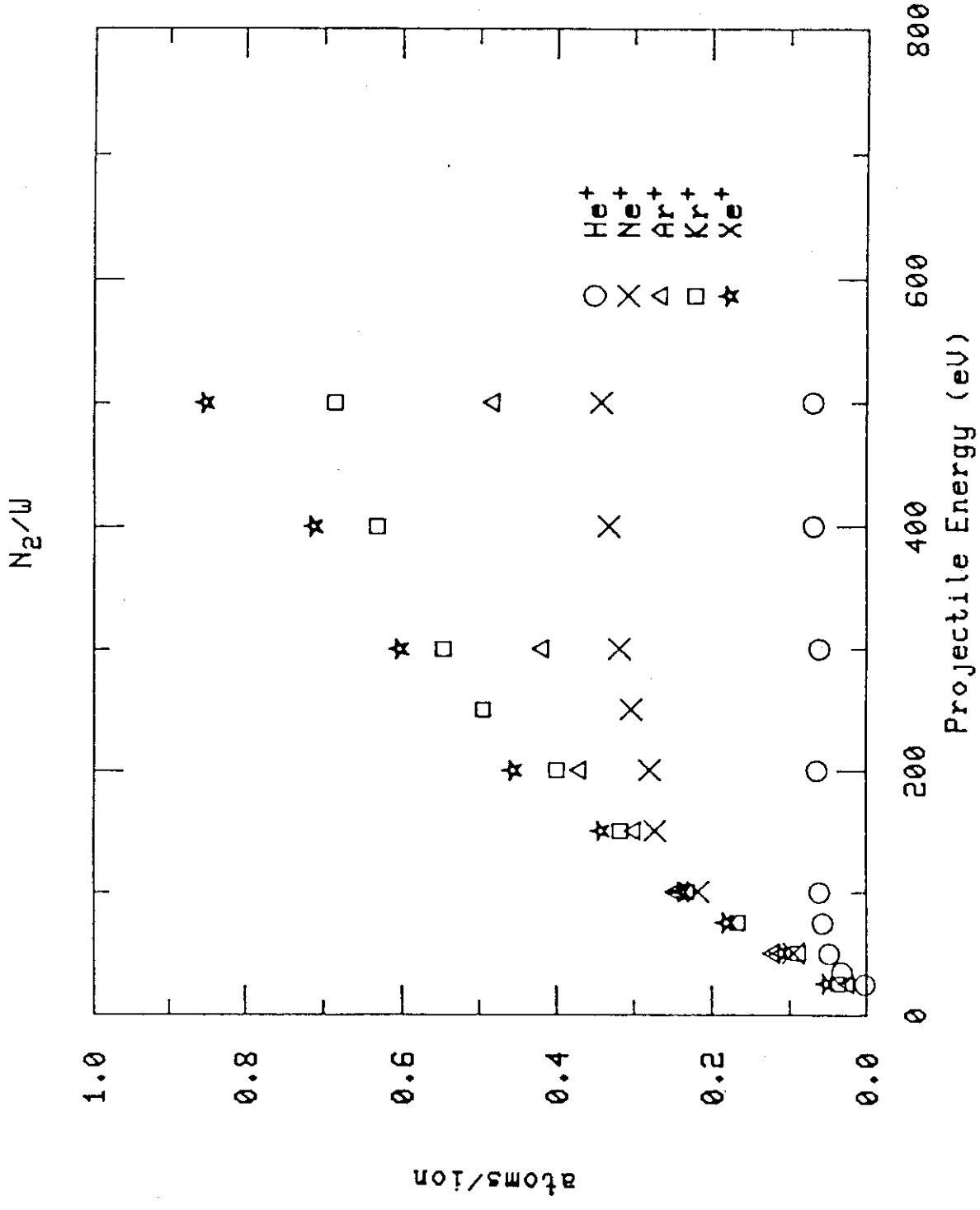

Fig.34 Desorption efficiency as a function of incident energy

DATA LIST

Substrate	Incident ion species	Incident energy (eV)	Incident angle from normal (deg.)	Method	Atoms per incident ion	Ref.
W	He+	0.250E+02	0	MS	0.238E-02	72Wi02
W	He+	0.350E+02	0	MS	0.320E-01	72Wi02
W	He+	0.500E+02	0	MS	0.490E-01	72Wi02
W	He+	0.750E+02	0	MS	0.577E-01	72Wi02
W	He+	0.100E+03	0	MS	0.622E-01	72Wi02
W	He+	0.200E+03	0	MS	0.653E-01	72Wi02
W	He+	0.300E+03	0	MS	0.622E-01	72Wi02
W	He+	0.400E+03	0	MS	0.696E-01	72Wi02
W	He+	0.500E+03	0	MS	0.706E-01	72Wi02
W	Ne+	0.500E+02	0	MS	0.954E-01	72Wi02
W	Ne+	0.100E+03	0	MS	0.218E+00	72Wi02
W	Ne+	0.150E+03	0	MS	0.273E+00	72Wi02
W	Ne+	0.200E+03	0	MS	0.280E+00	72Wi02
W	Ne+	0.250E+03	0	MS	0.304E+00	72Wi02
W	Ne+	0.300E+03	0	MS	0.319E+00	72Wi02
W	Ne+	0.400E+03	0	MS	0.333E+00	72Wi02
W	Ne+	0.500E+03	0	MS	0.343E+00	72Wi02
W	Ar+	0.250E+02	0	MS	0.235E-01	72Wi02
W	Ar+	0.500E+02	0	MS	0.121E+00	72Wi02
W	Ar+	0.100E+03	0	MS	0.246E+00	72Wi02
W	Ar+	0.150E+03	0	MS	0.299E+00	72Wi02
W	Ar+	0.200E+03	0	MS	0.369E+00	72Wi02
W	Ar+	0.300E+03	0	MS	0.418E+00	72Wi02
W	Ar+	0.500E+03	0	MS	0.482E+00	72Wi02
W	Kr+	0.250E+02	0	MS	0.361E-01	72Wi02
W	Kr+	0.500E+02	0	MS	0.891E-01	72Wi02
W	Kr+	0.750E+02	0	MS	0.167E+00	72Wi02
W	Kr+	0.100E+03	0	MS	0.233E+00	72Wi02
W	Kr+	0.150E+03	0	MS	0.318E+00	72Wi02
W	Kr+	0.200E+03	0	MS	0.400E+00	72Wi02
W	Kr+	0.250E+03	0	MS	0.496E+00	72Wi02
W	Kr+	0.300E+03	0	MS	0.547E+00	72Wi02
W	Kr+	0.400E+03	0	MS	0.632E+00	72Wi02
W	Kr+	0.500E+03	0	MS	0.686E+00	72Wi02
W	Xe+	0.250E+02	0	MS	0.530E-01	72Wi02
W	Xe+	0.500E+02	0	MS	0.112E+00	72Wi02
W	Xe+	0.750E+02	0	MS	0.182E+00	72Wi02
W	Xe+	0.100E+03	0	MS	0.239E+00	72Wi02
W	Xe+	0.150E+03	0	MS	0.343E+00	72Wi02
W	Xe+	0.200E+03	0	MS	0.457E+00	72Wi02
W	Xe+	0.300E+03	0	MS	0.604E+00	72Wi02
W	Xe+	0.400E+03	0	MS	0.714E+00	72Wi02
W	Xe+	0.500E+03	0	MS	0.853E+00	72Wi02

Surface coverage 6.0E+14 (atoms/cm**2)

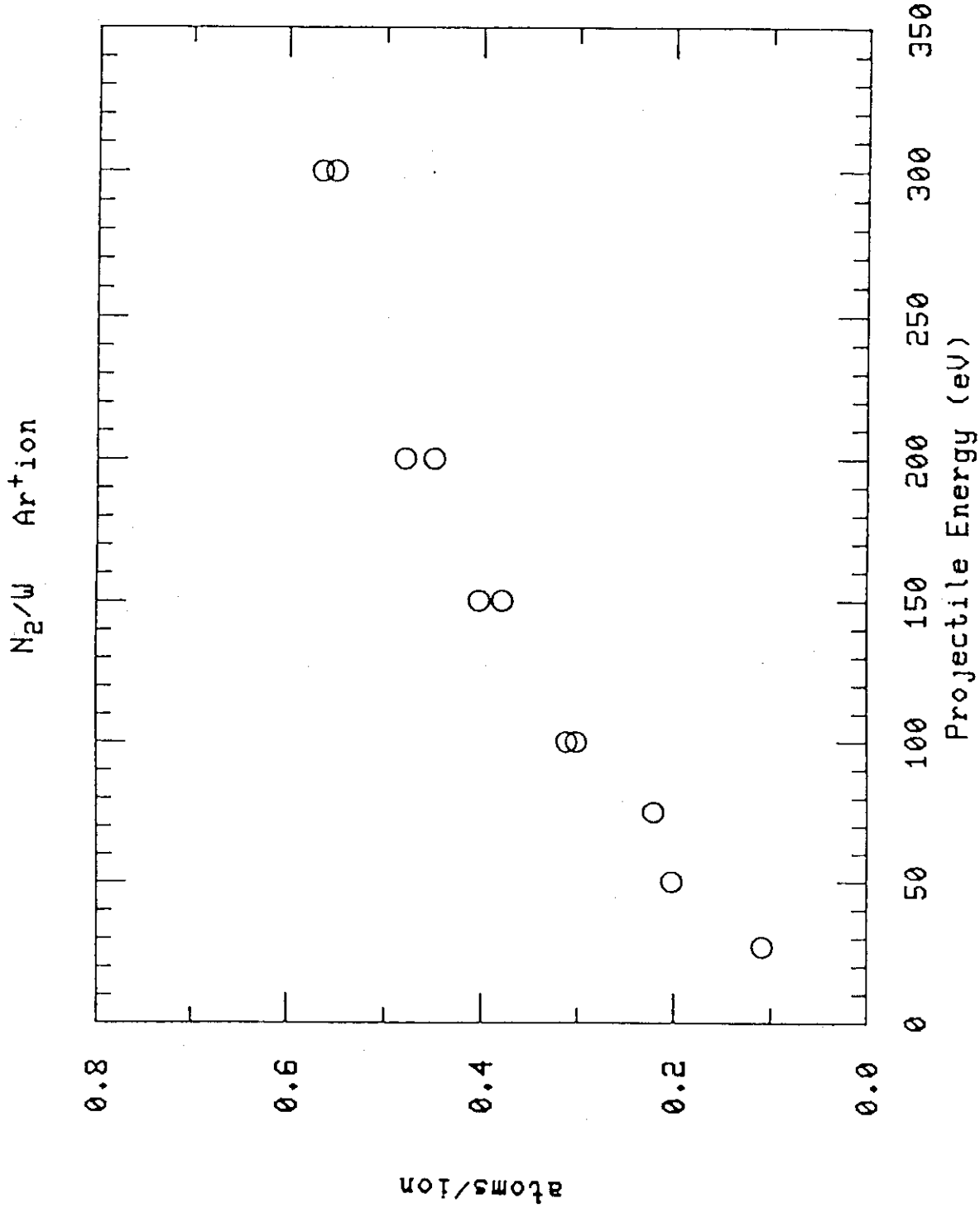

Fig.35 Desorption efficiency as a function of incident energy

DATA LIST

Substrate	Incident ion species	Incident energy (eV)	Incident angle from normal (deg.)	Method	Atoms per incident ion	Ref.
W	Ar+	0.270E+02	0	MS	0.109E+00	71Wi01
W	Ar+	0.500E+02	0	MS	0.202E+00	71Wi01
W	Ar+	0.750E+02	0	MS	0.221E+00	71Wi01
W	Ar+	0.100E+03	0	MS	0.301E+00	71Wi01
W	Ar+	0.100E+03	0	MS	0.311E+00	71Wi01
W	Ar+	0.150E+03	0	MS	0.402E+00	71Wi01
W	Ar+	0.150E+03	0	MS	0.378E+00	71Wi01
W	Ar+	0.200E+03	0	MS	0.479E+00	71Wi01
W	Ar+	0.200E+03	0	MS	0.449E+00	71Wi01
W	Ar+	0.300E+03	0	MS	0.565E+00	71Wi01
W	Ar+	0.300E+03	0	MS	0.551E+00	71Wi01

Surface coverage 6.0E+14 (atoms/cm**2)

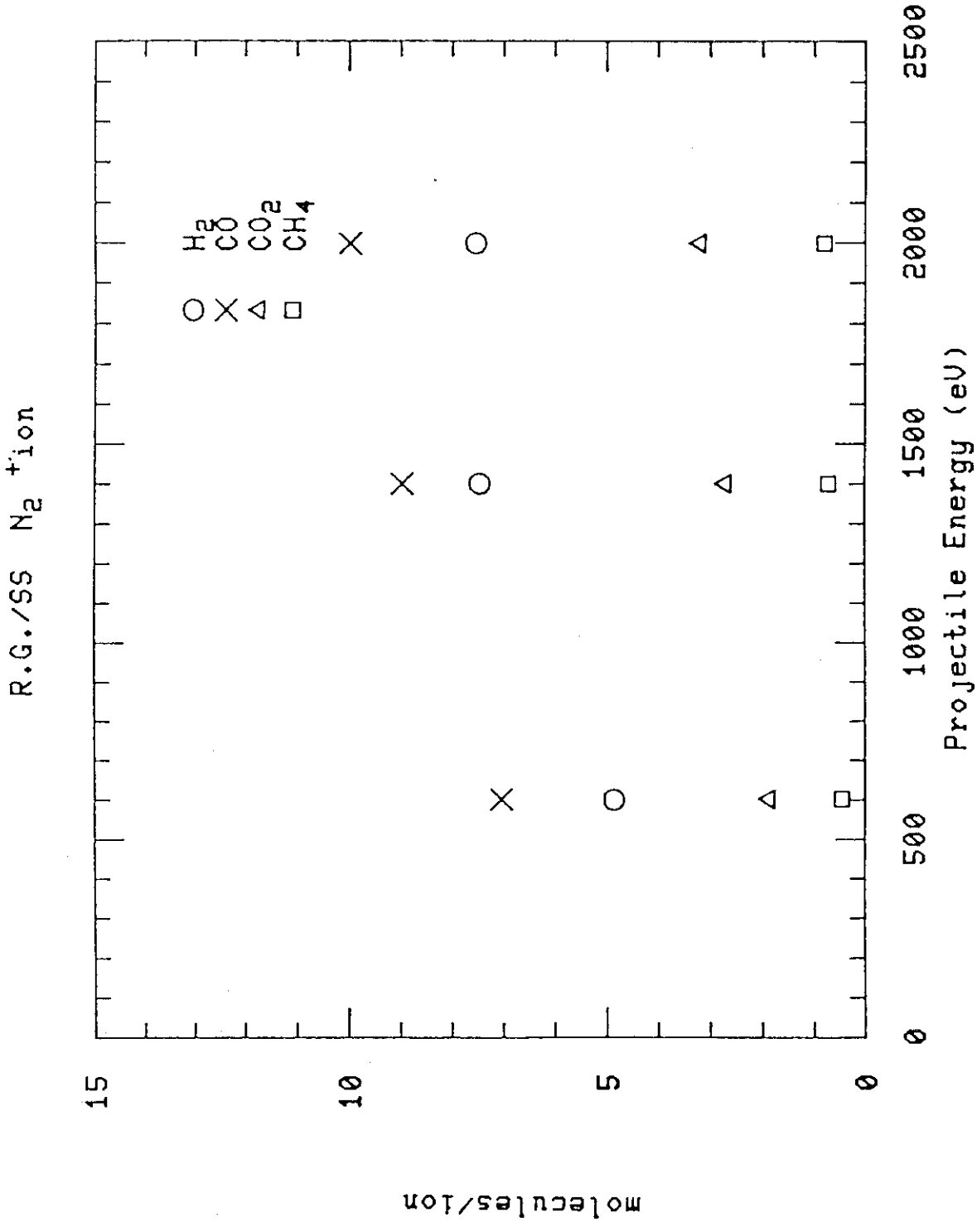

Fig.36 Desorption efficiency as a function of incident energy

DATA LIST

Substrate	Desorbed species	Incident energy (eV)	Incident ion species	Method	Molecules per incident ion	Ref.
SS	H2	0.600E+03	N2 +	MS	0.486E+01	76Ma01
SS	H2	0.140E+04	N2 +	MS	0.746E+01	76Ma01
SS	H2	0.200E+04	N2 +	MS	0.753E+01	76Ma01
SS	CO	0.600E+03	N2 +	MS	0.704E+01	76Ma01
SS	CO	0.140E+04	N2 +	MS	0.897E+01	76Ma01
SS	CO	0.200E+04	N2 +	MS	0.997E+01	76Ma01
SS	CO2	0.600E+03	N2 +	MS	0.186E+01	76Ma01
SS	CO2	0.140E+04	N2 +	MS	0.270E+01	76Ma01
SS	CO2	0.200E+04	N2 +	MS	0.318E+01	76Ma01
SS	CH4	0.600E+03	N2 +	MS	0.441E+00	76Ma01
SS	CH4	0.140E+04	N2 +	MS	0.706E+00	76Ma01
SS	CH4	0.200E+04	N2 +	MS	0.784E+00	76Ma01

SS : Stainless steel (unbaked)

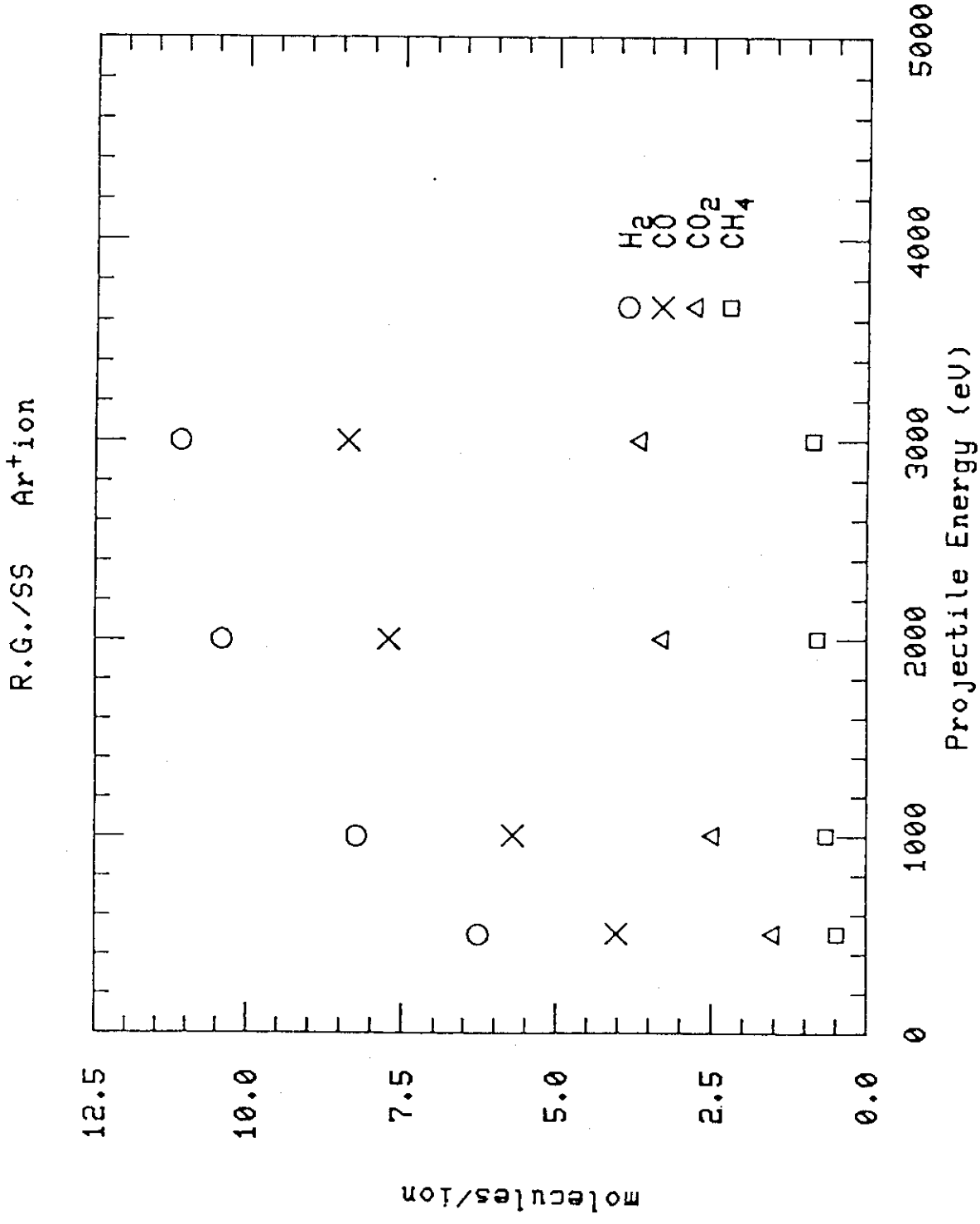

Fig.37 Desorption efficiency as a function of incident energy

DATA LIST

Substrate	Desorbed species	Incident energy (eV)	Incident ion species	Method	Molecules per incident ion	Ref.
SS	H2	0.500E+03	Ar +	MS	0.626E+01	76Ma01
SS	H2	0.100E+04	Ar +	MS	0.824E+01	76Ma01
SS	H2	0.200E+04	Ar +	MS	0.104E+02	76Ma01
SS	H2	0.300E+04	Ar +	MS	0.111E+02	76Ma01
SS	CO	0.500E+03	Ar +	MS	0.402E+01	76Ma01
SS	CO	0.100E+04	Ar +	MS	0.570E+01	76Ma01
SS	CO	0.200E+04	Ar +	MS	0.772E+01	76Ma01
SS	CO	0.300E+04	Ar +	MS	0.839E+01	76Ma01
SS	CO2	0.500E+03	Ar +	MS	0.150E+01	76Ma01
SS	CO2	0.100E+04	Ar +	MS	0.247E+01	76Ma01
SS	CO2	0.200E+04	Ar +	MS	0.329E+01	76Ma01
SS	CO2	0.300E+04	Ar +	MS	0.365E+01	76Ma01
SS	CH4	0.500E+03	Ar +	MS	0.482E+00	76Ma01
SS	CH4	0.100E+04	Ar +	MS	0.664E+00	76Ma01
SS	CH4	0.200E+04	Ar +	MS	0.802E+00	76Ma01
SS	CH4	0.300E+04	Ar +	MS	0.884E+00	76Ma01

SS : Stainless steel (unbaked)

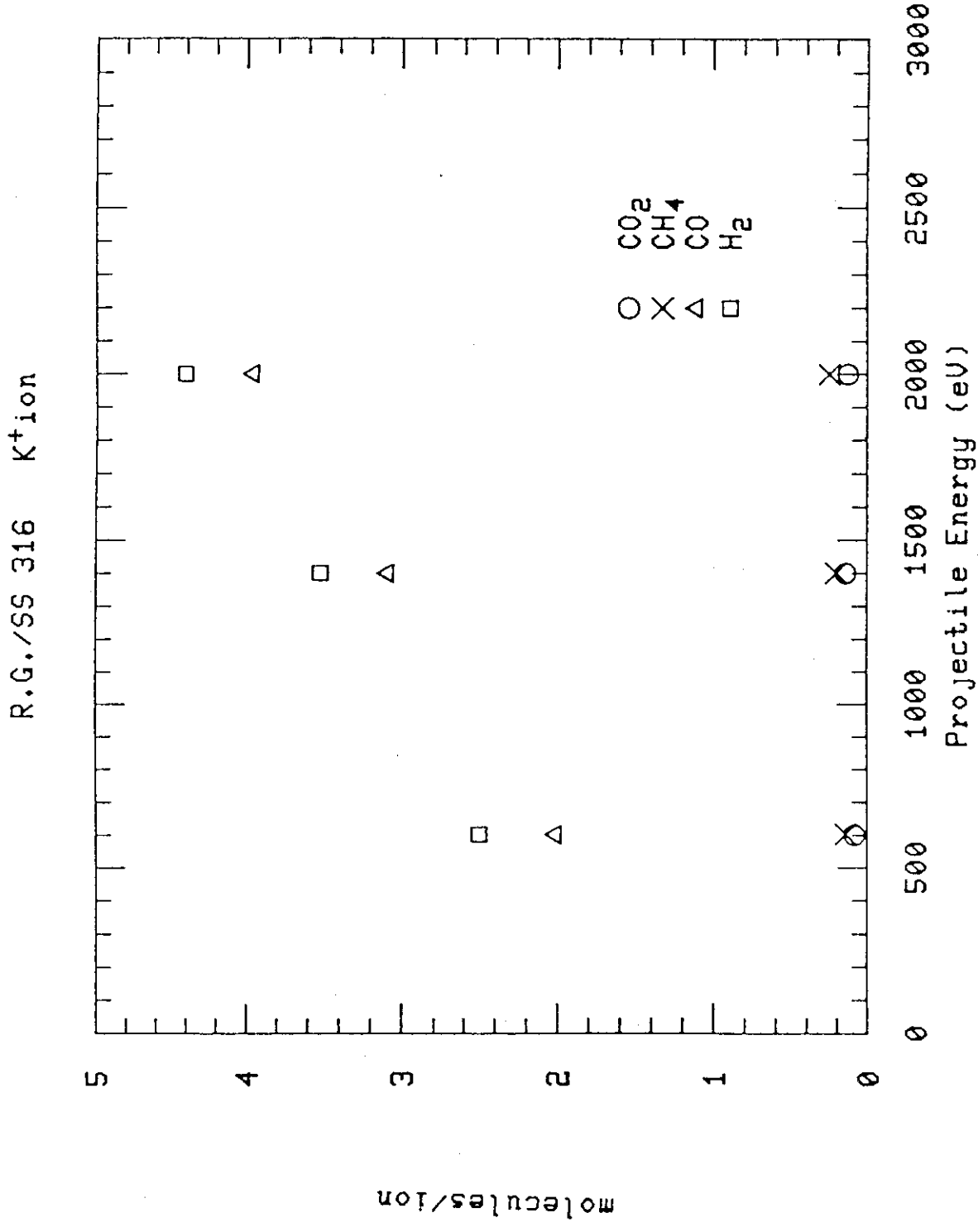

Fig.38 Desorption efficiency as a function of incident energy

DATA LIST

Substrate	Desorbed species	Incident energy (eV)	Incident ion species	Method	Molecules per incident ion	Ref.
SS 316	CO2	0.600E+03	K+	AES	0.856E-01	77Ma02
SS 316	CO2	0.140E+04	K+	AES	0.142E+00	77Ma02
SS 316	CO2	0.200E+04	K+	AES	0.127E+00	77Ma02
SS 316	CH4	0.600E+03	K+	AES	0.139E+00	77Ma02
SS 316	CH4	0.140E+04	K+	AES	0.202E+00	77Ma02
SS 316	CH4	0.200E+04	K+	AES	0.248E+00	77Ma02
SS 316	CO	0.600E+03	K+	AES	0.201E+01	77Ma02
SS 316	CO	0.140E+04	K+	AES	0.309E+01	77Ma02
SS 316	CO	0.200E+04	K+	AES	0.396E+01	77Ma02
SS 316	H2	0.600E+03	K+	AES	0.250E+01	77Ma02
SS 316	H2	0.140E+04	K+	AES	0.352E+01	77Ma02
SS 316	H2	0.200E+04	K+	AES	0.441E+01	77Ma02

SS 316 : Stainless steel 316

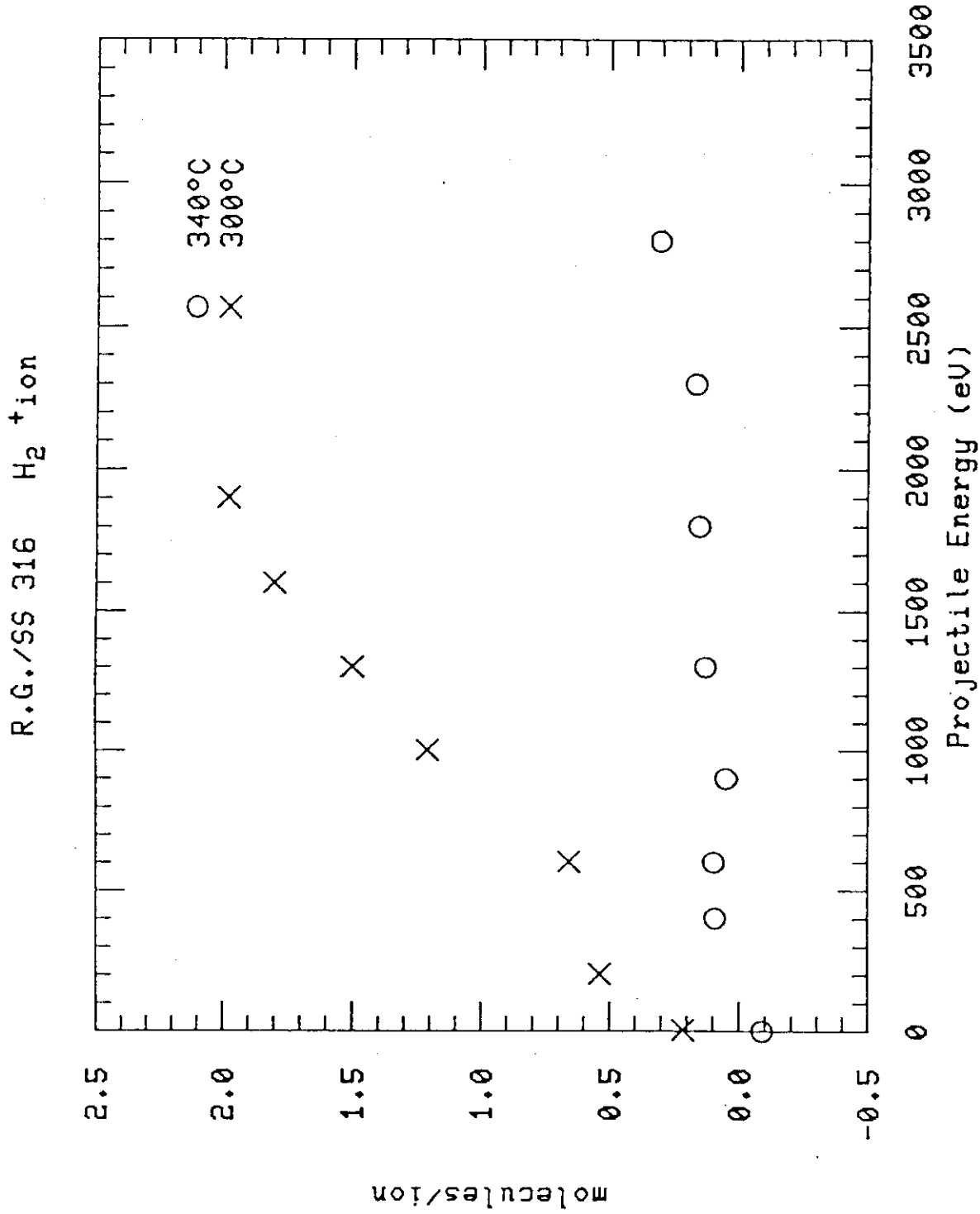

Fig.39 Desorption efficiency as a function of incident energy

DATA LIST

Substrate	Incident ion species	Incident energy (eV)	Incident angle from normal (deg.)	Method	Molecules per incident ion	Ref.
SS 316	H2 +	0.000E+00	?	AES	-0.895E-01	74Ca01
SS 316	H2 +	0.400E+03	?	AES	0.927E-01	74Ca01
SS 316	H2 +	0.600E+03	?	AES	0.973E-01	74Ca01
SS 316	H2 +	0.900E+03	?	AES	0.520E-01	74Ca01
SS 316	H2 +	0.130E+04	?	AES	0.130E+00	74Ca01
SS 316	H2 +	0.180E+04	?	AES	0.152E+00	74Ca01
SS 316	H2 +	0.230E+04	?	AES	0.167E+00	74Ca01
SS 316	H2 +	0.280E+04	?	AES	0.306E+00	74Ca01
SS 316	H2 +	0.000E+00	?	AES	0.215E+00	74Ca01
SS 316	H2 +	0.200E+03	?	AES	0.538E+00	74Ca01
SS 316	H2 +	0.600E+03	?	AES	0.658E+00	74Ca01
SS 316	H2 +	0.100E+04	?	AES	0.121E+01	74Ca01
SS 316	H2 +	0.130E+04	?	AES	0.150E+01	74Ca01
SS 316	H2 +	0.160E+04	?	AES	0.180E+01	74Ca01
SS 316	H2 +	0.190E+04	?	AES	0.198E+01	74Ca01

Desorption yield for the ISR stainless steel vacuum chamber
(ISR proton beam current 3mA).
Desorbed species were mostly CO and H2.
The bakeout temperatures were shown in Figure.
SS 316 : Stainless steel 316.

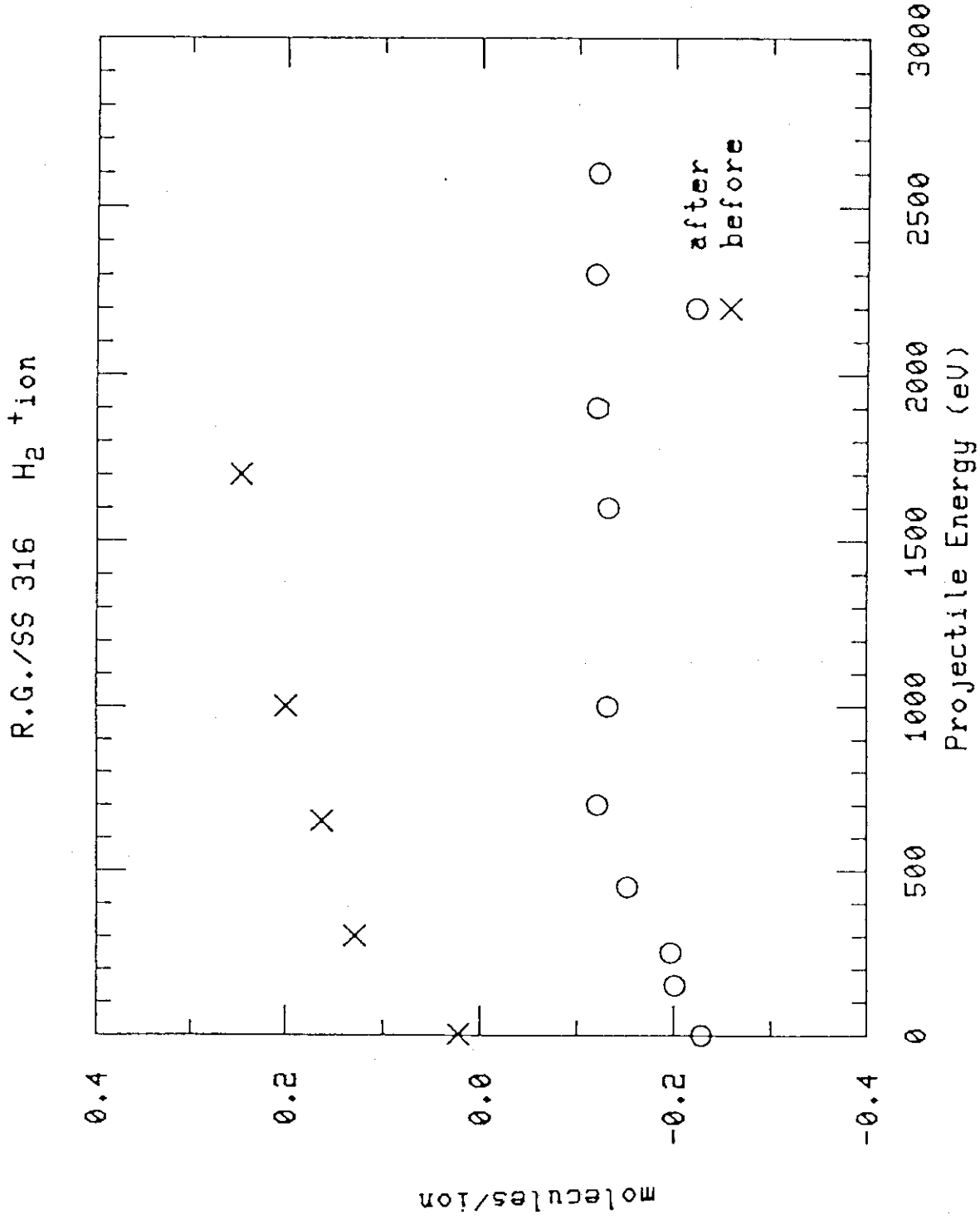

Fig.40 Desorption efficiency as a function of incident energy

DATA LIST

Substrate	Incident ion species	Incident energy (eV)	Incident angle from normal (deg.)	Method	Molecules per incident ion	Ref.	Remark
SS 316	H2 +	0.000E+00	?	AES	-0.228E+00	74Ca01	*1)
SS 316	H2 +	0.150E+03	?	AES	-0.201E+00	74Ca01	*1)
SS 316	H2 +	0.250E+03	?	AES	-0.197E+00	74Ca01	*1)
SS 316	H2 +	0.450E+03	?	AES	-0.152E+00	74Ca01	*1)
SS 316	H2 +	0.700E+03	?	AES	-0.121E+00	74Ca01	*1)
SS 316	H2 +	0.100E+04	?	AES	-0.132E+00	74Ca01	*1)
SS 316	H2 +	0.160E+04	?	AES	-0.132E+00	74Ca01	*1)
SS 316	H2 +	0.190E+04	?	AES	-0.120E+00	74Ca01	*1)
SS 316	H2 +	0.230E+04	?	AES	-0.119E+00	74Ca01	*1)
SS 316	H2 +	0.260E+04	?	AES	-0.121E+00	74Ca01	*1)
SS 316	H2 +	0.000E+00	?	AES	0.226E-01	74Ca01	*2)
SS 316	H2 +	0.300E+03	?	AES	0.129E+00	74Ca01	*2)
SS 316	H2 +	0.650E+03	?	AES	0.163E+00	74Ca01	*2)
SS 316	H2 +	0.100E+04	?	AES	0.200E+00	74Ca01	*2)
SS 316	H2 +	0.170E+04	?	AES	0.247E+00	74Ca01	*2)

Desorption yield for the ISR stainless steel vacuum chamber
(ISR proton beam current 3mA).
Desorbed species were mostly CO and H2.
The bakeout temperatures were shown in Figure.
SS 316 : Stainless steel 316.
*1) After an Ar glow discharge cleaning
*2) Before an Ar glow discharge cleaning

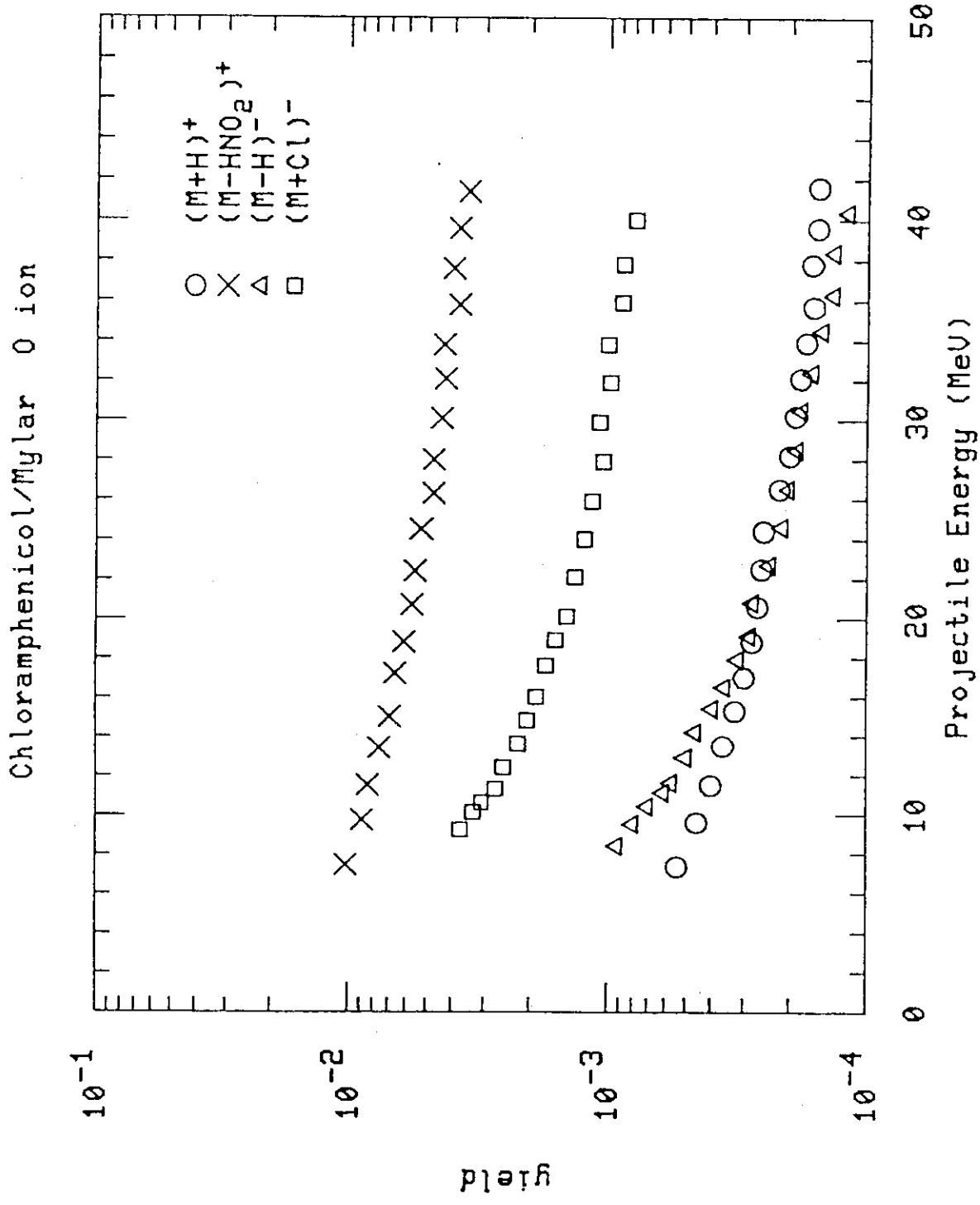

Fig.41 Desorption efficiency as a function of incident energy

DATA LIST

Substrate	Incident ion species	Incident energy (MeV)	Incident angle from normal (deg.)	Method	Yield	Ref.	Remark
Mylar	O ion	0.733E+01	0	TOF	0.538E-03	84Ne01	*1)
Mylar	O ion	0.960E+01	0	TOF	0.452E-03	84Ne01	*1)
Mylar	O ion	0.115E+02	0	TOF	0.399E-03	84Ne01	*1)
Mylar	O ion	0.135E+02	0	TOF	0.359E-03	84Ne01	*1)
Mylar	O ion	0.153E+02	0	TOF	0.324E-03	84Ne01	*1)
Mylar	O ion	0.170E+02	0	TOF	0.299E-03	84Ne01	*1)
Mylar	O ion	0.188E+02	0	TOF	0.279E-03	84Ne01	*1)
Mylar	O ion	0.206E+02	0	TOF	0.266E-03	84Ne01	*1)
Mylar	O ion	0.225E+02	0	TOF	0.257E-03	84Ne01	*1)
Mylar	O ion	0.244E+02	0	TOF	0.252E-03	84Ne01	*1)
Mylar	O ion	0.265E+02	0	TOF	0.219E-03	84Ne01	*1)
Mylar	O ion	0.282E+02	0	TOF	0.200E-03	84Ne01	*1)
Mylar	O ion	0.302E+02	0	TOF	0.191E-03	84Ne01	*1)
Mylar	O ion	0.321E+02	0	TOF	0.183E-03	84Ne01	*1)
Mylar	O ion	0.339E+02	0	TOF	0.174E-03	84Ne01	*1)
Mylar	O ion	0.357E+02	0	TOF	0.163E-03	84Ne01	*1)
Mylar	O ion	0.378E+02	0	TOF	0.165E-03	84Ne01	*1)
Mylar	O ion	0.396E+02	0	TOF	0.157E-03	84Ne01	*1)
Mylar	O ion	0.416E+02	0	TOF	0.156E-03	84Ne01	*1)
Mylar	O ion	0.741E+01	0	TOF	0.102E-01	84Ne01	*2)
Mylar	O ion	0.971E+01	0	TOF	0.882E-02	84Ne01	*2)
Mylar	O ion	0.115E+02	0	TOF	0.842E-02	84Ne01	*2)
Mylar	O ion	0.134E+02	0	TOF	0.759E-02	84Ne01	*2)
Mylar	O ion	0.150E+02	0	TOF	0.692E-02	84Ne01	*2)
Mylar	O ion	0.172E+02	0	TOF	0.661E-02	84Ne01	*2)
Mylar	O ion	0.188E+02	0	TOF	0.610E-02	84Ne01	*2)
Mylar	O ion	0.207E+02	0	TOF	0.569E-02	84Ne01	*2)
Mylar	O ion	0.224E+02	0	TOF	0.556E-02	84Ne01	*2)
Mylar	O ion	0.245E+02	0	TOF	0.531E-02	84Ne01	*2)
Mylar	O ion	0.263E+02	0	TOF	0.473E-02	84Ne01	*2)
Mylar	O ion	0.280E+02	0	TOF	0.473E-02	84Ne01	*2)
Mylar	O ion	0.301E+02	0	TOF	0.442E-02	84Ne01	*2)
Mylar	O ion	0.321E+02	0	TOF	0.427E-02	84Ne01	*2)
Mylar	O ion	0.338E+02	0	TOF	0.432E-02	84Ne01	*2)
Mylar	O ion	0.358E+02	0	TOF	0.377E-02	84Ne01	*2)
Mylar	O ion	0.376E+02	0	TOF	0.399E-02	84Ne01	*2)
Mylar	O ion	0.396E+02	0	TOF	0.377E-02	84Ne01	*2)
Mylar	O ion	0.414E+02	0	TOF	0.348E-02	84Ne01	*2)
Mylar	O ion	0.839E+01	0	TOF	0.911E-03	84Ne01	*3)
Mylar	O ion	0.950E+01	0	TOF	0.792E-03	84Ne01	*3)

./..

Mylar	O ion	0.104E+02	0	TOF	0.697E-03	84Ne01 *3)
Mylar	O ion	0.111E+02	0	TOF	0.605E-03	84Ne01 *3)
Mylar	O ion	0.116E+02	0	TOF	0.564E-03	84Ne01 *3)
Mylar	O ion	0.129E+02	0	TOF	0.502E-03	84Ne01 *3)
Mylar	O ion	0.142E+02	0	TOF	0.457E-03	84Ne01 *3)
Mylar	O ion	0.154E+02	0	TOF	0.393E-03	84Ne01 *3)
Mylar	O ion	0.165E+02	0	TOF	0.354E-03	84Ne01 *3)
Mylar	O ion	0.179E+02	0	TOF	0.315E-03	84Ne01 *3)
Mylar	O ion	0.191E+02	0	TOF	0.284E-03	84Ne01 *3)
Mylar	O ion	0.208E+02	0	TOF	0.277E-03	84Ne01 *3)
Mylar	O ion	0.227E+02	0	TOF	0.238E-03	84Ne01 *3)
Mylar	O ion	0.246E+02	0	TOF	0.214E-03	84Ne01 *3)
Mylar	O ion	0.265E+02	0	TOF	0.202E-03	84Ne01 *3)
Mylar	O ion	0.285E+02	0	TOF	0.187E-03	84Ne01 *3)
Mylar	O ion	0.305E+02	0	TOF	0.180E-03	84Ne01 *3)
Mylar	O ion	0.324E+02	0	TOF	0.164E-03	84Ne01 *3)
Mylar	O ion	0.345E+02	0	TOF	0.150E-03	84Ne01 *3)
Mylar	O ion	0.363E+02	0	TOF	0.136E-03	84Ne01 *3)
Mylar	O ion	0.384E+02	0	TOF	0.135E-03	84Ne01 *3)
Mylar	O ion	0.404E+02	0	TOF	0.119E-03	84Ne01 *3)
Mylar	O ion	0.920E+01	0	TOF	0.369E-02	84Ne01 *4)
Mylar	O ion	0.101E+02	0	TOF	0.329E-02	84Ne01 *4)
Mylar	O ion	0.106E+02	0	TOF	0.307E-02	84Ne01 *4)
Mylar	O ion	0.113E+02	0	TOF	0.270E-02	84Ne01 *4)
Mylar	O ion	0.124E+02	0	TOF	0.252E-02	84Ne01 *4)
Mylar	O ion	0.136E+02	0	TOF	0.221E-02	84Ne01 *4)
Mylar	O ion	0.148E+02	0	TOF	0.204E-02	84Ne01 *4)
Mylar	O ion	0.160E+02	0	TOF	0.188E-02	84Ne01 *4)
Mylar	O ion	0.176E+02	0	TOF	0.173E-02	84Ne01 *4)
Mylar	O ion	0.189E+02	0	TOF	0.159E-02	84Ne01 *4)
Mylar	O ion	0.201E+02	0	TOF	0.144E-02	84Ne01 *4)
Mylar	O ion	0.221E+02	0	TOF	0.134E-02	84Ne01 *4)
Mylar	O ion	0.240E+02	0	TOF	0.123E-02	84Ne01 *4)
Mylar	O ion	0.259E+02	0	TOF	0.115E-02	84Ne01 *4)
Mylar	O ion	0.279E+02	0	TOF	0.104E-02	84Ne01 *4)
Mylar	O ion	0.299E+02	0	TOF	0.108E-02	84Ne01 *4)
Mylar	O ion	0.319E+02	0	TOF	0.983E-03	84Ne01 *4)
Mylar	O ion	0.338E+02	0	TOF	0.100E-02	84Ne01 *4)
Mylar	O ion	0.359E+02	0	TOF	0.883E-03	84Ne01 *4)
Mylar	O ion	0.378E+02	0	TOF	0.872E-03	84Ne01 *4)
Mylar	O ion	0.400E+02	0	TOF	0.785E-03	84Ne01 *4)

*1) Desorbed species : [M+H]+
*2) Desorbed species : [M-HNO2]+
*3) Desorbed species : [M-H]-
*4) Desorbed species : [M+Cl]-
Thickness 30~50 ug/cm**2

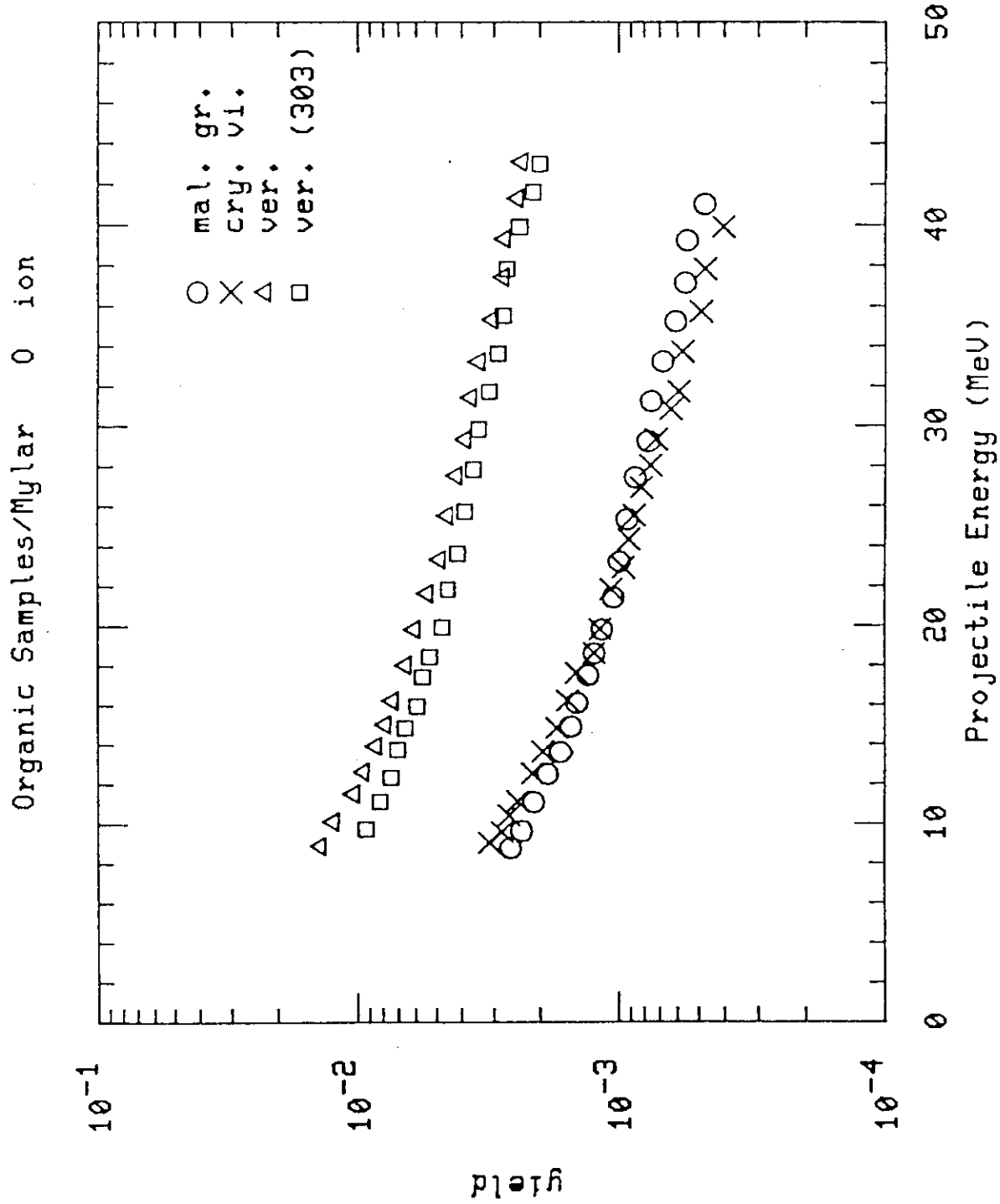

Fig.42 Desorption efficiency as a function of incident energy

DATA LIST

Substrate	Incident ion species	Incident energy (MeV)	Incident angle from normal (deg.)	Method	Yield	Ref.	Remark
Mylar	O ion	0.879E+01	0	TOF	0.258E-02	84Ne01	*1)
Mylar	O ion	0.965E+01	0	TOF	0.234E-02	84Ne01	*1)
Mylar	O ion	0.111E+02	0	TOF	0.210E-02	84Ne01	*1)
Mylar	O ion	0.125E+02	0	TOF	0.186E-02	84Ne01	*1)
Mylar	O ion	0.136E+02	0	TOF	0.166E-02	84Ne01	*1)
Mylar	O ion	0.149E+02	0	TOF	0.151E-02	84Ne01	*1)
Mylar	O ion	0.161E+02	0	TOF	0.143E-02	84Ne01	*1)
Mylar	O ion	0.175E+02	0	TOF	0.130E-02	84Ne01	*1)
Mylar	O ion	0.186E+02	0	TOF	0.123E-02	84Ne01	*1)
Mylar	O ion	0.198E+02	0	TOF	0.115E-02	84Ne01	*1)
Mylar	O ion	0.214E+02	0	TOF	0.104E-02	84Ne01	*1)
Mylar	O ion	0.232E+02	0	TOF	0.985E-03	84Ne01	*1)
Mylar	O ion	0.253E+02	0	TOF	0.919E-03	84Ne01	*1)
Mylar	O ion	0.274E+02	0	TOF	0.857E-03	84Ne01	*1)
Mylar	O ion	0.292E+02	0	TOF	0.767E-03	84Ne01	*1)
Mylar	O ion	0.312E+02	0	TOF	0.746E-03	84Ne01	*1)
Mylar	O ion	0.332E+02	0	TOF	0.677E-03	84Ne01	*1)
Mylar	O ion	0.352E+02	0	TOF	0.606E-03	84Ne01	*1)
Mylar	O ion	0.371E+02	0	TOF	0.558E-03	84Ne01	*1)
Mylar	O ion	0.392E+02	0	TOF	0.549E-03	84Ne01	*1)
Mylar	O ion	0.410E+02	0	TOF	0.472E-03	84Ne01	*1)
Mylar	O ion	0.901E+01	0	TOF	0.311E-02	84Ne01	*2)
Mylar	O ion	0.956E+01	0	TOF	0.278E-02	84Ne01	*2)
Mylar	O ion	0.104E+02	0	TOF	0.261E-02	84Ne01	*2)
Mylar	O ion	0.111E+02	0	TOF	0.242E-02	84Ne01	*2)
Mylar	O ion	0.125E+02	0	TOF	0.213E-02	84Ne01	*2)
Mylar	O ion	0.136E+02	0	TOF	0.194E-02	84Ne01	*2)
Mylar	O ion	0.148E+02	0	TOF	0.171E-02	84Ne01	*2)
Mylar	O ion	0.162E+02	0	TOF	0.155E-02	84Ne01	*2)
Mylar	O ion	0.176E+02	0	TOF	0.144E-02	84Ne01	*2)
Mylar	O ion	0.186E+02	0	TOF	0.123E-02	84Ne01	*2)
Mylar	O ion	0.198E+02	0	TOF	0.117E-02	84Ne01	*2)
Mylar	O ion	0.218E+02	0	TOF	0.106E-02	84Ne01	*2)
Mylar	O ion	0.229E+02	0	TOF	0.951E-03	84Ne01	*2)
Mylar	O ion	0.243E+02	0	TOF	0.906E-03	84Ne01	*2)
Mylar	O ion	0.255E+02	0	TOF	0.864E-03	84Ne01	*2)
Mylar	O ion	0.269E+02	0	TOF	0.811E-03	84Ne01	*2)
Mylar	O ion	0.280E+02	0	TOF	0.748E-03	84Ne01	*2)
Mylar	O ion	0.293E+02	0	TOF	0.713E-03	84Ne01	*2)
Mylar	O ion	0.308E+02	0	TOF	0.628E-03	84Ne01	*2)
Mylar	O ion	0.317E+02	0	TOF	0.589E-03	84Ne01	*2)
Mylar	O ion	0.337E+02	0	TOF	0.570E-03	84Ne01	*2)
Mylar	O ion	0.357E+02	0	TOF	0.486E-03	84Ne01	*2)
Mylar	O ion	0.378E+02	0	TOF	0.470E-03	84Ne01	*2)
Mylar	O ion	0.399E+02	0	TOF	0.400E-03	84Ne01	*2)

./..

Mylar	O ion	0.886E+01	0	TOF	0.138E-01	84Ne01 *3)
Mylar	O ion	0.101E+02	0	TOF	0.123E-01	84Ne01 *3)
Mylar	O ion	0.115E+02	0	TOF	0.103E-01	84Ne01 *3)
Mylar	O ion	0.126E+02	0	TOF	0.948E-02	84Ne01 *3)
Mylar	O ion	0.139E+02	0	TOF	0.846E-02	84Ne01 *3)
Mylar	O ion	0.150E+02	0	TOF	0.780E-02	84Ne01 *3)
Mylar	O ion	0.162E+02	0	TOF	0.732E-02	84Ne01 *3)
Mylar	O ion	0.180E+02	0	TOF	0.653E-02	84Ne01 *3)
Mylar	O ion	0.198E+02	0	TOF	0.603E-02	84Ne01 *3)
Mylar	O ion	0.216E+02	0	TOF	0.538E-02	84Ne01 *3)
Mylar	O ion	0.233E+02	0	TOF	0.481E-02	84Ne01 *3)
Mylar	O ion	0.255E+02	0	TOF	0.451E-02	84Ne01 *3)
Mylar	O ion	0.275E+02	0	TOF	0.416E-02	84Ne01 *3)
Mylar	O ion	0.293E+02	0	TOF	0.384E-02	84Ne01 *3)
Mylar	O ion	0.314E+02	0	TOF	0.366E-02	84Ne01 *3)
Mylar	O ion	0.332E+02	0	TOF	0.344E-02	84Ne01 *3)
Mylar	O ion	0.353E+02	0	TOF	0.303E-02	84Ne01 *3)
Mylar	O ion	0.374E+02	0	TOF	0.275E-02	84Ne01 *3)
Mylar	O ion	0.393E+02	0	TOF	0.271E-02	84Ne01 *3)
Mylar	O ion	0.413E+02	0	TOF	0.242E-02	84Ne01 *3)
Mylar	O ion	0.431E+02	0	TOF	0.235E-02	84Ne01 *3)
Mylar	O ion	0.971E+01	0	TOF	0.925E-02	84Ne01 *4)
Mylar	O ion	0.111E+02	0	TOF	0.816E-02	84Ne01 *4)
Mylar	O ion	0.123E+02	0	TOF	0.743E-02	84Ne01 *4)
Mylar	O ion	0.137E+02	0	TOF	0.698E-02	84Ne01 *4)
Mylar	O ion	0.148E+02	0	TOF	0.655E-02	84Ne01 *4)
Mylar	O ion	0.159E+02	0	TOF	0.588E-02	84Ne01 *4)
Mylar	O ion	0.174E+02	0	TOF	0.561E-02	84Ne01 *4)
Mylar	O ion	0.184E+02	0	TOF	0.527E-02	84Ne01 *4)
Mylar	O ion	0.199E+02	0	TOF	0.472E-02	84Ne01 *4)
Mylar	O ion	0.218E+02	0	TOF	0.451E-02	84Ne01 *4)
Mylar	O ion	0.236E+02	0	TOF	0.411E-02	84Ne01 *4)
Mylar	O ion	0.257E+02	0	TOF	0.386E-02	84Ne01 *4)
Mylar	O ion	0.278E+02	0	TOF	0.357E-02	84Ne01 *4)
Mylar	O ion	0.298E+02	0	TOF	0.341E-02	84Ne01 *4)
Mylar	O ion	0.317E+02	0	TOF	0.311E-02	84Ne01 *4)
Mylar	O ion	0.336E+02	0	TOF	0.288E-02	84Ne01 *4)
Mylar	O ion	0.355E+02	0	TOF	0.275E-02	84Ne01 *4)
Mylar	O ion	0.378E+02	0	TOF	0.266E-02	84Ne01 *4)
Mylar	O ion	0.399E+02	0	TOF	0.239E-02	84Ne01 *4)
Mylar	O ion	0.416E+02	0	TOF	0.211E-02	84Ne01 *4)
Mylar	O ion	0.430E+02	0	TOF	0.199E-02	84Ne01 *4)

*1) Desorbed species : cation of malachite green
*2) Desorbed species : cation of crystal violet
*3) Desorbed species : cation of verapamil
*4) Desorbed species : cation of verapamil mass number = 303

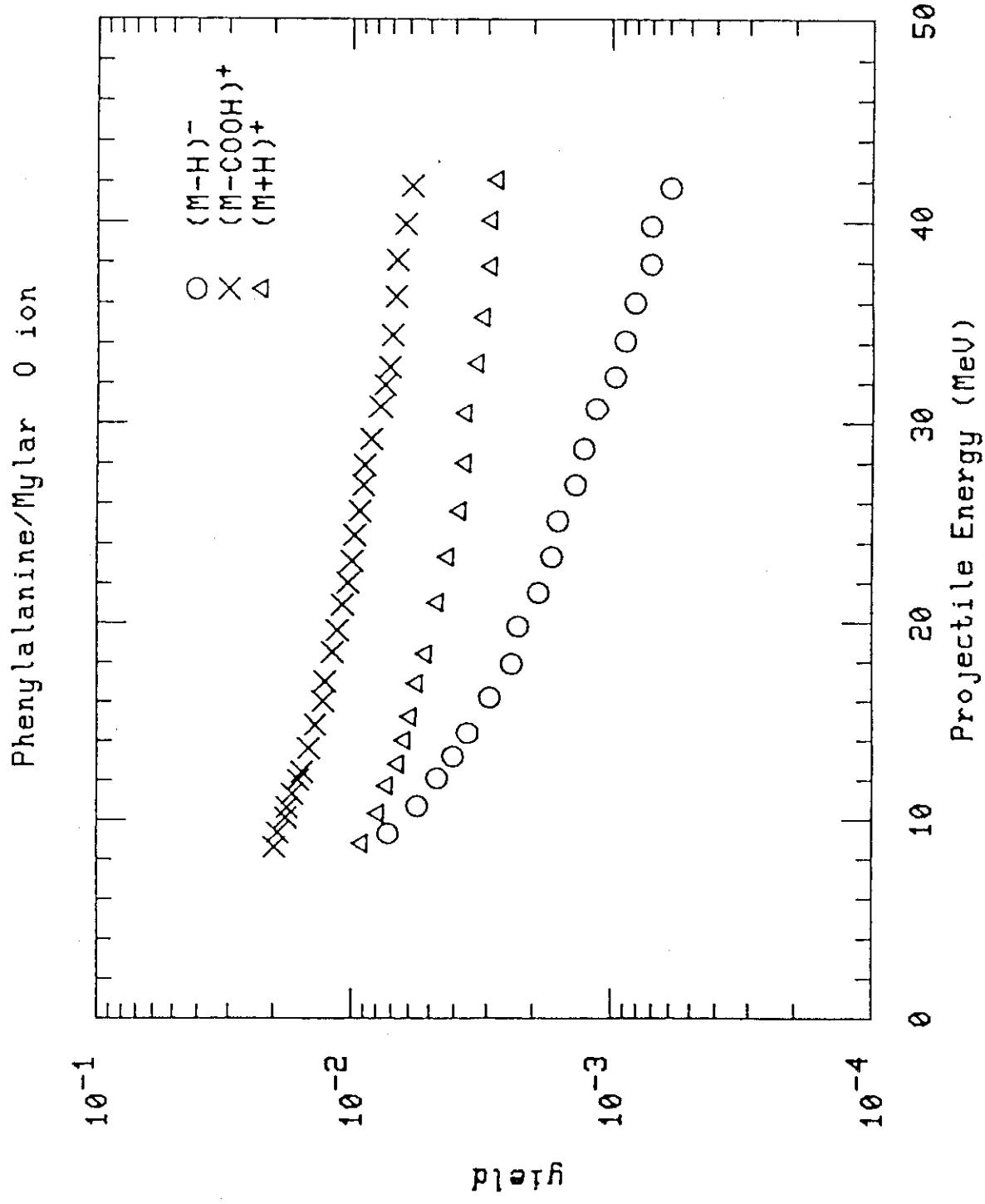

Fig.43 Desorption efficiency as a function of incident energy

DATA LIST

Substrate	Incident ion species	Incident energy (MeV)	Incident angle from normal (deg.)	Method	Yield	Ref.	Remark
Mylar	O ion	0.932E+01	0	TOF	0.719E-02	84Ne01	*1)
Mylar	O ion	0.107E+02	0	TOF	0.554E-02	84Ne01	*1)
Mylar	O ion	0.121E+02	0	TOF	0.466E-02	84Ne01	*1)
Mylar	O ion	0.132E+02	0	TOF	0.404E-02	84Ne01	*1)
Mylar	O ion	0.144E+02	0	TOF	0.355E-02	84Ne01	*1)
Mylar	O ion	0.162E+02	0	TOF	0.291E-02	84Ne01	*1)
Mylar	O ion	0.179E+02	0	TOF	0.240E-02	84Ne01	*1)
Mylar	O ion	0.198E+02	0	TOF	0.227E-02	84Ne01	*1)
Mylar	O ion	0.215E+02	0	TOF	0.190E-02	84Ne01	*1)
Mylar	O ion	0.233E+02	0	TOF	0.169E-02	84Ne01	*1)
Mylar	O ion	0.251E+02	0	TOF	0.160E-02	84Ne01	*1)
Mylar	O ion	0.269E+02	0	TOF	0.137E-02	84Ne01	*1)
Mylar	O ion	0.287E+02	0	TOF	0.127E-02	84Ne01	*1)
Mylar	O ion	0.307E+02	0	TOF	0.114E-02	84Ne01	*1)
Mylar	O ion	0.323E+02	0	TOF	0.966E-03	84Ne01	*1)
Mylar	O ion	0.341E+02	0	TOF	0.885E-03	84Ne01	*1)
Mylar	O ion	0.360E+02	0	TOF	0.810E-03	84Ne01	*1)
Mylar	O ion	0.379E+02	0	TOF	0.704E-03	84Ne01	*1)
Mylar	O ion	0.398E+02	0	TOF	0.702E-03	84Ne01	*1)
Mylar	O ion	0.417E+02	0	TOF	0.592E-03	84Ne01	*1)
Mylar	O ion	0.859E+01	0	TOF	0.198E-01	84Ne01	*2)
Mylar	O ion	0.934E+01	0	TOF	0.192E-01	84Ne01	*2)
Mylar	O ion	0.101E+02	0	TOF	0.179E-01	84Ne01	*2)
Mylar	O ion	0.106E+02	0	TOF	0.177E-01	84Ne01	*2)
Mylar	O ion	0.113E+02	0	TOF	0.169E-01	84Ne01	*2)
Mylar	O ion	0.120E+02	0	TOF	0.160E-01	84Ne01	*2)
Mylar	O ion	0.124E+02	0	TOF	0.155E-01	84Ne01	*2)
Mylar	O ion	0.136E+02	0	TOF	0.146E-01	84Ne01	*2)
Mylar	O ion	0.148E+02	0	TOF	0.138E-01	84Ne01	*2)
Mylar	O ion	0.160E+02	0	TOF	0.128E-01	84Ne01	*2)
Mylar	O ion	0.170E+02	0	TOF	0.126E-01	84Ne01	*2)
Mylar	O ion	0.185E+02	0	TOF	0.118E-01	84Ne01	*2)
Mylar	O ion	0.196E+02	0	TOF	0.113E-01	84Ne01	*2)
Mylar	O ion	0.209E+02	0	TOF	0.108E-01	84Ne01	*2)
Mylar	O ion	0.220E+02	0	TOF	0.103E-01	84Ne01	*2)
Mylar	O ion	0.231E+02	0	TOF	0.997E-02	84Ne01	*2)
Mylar	O ion	0.244E+02	0	TOF	0.974E-02	84Ne01	*2)
Mylar	O ion	0.256E+02	0	TOF	0.931E-02	84Ne01	*2)
Mylar	O ion	0.269E+02	0	TOF	0.901E-02	84Ne01	*2)
Mylar	O ion	0.279E+02	0	TOF	0.890E-02	84Ne01	*2)
Mylar	O ion	0.292E+02	0	TOF	0.842E-02	84Ne01	*2)
Mylar	O ion	0.308E+02	0	TOF	0.780E-02	84Ne01	*2)
Mylar	O ion	0.319E+02	0	TOF	0.747E-02	84Ne01	*2)

·/··

Mylar	O ion	0.328E+02	0	TOF	0.715E-02	84Ne01 *2)
Mylar	O ion	0.344E+02	0	TOF	0.699E-02	84Ne01 *2)
Mylar	O ion	0.363E+02	0	TOF	0.676E-02	84Ne01 *2)
Mylar	O ion	0.381E+02	0	TOF	0.668E-02	84Ne01 *2)
Mylar	O ion	0.399E+02	0	TOF	0.619E-02	84Ne01 *2)
Mylar	O ion	0.418E+02	0	TOF	0.586E-02	84Ne01 *2)
Mylar	O ion	0.877E+01	0	TOF	0.908E-02	84Ne01 *3)
Mylar	O ion	0.103E+02	0	TOF	0.786E-02	84Ne01 *3)
Mylar	O ion	0.117E+02	0	TOF	0.727E-02	84Ne01 *3)
Mylar	O ion	0.128E+02	0	TOF	0.658E-02	84Ne01 *3)
Mylar	O ion	0.140E+02	0	TOF	0.622E-02	84Ne01 *3)
Mylar	O ion	0.152E+02	0	TOF	0.589E-02	84Ne01 *3)
Mylar	O ion	0.169E+02	0	TOF	0.556E-02	84Ne01 *3)
Mylar	O ion	0.184E+02	0	TOF	0.515E-02	84Ne01 *3)
Mylar	O ion	0.210E+02	0	TOF	0.465E-02	84Ne01 *3)
Mylar	O ion	0.233E+02	0	TOF	0.425E-02	84Ne01 *3)
Mylar	O ion	0.256E+02	0	TOF	0.381E-02	84Ne01 *3)
Mylar	O ion	0.280E+02	0	TOF	0.364E-02	84Ne01 *3)
Mylar	O ion	0.305E+02	0	TOF	0.363E-02	84Ne01 *3)
Mylar	O ion	0.330E+02	0	TOF	0.328E-02	84Ne01 *3)
Mylar	O ion	0.353E+02	0	TOF	0.310E-02	84Ne01 *3)
Mylar	O ion	0.378E+02	0	TOF	0.290E-02	84Ne01 *3)
Mylar	O ion	0.401E+02	0	TOF	0.289E-02	84Ne01 *3)
Mylar	O ion	0.421E+02	0	TOF	0.274E-02	84Ne01 *3)

*1) Desorbed species : [M-H]-
*2) Desorbed species : [M-COOH]+
*3) Desorbed species : [M+H]+
Thickness 30~50 ug/cm**2

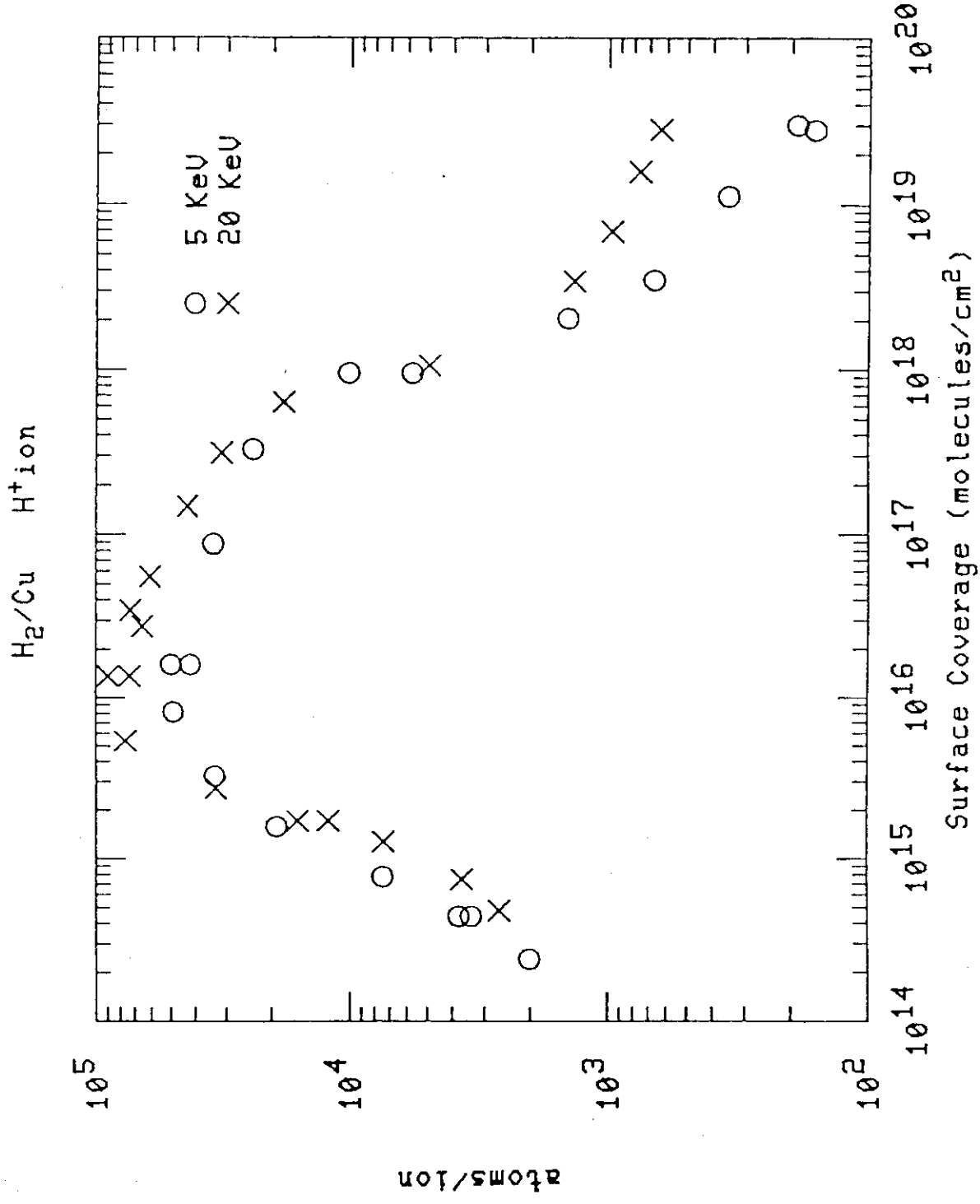

Fig.44 Desorption efficiency as a function of surface coverage

DATA LIST

Substrate	Incident ion species	Surface coverage (mol. /cm**2)	Incident energy (eV)	Method	Atoms per incident ion	Ref.
Cu	H+	0.240E+15	5000	MS	0.201E+04	73Er01
Cu	H+	0.438E+15	5000	MS	0.338E+04	73Er01
Cu	H+	0.438E+15	5000	MS	0.378E+04	73Er01
Cu	H+	0.769E+15	5000	MS	0.744E+04	73Er01
Cu	H+	0.158E+16	5000	MS	0.191E+05	73Er01
Cu	H+	0.323E+16	5000	MS	0.335E+05	73Er01
Cu	H+	0.811E+16	5000	MS	0.491E+05	73Er01
Cu	H+	0.160E+17	5000	MS	0.501E+05	73Er01
Cu	H+	0.160E+17	5000	MS	0.418E+05	73Er01
Cu	H+	0.873E+17	5000	MS	0.340E+05	73Er01
Cu	H+	0.327E+18	5000	MS	0.237E+05	73Er01
Cu	H+	0.950E+18	5000	MS	0.575E+04	73Er01
Cu	H+	0.950E+18	5000	MS	0.101E+05	73Er01
Cu	H+	0.204E+19	5000	MS	0.143E+04	73Er01
Cu	H+	0.349E+19	5000	MS	0.668E+03	73Er01
Cu	H+	0.112E+20	5000	MS	0.349E+03	73Er01
Cu	H+	0.279E+20	5000	MS	0.163E+03	73Er01
Cu	H+	0.299E+20	5000	MS	0.191E+03	73Er01
Cu	H+	0.470E+15	20000	MS	0.263E+04	73Er01
Cu	H+	0.736E+15	20000	MS	0.368E+04	73Er01
Cu	H+	0.126E+16	20000	MS	0.739E+04	73Er01
Cu	H+	0.170E+16	20000	MS	0.121E+05	73Er01
Cu	H+	0.170E+16	20000	MS	0.159E+05	73Er01
Cu	H+	0.271E+16	20000	MS	0.333E+05	73Er01
Cu	H+	0.533E+16	20000	MS	0.778E+05	73Er01
Cu	H+	0.135E+17	20000	MS	0.906E+05	73Er01
Cu	H+	0.135E+17	20000	MS	0.740E+05	73Er01
Cu	H+	0.274E+17	20000	MS	0.659E+05	73Er01
Cu	H+	0.344E+17	20000	MS	0.736E+05	73Er01
Cu	H+	0.551E+17	20000	MS	0.613E+05	73Er01
Cu	H+	0.148E+18	20000	MS	0.436E+05	73Er01
Cu	H+	0.310E+18	20000	MS	0.317E+05	73Er01
Cu	H+	0.634E+18	20000	MS	0.181E+05	73Er01
Cu	H+	0.106E+19	20000	MS	0.494E+04	73Er01
Cu	H+	0.344E+19	20000	MS	0.135E+04	73Er01
Cu	H+	0.689E+19	20000	MS	0.966E+03	73Er01
Cu	H+	0.158E+20	20000	MS	0.756E+03	73Er01
Cu	H+	0.282E+20	20000	MS	0.632E+03	73Er01

The gas desorption rate was measured dynamically with QMS.
The angle of incidence was normal to the condensed layer.
Surface temp. 3.2K

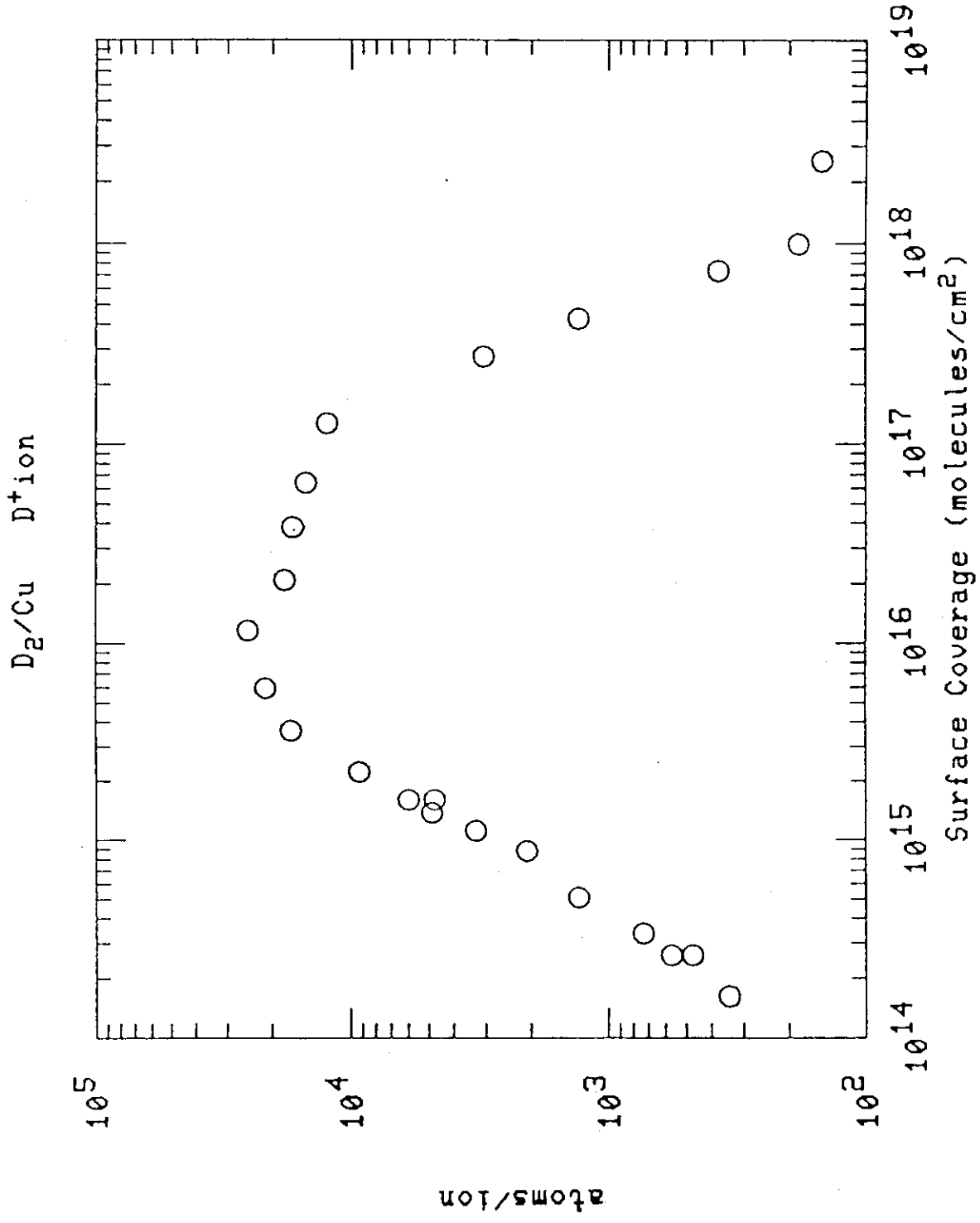

Fig.45 Desorption efficiency as a function of surface coverage

DATA LIST

Substrate	Incident ion species	Surface coverage (mol. /cm**2)	Incident energy (eV)	Method	Atoms per incident ion	Ref.
Cu	D+	0.161E+15	5000	MS	0.341E+03	73Er01
Cu	D+	0.260E+15	5000	MS	0.471E+03	73Er01
Cu	D+	0.260E+15	5000	MS	0.567E+03	73Er01
Cu	D+	0.335E+15	5000	MS	0.731E+03	73Er01
Cu	D+	0.508E+15	5000	MS	0.130E+04	73Er01
Cu	D+	0.879E+15	5000	MS	0.207E+04	73Er01
Cu	D+	0.111E+16	5000	MS	0.328E+04	73Er01
Cu	D+	0.137E+16	5000	MS	0.486E+04	73Er01
Cu	D+	0.160E+16	5000	MS	0.474E+04	73Er01
Cu	D+	0.160E+16	5000	MS	0.598E+04	73Er01
Cu	D+	0.222E+16	5000	MS	0.927E+04	73Er01
Cu	D+	0.360E+16	5000	MS	0.169E+05	73Er01
Cu	D+	0.592E+16	5000	MS	0.212E+05	73Er01
Cu	D+	0.116E+17	5000	MS	0.248E+05	73Er01
Cu	D+	0.208E+17	5000	MS	0.179E+05	73Er01
Cu	D+	0.380E+17	5000	MS	0.167E+05	73Er01
Cu	D+	0.636E+17	5000	MS	0.148E+05	73Er01
Cu	D+	0.127E+18	5000	MS	0.123E+05	73Er01
Cu	D+	0.274E+18	5000	MS	0.306E+04	73Er01
Cu	D+	0.424E+18	5000	MS	0.130E+04	73Er01
Cu	D+	0.730E+18	5000	MS	0.374E+03	73Er01
Cu	D+	0.991E+18	5000	MS	0.183E+03	73Er01
Cu	D+	0.254E+19	5000	MS	0.148E+03	73Er01

The gas desorption rate was measured dynamically with QMS.
The angle of incidence was normal to the condensed layer.
Surface temperature 4.2K

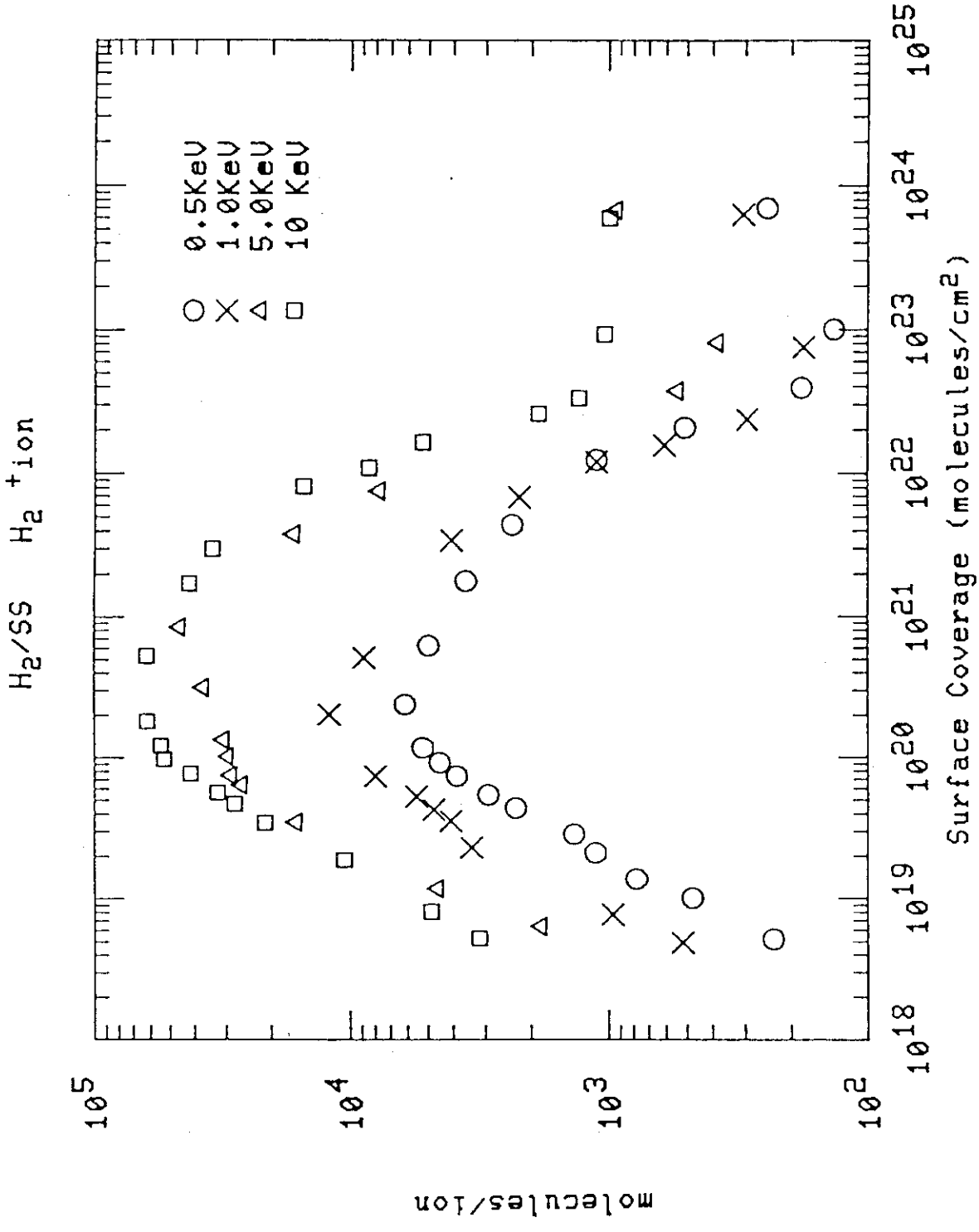

Fig.46 Desorption efficiency as a function of surface coverage

DATA LIST

Substrate	Incident ion species	Surface coverage (mol. /cm**2)	Incident energy (eV)	Method	Molecules per incident ion	Ref.
SS	H2 +	0.514E+19	500	*1)	0.233E+03	77Hi01
SS	H2 +	0.100E+20	500	*1)	0.474E+03	77Hi01
SS	H2 +	0.137E+20	500	*1)	0.776E+03	77Hi01
SS	H2 +	0.210E+20	500	*1)	0.112E+04	77Hi01
SS	H2 +	0.286E+20	500	*1)	0.135E+04	77Hi01
SS	H2 +	0.438E+20	500	*1)	0.228E+04	77Hi01
SS	H2 +	0.542E+20	500	*1)	0.292E+04	77Hi01
SS	H2 +	0.736E+20	500	*1)	0.385E+04	77Hi01
SS	H2 +	0.912E+20	500	*1)	0.449E+04	77Hi01
SS	H2 +	0.117E+21	500	*1)	0.524E+04	77Hi01
SS	H2 +	0.237E+21	500	*1)	0.613E+04	77Hi01
SS	H2 +	0.620E+21	500	*1)	0.498E+04	77Hi01
SS	H2 +	0.178E+22	500	*1)	0.358E+04	77Hi01
SS	H2 +	0.440E+22	500	*1)	0.236E+04	77Hi01
SS	H2 +	0.124E+23	500	*1)	0.111E+04	77Hi01
SS	H2 +	0.206E+23	500	*1)	0.508E+03	77Hi01
SS	H2 +	0.391E+23	500	*1)	0.182E+03	77Hi01
SS	H2 +	0.999E+23	500	*1)	0.136E+03	77Hi01
SS	H2 +	0.697E+24	500	*1)	0.246E+03	77Hi01
SS	H2 +	0.479E+19	1000	*1)	0.516E+03	77Hi01
SS	H2 +	0.757E+19	1000	*1)	0.956E+03	77Hi01
SS	H2 +	0.227E+20	1000	*1)	0.338E+04	77Hi01
SS	H2 +	0.350E+20	1000	*1)	0.407E+04	77Hi01
SS	H2 +	0.420E+20	1000	*1)	0.475E+04	77Hi01
SS	H2 +	0.521E+20	1000	*1)	0.554E+04	77Hi01
SS	H2 +	0.729E+20	1000	*1)	0.801E+04	77Hi01
SS	H2 +	0.201E+21	1000	*1)	0.120E+05	77Hi01
SS	H2 +	0.510E+21	1000	*1)	0.887E+04	77Hi01
SS	H2 +	0.341E+22	1000	*1)	0.407E+04	77Hi01
SS	H2 +	0.680E+22	1000	*1)	0.222E+04	77Hi01
SS	H2 +	0.120E+23	1000	*1)	0.111E+04	77Hi01
SS	H2 +	0.156E+23	1000	*1)	0.607E+03	77Hi01
SS	H2 +	0.236E+23	1000	*1)	0.295E+03	77Hi01
SS	H2 +	0.751E+23	1000	*1)	0.178E+03	77Hi01
SS	H2 +	0.632E+24	1000	*1)	0.304E+03	77Hi01
SS	H2 +	0.624E+19	5000	*1)	0.182E+04	77Hi01
SS	H2 +	0.115E+20	5000	*1)	0.457E+04	77Hi01
SS	H2 +	0.344E+20	5000	*1)	0.161E+05	77Hi01
SS	H2 +	0.634E+20	5000	*1)	0.263E+05	77Hi01
SS	H2 +	0.739E+20	5000	*1)	0.289E+05	77Hi01
SS	H2 +	0.101E+21	5000	*1)	0.298E+05	77Hi01
SS	H2 +	0.133E+21	5000	*1)	0.308E+05	77Hi01

·/··

SS	H2 +	0.314E+21	5000	*1)	0.370E+05	77Hi01
SS	H2 +	0.841E+21	5000	*1)	0.460E+05	77Hi01
SS	H2 +	0.377E+22	5000	*1)	0.165E+05	77Hi01
SS	H2 +	0.753E+22	5000	*1)	0.773E+04	77Hi01
SS	H2 +	0.372E+23	5000	*1)	0.542E+03	77Hi01
SS	H2 +	0.812E+23	5000	*1)	0.380E+03	77Hi01
SS	H2 +	0.677E+24	5000	*1)	0.929E+03	77Hi01
SS	H2 +	0.515E+19	10000	*1)	0.315E+04	77Hi01
SS	H2 +	0.791E+19	10000	*1)	0.485E+04	77Hi01
SS	H2 +	0.186E+20	10000	*1)	0.105E+05	77Hi01
SS	H2 +	0.343E+20	10000	*1)	0.212E+05	77Hi01
SS	H2 +	0.465E+20	10000	*1)	0.280E+05	77Hi01
SS	H2 +	0.559E+20	10000	*1)	0.326E+05	77Hi01
SS	H2 +	0.759E+20	10000	*1)	0.417E+05	77Hi01
SS	H2 +	0.968E+20	10000	*1)	0.532E+05	77Hi01
SS	H2 +	0.120E+21	10000	*1)	0.549E+05	77Hi01
SS	H2 +	0.179E+21	10000	*1)	0.621E+05	77Hi01
SS	H2 +	0.527E+21	10000	*1)	0.623E+05	77Hi01
SS	H2 +	0.171E+22	10000	*1)	0.421E+05	77Hi01
SS	H2 +	0.300E+22	10000	*1)	0.341E+05	77Hi01
SS	H2 +	0.816E+22	10000	*1)	0.151E+05	77Hi01
SS	H2 +	0.109E+23	10000	*1)	0.848E+04	77Hi01
SS	H2 +	0.164E+23	10000	*1)	0.523E+04	77Hi01
SS	H2 +	0.258E+23	10000	*1)	0.187E+04	77Hi01
SS	H2 +	0.333E+23	10000	*1)	0.130E+04	77Hi01
SS	H2 +	0.930E+23	10000	*1)	0.103E+04	77Hi01
SS	H2 +	0.597E+24	10000	*1)	0.986E+03	77Hi01

*1) The desorption yield was obtained from the measured ion currrnt and pressure incrase during ion bombardment.
Surface temperature 3.2K
SS : Stainless steel

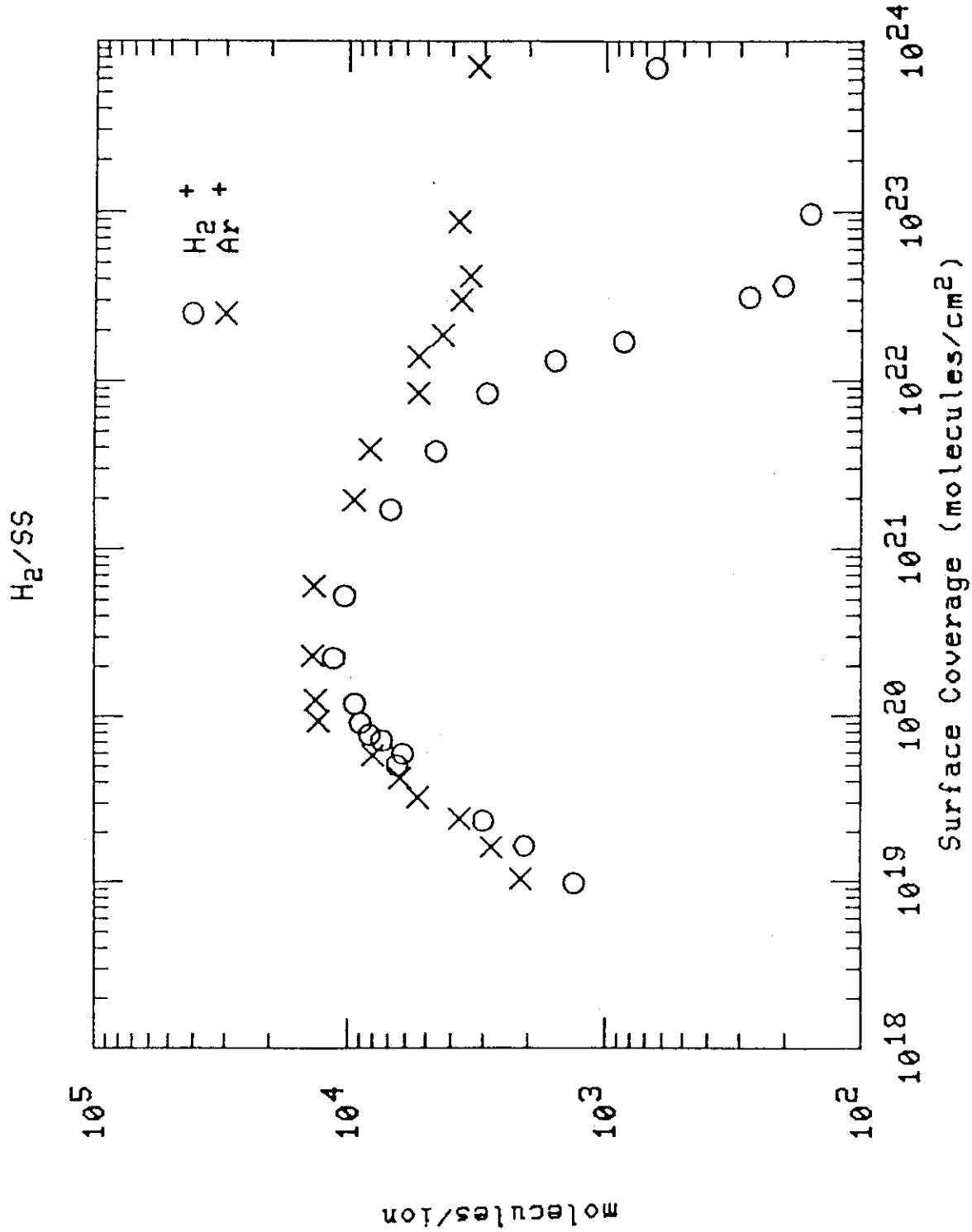

Fig.47 Desorption efficiency as a function of surface coverage

DATA LIST

Substrate	Incident ion species	Surface coverage (mol. /cm**2)	Incident energy (eV)	Method	Molecules per incident ion	Ref.
SS	H2 +	0.967E+19	1000	*1)	0.131E+04	77Hi01
SS	H2 +	0.164E+20	1000	*1)	0.206E+04	77Hi01
SS	H2 +	0.232E+20	1000	*1)	0.299E+04	77Hi01
SS	H2 +	0.502E+20	1000	*1)	0.647E+04	77Hi01
SS	H2 +	0.589E+20	1000	*1)	0.613E+04	77Hi01
SS	H2 +	0.709E+20	1000	*1)	0.738E+04	77Hi01
SS	H2 +	0.768E+20	1000	*1)	0.821E+04	77Hi01
SS	H2 +	0.902E+20	1000	*1)	0.888E+04	77Hi01
SS	H2 +	0.118E+21	1000	*1)	0.936E+04	77Hi01
SS	H2 +	0.223E+21	1000	*1)	0.113E+05	77Hi01
SS	H2 +	0.525E+21	1000	*1)	0.103E+05	77Hi01
SS	H2 +	0.170E+22	1000	*1)	0.689E+04	77Hi01
SS	H2 +	0.377E+22	1000	*1)	0.460E+04	77Hi01
SS	H2 +	0.837E+22	1000	*1)	0.291E+04	77Hi01
SS	H2 +	0.131E+23	1000	*1)	0.157E+04	77Hi01
SS	H2 +	0.171E+23	1000	*1)	0.847E+03	77Hi01
SS	H2 +	0.312E+23	1000	*1)	0.275E+03	77Hi01
SS	H2 +	0.365E+23	1000	*1)	0.204E+03	77Hi01
SS	H2 +	0.973E+23	1000	*1)	0.160E+03	77Hi01
SS	H2 +	0.704E+24	1000	*1)	0.636E+03	77Hi01
SS	Ar+	0.102E+20	1000	*1)	0.212E+04	77Hi01
SS	Ar+	0.160E+20	1000	*1)	0.277E+04	77Hi01
SS	Ar+	0.238E+20	1000	*1)	0.370E+04	77Hi01
SS	Ar+	0.319E+20	1000	*1)	0.538E+04	77Hi01
SS	Ar+	0.416E+20	1000	*1)	0.630E+04	77Hi01
SS	Ar+	0.573E+20	1000	*1)	0.800E+04	77Hi01
SS	Ar+	0.925E+20	1000	*1)	0.129E+05	77Hi01
SS	Ar+	0.124E+21	1000	*1)	0.132E+05	77Hi01
SS	Ar+	0.229E+21	1000	*1)	0.136E+05	77Hi01
SS	Ar+	0.600E+21	1000	*1)	0.135E+05	77Hi01
SS	Ar+	0.194E+22	1000	*1)	0.949E+04	77Hi01
SS	Ar+	0.388E+22	1000	*1)	0.828E+04	77Hi01
SS	Ar+	0.839E+22	1000	*1)	0.538E+04	77Hi01
SS	Ar+	0.139E+23	1000	*1)	0.537E+04	77Hi01
SS	Ar+	0.187E+23	1000	*1)	0.433E+04	77Hi01
SS	Ar+	0.301E+23	1000	*1)	0.368E+04	77Hi01
SS	Ar+	0.414E+23	1000	*1)	0.339E+04	77Hi01
SS	Ar+	0.875E+23	1000	*1)	0.376E+04	77Hi01
SS	Ar+	0.717E+24	1000	*1)	0.317E+04	77Hi01

*1) The desorption yield was obtained from the measured ion current and pressure increase during ion bombardment.
Surface temperature 3.18K
SS : Stainless steel

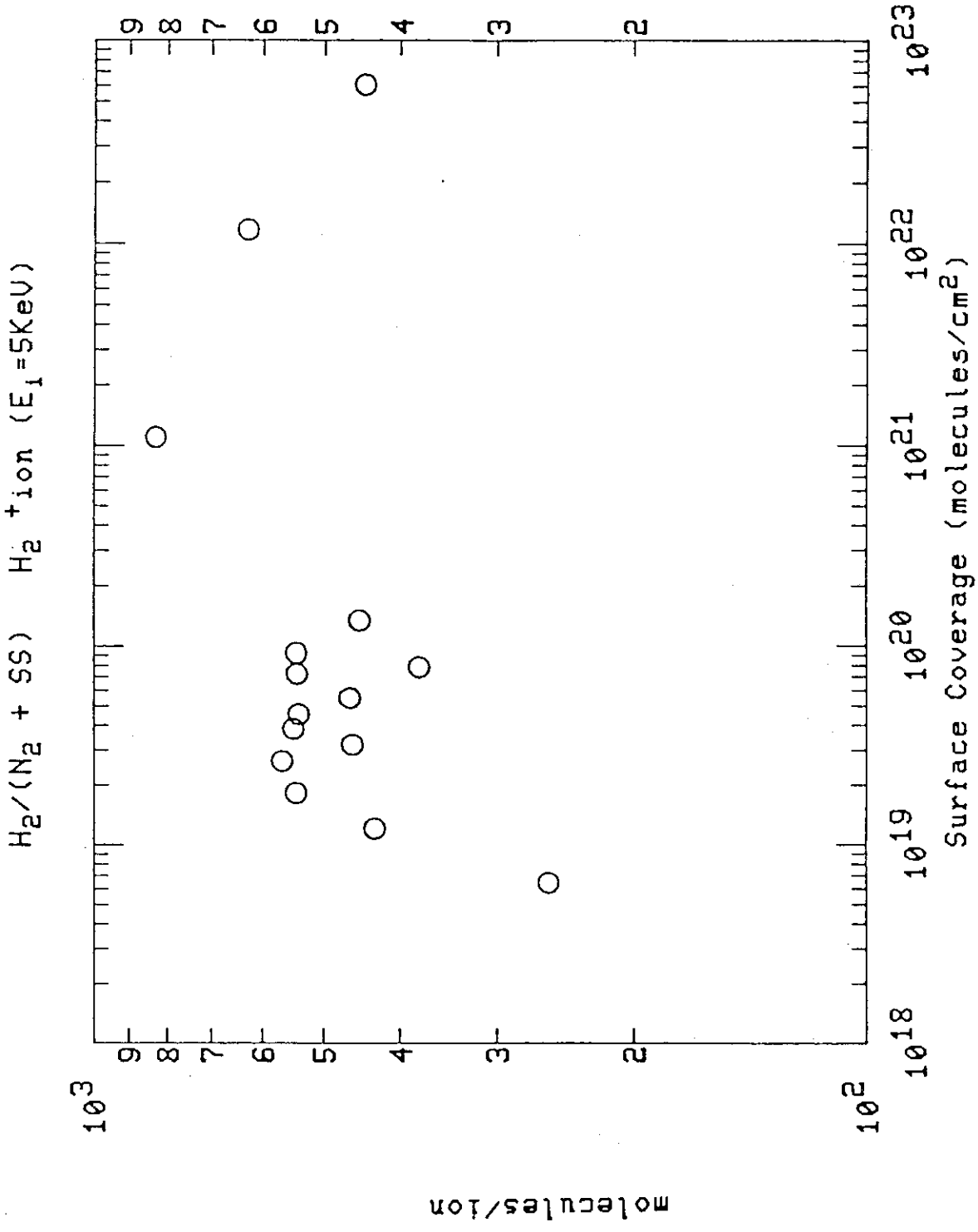

Fig.48 Desorption efficiency as a function of surface coverage

DATA LIST

Substrate	Incident ion species	Surface coverage (mol. /cm**2)	Incident energy (eV)	Method	Molecules per incident ion	Ref.
SS	H2 +	0.641E+19	5000	*1)	0.257E+03	77Hi01
SS	H2 +	0.120E+20	5000	*1)	0.431E+03	77Hi01
SS	H2 +	0.181E+20	5000	*1)	0.543E+03	77Hi01
SS	H2 +	0.263E+20	5000	*1)	0.566E+03	77Hi01
SS	H2 +	0.318E+20	5000	*1)	0.460E+03	77Hi01
SS	H2 +	0.382E+20	5000	*1)	0.547E+03	77Hi01
SS	H2 +	0.452E+20	5000	*1)	0.538E+03	77Hi01
SS	H2 +	0.546E+20	5000	*1)	0.463E+03	77Hi01
SS	H2 +	0.721E+20	5000	*1)	0.541E+03	77Hi01
SS	H2 +	0.779E+20	5000	*1)	0.377E+03	77Hi01
SS	H2 +	0.919E+20	5000	*1)	0.542E+03	77Hi01
SS	H2 +	0.134E+21	5000	*1)	0.450E+03	77Hi01
SS	H2 +	0.110E+22	5000	*1)	0.830E+03	77Hi01
SS	H2 +	0.117E+23	5000	*1)	0.628E+03	77Hi01
SS	H2 +	0.608E+23	5000	*1)	0.444E+03	77Hi01

*1) The desorption yield was obtained from the measured ion current and pressure increase during ion bombardment.
Surface temperature 2.78K
SS : Stainless steel
Hydrogen was condensed on a nitrogen layer (1.7E+21 mol/m**2)

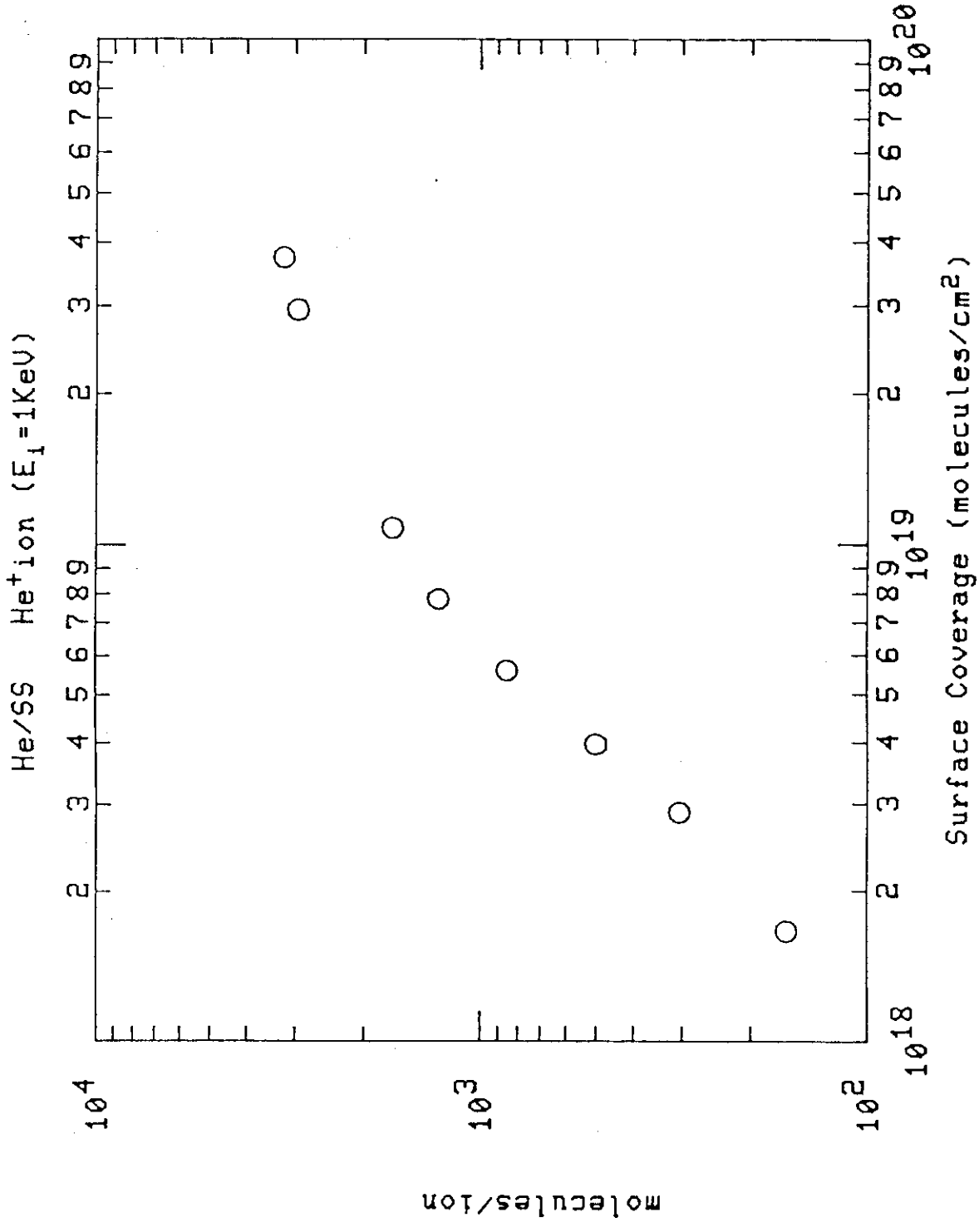

Fig.49 Desorption efficiency as a function of surface coverage

DATA LIST

Substrate	Incident ion species	Surface coverage (mol. /cm**2)	Incident energy (eV)	Method	Molecules per incident ion	Ref.
SS	He+	0.166E+19	1000	*1)	0.162E+03	77Hi01
SS	He+	0.288E+19	1000	*1)	0.304E+03	77Hi01
SS	He+	0.397E+19	1000	*1)	0.499E+03	77Hi01
SS	He+	0.560E+19	1000	*1)	0.849E+03	77Hi01
SS	He+	0.780E+19	1000	*1)	0.128E+04	77Hi01
SS	He+	0.108E+20	1000	*1)	0.168E+04	77Hi01
SS	He+	0.294E+20	1000	*1)	0.295E+04	77Hi01
SS	He+	0.373E+20	1000	*1)	0.320E+04	77Hi01

*1) The desorption yield was obtained from the measured ion current and pressure increase during ion bombardment.
The desorption yield of physisorbed helium.
Surface temperature 2.23K
SS : Stainless steel

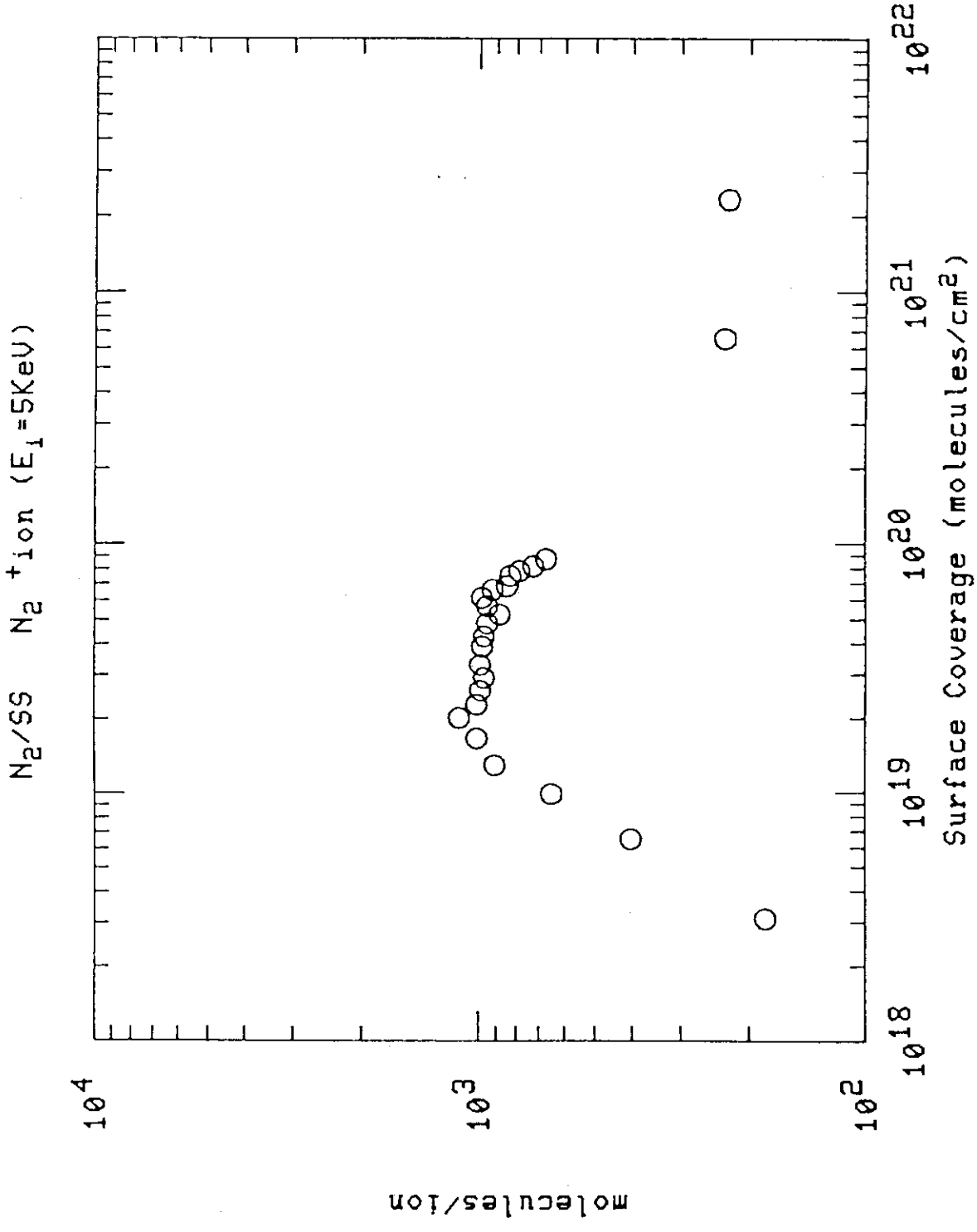

Fig.50 Desorption efficiency as a function of surface coverage

DATA LIST

Substrate	Incident ion species	Surface coverage (mol. /cm**2)	Incident energy (eV)	Method	Molecules per incident ion	Ref.
SS	N2 +	0.309E+19	5000	*1)	0.182E+03	77Hi01
SS	N2 +	0.650E+19	5000	*1)	0.404E+03	77Hi01
SS	N2 +	0.989E+19	5000	*1)	0.649E+03	77Hi01
SS	N2 +	0.129E+20	5000	*1)	0.909E+03	77Hi01
SS	N2 +	0.166E+20	5000	*1)	0.101E+04	77Hi01
SS	N2 +	0.201E+20	5000	*1)	0.112E+04	77Hi01
SS	N2 +	0.227E+20	5000	*1)	0.101E+04	77Hi01
SS	N2 +	0.258E+20	5000	*1)	0.990E+03	77Hi01
SS	N2 +	0.290E+20	5000	*1)	0.969E+03	77Hi01
SS	N2 +	0.327E+20	5000	*1)	0.990E+03	77Hi01
SS	N2 +	0.388E+20	5000	*1)	0.979E+03	77Hi01
SS	N2 +	0.427E+20	5000	*1)	0.969E+03	77Hi01
SS	N2 +	0.481E+20	5000	*1)	0.949E+03	77Hi01
SS	N2 +	0.524E+20	5000	*1)	0.881E+03	77Hi01
SS	N2 +	0.565E+20	5000	*1)	0.949E+03	77Hi01
SS	N2 +	0.610E+20	5000	*1)	0.979E+03	77Hi01
SS	N2 +	0.657E+20	5000	*1)	0.919E+03	77Hi01
SS	N2 +	0.679E+20	5000	*1)	0.845E+03	77Hi01
SS	N2 +	0.748E+20	5000	*1)	0.827E+03	77Hi01
SS	N2 +	0.780E+20	5000	*1)	0.784E+03	77Hi01
SS	N2 +	0.815E+20	5000	*1)	0.721E+03	77Hi01
SS	N2 +	0.869E+20	5000	*1)	0.669E+03	77Hi01
SS	N2 +	0.654E+21	5000	*1)	0.232E+03	77Hi01
SS	N2 +	0.233E+22	5000	*1)	0.227E+03	77Hi01

*1) The desorption yield was obtained from the measured ion current and pressure increase during ion bombardment.
Surface temperature 4.2K
SS : Stainless steel

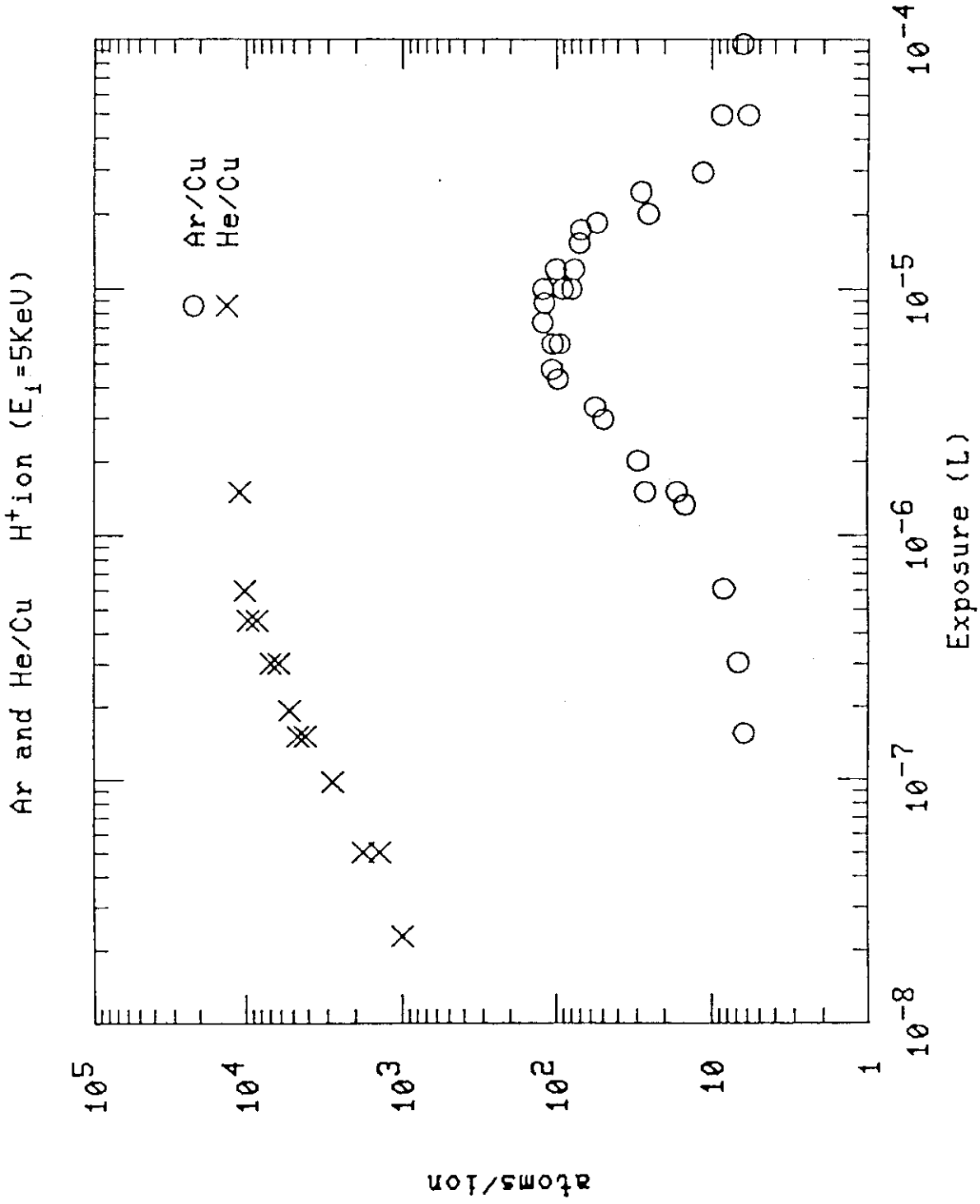

Fig.51 Desorption efficiency as a function of exposure

DATA LIST

Substrate	Incident ion species	Exposure (L)	Incident energy (eV)	Method	Atoms per incident ion	Ref.	Remark
Cu	H+	0.154E-06	5000	MS	0.625E+01	75Er02	*1)
Cu	H+	0.302E-06	5000	MS	0.678E+01	75Er02	*1)
Cu	H+	0.604E-06	5000	MS	0.838E+01	75Er02	*1)
Cu	H+	0.133E-05	5000	MS	0.148E+02	75Er02	*1)
Cu	H+	0.150E-05	5000	MS	0.165E+02	75Er02	*1)
Cu	H+	0.150E-05	5000	MS	0.263E+02	75Er02	*1)
Cu	H+	0.200E-05	5000	MS	0.293E+02	75Er02	*1)
Cu	H+	0.296E-05	5000	MS	0.492E+02	75Er02	*1)
Cu	H+	0.331E-05	5000	MS	0.559E+02	75Er02	*1)
Cu	H+	0.431E-05	5000	MS	0.975E+02	75Er02	*1)
Cu	H+	0.473E-05	5000	MS	0.107E+03	75Er02	*1)
Cu	H+	0.600E-05	5000	MS	0.106E+03	75Er02	*1)
Cu	H+	0.600E-05	5000	MS	0.951E+02	75Er02	*1)
Cu	H+	0.733E-05	5000	MS	0.123E+03	75Er02	*1)
Cu	H+	0.878E-05	5000	MS	0.120E+03	75Er02	*1)
Cu	H+	0.100E-04	5000	MS	0.122E+03	75Er02	*1)
Cu	H+	0.100E-04	5000	MS	0.907E+02	75Er02	*1)
Cu	H+	0.100E-04	5000	MS	0.796E+02	75Er02	*1)
Cu	H+	0.120E-04	5000	MS	0.101E+03	75Er02	*1)
Cu	H+	0.120E-04	5000	MS	0.763E+02	75Er02	*1)
Cu	H+	0.153E-04	5000	MS	0.705E+02	75Er02	*1)
Cu	H+	0.173E-04	5000	MS	0.691E+02	75Er02	*1)
Cu	H+	0.185E-04	5000	MS	0.541E+02	75Er02	*1)
Cu	H+	0.200E-04	5000	MS	0.251E+02	75Er02	*1)
Cu	H+	0.245E-04	5000	MS	0.280E+02	75Er02	*1)
Cu	H+	0.294E-04	5000	MS	0.114E+02	75Er02	*1)
Cu	H+	0.500E-04	5000	MS	0.867E+01	75Er02	*1)
Cu	H+	0.500E-04	5000	MS	0.585E+01	75Er02	*1)
Cu	H+	0.962E-04	5000	MS	0.635E+01	75Er02	*1)
Cu	H+	0.226E-07	5000	MS	0.100E+04	75Er02	*2)
Cu	H+	0.500E-07	5000	MS	0.179E+04	75Er02	*2)
Cu	H+	0.500E-07	5000	MS	0.140E+04	75Er02	*2)
Cu	H+	0.974E-07	5000	MS	0.280E+04	75Er02	*2)
Cu	H+	0.150E-06	5000	MS	0.468E+04	75Er02	*2)
Cu	H+	0.150E-06	5000	MS	0.418E+04	75Er02	*2)
Cu	H+	0.192E-06	5000	MS	0.530E+04	75Er02	*2)
Cu	H+	0.300E-06	5000	MS	0.708E+04	75Er02	*2)
Cu	H+	0.300E-06	5000	MS	0.621E+04	75Er02	*2)
Cu	H+	0.450E-06	5000	MS	0.981E+04	75Er02	*2)
Cu	H+	0.450E-06	5000	MS	0.861E+04	75Er02	*2)
Cu	H+	0.596E-06	5000	MS	0.103E+05	75Er02	*2)
Cu	H+	0.150E-05	5000	MS	0.111E+05	75Er02	*2)

*1) Ar-exposure, Surface temperature 4.2K
*2) He-exposure, Surface temperature 4.2K

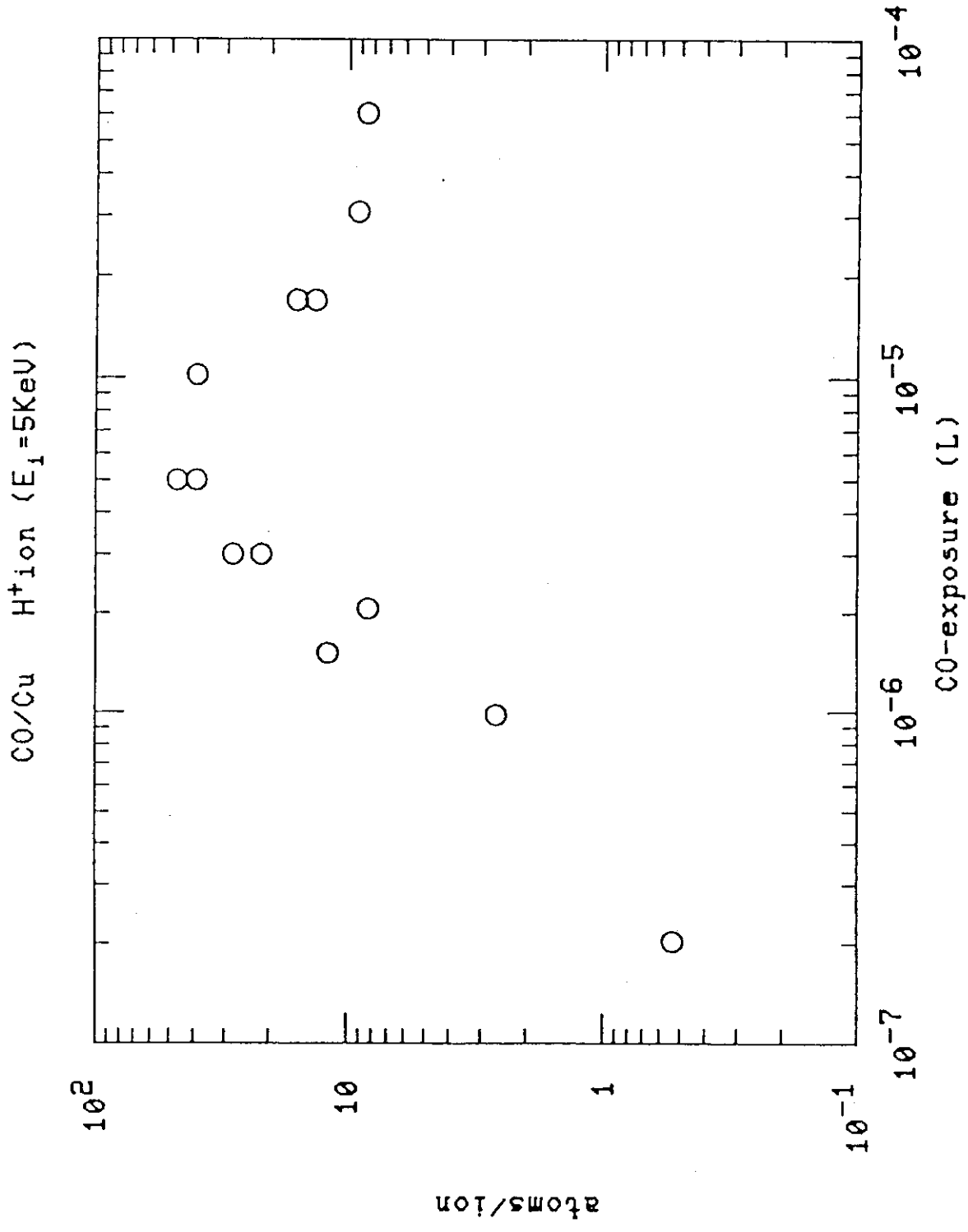

Fig.52 Desorption efficiency as a function of exposure

DATA LIST

Substrate	Incident ion species	Exposure (L)	Incident energy (eV)	Method	Atoms per incident ion	Ref.
Cu	H+	0.203E-06	5000	MS	0.531E+00	75Er02
Cu	H+	0.980E-06	5000	MS	0.261E+01	75Er02
Cu	H+	0.151E-05	5000	MS	0.118E+02	75Er02
Cu	H+	0.206E-05	5000	MS	0.827E+01	75Er02
Cu	H+	0.300E-05	5000	MS	0.278E+02	75Er02
Cu	H+	0.300E-05	5000	MS	0.215E+02	75Er02
Cu	H+	0.500E-05	5000	MS	0.467E+02	75Er02
Cu	H+	0.500E-05	5000	MS	0.389E+02	75Er02
Cu	H+	0.102E-04	5000	MS	0.389E+02	75Er02
Cu	H+	0.170E-04	5000	MS	0.157E+02	75Er02
Cu	H+	0.170E-04	5000	MS	0.133E+02	75Er02
Cu	H+	0.308E-04	5000	MS	0.912E+01	75Er02
Cu	H+	0.605E-04	5000	MS	0.849E+01	75Er02

Surface temperature 4.2K

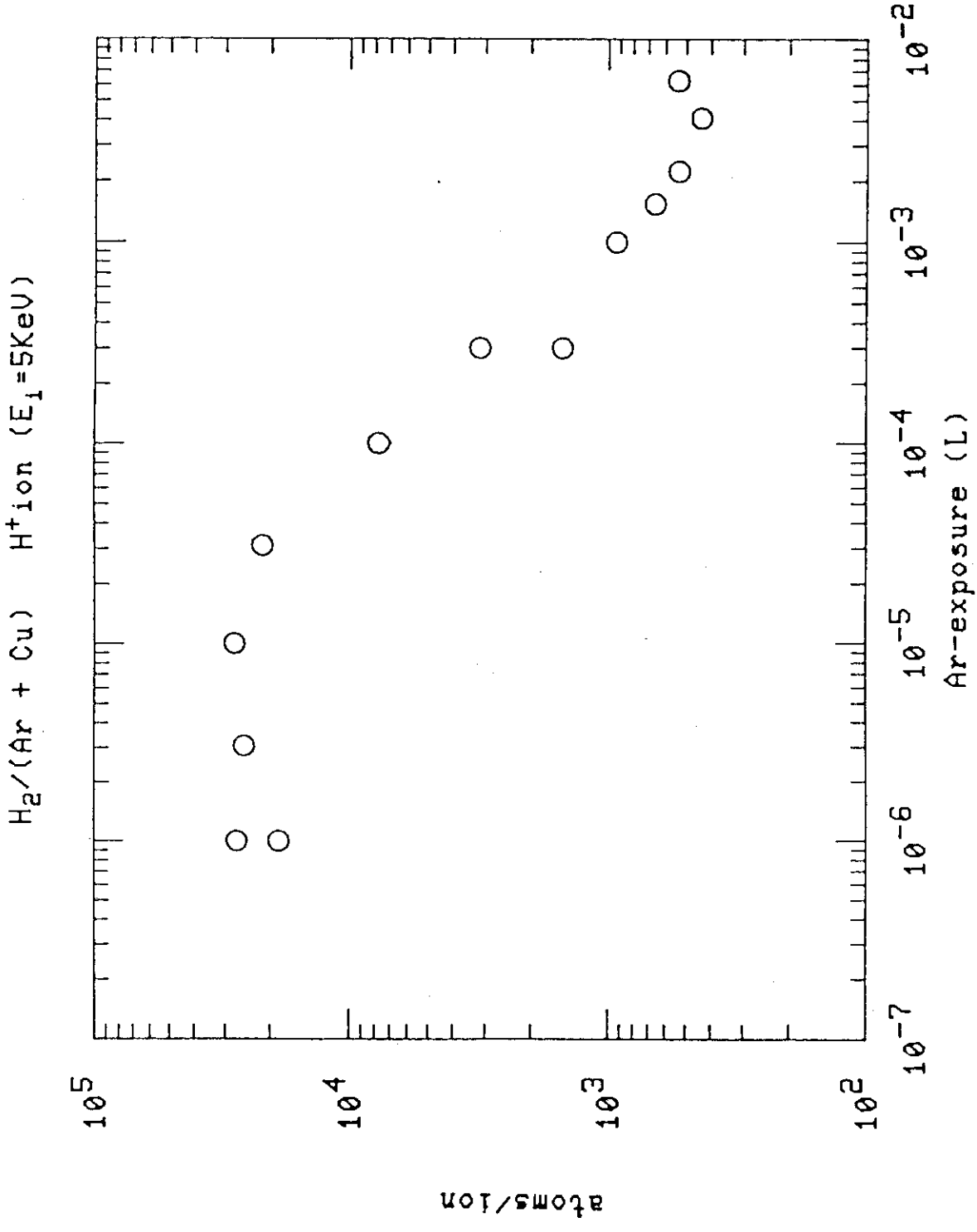

Fig.53 Desorption efficiency as a function of exposure

DATA LIST

Substrate	Incident ion species	Exposure (L)	Incident energy (eV)	Method	Atoms per incident ion	Ref.
Cu	H+	0.100E-05	5000	MS	0.270E+05	75Er02
Cu	H+	0.100E-05	5000	MS	0.185E+05	75Er02
Cu	H+	0.306E-05	5000	MS	0.253E+05	75Er02
Cu	H+	0.100E-04	5000	MS	0.276E+05	75Er02
Cu	H+	0.310E-04	5000	MS	0.214E+05	75Er02
Cu	H+	0.100E-03	5000	MS	0.775E+04	75Er02
Cu	H+	0.300E-03	5000	MS	0.315E+04	75Er02
Cu	H+	0.300E-03	5000	MS	0.150E+04	75Er02
Cu	H+	0.100E-02	5000	MS	0.923E+03	75Er02
Cu	H+	0.154E-02	5000	MS	0.654E+03	75Er02
Cu	H+	0.223E-02	5000	MS	0.529E+03	75Er02
Cu	H+	0.411E-02	5000	MS	0.435E+03	75Er02
Cu	H+	0.629E-02	5000	MS	0.535E+03	75Er02

Desorption of hydrogen from a layer of hydrogen condensed on top of a layer of argon.
Hydrogen layer thickness ~2.0E+16 mol./cm**2
Surface temp. 2.5K

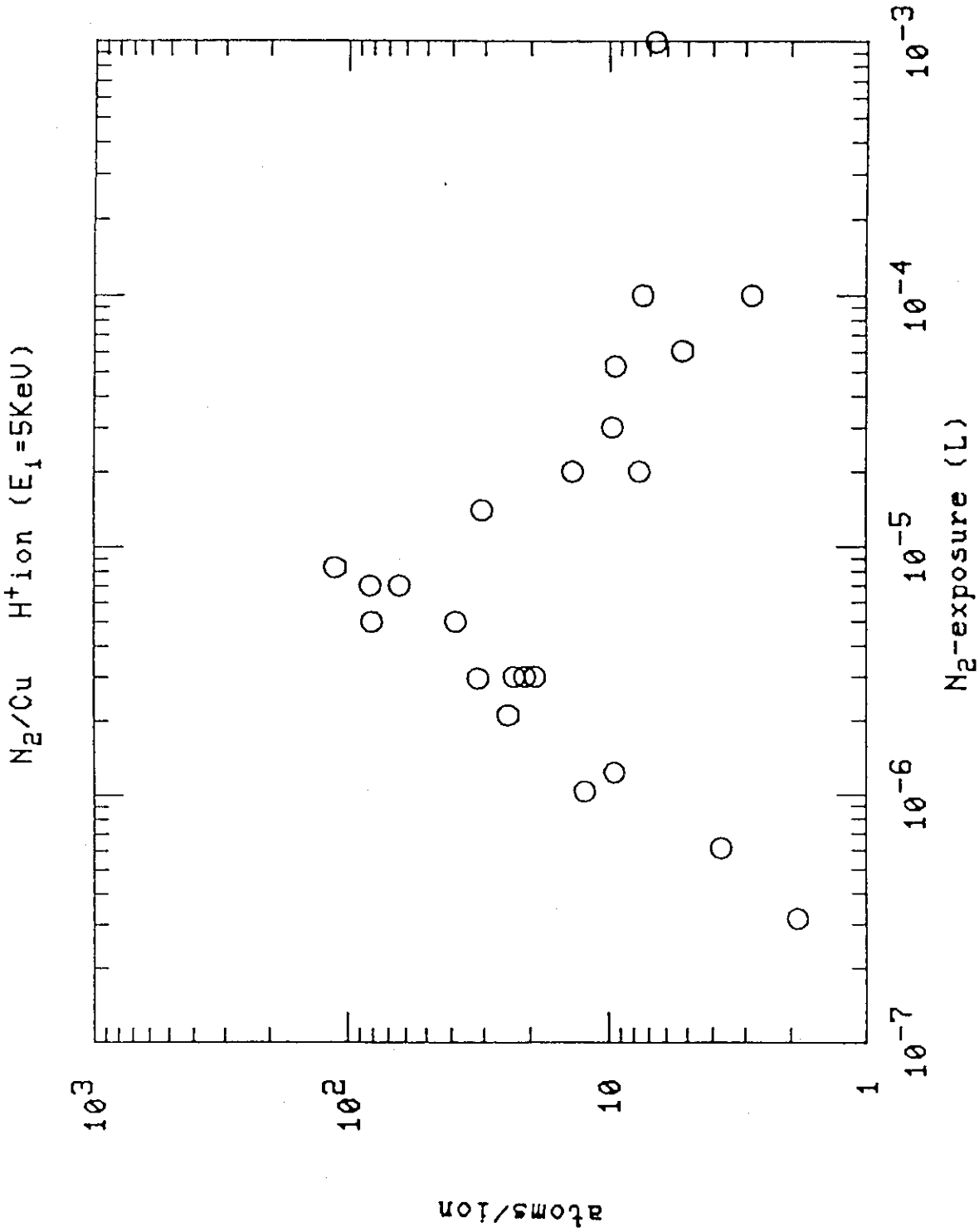

Fig.54 Desorption efficiency as a function of exposure

DATA LIST

Substrate	Incident ion species	Exposure (L)	Incident energy (eV)	Method	Atoms per incident ion	Ref.
Cu	H+	0.315E-06	5000	MS	0.187E+01	75Er02
Cu	H+	0.610E-06	5000	MS	0.369E+01	75Er02
Cu	H+	0.103E-05	5000	MS	0.123E+02	75Er02
Cu	H+	0.123E-05	5000	MS	0.947E+01	75Er02
Cu	H+	0.210E-05	5000	MS	0.243E+02	75Er02
Cu	H+	0.296E-05	5000	MS	0.315E+02	75Er02
Cu	H+	0.300E-05	5000	MS	0.229E+02	75Er02
Cu	H+	0.300E-05	5000	MS	0.209E+02	75Er02
Cu	H+	0.300E-05	5000	MS	0.191E+02	75Er02
Cu	H+	0.500E-05	5000	MS	0.807E+02	75Er02
Cu	H+	0.500E-05	5000	MS	0.384E+02	75Er02
Cu	H+	0.700E-05	5000	MS	0.820E+02	75Er02
Cu	H+	0.700E-05	5000	MS	0.633E+02	75Er02
Cu	H+	0.828E-05	5000	MS	0.112E+03	75Er02
Cu	H+	0.140E-04	5000	MS	0.305E+02	75Er02
Cu	H+	0.200E-04	5000	MS	0.137E+02	75Er02
Cu	H+	0.200E-04	5000	MS	0.758E+01	75Er02
Cu	H+	0.300E-04	5000	MS	0.962E+01	75Er02
Cu	H+	0.527E-04	5000	MS	0.941E+01	75Er02
Cu	H+	0.606E-04	5000	MS	0.520E+01	75Er02
Cu	H+	0.100E-03	5000	MS	0.737E+01	75Er02
Cu	H+	0.100E-03	5000	MS	0.281E+01	75Er02
Cu	H+	0.100E-02	5000	MS	0.659E+01	75Er02

Surface temperature 4.2K

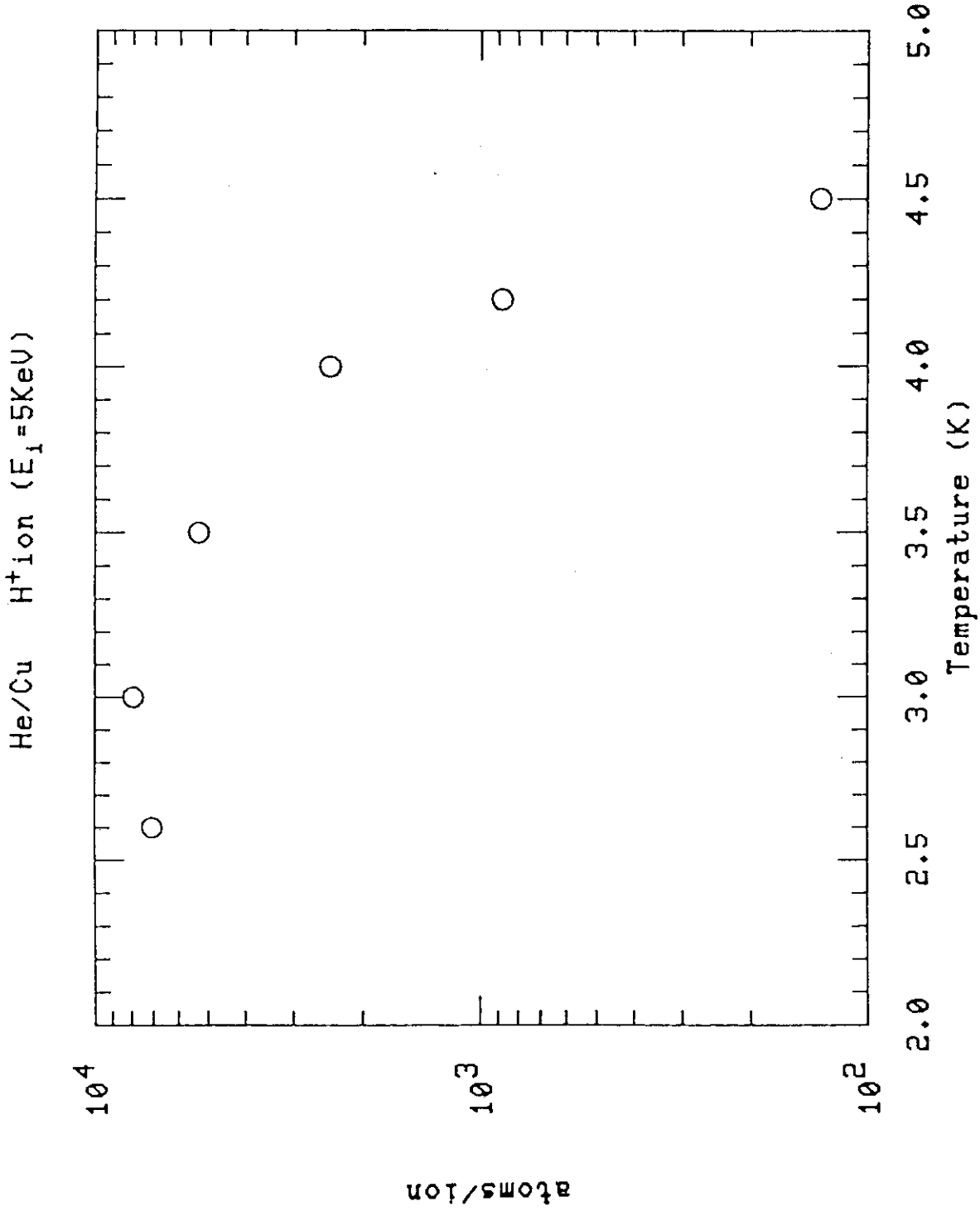

Fig.55 Desorption efficiency as a function of temperature

DATA LIST

Substrate	Incident ion species	Temp. (K)	Incident energy (eV)	Method	Atoms per incident ion	Ref.
Cu	H+	0.260E+01	5000	MS	0.704E+04	75Er02
Cu	H+	0.300E+01	5000	MS	0.792E+04	75Er02
Cu	H+	0.350E+01	5000	MS	0.530E+04	75Er02
Cu	H+	0.400E+01	5000	MS	0.242E+04	75Er02
Cu	H+	0.420E+01	5000	MS	0.878E+03	75Er02
Cu	H+	0.450E+01	5000	MS	0.132E+03	75Er02

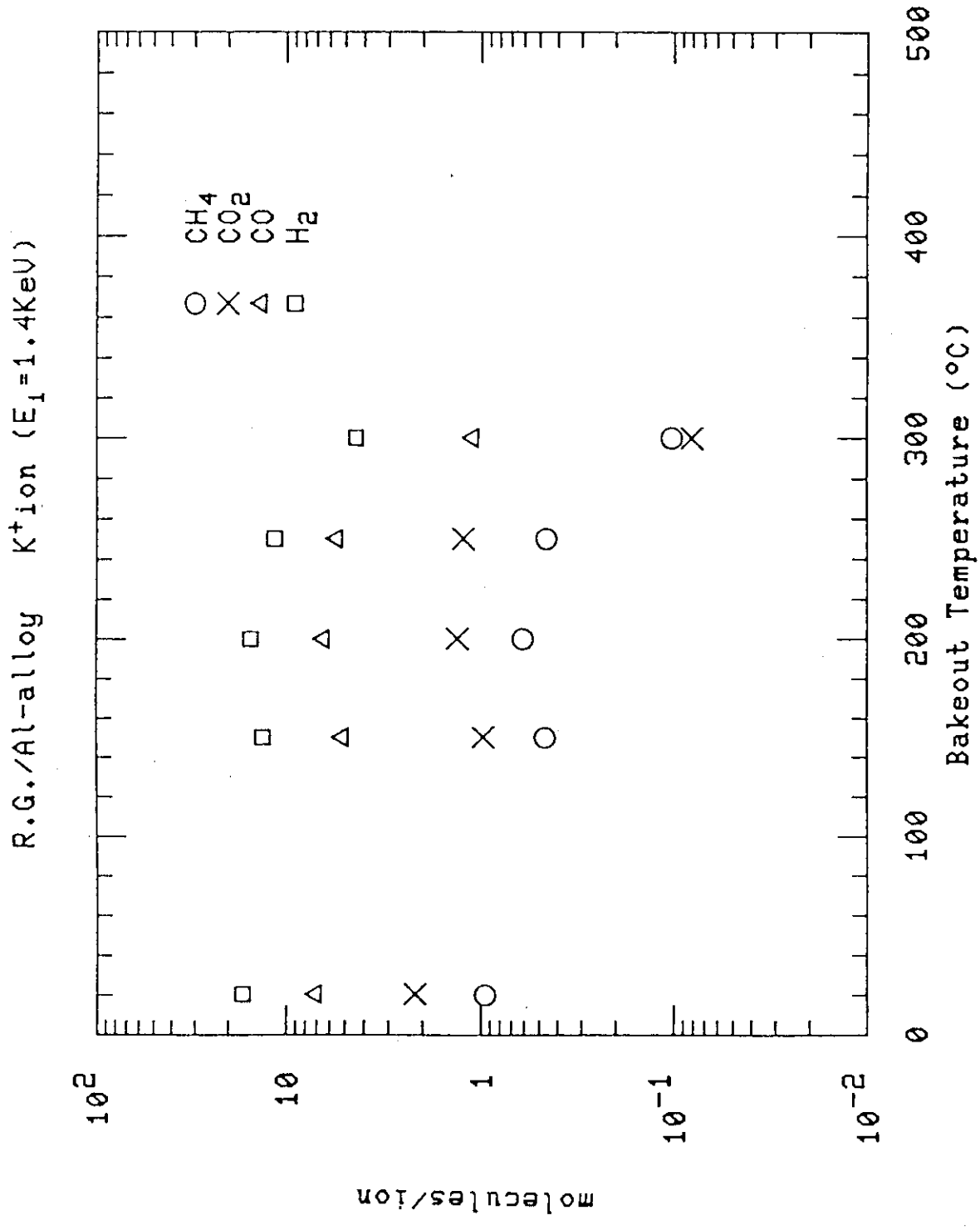

Fig.56 Desorption efficiency as a function of bakeout temperature

DATA LIST

Substrate	Desorbed species	Bakeout temp. (deg.C)	Incident energy (eV)	Method	Molecules per ion	Ref.
Al-alloy	CH4	0.200E+02	1400	MS	0.948E+00	79Ac01
Al-alloy	CH4	0.150E+03	1400	MS	0.466E+00	79Ac01
Al-alloy	CH4	0.200E+03	1400	MS	0.604E+00	79Ac01
Al-alloy	CH4	0.250E+03	1400	MS	0.457E+00	79Ac01
Al-alloy	CH4	0.300E+03	1400	MS	0.102E+00	79Ac01
Al-alloy	CO2	0.200E+02	1400	MS	0.219E+01	79Ac01
Al-alloy	CO2	0.150E+03	1400	MS	0.972E+00	79Ac01
Al-alloy	CO2	0.200E+03	1400	MS	0.132E+01	79Ac01
Al-alloy	CO2	0.250E+03	1400	MS	0.123E+01	79Ac01
Al-alloy	CO2	0.300E+03	1400	MS	0.801E-01	79Ac01
Al-alloy	CO	0.200E+02	1400	MS	0.710E+01	79Ac01
Al-alloy	CO	0.150E+03	1400	MS	0.513E+01	79Ac01
Al-alloy	CO	0.200E+03	1400	MS	0.642E+01	79Ac01
Al-alloy	CO	0.250E+03	1400	MS	0.551E+01	79Ac01
Al-alloy	CO	0.300E+03	1400	MS	0.110E+01	79Ac01
Al-alloy	H2	0.200E+02	1400	MS	0.169E+02	79Ac01
Al-alloy	H2	0.150E+03	1400	MS	0.132E+02	79Ac01
Al-alloy	H2	0.200E+03	1400	MS	0.152E+02	79Ac01
Al-alloy	H2	0.250E+03	1400	MS	0.115E+02	79Ac01
Al-alloy	H2	0.300E+03	1400	MS	0.444E+01	79Ac01

A bombardment energy of K+ ions was corresponding to the energy of residual gas ion produced by a typical ISR proton beam.
The angle of incidence was normal to the surface, judging from the experimental arrangements.
Al-alloy : 5086

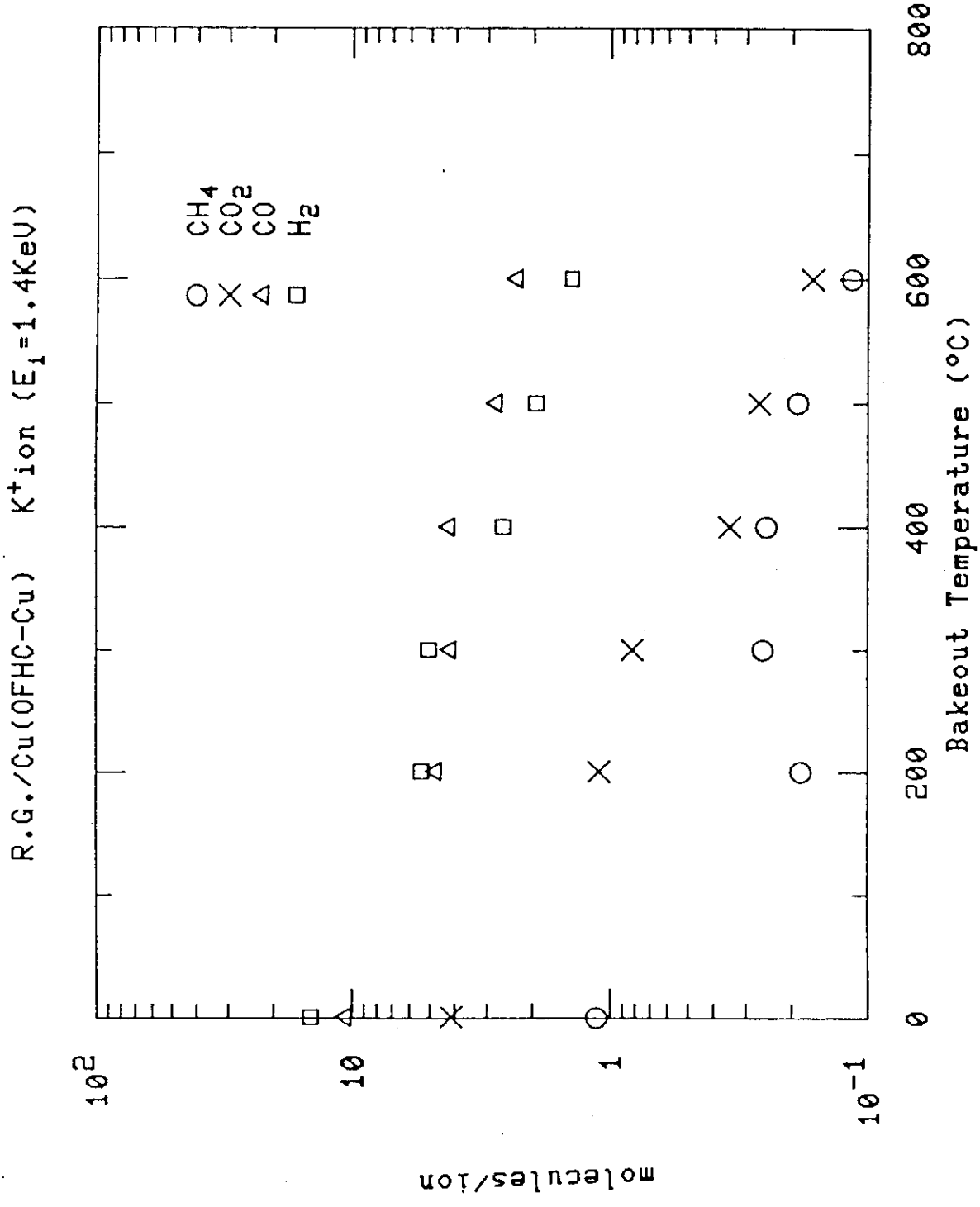

Fig.57 Desorption efficiency as a function of bakeout temperature

DATA LIST

Substrate	Desorbed species	Bakeout temp. (deg.C)	Incident energy (eV)	Method	Molecules per ion	Ref.
OFHC-Cu	CH4	0.000E+00	1400	MS	0.113E+01	79Ac01
OFHC-Cu	CH4	0.200E+03	1400	MS	0.184E+00	79Ac01
OFHC-Cu	CH4	0.300E+03	1400	MS	0.258E+00	79Ac01
OFHC-Cu	CH4	0.400E+03	1400	MS	0.250E+00	79Ac01
OFHC-Cu	CH4	0.500E+03	1400	MS	0.189E+00	79Ac01
OFHC-Cu	CH4	0.600E+03	1400	MS	0.116E+00	79Ac01
OFHC-Cu	CO2	0.000E+00	1400	MS	0.413E+01	79Ac01
OFHC-Cu	CO2	0.200E+03	1400	MS	0.110E+01	79Ac01
OFHC-Cu	CO2	0.300E+03	1400	MS	0.818E+00	79Ac01
OFHC-Cu	CO2	0.400E+03	1400	MS	0.345E+00	79Ac01
OFHC-Cu	CO2	0.500E+03	1400	MS	0.266E+00	79Ac01
OFHC-Cu	CO2	0.600E+03	1400	MS	0.166E+00	79Ac01
OFHC-Cu	CO	0.000E+00	1400	MS	0.106E+02	79Ac01
OFHC-Cu	CO	0.200E+03	1400	MS	0.471E+01	79Ac01
OFHC-Cu	CO	0.300E+03	1400	MS	0.414E+01	79Ac01
OFHC-Cu	CO	0.400E+03	1400	MS	0.421E+01	79Ac01
OFHC-Cu	CO	0.500E+03	1400	MS	0.276E+01	79Ac01
OFHC-Cu	CO	0.600E+03	1400	MS	0.231E+01	79Ac01
OFHC-Cu	H2	0.000E+00	1400	MS	0.144E+02	79Ac01
OFHC-Cu	H2	0.200E+03	1400	MS	0.537E+01	79Ac01
OFHC-Cu	H2	0.300E+03	1400	MS	0.503E+01	79Ac01
OFHC-Cu	H2	0.400E+03	1400	MS	0.259E+01	79Ac01
OFHC-Cu	H2	0.500E+03	1400	MS	0.193E+01	79Ac01
OFHC-Cu	H2	0.600E+03	1400	MS	0.142E+01	79Ac01

A bombardment energy of K+ ions was corresponding to the energy of residual gas ion produced by a typical ISR proton beam.
The angle of incidence was normal to the surface, judging from the experimental arrangements.
OFHC : Oxygen Free High Conductivity

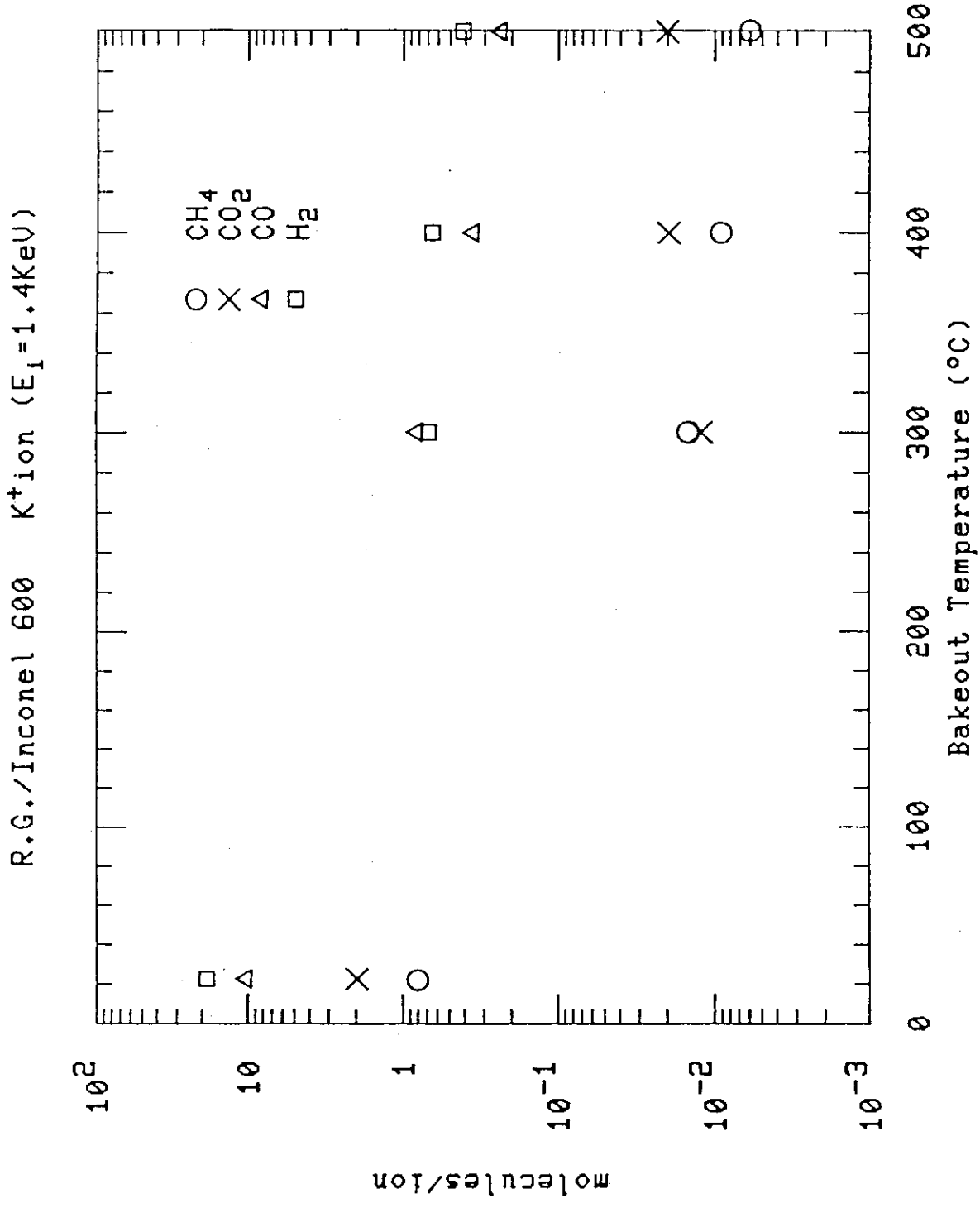

Fig.58 Desorption efficiency as a function of bakeout temperature

DATA LIST

Substrate	Desorbed species	Bakeout temp. (deg.C)	Incident energy (eV)	Method	Molecules per ion	Ref.
Inco.600	CH4	0.220E+02	1400	MS	0.803E+00	79Ac01
Inco.600	CH4	0.300E+03	1400	MS	0.147E-01	79Ac01
Inco.600	CH4	0.400E+03	1400	MS	0.911E-02	79Ac01
Inco.600	CH4	0.500E+03	1400	MS	0.594E-02	79Ac01
Inco.600	CO2	0.220E+02	1400	MS	0.199E+01	79Ac01
Inco.600	CO2	0.300E+03	1400	MS	0.121E-01	79Ac01
Inco.600	CO2	0.400E+03	1400	MS	0.195E-01	79Ac01
Inco.600	CO2	0.500E+03	1400	MS	0.200E-01	79Ac01
Inco.600	CO	0.220E+02	1400	MS	0.104E+02	79Ac01
Inco.600	CO	0.300E+03	1400	MS	0.814E+00	79Ac01
Inco.600	CO	0.400E+03	1400	MS	0.354E+00	79Ac01
Inco.600	CO	0.500E+03	1400	MS	0.235E+00	79Ac01
Inco.600	H2	0.220E+02	1400	MS	0.189E+02	79Ac01
Inco.600	H2	0.300E+03	1400	MS	0.682E+00	79Ac01
Inco.600	H2	0.400E+03	1400	MS	0.655E+00	79Ac01
Inco.600	H2	0.500E+03	1400	MS	0.414E+00	79Ac01

A bombardment energy of K+ ions was corresponding to the energy of residual gas ion produced by a typical ISR proton beam.
The angle of incidence was normal to the surface, judging from the experimental arrangements.
Inco.600 : Inconel 600

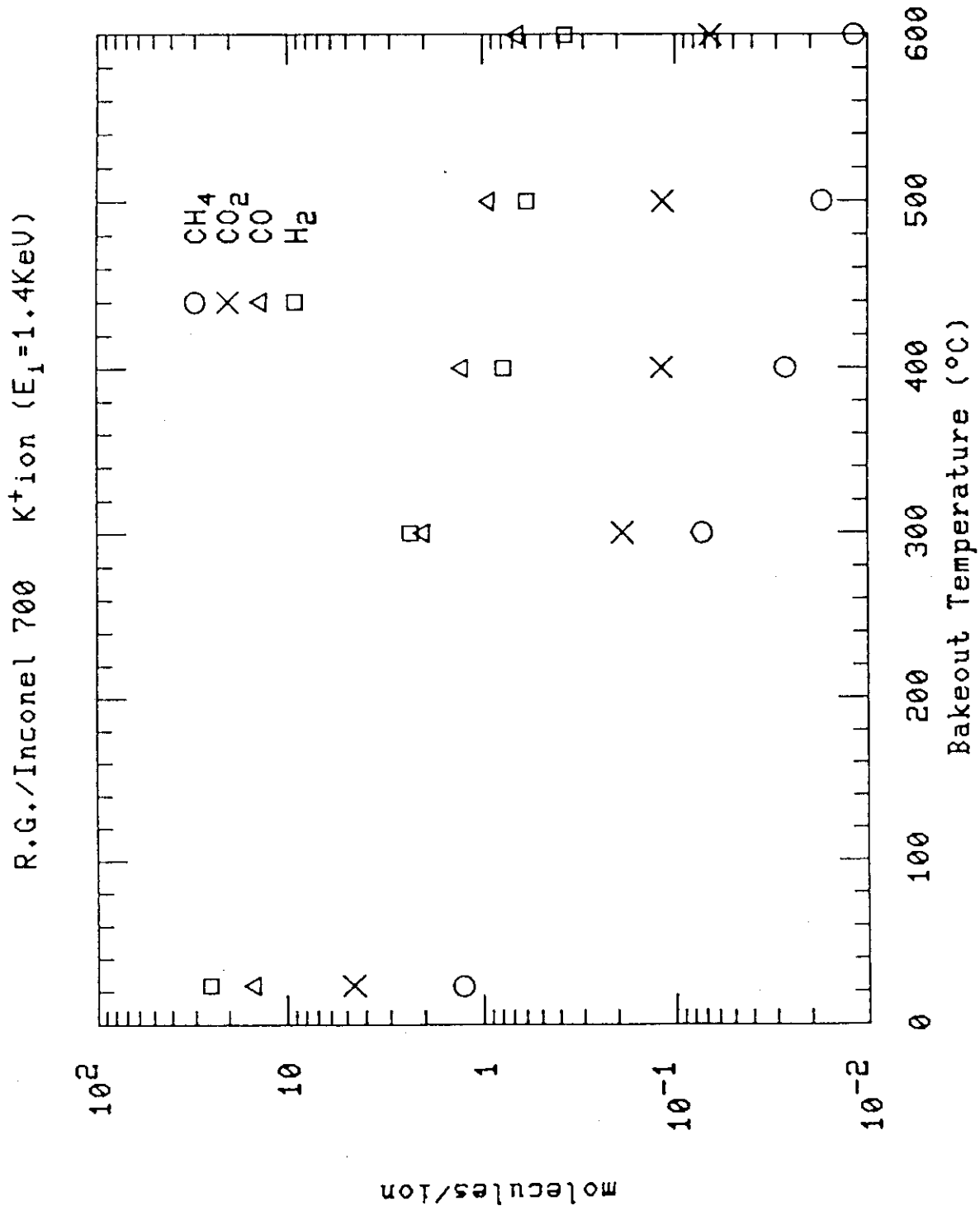

Fig.59 Desorption efficiency as a function of bakeout temperature

DATA LIST

Substrate	Desorbed species	Bakeout temp. (deg.C)	Incident energy (eV)	Method	Molecules per ion	Ref.
Inco.700	CH4	0.230E+02	1400	MS	0.127E+01	79Ac01
Inco.700	CH4	0.300E+03	1400	MS	0.725E-01	79Ac01
Inco.700	CH4	0.400E+03	1400	MS	0.270E-01	79Ac01
Inco.700	CH4	0.500E+03	1400	MS	0.174E-01	79Ac01
Inco.700	CH4	0.600E+03	1400	MS	0.118E-01	79Ac01
Inco.700	CO2	0.230E+02	1400	MS	0.462E+01	79Ac01
Inco.700	CO2	0.300E+03	1400	MS	0.188E+00	79Ac01
Inco.700	CO2	0.400E+03	1400	MS	0.117E+00	79Ac01
Inco.700	CO2	0.500E+03	1400	MS	0.115E+00	79Ac01
Inco.700	CO2	0.600E+03	1400	MS	0.652E-01	79Ac01
Inco.700	CO	0.230E+02	1400	MS	0.148E+02	79Ac01
Inco.700	CO	0.300E+03	1400	MS	0.200E+01	79Ac01
Inco.700	CO	0.400E+03	1400	MS	0.127E+01	79Ac01
Inco.700	CO	0.500E+03	1400	MS	0.927E+00	79Ac01
Inco.700	CO	0.600E+03	1400	MS	0.668E+00	79Ac01
Inco.700	H2	0.230E+02	1400	MS	0.253E+02	79Ac01
Inco.700	H2	0.300E+03	1400	MS	0.235E+01	79Ac01
Inco.700	H2	0.400E+03	1400	MS	0.779E+00	79Ac01
Inco.700	H2	0.500E+03	1400	MS	0.589E+00	79Ac01
Inco.700	H2	0.600E+03	1400	MS	0.373E+00	79Ac01

A bombardment energy of K+ ions was corresponding to the energy of residual gas ion produced by a typical ISR proton beam.
The angle of incidence was normal to the surface, judging from the experimental arrangements.
Inco.700 : Inconel 700

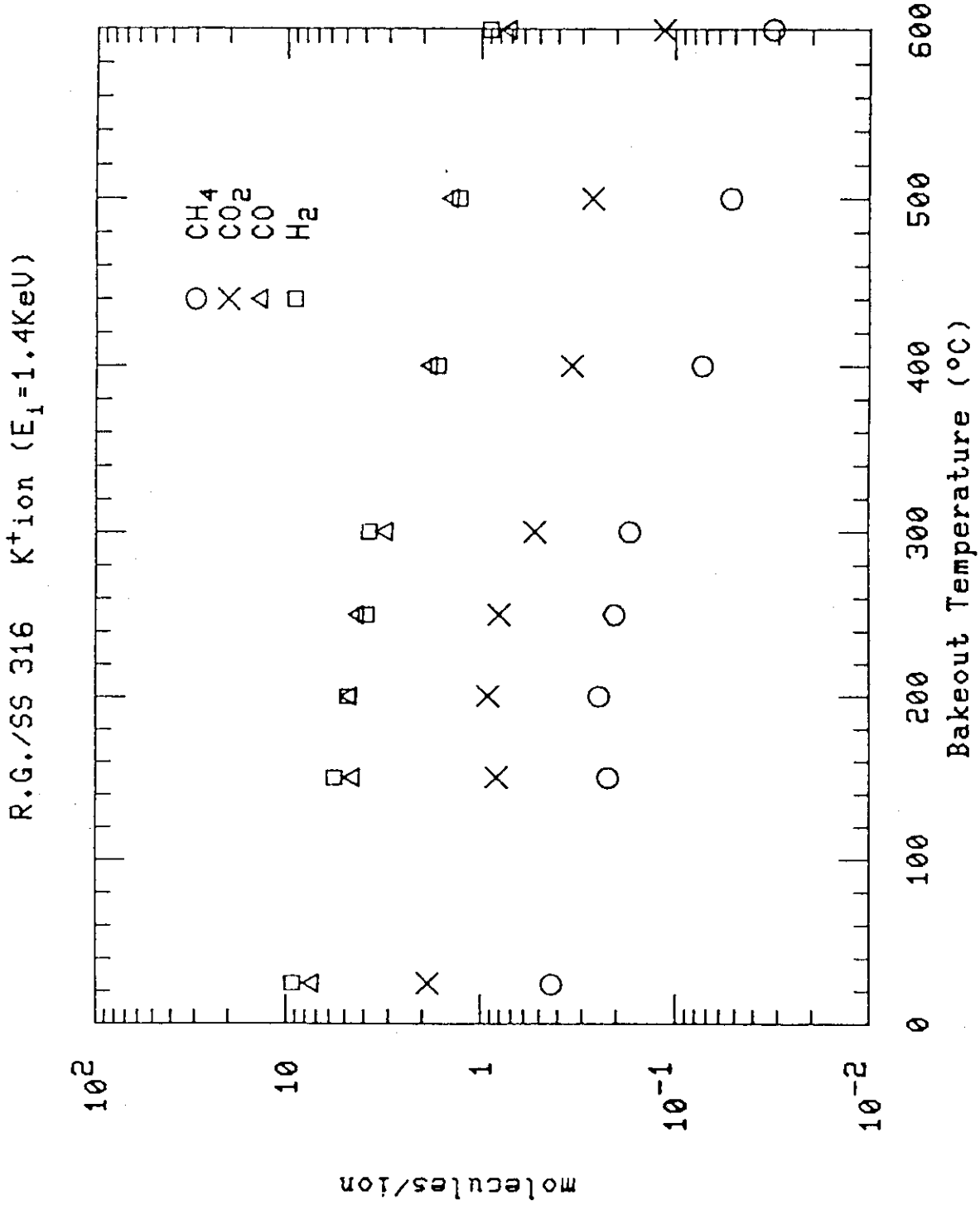

Fig.60 Desorption efficiency as a function of bakeout temperature

DATA LIST

Substrate	Desorbed species	Bakeout temp. (deg.C)	Incident energy (eV)	Method	Molecules per ion	Ref.
SS 316	CH4	0.240E+02	1400	MS	0.431E+00	78Ma03
SS 316	CH4	0.150E+03	1400	MS	0.220E+00	78Ma03
SS 316	CH4	0.200E+03	1400	MS	0.243E+00	78Ma03
SS 316	CH4	0.250E+03	1400	MS	0.203E+00	78Ma03
SS 316	CH4	0.300E+03	1400	MS	0.169E+00	78Ma03
SS 316	CH4	0.400E+03	1400	MS	0.726E-01	78Ma03
SS 316	CH4	0.500E+03	1400	MS	0.516E-01	78Ma03
SS 316	CH4	0.600E+03	1400	MS	0.317E-01	78Ma03
SS 316	CO2	0.240E+02	1400	MS	0.188E+01	78Ma03
SS 316	CO2	0.150E+03	1400	MS	0.828E+00	78Ma03
SS 316	CO2	0.200E+03	1400	MS	0.912E+00	78Ma03
SS 316	CO2	0.250E+03	1400	MS	0.799E+00	78Ma03
SS 316	CO2	0.300E+03	1400	MS	0.522E+00	78Ma03
SS 316	CO2	0.400E+03	1400	MS	0.336E+00	78Ma03
SS 316	CO2	0.500E+03	1400	MS	0.263E+00	78Ma03
SS 316	CO2	0.600E+03	1400	MS	0.113E+00	78Ma03
SS 316	CO	0.240E+02	1400	MS	0.732E+01	78Ma03
SS 316	CO	0.150E+03	1400	MS	0.453E+01	78Ma03
SS 316	CO	0.200E+03	1400	MS	0.467E+01	78Ma03
SS 316	CO	0.250E+03	1400	MS	0.429E+01	78Ma03
SS 316	CO	0.300E+03	1400	MS	0.309E+01	78Ma03
SS 316	CO	0.400E+03	1400	MS	0.180E+01	78Ma03
SS 316	CO	0.500E+03	1400	MS	0.140E+01	78Ma03
SS 316	CO	0.600E+03	1400	MS	0.707E+00	78Ma03
SS 316	H2	0.240E+02	1400	MS	0.935E+01	78Ma03
SS 316	H2	0.150E+03	1400	MS	0.569E+01	78Ma03
SS 316	H2	0.200E+03	1400	MS	0.482E+01	78Ma03
SS 316	H2	0.250E+03	1400	MS	0.389E+01	78Ma03
SS 316	H2	0.300E+03	1400	MS	0.376E+01	78Ma03
SS 316	H2	0.400E+03	1400	MS	0.166E+01	78Ma03
SS 316	H2	0.500E+03	1400	MS	0.129E+01	78Ma03
SS 316	H2	0.600E+03	1400	MS	0.902E+00	78Ma03

A bombardment energy of K+ ions was corresponding to the energy of residual gas ion produced by a typical ISR proton beam.
The angle of incidence was normal to the surface, judging from the experimental arrangements.
SS 316 : Stainless steel 316L+N

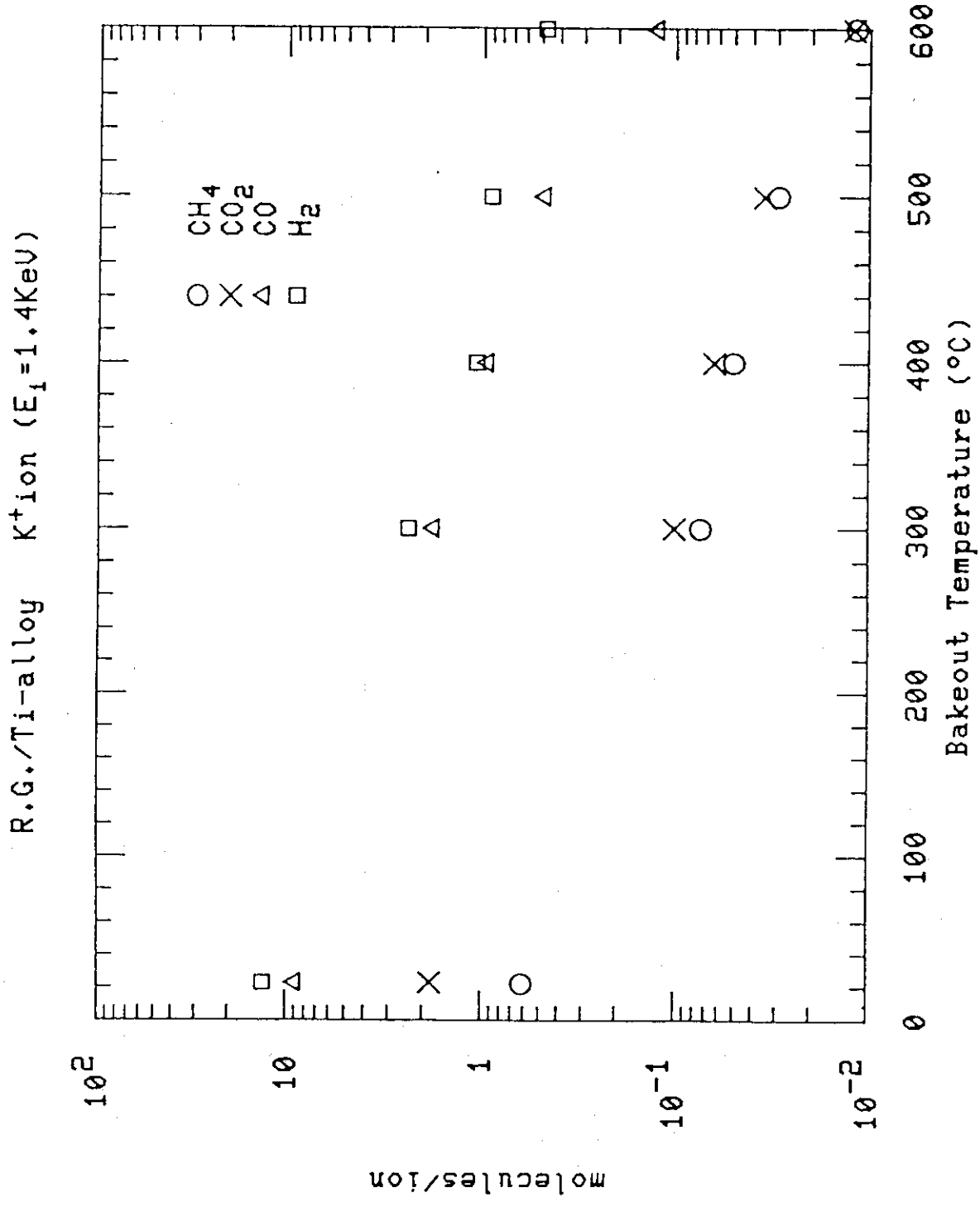

Fig.61 Desorption efficiency as a function of bakeout temperature

DATA LIST

Substrate	Desorbed species	Bakeout temp. (deg.C)	Incident energy (eV)	Method	Molecules per ion	Ref.
Ti-alloy	CH4	0.220E+02	1400	MS	0.610E+00	79Ac01
Ti-alloy	CH4	0.300E+03	1400	MS	0.734E-01	79Ac01
Ti-alloy	CH4	0.400E+03	1400	MS	0.500E-01	79Ac01
Ti-alloy	CH4	0.500E+03	1400	MS	0.295E-01	79Ac01
Ti-alloy	CH4	0.600E+03	1400	MS	0.118E-01	79Ac01
Ti-alloy	CO2	0.220E+02	1400	MS	0.183E+01	79Ac01
Ti-alloy	CO2	0.300E+03	1400	MS	0.999E-01	79Ac01
Ti-alloy	CO2	0.400E+03	1400	MS	0.628E-01	79Ac01
Ti-alloy	CO2	0.500E+03	1400	MS	0.347E-01	79Ac01
Ti-alloy	CO2	0.600E+03	1400	MS	0.120E-01	79Ac01
Ti-alloy	CO	0.220E+02	1400	MS	0.897E+01	79Ac01
Ti-alloy	CO	0.300E+03	1400	MS	0.179E+01	79Ac01
Ti-alloy	CO	0.400E+03	1400	MS	0.942E+00	79Ac01
Ti-alloy	CO	0.500E+03	1400	MS	0.480E+00	79Ac01
Ti-alloy	CO	0.600E+03	1400	MS	0.124E+00	79Ac01
Ti-alloy	H2	0.220E+02	1400	MS	0.132E+02	79Ac01
Ti-alloy	H2	0.300E+03	1400	MS	0.239E+01	79Ac01
Ti-alloy	H2	0.400E+03	1400	MS	0.107E+01	79Ac01
Ti-alloy	H2	0.500E+03	1400	MS	0.903E+00	79Ac01
Ti-alloy	H2	0.600E+03	1400	MS	0.475E+00	79Ac01

A bombardment energy of K+ ions was corresponding to the energy of residual gas ion produced by a typical ISR proton beam.
The angle of incidence was normal to the surface, judging from the experimental arrangements.
Ti-alloy : Ti Al 6V4

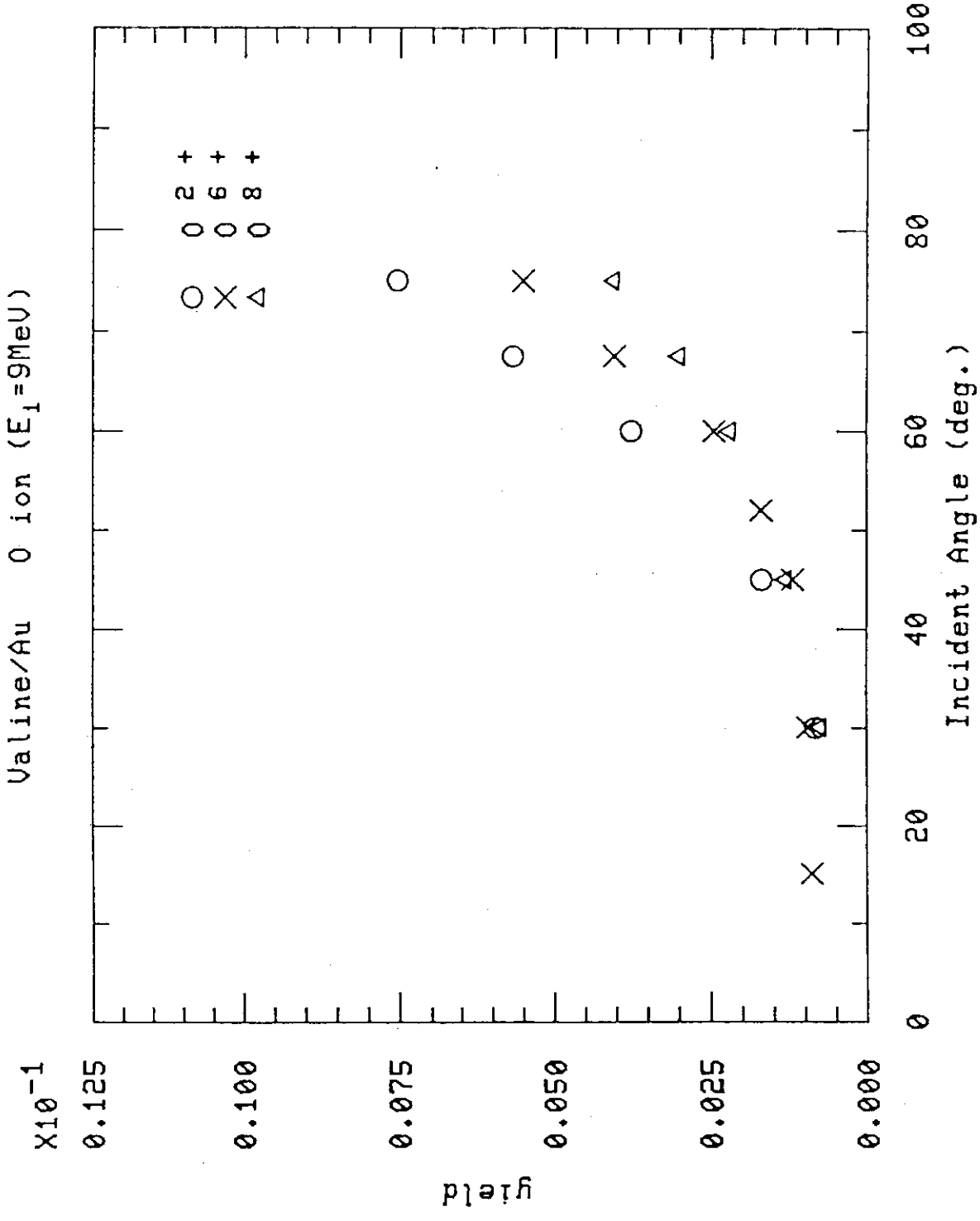

Fig.62 Desorption efficiency as a function of incidnt angle

DATA LIST

Substrate	Incident ion species	Incident energy (eV)	Incident angle from normal (deg.)	Method	[M+H]+ yield	Ref.
Au	O +2	0.900E+07	30	TOF	0.841E-03	84Ni01
Au	O +2	0.900E+07	45	TOF	0.170E-02	84Ni01
Au	O +2	0.900E+07	60	TOF	0.376E-02	84Ni01
Au	O +2	0.900E+07	67.5	TOF	0.568E-02	84Ni01
Au	O +2	0.900E+07	75	TOF	0.905E-02	84Ni01
Au	O +6	0.900E+07	15	TOF	0.889E-03	84Ni01
Au	O +6	0.900E+07	30	TOF	0.954E-03	84Ni01
Au	O +6	0.900E+07	45	TOF	0.120E-02	84Ni01
Au	O +6	0.900E+07	52	TOF	0.170E-02	84Ni01
Au	O +6	0.900E+07	60	TOF	0.244E-02	84Ni01
Au	O +6	0.900E+07	67.5	TOF	0.403E-02	84Ni01
Au	O +6	0.900E+07	75	TOF	0.551E-02	84Ni01
Au	O +8	0.900E+07	30	TOF	0.744E-03	84Ni01
Au	O +8	0.900E+07	45	TOF	0.131E-02	84Ni01
Au	O +8	0.900E+07	60	TOF	0.219E-02	84Ni01
Au	O +8	0.900E+07	67.5	TOF	0.300E-02	84Ni01
Au	O +8	0.900E+07	75	TOF	0.405E-02	84Ni01

Thickness 15ug/cm**2
Mass number of Valine 117

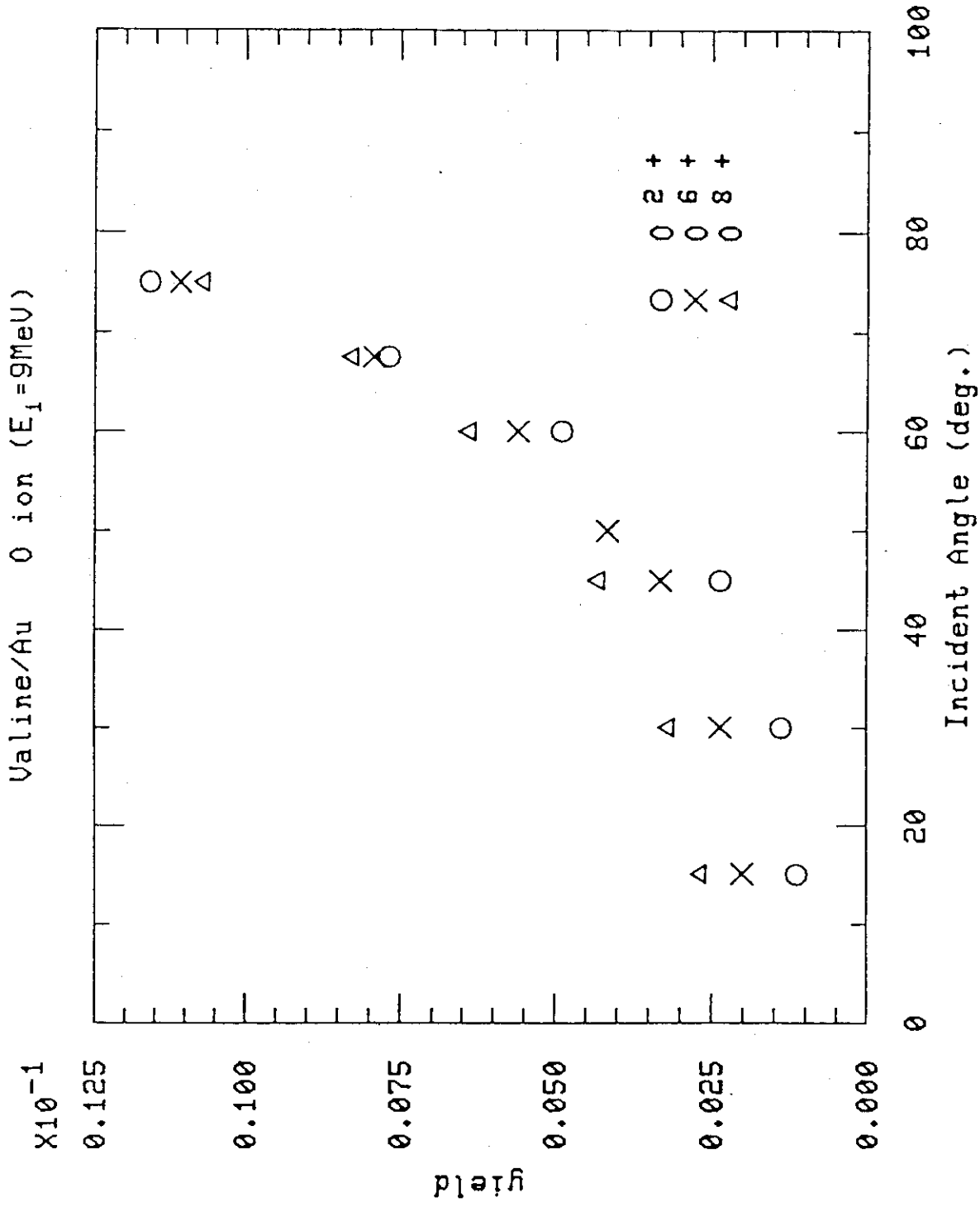

Fig.63 Desorption efficiency as a function of incidnt angle

DATA LIST

Substrate	Incident ion species	Incident energy (eV)	Incident angle from normal (deg.)	Method	[M-COOH]+ yield	Ref.
Au	O +2	0.900E+07	15	TOF	0.114E-02	84Ni01
Au	O +2	0.900E+07	30	TOF	0.139E-02	84Ni01
Au	O +2	0.900E+07	45	TOF	0.237E-02	84Ni01
Au	O +2	0.900E+07	60	TOF	0.489E-02	84Ni01
Au	O +2	0.900E+07	67.5	TOF	0.768E-02	84Ni01
Au	O +2	0.900E+07	75	TOF	0.116E-01	84Ni01
Au	O +6	0.900E+07	15	TOF	0.201E-02	84Ni01
Au	O +6	0.900E+07	30	TOF	0.236E-02	84Ni01
Au	O +6	0.900E+07	45	TOF	0.331E-02	84Ni01
Au	O +6	0.900E+07	50	TOF	0.416E-02	84Ni01
Au	O +6	0.900E+07	60	TOF	0.560E-02	84Ni01
Au	O +6	0.900E+07	67.5	TOF	0.793E-02	84Ni01
Au	O +6	0.900E+07	75	TOF	0.111E-01	84Ni01
Au	O +8	0.900E+07	15	TOF	0.267E-02	84Ni01
Au	O +8	0.900E+07	30	TOF	0.317E-02	84Ni01
Au	O +8	0.900E+07	45	TOF	0.431E-02	84Ni01
Au	O +8	0.900E+07	60	TOF	0.639E-02	84Ni01
Au	O +8	0.900E+07	67.5	TOF	0.827E-02	84Ni01
Au	O +8	0.900E+07	75	TOF	0.107E-01	84Ni01

Thickness 15ug/cm**2
Mass number of Valine 117

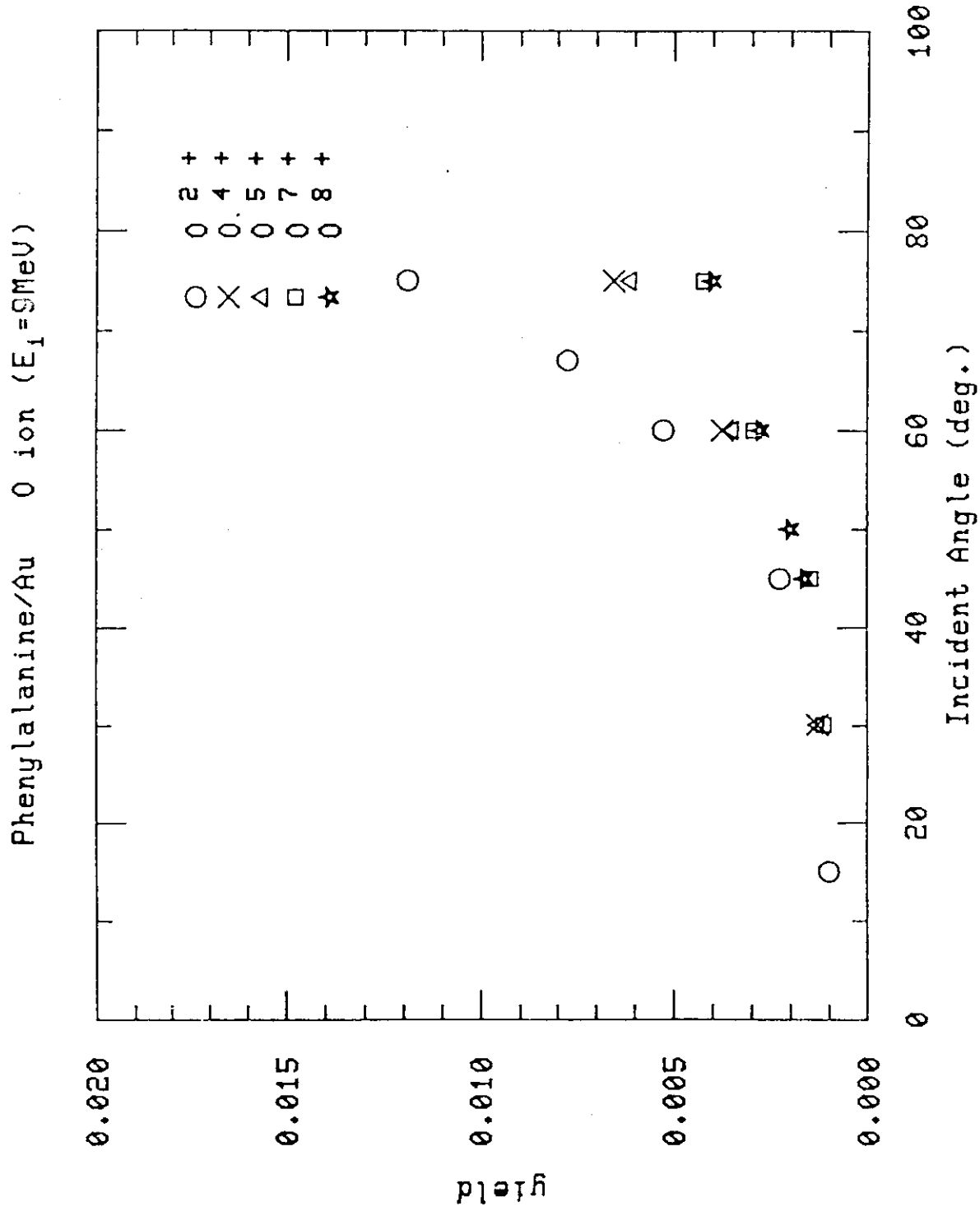

Fig.64 Desorption efficiency as a function of incidnt angle

DATA LIST

Substrate	Incident ion species	Incident energy (eV)	Incident angle from normal (deg.)	Method	[M+H]+ yield	Ref.
Au	O +2	0.900E+07	15	TOF	0.101E-02	84Ni01
Au	O +2	0.900E+07	45	TOF	0.229E-02	84Ni01
Au	O +2	0.900E+07	60	TOF	0.525E-02	84Ni01
Au	O +2	0.900E+07	67	TOF	0.774E-02	84Ni01
Au	O +2	0.900E+07	75	TOF	0.119E-01	84Ni01
Au	O +4	0.900E+07	30	TOF	0.130E-02	84Ni01
Au	O +4	0.900E+07	60	TOF	0.374E-02	84Ni01
Au	O +4	0.900E+07	75	TOF	0.654E-02	84Ni01
Au	O +5	0.900E+07	30	TOF	0.128E-02	84Ni01
Au	O +5	0.900E+07	60	TOF	0.348E-02	84Ni01
Au	O +5	0.900E+07	75	TOF	0.610E-02	84Ni01
Au	O +7	0.900E+07	30	TOF	0.114E-02	84Ni01
Au	O +7	0.900E+07	45	TOF	0.148E-02	84Ni01
Au	O +7	0.900E+07	60	TOF	0.293E-02	84Ni01
Au	O +7	0.900E+07	75	TOF	0.423E-02	84Ni01
Au	O +8	0.900E+07	45	TOF	0.164E-02	84Ni01
Au	O +8	0.900E+07	50	TOF	0.202E-02	84Ni01
Au	O +8	0,900E+07	60	TOF	0.277E-02	84Ni01
Au	O +8	0.900E+07	75	TOF	0.402E-02	84Ni01

Tickness 15ug/cm**2
Mass number of phenylalanine 165

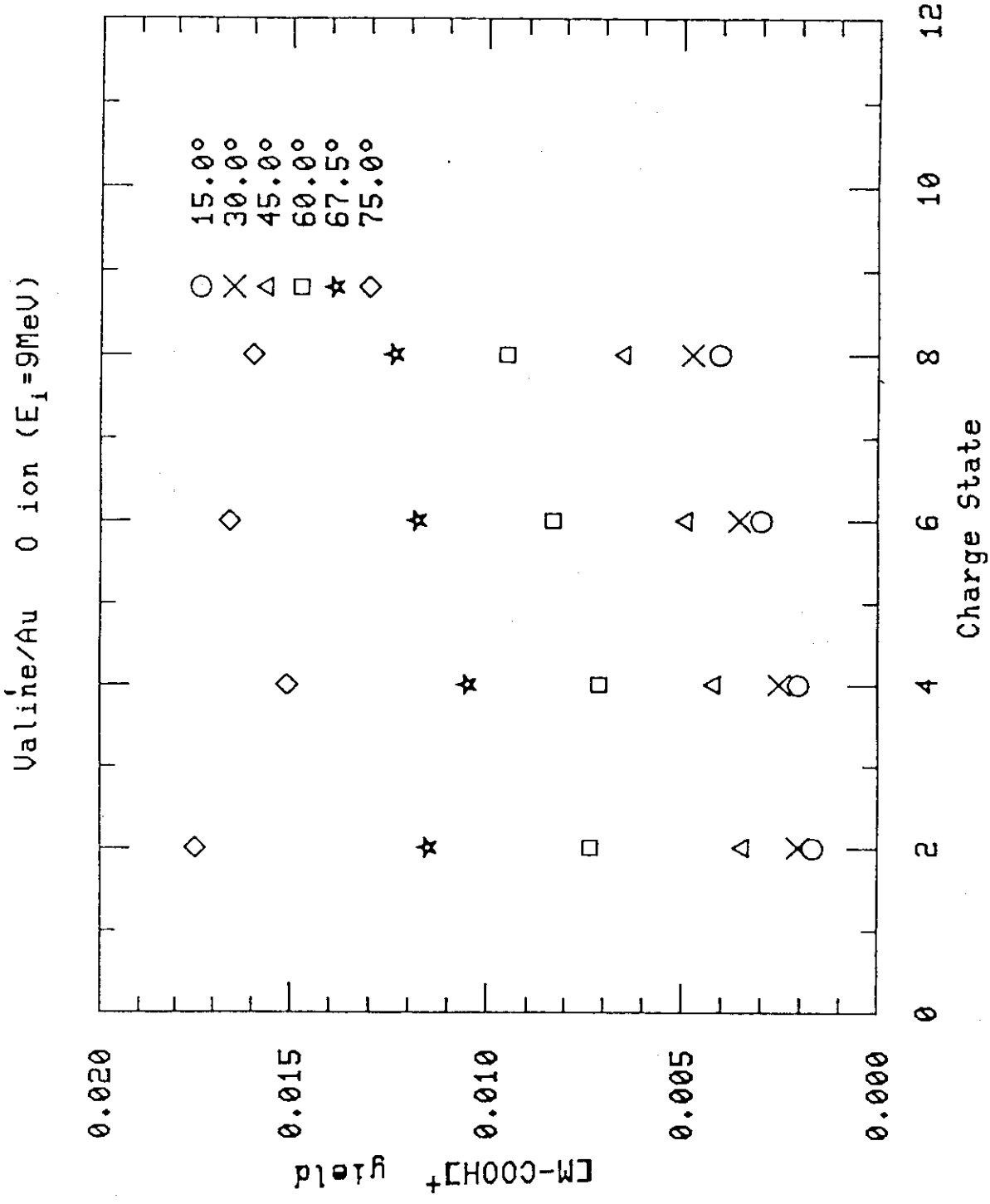

Fig.65 Desorption efficiency as a function of charge state of incident ion

DATA LIST

Substrate	Incident ion species	Incident energy (eV)	Incident angle from normal (deg.)	Method	[M-COOH]+ yield	Ref.
Au	O +2	0.900E+07	15	TOF	0.169E-02	84Ni01
Au	O +4	0.900E+07	15	TOF	0.206E-02	84Ni01
Au	O +6	0.900E+07	15	TOF	0.301E-02	84Ni01
Au	O +8	0.900E+07	15	TOF	0.407E-02	84Ni01
Au	O +2	0.900E+07	30	TOF	0.205E-02	84Ni01
Au	O +4	0.900E+07	30	TOF	0.254E-02	84Ni01
Au	O +6	0.900E+07	30	TOF	0.356E-02	84Ni01
Au	O +8	0.900E+07	30	TOF	0.476E-02	84Ni01
Au	O +2	0.900E+07	45	TOF	0.344E-02	84Ni01
Au	O +4	0.900E+07	45	TOF	0.417E-02	84Ni01
Au	O +6	0.900E+07	45	TOF	0.490E-02	84Ni01
Au	O +8	0.900E+07	45	TOF	0.650E-02	84Ni01
Au	O +2	0.900E+07	60	TOF	0.734E-02	84Ni01
Au	O +4	0.900E+07	60	TOF	0.712E-02	84Ni01
Au	O +6	0.900E+07	60	TOF	0.832E-02	84Ni01
Au	O +8	0.900E+07	60	TOF	0.951E-02	84Ni01
Au	O +2	0.900E+07	67.5	TOF	0.115E-01	84Ni01
Au	O +4	0.900E+07	67.5	TOF	0.105E-01	84Ni01
Au	O +6	0.900E+07	67.5	TOF	0.118E-01	84Ni01
Au	O +8	0.900E+07	67.5	TOF	0.124E-01	84Ni01
Au	O +2	0.900E+07	75	TOF	0.175E-01	84Ni01
Au	O +4	0.900E+07	75	TOF	0.151E-01	84Ni01
Au	O +6	0.900E+07	75	TOF	0.166E-01	84Ni01
Au	O +8	0.900E+07	75	TOF	0.160E-01	84Ni01

Thickness 15ug/cm**2
Mass number of Valine 117

5.1.4 Lists for Miscellaneous Data of IID

DATA LIST FOR IID 1 -- DESORPTION CROSS SECTION --

Substrate	Adsorbate and coverage	Incident ion species	Incident energy (eV)	Incident angle from normal (deg.)	Method	Desorption cross section (cm^2)	Ref.	Remark
Ni poly	H_2 (γ)	Ar^+	3000	60	SIMS	5.0×10^{-14}	81Be04	*1)
Ni poly	H_2 (β)	Ar^+	3000	60	SIMS	5.0×10^{-15}	81Be04	*1)
Ni oxide	H_2	H^+	500	?	SIMS	1.5×10^{-15}	82Bo01	
W	H_2	He^+	500	?	ISS	3.0×10^{-16}	84Tal2	
W	H_2	He^+	500	?	MS	1.25×10^{-16}	84Tal2	*2)
W(100)	H_2	$^3He^+$	1000	60	ISS	1.21×10^{-16}	78Ta06	*3)
SS	H_2	D^+	5600	0	MS	2.0×10^{-17}	74Mc01	*4)
SS	H_2	D^+	5600	0	MS	$> 10^{-16}$	74Mc01	*5)
Ti	O	H^+	500	50	SIMS	1.65×10^{-17}	84Su01	
Ti	O	H^+	700	50	SIMS	1.45×10^{-17}	84Su01	
Ti	O	H^+	1000	50	SIMS	1.42×10^{-17}	84Su01	
Ti	O	H^+	1500	50	SIMS	1.35×10^{-17}	84Su01	
Ti	O	H^+	2000	50	SIMS	9.50×10^{-18}	84Su01	

Ti	O		Ar^+	500	50	SIMS	1.2×10^{-16}	84Su01	
Ti	O		Ar^+	1000	50	SIMS	1.28×10^{-16}	84Su01	
Ti	O		Ar^+	2000	50	SIMS	1.52×10^{-16}	84Su01	
Ti	O		Ar^+	3000	50	SIMS	1.6×10^{-16}	84Su01	
Ti	O		Ar^+	5000	50	SIMS	1.38×10^{-16}	84Su01	
Fe poly	O_2		H^+	50000	60	AES	2.78×10^{-18}	81Le01	
Fe poly	O_2		H^+	100000	60	AES	1.96×10^{-18}	81Le01	
Ni	O	<1 ML	He^+	500	60	ISS	1.0×10^{-16}	76Ta02	
Ni(110)	O_2	1 ML	$^3He^+$	1200	60	ISS	6.0×10^{-17}	77Ta04	
Ni(110)	O		$^3He^+$	1400	60	ISS	2.8×10^{-17}	77Ta05	
Ni(110)	O		He^+	1000	60	ISS	1.0×10^{-16}	77Ta05	
Ni(110)	O		Ne^+	1000	60	ISS	5.0×10^{-16}	77Ta05	
Cu poly	O_2		He^+	500	30	ISS	1.5×10^{-16}	80Ta10	
Mo	O_2		He^+	1500	45	ISS	1.6×10^{-17}	78Ak01	*6)
Ti	CO		Ar^+	1500	45	ISS	1.3×10^{-16}	80Sa02	
Ti	CO		He^+	1500	45	ISS	1.7×10^{-15}	80Sa02	
Ni	CO		He^+	500	?	ISS	5.0×10^{-15}	84Ta12	

Ni poly	CO		He^+	2000	45	IPP	2.6×10^{-15}	80Ma04	*7)
Ni poly	CO		Ne^+	2000	45	IPP	7.7×10^{-15}	80Ma04	*7)
Ni poly	CO		Ar^+	2000	45	IPP	1.8×10^{-14}	80Ma04	*7)
Mo	CO		He^+	1500	45	ISS	5.7×10^{-15}	80Sa02	
Mo	CO		Ar^+	1500	45	ISS	3.0×10^{-16}	80Sa02	
Ni	S		Ar^+	500	30	MS	1.0×10^{-15}	74Wi02	
Ni	S	<1 ML	He^+	500	60	ISS	6.3×10^{-16}	76Ta02	
Ni	S	<1 ML	Ne^+	500	60	ISS	8.0×10^{-16}	76Ta02	
Ni	S	<1 ML	Ar^+	500	60	ISS	1.1×10^{-15}	76Ta02	
Ni foil	S		Ar^+	500	30	AES	6.0×10^{-16}	78Wi03	
Ni foil	S		Ar^+	500	30	ISS	6.0×10^{-16}	77Ta05	
Ni foil	S		H_3^+	500	30	AES	2.00×10^{-17}	78Wi03	
Ni poly	S		He^+	1000	45	ISS	1.48×10^{-16}	81Sa03	*8)
Ni (111)	S		Ne^+	2000	45	ISS	1.4×10^{-15}	75Ta01	
Ni (111)	S		Ne^+	1000	60	ISS	3.0×10^{-15}	77Ta05	*9)
Ni (111)	S		Ne^+	1000	20	ISS	1.0×10^{-15}	77Ta05	*9)
Ni (110)	S		Ne^+	1000	60	ISS	2.5×10^{-15}	77Ta05	*9)
Ni (110)	S		Ne^+	1000	60	ISS	8.0×10^{-16}	77Ta05	*9)
TiC	O		H^+	500	50	SIMS	3.7×10^{-17}	84Su01	
TiC	O		H^+	700	50	SIMS	4.2×10^{-17}	84Su01	
TiC	O		H^+	1000	50	SIMS	4.1×10^{-17}	84Su01	

TiC	O	H^+	1500	50	SIMS	3.7×10^{-17}	84Su01	
TiC	O	H^+	2000	50	SIMS	2.85×10^{-17}	84Su01	
TiC	O	H^+	3000	50	SIMS	2.2×10^{-17}	84Su01	
TiC	O	Ar^+	500	50	SIMS	3.2×10^{-17}	84Su01	
TiC	O	Ar^+	700	50	SIMS	4.2×10^{-17}	84Su01	
TiC	O	Ar^+	1000	50	SIMS	5.0×10^{-17}	84Su01	
TiC	O	Ar^+	1500	50	SIMS	6.0×10^{-17}	84Su01	
TiC	O	Ar^+	2000	50	SIMS	5.0×10^{-17}	84Su01	
TiC	O	Ar^+	3000	50	SIMS	6.2×10^{-17}	84Su01	
TiC	O	Ar^+	5000	50	SIMS	6.2×10^{-17}	84Su01	
Si (111)	Impurites	$^4He^+$	1000	45	ISS	8.9×10^{-17}	80On01	*10)
Si (111)	Impurites	$^4He^+$	1000	45	ISS	5.4×10^{-17}	80On01	*11)

*1) Desorbed species H_2^+, NiH_2^+ for γ state ; Ni_2H^+ for β state.
*2) Refer to 74Wi02
*3) Saturation coverage
*4) Baked stainless steel, desorbed species; hydrogen molecules.
*5) Unbaked stainless steel, desorbed species; hydrogen molecules.
*6) Electron beam melted Mo
*7) Ni I 352.5nm
*8) Surface segregation due to sample heating
*9) Sulfer was brought to crystal surface simply by heating it to about 800°C for some time.
*10) Segregated impurities (As, Se, Br) due to sample heating. Speciemen temp. 300K
*11) Segregated impurities (As, Se, Br) due to sample heating. Speciemen temp. 973K

DATA LIST FOR IID 2 --ATOMS PER ION--

Substrate	Adsorbate and coverage	Incident ion species	Incident energy (eV)	Incident angle from normal (deg.)	Desorbed species	Temp. (K)	Method	Atoms per ion	Ref.	Remark
Ti	H_2	Ar^+	1500	45	H		MS	0.01	80Sa02	*1)
Ti	H_2	He^+	1500	45	H		MS	0.003	80Sa02	*1)
W(100)	H_2 1 ML	$^3He^+$	1000	60				0.12	78Ta06	*2)
SS(Baked)	H_2	D^+	5600	0	H_2	300	MS	2.0	74Mc01	
Be	D_2	H^+	1000	30	D^-		SIMS	0.22	84Ba05	*3)
SS 316	D_2 1 ML	H_3^+	1000	30	D^-		SIMS	0.2	81Ba03	*3)
Mo poly	O_2	H^+	20000	60°			*4)	0.0029	77Ra01	
Mo poly	O_2	H_2^+	20000	60			*4)	0.011	77Ra01	
Mo poly	O_2	H_3^+	20000	60			*4)	0.017	77Ra01	
Mo poly	O_2	H^+	20000	30°			*4)	0.0012	78Ra02	
Ti	CO	He^+	1500	45	CO		*4)	0.012	80Sa02	*5)

Mo	CO	He^+	1500	45	CO		ISS	0.04	80Sa02	*5)
Mo	CO	Ar^+	1500	45	CO		ISS	0.21	80Sa02	*5)
Ni(111)	S	Ne^+	2000	45			ISS	1.2	75Ta01	*6)
SS	CH_4	D^+	5600	0	H_2	77	MS	0.025	74Mc01	
SS	CH_4 etc.	D^+	5600	0		75	MS	< 0.1	74Mc01	*7)
SS	CO_2	D^+	5600	0	CO	77	MS	10	74Mc01	
SS(babed)	R. G.	D^+	5600	0	H_2	300	MS	1 ∿ 10	74Mc01	

*1) Residual gas analyser
*2) Surface coverage 1×10^{15} atoms/cm^2
*3) Surface coverage 2×10^{15} atoms/cm^2
*4) Hydrogen Balmer-β line intensity from excited H atoms was measured.
*5) Surface coverage 7.0×10^{14} molecules/cm^2
*6) Surface coverage 8.6×10^{14} atoms/cm^2
*7) Adsorbates : CH_4, Kr, Ar, CO

DATA LIST FOR IID 3 --MOLECULES PER ION--

Substrate	Adsorbate and coverage	Incident ion species	Incident energy (eV)	Incident angle from normal (deg.)	Desorbed species	Temp.	Method	Molecules per ion	Ref.	Remark
Mo	H_2O	D^+	15000		H_2	300	MS	0.5 ∿ 6	74Mc01	
SS	CO	D^+	5600		CO	77	MS	10	74Mc01	
SS	H_2O	D^+	5600		H_2O	77	MS	120	74Mc01	

5.2 Experimental Data for PSD

5.2.1 Tables

In table 3, the first column shows the substrate and the first line the adsorbate. For a combination of adsorbate and substrate the references concerned are shown by registered symbols. The rule of the registered symbol is the same as that for the case of IID (see 5.1.1).

Table 4 shows the figure number of the subsequent graphs. In this table, DL indicates the list of miscellaneous data in section 5.2.4.

TABLE 3 ADSORBATE/SUBSTRATE SYSTEMS IN PSD

	O_2	CO	H_2O	NO	K,Na	R.G.
Ti	81Ha01		82St02			
Cr	84St02					
Ni	81Ja02	61La01		82Ja04	73De01	
		65Ad01				
		65La02				
		72Pa01				
		73Mc01				
		81Ja02				
		82Ja04				
Zr		65Ad01				
Mo		65Ad01				
Ru		81Ma02				
W	77Fr01	65Ad01				71Pe01
	80Ca01	65La02				77Fr01
	80Ma01	72Kr01				
		79Fr02				

$(CO_2 + CO)/Ni$: 71Ge01
$(CO + O_2)/W$: 77Fr01
$(H_2 + CO)/W$: 77Fr01
$R.G./(Nb + O_2)$: 77Li05
$(CH_3)_4C/Ag$: 84Ke01

TABLE 3 -CONTINUED

	N_2	O_2	CO	H_2O	C_2H_2	Na,K	R.G.
Al_2O_3	83Ro02*		83Ro02*		83Ro02*		76Br01 76Br02
TiO_2				79Kn01			76Co01 76Li03 76Li04
ZnO		76Dr01**					75Sh01 76Sh02 76Li03 76Li04 77Sh03 79Li07
CdS							76Li03 76Li04
Al- Alloy							68Ba01 83Gr01 84Mo02 84Ko02
SS						77Fr01	73Fa01 76Br01 76Br02 77Fr01
QUARTZ			65La02				
PYREX			65La02				

CH_3F/Nacl : 82He01, 83He02

*) Condensed-phase
**) Refer to 76Sh02

TABLE 4 FIGURE NUMBER OF GRAPHS AND DATA LIST (DL)

	O_2	CO	H_2O	NO	K,Na	R.G.
Ti	fig.81 fig.89 fig.90 fig.91		fig.82			
Cr	fig.80					
Ni	fig.79	fig.68 fig.76 DL		fig.78	fig.73	
Zr		fig.70				
Mo		DL				
Ru		fig.77				
W	DL	fig.71				DL

$(CO_2 + CO)/Ni$: fig.67
$(O_2 + CO)/W$: DL
$(H_2 + CO)/W$: DL
$R.G./(Nb + O_2)$: DL
$(CH_3)C/Ag$: fig.88

TABLE 4 -CONTINUED

	N_2	O_2	CO	H_2O	C_2H_2	Na,K	R.G.
Al_2O_3	fig.86 fig.87		fig.84 fig.85		fig.83		fig.74 DL
TiO_2				DL			DL
ZnO		fig.66					fig.66 DL
CdS							DL
Al-Alloy							DL
SS						DL	fig.72 fig.75 DL
QUARTZ			DL				
PYREX			fig.69				

CH_3F/NaCl: DL

5.2.2 Graph and Data List for Desorption Cross Section

Figure 66 shows an energy dependence of desorption cross section. The measurement was done using five specific lines of the Hg lamp spectra selected by three interference filters and a color filter. Photodesorption yields of CO_2, as well as those of O_2, showed an exponential decay with illumination time. From the decay constants, the desorption cross section was obtained (see section 2).

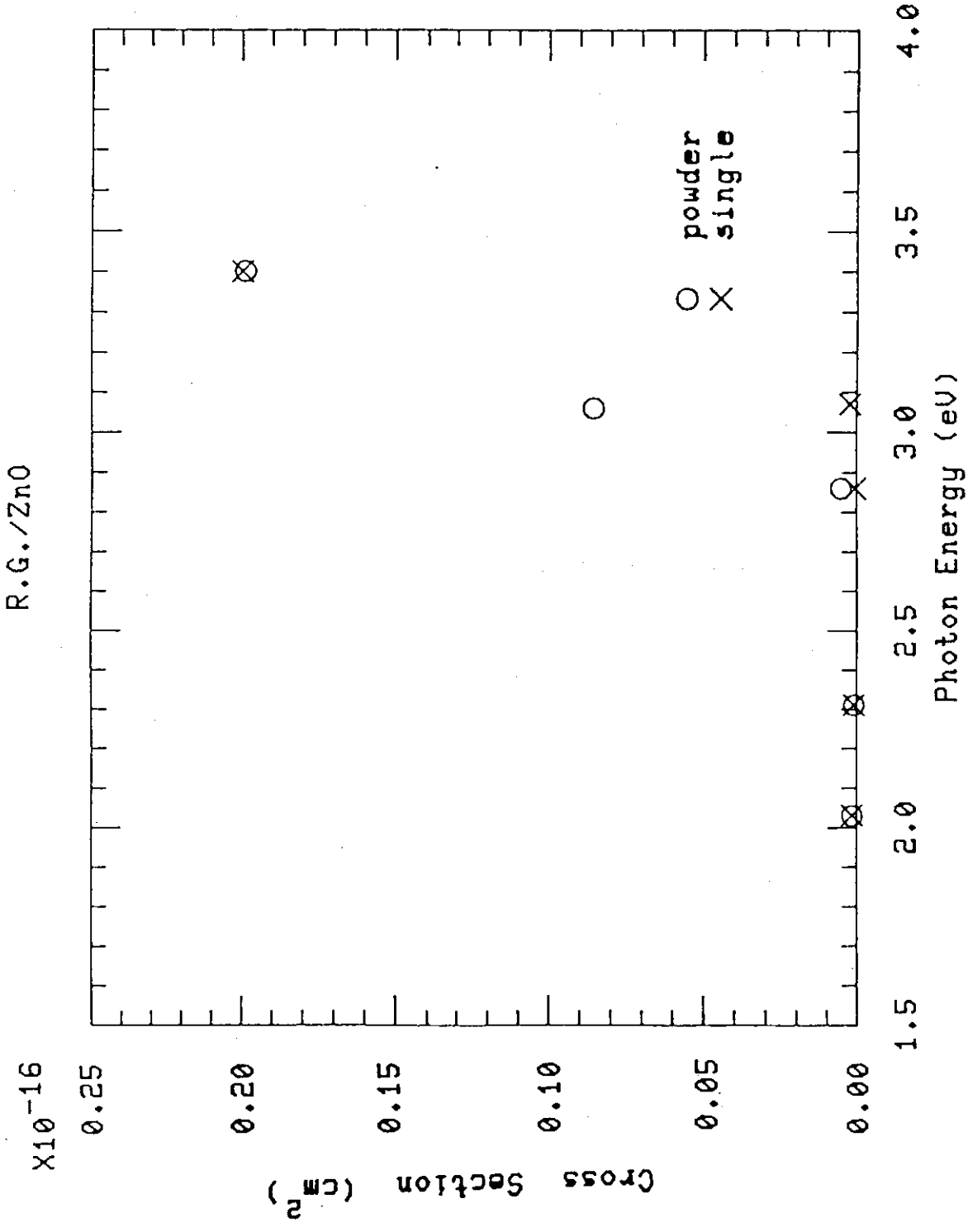

Fig.66 Desorption cross section as a function of incident energy

DATA LIST

Substrate	Adsorbed gases	Incident photon energy (eV)	Desorbed species	Method	Desorption cross section (cm**2)	Ref.
ZnO pow.	R.G.	0.203E+01	CO2	MS	0.155E-18	76Sh02
ZnO pow.	R.G.	0.231E+01	CO2	MS	0.899E-19	76Sh02
ZnO pow.	R.G.	0.286E+01	CO2	MS	0.521E-18	76Sh02
ZnO pow.	R.G.	0.306E+01	CO2	MS	0.855E-17	76Sh02
ZnO pow.	R.G.	0.340E+01	CO2	MS	0.199E-16	76Sh02
ZnO sin.	R.G.	0.203E+01	CO2	MS	0.155E-18	76Sh02
ZnO sin.	R.G.	0.231E+01	CO2	MS	0.899E-19	76Sh02
ZnO sin.	R.G.	0.286E+01	CO2	MS	0.279E-19	76Sh02
ZnO sin.	R.G.	0.307E+01	CO2	MS	0.217E-18	76Sh02
ZnO sin.	R.G.	0.340E+01	CO2	MS	0.200E-16	76Sh02

CO2 was the only photodesorbed species.
The photodesorption occurs only when the incident photon energy exceeds the ZnO band gap energy.
pow. : powder
sin. : single

5.2.3 Graphs and Data Lists for Desorption Yields

Desorption yields show distinct thresholds. In the desorption of molecules and some ions, the thresholds lie in the energy range of single one-electron excitations of the valence levels. The thresholds of positive ions lie in the energy ranges corresponding to ionizations of core level or complex multi-electron excitations.

The desorption yields of molecules or atoms are shown in Figs. 67 - 73 as a function of wavelength of photon. In general, the mass-analyzed yields decrease with increasing wavelength. The measurements were performed with use of photons of energies between visible to far UV range.

The data in Fig.74 and some data in Fig.75 were obtained using X-rays as photon sources.

Figures 76 - 88 show the energy dependence of desorbed ions. Desorption spectra show complex structures both in the region near threshold and well above threshold energy. These data were obtained using synchrotron orbital radiations with various monochrometers.

Figures 83 - 88 show the photon-stimulated ion desorption from surfaces with condensed gases. Gross differences between condensed-phase and gas-phase are found in desorption yields near threshold energy.

Figures 89 and 93 show the exposure dependence of desorption yields. The energy dependence of desorbed ions is also shown in Fig.91.

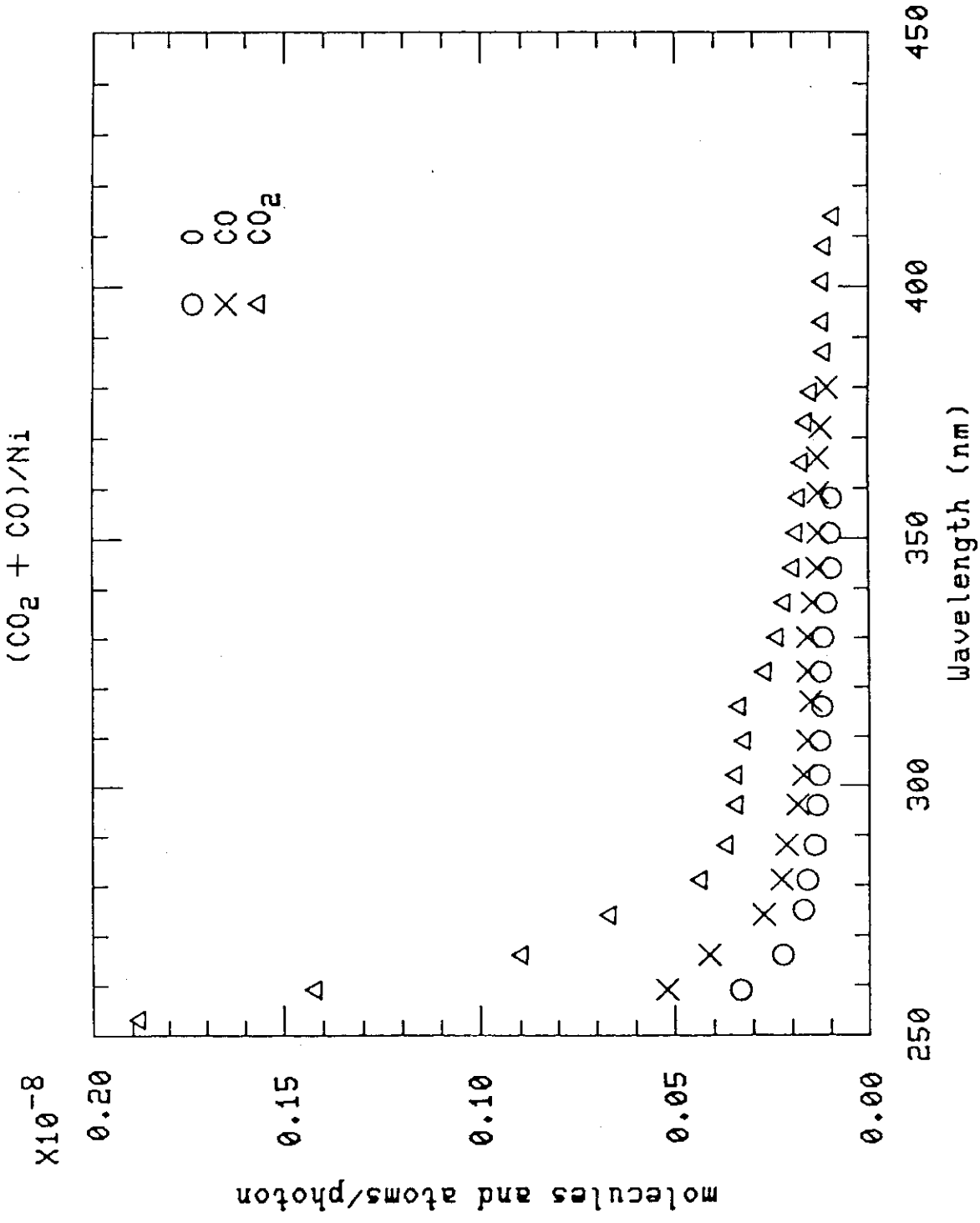

Fig.67 Desorption efficiency as a function of wavelength

DATA LIST

Substrate	Adsorbed gases	Incident photon energy (nm)	Desorbed species	Method	Molecules and atoms per photon	Ref.
Ni poly	CO2/CO	0.259E+03	O	MS	0.332E-09	71Ge01
Ni poly	CO2/CO	0.266E+03	O	MS	0.224E-09	71Ge01
Ni poly	CO2/CO	0.275E+03	O	MS	0.171E-09	71Ge01
Ni poly	CO2/CO	0.281E+03	O	MS	0.161E-09	71Ge01
Ni poly	CO2/CO	0.288E+03	O	MS	0.143E-09	71Ge01
Ni poly	CO2/CO	0.296E+03	O	MS	0.136E-09	71Ge01
Ni poly	CO2/CO	0.302E+03	O	MS	0.130E-09	71Ge01
Ni poly	CO2/CO	0.309E+03	O	MS	0.129E-09	71Ge01
Ni poly	CO2/CO	0.316E+03	O	MS	0.123E-09	71Ge01
Ni poly	CO2/CO	0.323E+03	O	MS	0.126E-09	71Ge01
Ni poly	CO2/CO	0.330E+03	O	MS	0.119E-09	71Ge01
Ni poly	CO2/CO	0.337E+03	O	MS	0.110E-09	71Ge01
Ni poly	CO2/CO	0.344E+03	O	MS	0.971E-10	71Ge01
Ni poly	CO2/CO	0.351E+03	O	MS	0.998E-10	71Ge01
Ni poly	CO2/CO	0.358E+03	O	MS	0.964E-10	71Ge01
Ni poly	CO2/CO	0.259E+03	CO	MS	0.519E-09	71Ge01
Ni poly	CO2/CO	0.266E+03	CO	MS	0.411E-09	71Ge01
Ni poly	CO2/CO	0.274E+03	CO	MS	0.272E-09	71Ge01
Ni poly	CO2/CO	0.281E+03	CO	MS	0.226E-09	71Ge01
Ni poly	CO2/CO	0.288E+03	CO	MS	0.213E-09	71Ge01
Ni poly	CO2/CO	0.296E+03	CO	MS	0.185E-09	71Ge01
Ni poly	CO2/CO	0.302E+03	CO	MS	0.170E-09	71Ge01
Ni poly	CO2/CO	0.309E+03	CO	MS	0.160E-09	71Ge01
Ni poly	CO2/CO	0.317E+03	CO	MS	0.151E-09	71Ge01
Ni poly	CO2/CO	0.323E+03	CO	MS	0.159E-09	71Ge01
Ni poly	CO2/CO	0.330E+03	CO	MS	0.159E-09	71Ge01
Ni poly	CO2/CO	0.337E+03	CO	MS	0.147E-09	71Ge01
Ni poly	CO2/CO	0.344E+03	CO	MS	0.134E-09	71Ge01
Ni poly	CO2/CO	0.351E+03	CO	MS	0.131E-09	71Ge01
Ni poly	CO2/CO	0.359E+03	CO	MS	0.130E-09	71Ge01
Ni poly	CO2/CO	0.366E+03	CO	MS	0.130E-09	71Ge01
Ni poly	CO2/CO	0.372E+03	CO	MS	0.123E-09	71Ge01
Ni poly	CO2/CO	0.380E+03	CO	MS	0.108E-09	71Ge01
Ni poly	CO2/CO	0.253E+03	CO2	MS	0.188E-08	71Ge01
Ni poly	CO2/CO	0.259E+03	CO2	MS	0.142E-08	71Ge01
Ni poly	CO2/CO	0.266E+03	CO2	MS	0.894E-09	71Ge01
Ni poly	CO2/CO	0.274E+03	CO2	MS	0.666E-09	71Ge01
Ni poly	CO2/CO	0.281E+03	CO2	MS	0.432E-09	71Ge01
Ni poly	CO2/CO	0.288E+03	CO2	MS	0.364E-09	71Ge01
Ni poly	CO2/CO	0.296E+03	CO2	MS	0.339E-09	71Ge01

./..

Ni poly	CO2/CO	0.302E+03	CO2	MS	0.342E-09	71Ge01
Ni poly	CO2/CO	0.309E+03	CO2	MS	0.320E-09	71Ge01
Ni poly	CO2/CO	0.316E+03	CO2	MS	0.332E-09	71Ge01
Ni poly	CO2/CO	0.323E+03	CO2	MS	0.267E-09	71Ge01
Ni poly	CO2/CO	0.330E+03	CO2	MS	0.236E-09	71Ge01
Ni poly	CO2/CO	0.337E+03	CO2	MS	0.217E-09	71Ge01
Ni poly	CO2/CO	0.344E+03	CO2	MS	0.195E-09	71Ge01
Ni poly	CO2/CO	0.351E+03	CO2	MS	0.186E-09	71Ge01
Ni poly	CO2/CO	0.358E+03	CO2	MS	0.179E-09	71Ge01
Ni poly	CO2/CO	0.365E+03	CO2	MS	0.170E-09	71Ge01
Ni poly	CO2/CO	0.373E+03	CO2	MS	0.160E-09	71Ge01
Ni poly	CO2/CO	0.379E+03	CO2	MS	0.148E-09	71Ge01
Ni poly	CO2/CO	0.387E+03	CO2	MS	0.114E-09	71Ge01
Ni poly	CO2/CO	0.393E+03	CO2	MS	0.119E-09	71Ge01
Ni poly	CO2/CO	0.401E+03	CO2	MS	0.119E-09	71Ge01
Ni poly	CO2/CO	0.408E+03	CO2	MS	0.113E-09	71Ge01
Ni poly	CO2/CO	0.414E+03	CO2	MS	0.908E-10	71Ge01

Ni film was evaporated on Pyrex glass.

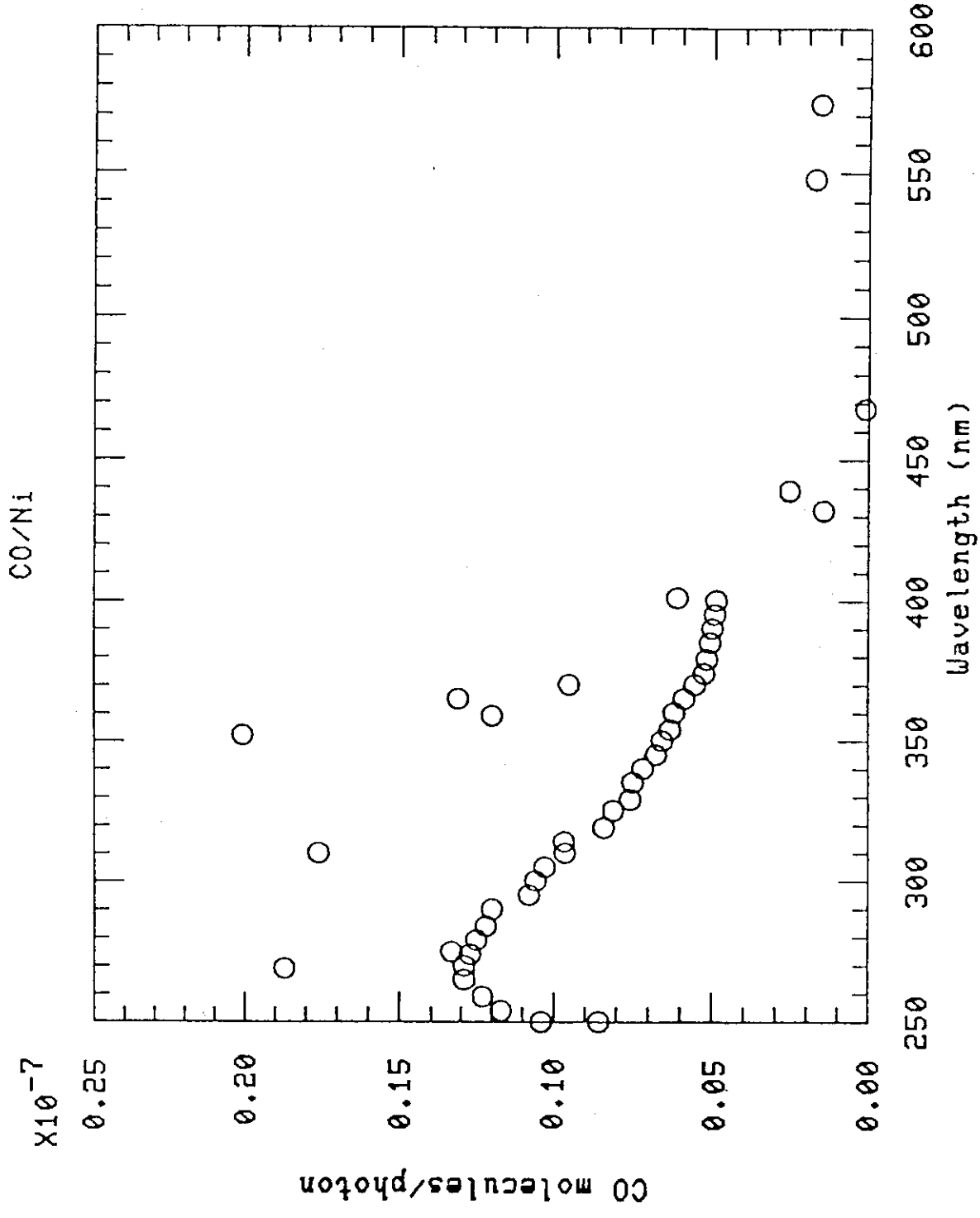

Fig.68 Desorption efficiency as a function of wavelength

DATA LIST

Substrate	Adsorbed gases	Incident photon energy (nm)	Desorbed species	Method	Molecules per photon	Ref.
Ni poly	CO	0.250E+03	CO	*1)	0.856E-08	65Ad01
Ni(110)	CO	0.250E+03	CO	*2)	0.104E-07	72Pa01
Ni(110)	CO	0.254E+03	CO	*2)	0.117E-07	72Pa01
Ni(110)	CO	0.259E+03	CO	*2)	0.123E-07	72Pa01
Ni(110)	CO	0.265E+03	CO	*2)	0.129E-07	72Pa01
Ni poly	CO	0.269E+03	CO	*1)	0.187E-07	65Ad01
Ni(110)	CO	0.270E+03	CO	*2)	0.129E-07	72Pa01
Ni(110)	CO	0.274E+03	CO	*2)	0.127E-07	72Pa01
Ni poly	CO	0.275E+03	CO	MS	0.133E-07	61La01
Ni(110)	CO	0.279E+03	CO	*2)	0.125E-07	72Pa01
Ni(110)	CO	0.284E+03	CO	*2)	0.122E-07	72Pa01
Ni(110)	CO	0.290E+03	CO	*2)	0.120E-07	72Pa01
Ni(110)	CO	0.295E+03	CO	*2)	0.108E-07	72Pa01
Ni(110)	CO	0.300E+03	CO	*2)	0.106E-07	72Pa01
Ni(110)	CO	0.305E+03	CO	*2)	0.103E-07	72Pa01
Ni(110)	CO	0.310E+03	CO	*2)	0.966E-08	72Pa01
Ni poly	CO	0.310E+03	CO	*1)	0.176E-07	65Ad01
Ni(110)	CO	0.314E+03	CO	*2)	0.969E-08	72Pa01
Ni(110)	CO	0.319E+03	CO	*2)	0.841E-08	72Pa01
Ni(110)	CO	0.325E+03	CO	*2)	0.812E-08	72Pa01
Ni(110)	CO	0.329E+03	CO	*2)	0.757E-08	72Pa01
Ni(110)	CO	0.335E+03	CO	*2)	0.749E-08	72Pa01
Ni(110)	CO	0.340E+03	CO	*2)	0.717E-08	72Pa01
Ni(110)	CO	0.345E+03	CO	*2)	0.676E-08	72Pa01
Ni(110)	CO	0.350E+03	CO	*2)	0.656E-08	72Pa01
Ni poly	CO	0.352E+03	CO	MS	0.201E-07	61La01
Ni(110)	CO	0.354E+03	CO	*2)	0.631E-08	72Pa01
Ni(110)	CO	0.360E+03	CO	*2)	0.618E-08	72Pa01
Ni poly	CO	0.359E+03	CO	MS	0.120E-07	61La01
Ni(110)	CO	0.365E+03	CO	*2)	0.587E-08	72Pa01
Ni poly	CO	0.365E+03	CO	MS	0.131E-07	61La01
Ni(110)	CO	0.370E+03	CO	*2)	0.553E-08	72Pa01
Ni poly	CO	0.370E+03	CO	*1)	0.953E-08	65Ad01
Ni(110)	CO	0.374E+03	CO	*2)	0.524E-08	72Pa01
Ni(110)	CO	0.379E+03	CO	*2)	0.515E-08	72Pa01
Ni(110)	CO	0.385E+03	CO	*2)	0.505E-08	72Pa01
Ni(110)	CO	0.390E+03	CO	*2)	0.499E-08	72Pa01
Ni(110)	CO	0.395E+03	CO	*2)	0.491E-08	72Pa01
Ni(110)	CO	0.400E+03	CO	*2)	0.487E-08	72Pa01
Ni poly	CO	0.401E+03	CO	MS	0.611E-08	61La01
Ni poly	CO	0.432E+03	CO	MS	0.146E-08	61La01
Ni poly	CO	0.439E+03	CO	*1)	0.256E-08	65Ad01
Ni poly	CO	0.468E+03	CO	MS	0.981E-10	61La01
Ni poly	CO	0.548E+03	CO	*1)	0.174E-08	65Ad01
Ni poly	CO	0.574E+03	CO	*1)	0.159E-08	65Ad01

*1) Total pressure change.
*2) A differential amplification method.

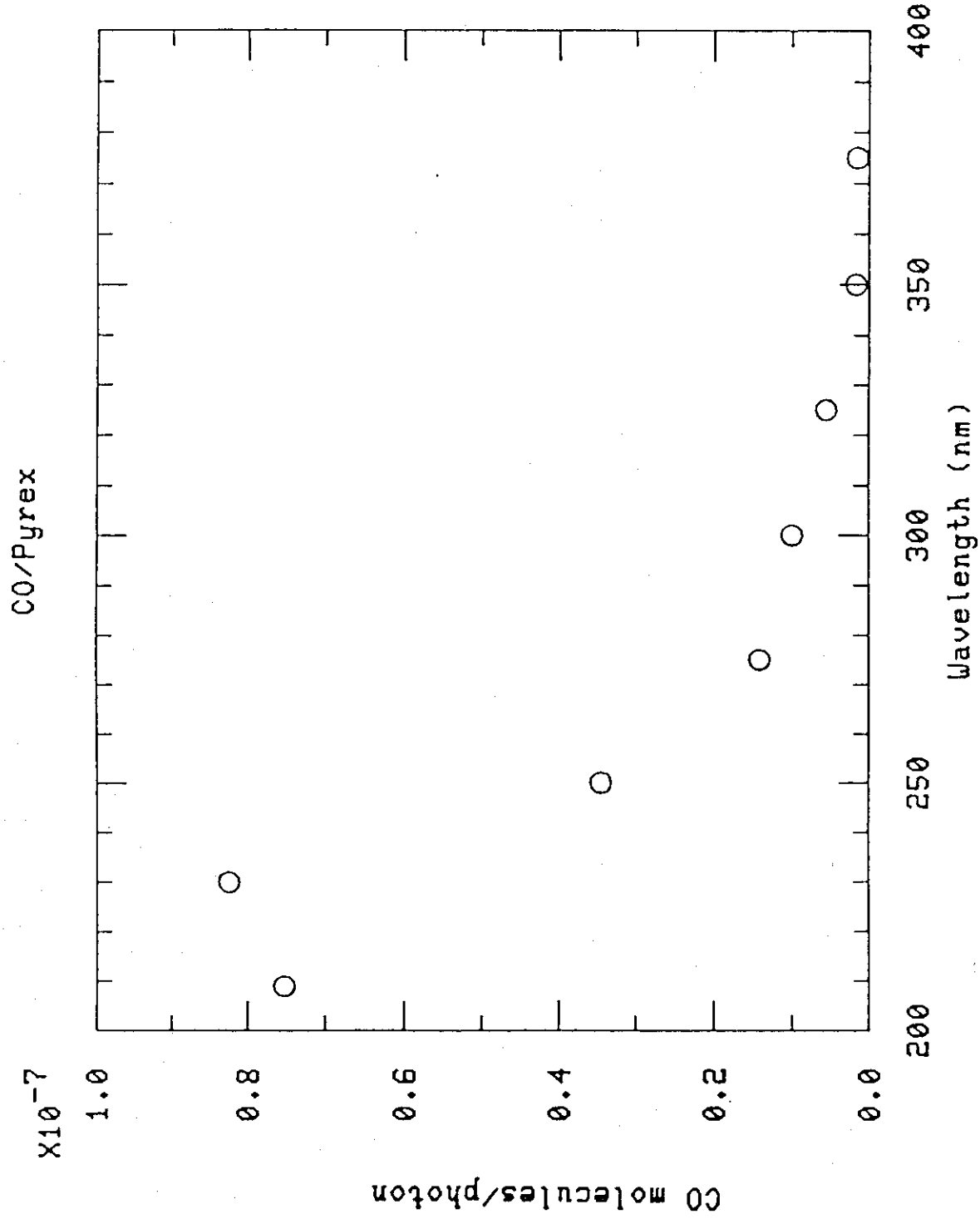

Fig.69 Desorption efficiency as a function of wavelength

DATA LIST

Substrate	Adsorbed gases	Incident photon energy (nm)	Desorbed species	Method	Molecules per photon	Ref.
Pyrex	CO	0.209E+03	CO	MS	0.752E-07	65La02
Pyrex	CO	0.230E+03	CO	MS	0.824E-07	65La02
Pyrex	CO	0.250E+03	CO	MS	0.345E-07	65La02
Pyrex	CO	0.275E+03	CO	MS	0.141E-07	65La02
Pyrex	CO	0.300E+03	CO	MS	0.996E-08	65La02
Pyrex	CO	0.325E+03	CO	MS	0.557E-08	65La02
Pyrex	CO	0.350E+03	CO	MS	0.170E-08	65La02
Pyrex	CO	0.375E+03	CO	MS	0.151E-08	65La02

Pyrex : borosilicate glass

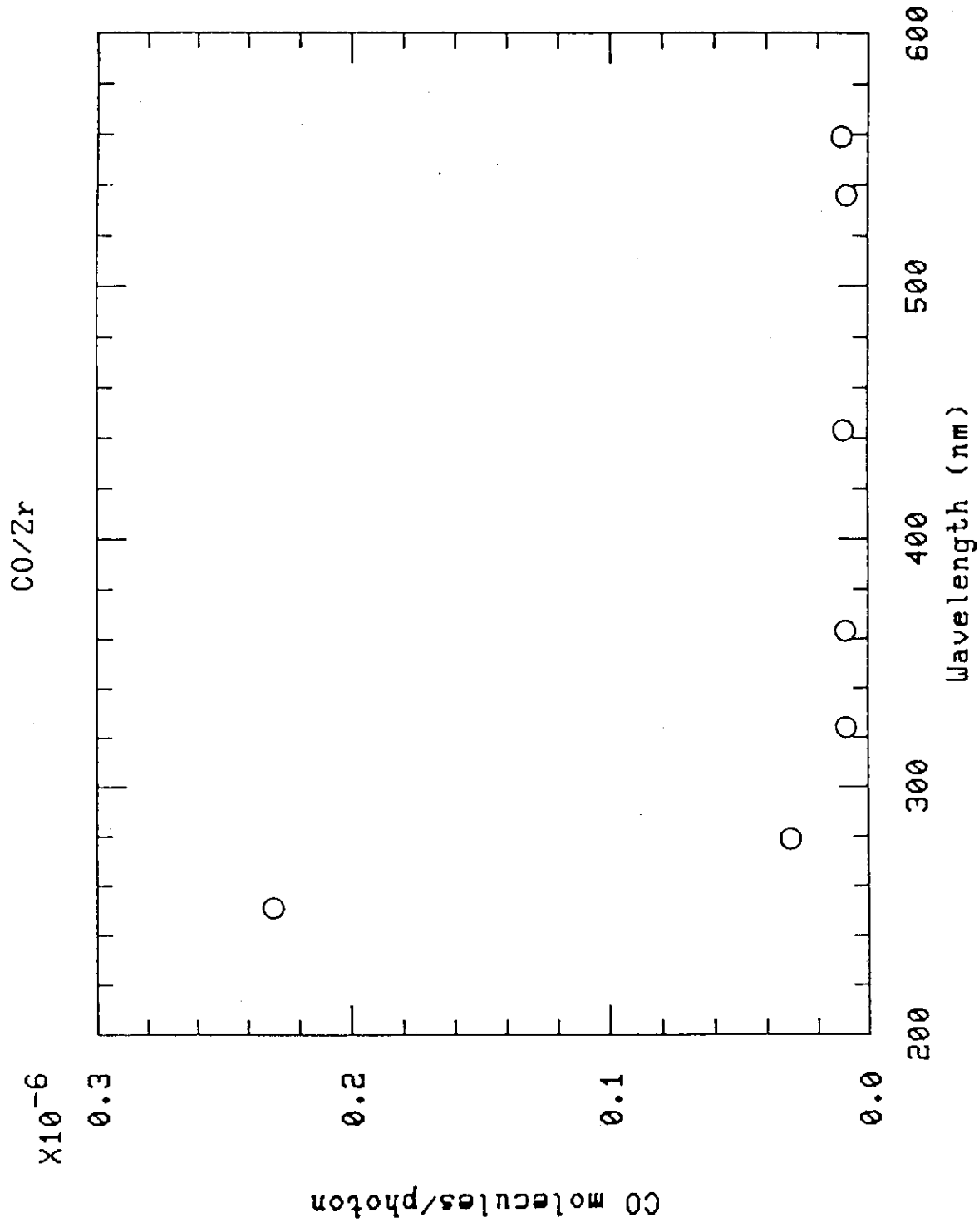

Fig.70 Desorption efficiency as a function of wavelength

DATA LIST

Substrate	Adsorbed gases	Incident photon energy (nm)	Desorbed species	Method	Molecules per photon	Ref.
Zr film	CO	0.251E+03	CO	*1)	0.230E-06	65Ad01
Zr film	CO	0.279E+03	CO	*1)	0.306E-07	65Ad01
Zr film	CO	0.324E+03	CO	*1)	0.880E-08	65Ad01
Zr film	CO	0.363E+03	CO	*1)	0.906E-08	65Ad01
Zr film	CO	0.443E+03	CO	*1)	0.960E-08	65Ad01
Zr film	CO	0.536E+03	CO	*1)	0.846E-08	65Ad01
Zr film	CO	0.559E+03	CO	*1)	0.104E-07	65Ad01

*1) Measurement of total pressure change.

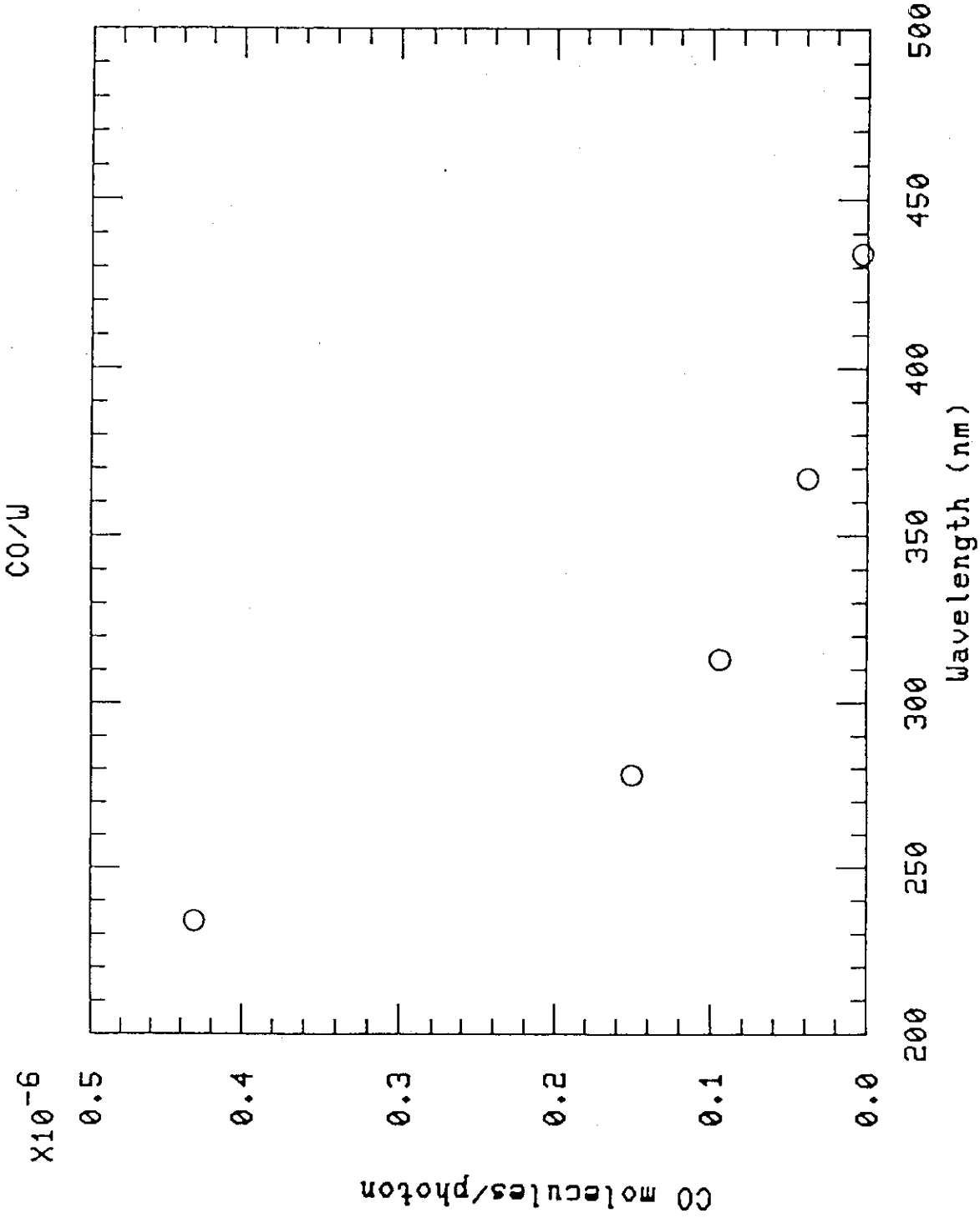

Fig.71 Desorption efficiency as a function of wavelength

DATA LIST

Substrate	Adsorbed gases	Incident photon energy (nm)	Desorbed species	Method	Molecules per photon	Ref.
W poly	CO alpha	0.234E+03	CO	MS	0.431E-06	72Kr01
W poly	CO alpha	0.278E+03	CO	MS	0.150E-06	72Kr01
W poly	CO alpha	0.313E+03	CO	MS	0.942E-07	72Kr01
W poly	CO alpha	0.367E+03	CO	MS	0.384E-07	72Kr01
W poly	CO alpha	0.434E+03	CO	MS	0.328E-08	72Kr01

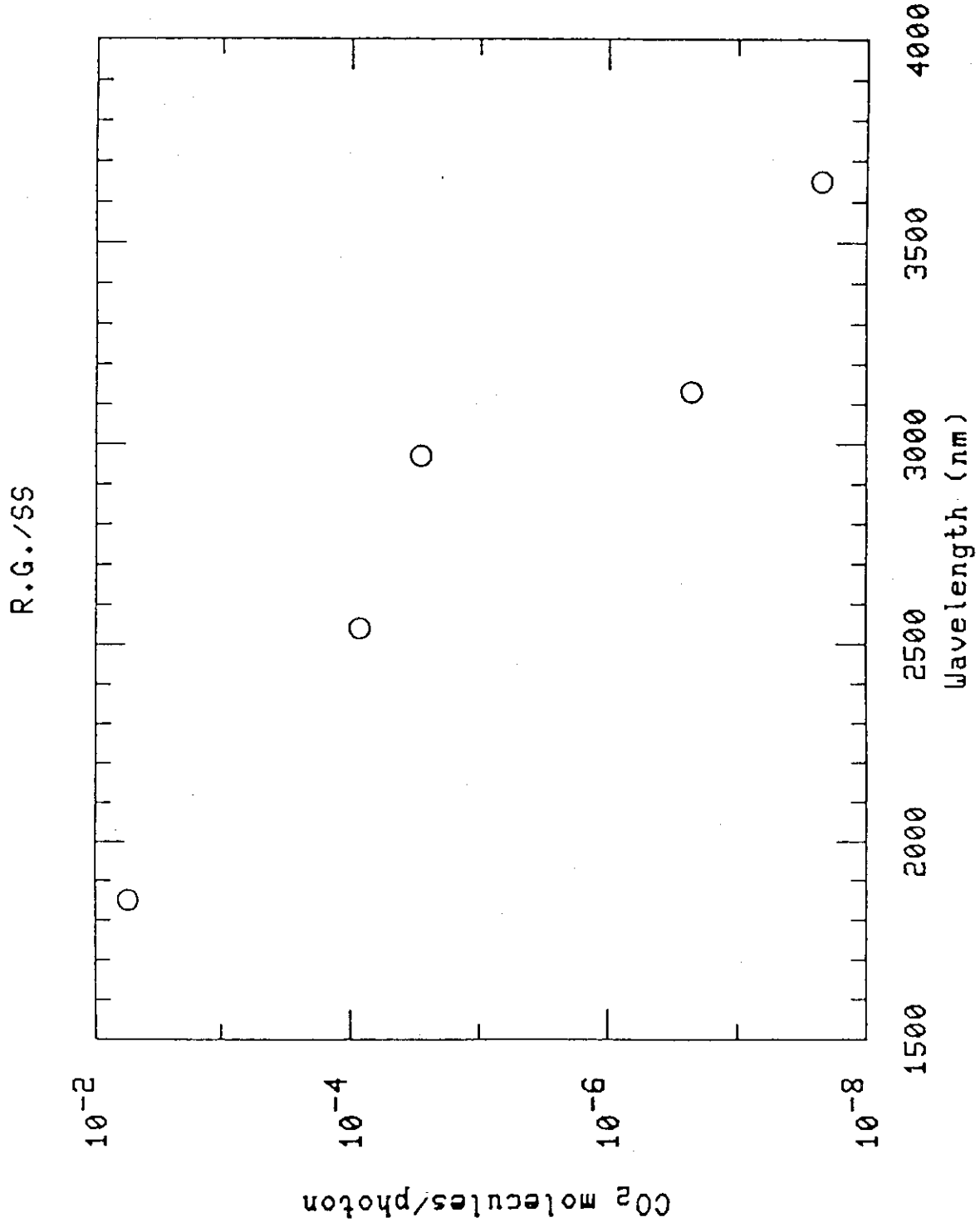

Fig.72 Desorption efficiency as a function of wavelength

DATA LIST

Substrate	Adsorbed gases	Incident photon energy (nm)	Desorbed species	Method	Molecules per photon	Ref.
SS 304	CO2	0.185E+04	CO2	MS	0.548E-02	73Fa01
SS 304	CO2	0.254E+04	CO2	MS	0.846E-04	73Fa01
SS 304	CO2	0.297E+04	CO2	MS	0.282E-04	73Fa01
SS 304	CO2	0.313E+04	CO2	MS	0.225E-06	73Fa01
SS 304	CO2	0.365E+04	CO2	MS	0.225E-07	73Fa01

The signals of other desorbed molecules were very weak.

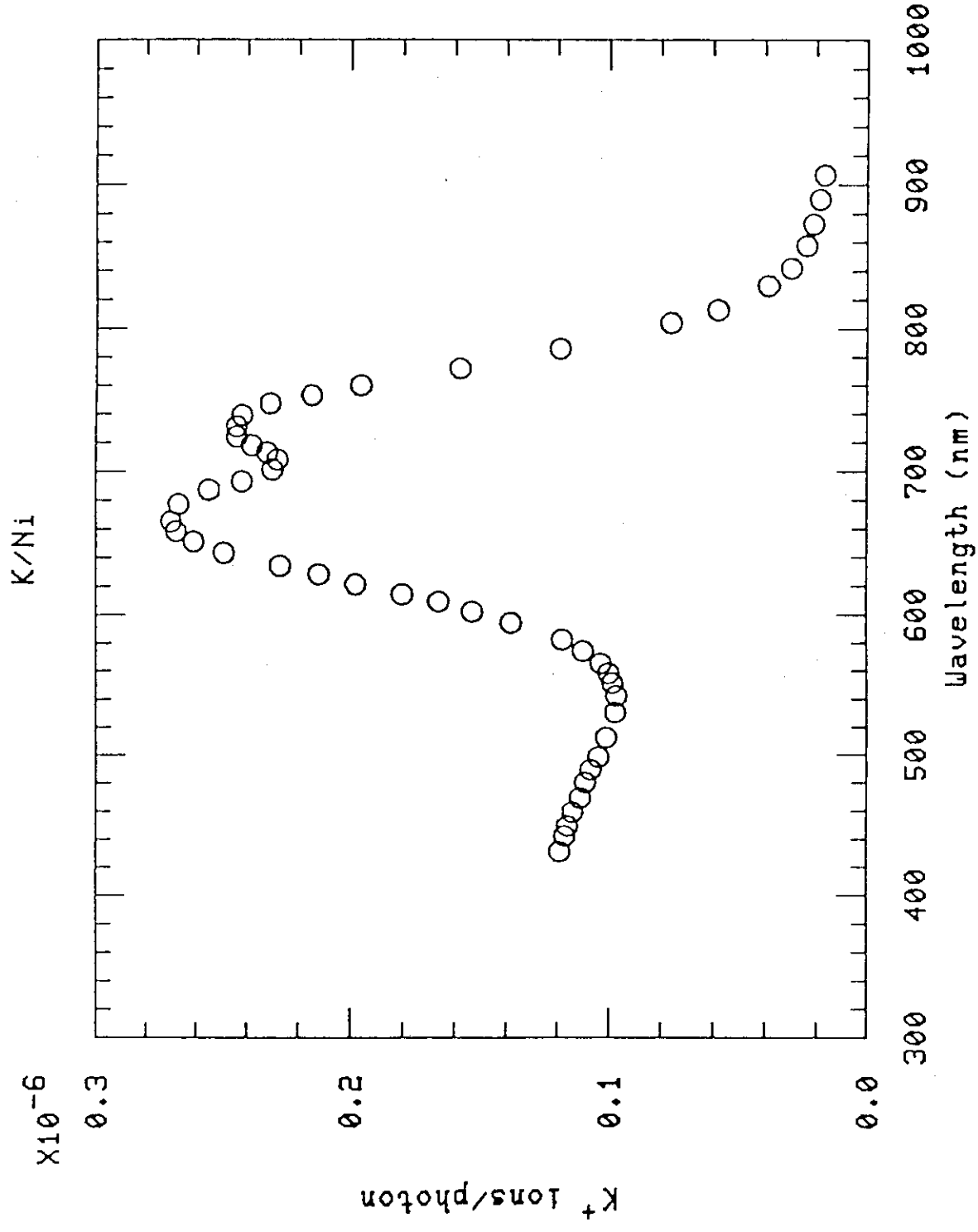

Fig.73 Desorption efficiency as a function of wavelength

DATA LIST

Substrate	Adsorbed gases	Incident photon energy (nm)	Desorbed species	Method	Ions per photon	Ref.
Ni	K	0.431E+03	K+	?	0.119E-06	73De01
Ni	K	0.442E+03	K+	?	0.117E-06	73De01
Ni	K	0.449E+03	K+	?	0.116E-06	73De01
Ni	K	0.459E+03	K+	?	0.114E-06	73De01
Ni	K	0.469E+03	K+	?	0.111E-06	73De01
Ni	K	0.480E+03	K+	?	0.109E-06	73De01
Ni	K	0.489E+03	K+	?	0.107E-06	73De01
Ni	K	0.498E+03	K+	?	0.104E-06	73De01
Ni	K	0.512E+03	K+	?	0.101E-06	73De01
Ni	K	0.530E+03	K+	?	0.975E-07	73De01
Ni	K	0.542E+03	K+	?	0.970E-07	73De01
Ni	K	0.551E+03	K+	?	0.986E-07	73De01
Ni	K	0.558E+03	K+	?	0.100E-06	73De01
Ni	K	0.565E+03	K+	?	0.103E-06	73De01
Ni	K	0.574E+03	K+	?	0.110E-06	73De01
Ni	K	0.582E+03	K+	?	0.118E-06	73De01
Ni	K	0.594E+03	K+	?	0.138E-06	73De01
Ni	K	0.602E+03	K+	?	0.153E-06	73De01
Ni	K	0.609E+03	K+	?	0.166E-06	73De01
Ni	K	0.614E+03	K+	?	0.180E-06	73De01
Ni	K	0.621E+03	K+	?	0.198E-06	73De01
Ni	K	0.628E+03	K+	?	0.212E-06	73De01
Ni	K	0.634E+03	K+	?	0.227E-06	73De01
Ni	K	0.643E+03	K+	?	0.249E-06	73De01
Ni	K	0.651E+03	K+	?	0.261E-06	73De01
Ni	K	0.658E+03	K+	?	0.268E-06	73De01
Ni	K	0.665E+03	K+	?	0.270E-06	73De01
Ni	K	0.677E+03	K+	?	0.267E-06	73De01
Ni	K	0.687E+03	K+	?	0.255E-06	73De01
Ni	K	0.693E+03	K+	?	0.242E-06	73De01
Ni	K	0.701E+03	K+	?	0.230E-06	73De01
Ni	K	0.708E+03	K+	?	0.228E-06	73De01
Ni	K	0.713E+03	K+	?	0.232E-06	73De01
Ni	K	0.718E+03	K+	?	0.238E-06	73De01
Ni	K	0.724E+03	K+	?	0.244E-06	73De01
Ni	K	0.731E+03	K+	?	0.244E-06	73De01
Ni	K	0.739E+03	K+	?	0.242E-06	73De01
Ni	K	0.747E+03	K+	?	0.231E-06	73De01
Ni	K	0.753E+03	K+	?	0.215E-06	73De01
Ni	K	0.760E+03	K+	?	0.196E-06	73De01
Ni	K	0.772E+03	K+	?	0.158E-06	73De01
Ni	K	0.786E+03	K+	?	0.119E-06	73De01
Ni	K	0.804E+03	K+	?	0.761E-07	73De01
Ni	K	0.813E+03	K+	?	0.580E-07	73De01
Ni	K	0.830E+03	K+	?	0.386E-07	73De01
Ni	K	0.842E+03	K+	?	0.296E-07	73De01
Ni	K	0.858E+03	K+	?	0.236E-07	73De01
Ni	K	0.873E+03	K+	?	0.210E-07	73De01
Ni	K	0.890E+03	K+	?	0.185E-07	73De01
Ni	K	0.907E+03	K+	?	0.167E-07	73De01

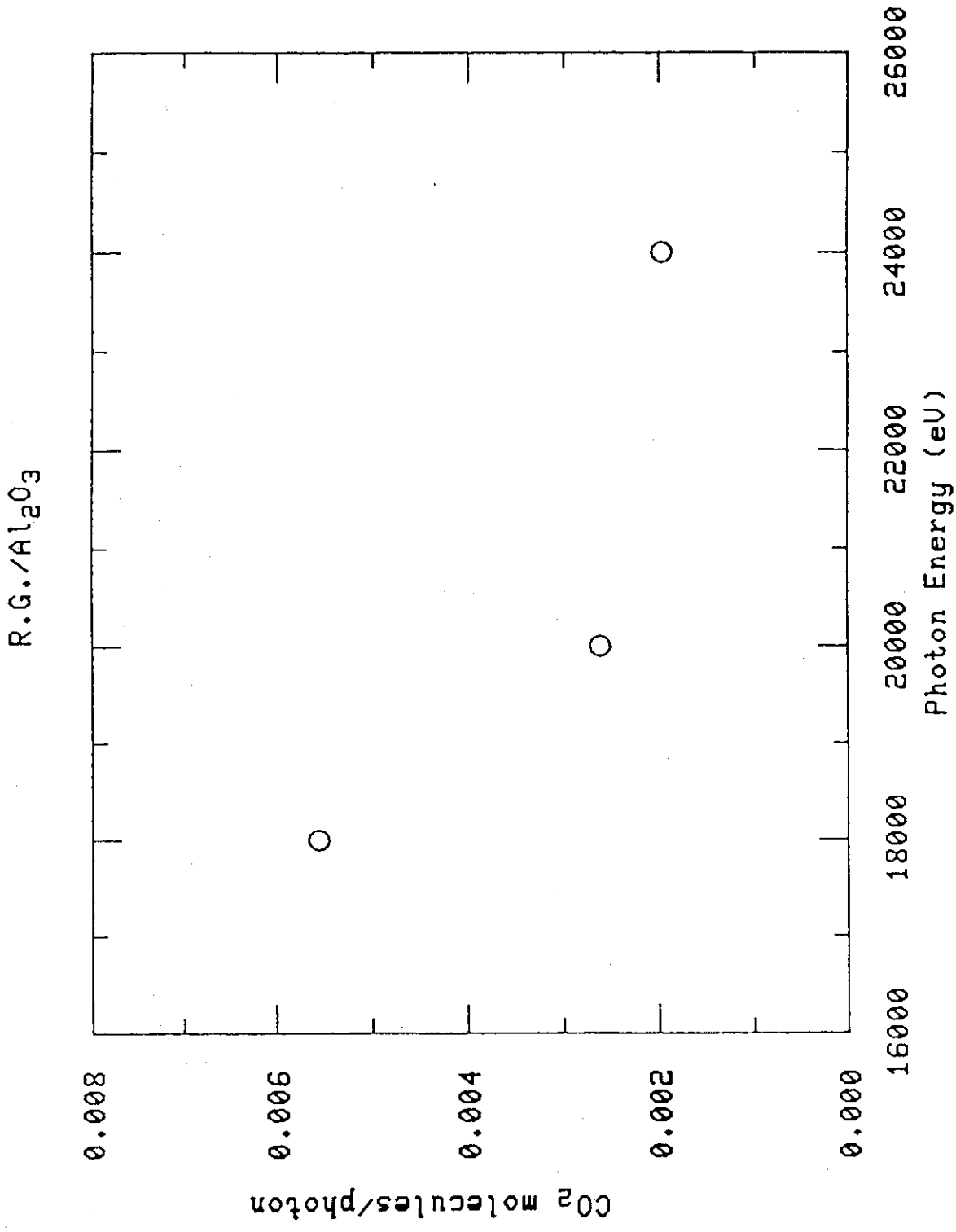

Fig.74 Desorption efficiency as a function of incident energy

DATA LIST

Substrate	Adsorbed gases	Incident photon energy (eV)	Desorbed species	Method	Molecules per photon	Ref.
Al2O3	R.G.	0.180E+05	CO2	MS	0.556E-02	76Br01
Al2O3	R.G.	0.200E+05	CO2	MS	0.262E-02	76Br01
Al2O3	R.G.	0.240E+05	CO2	MS	0.196E-02	76Br01

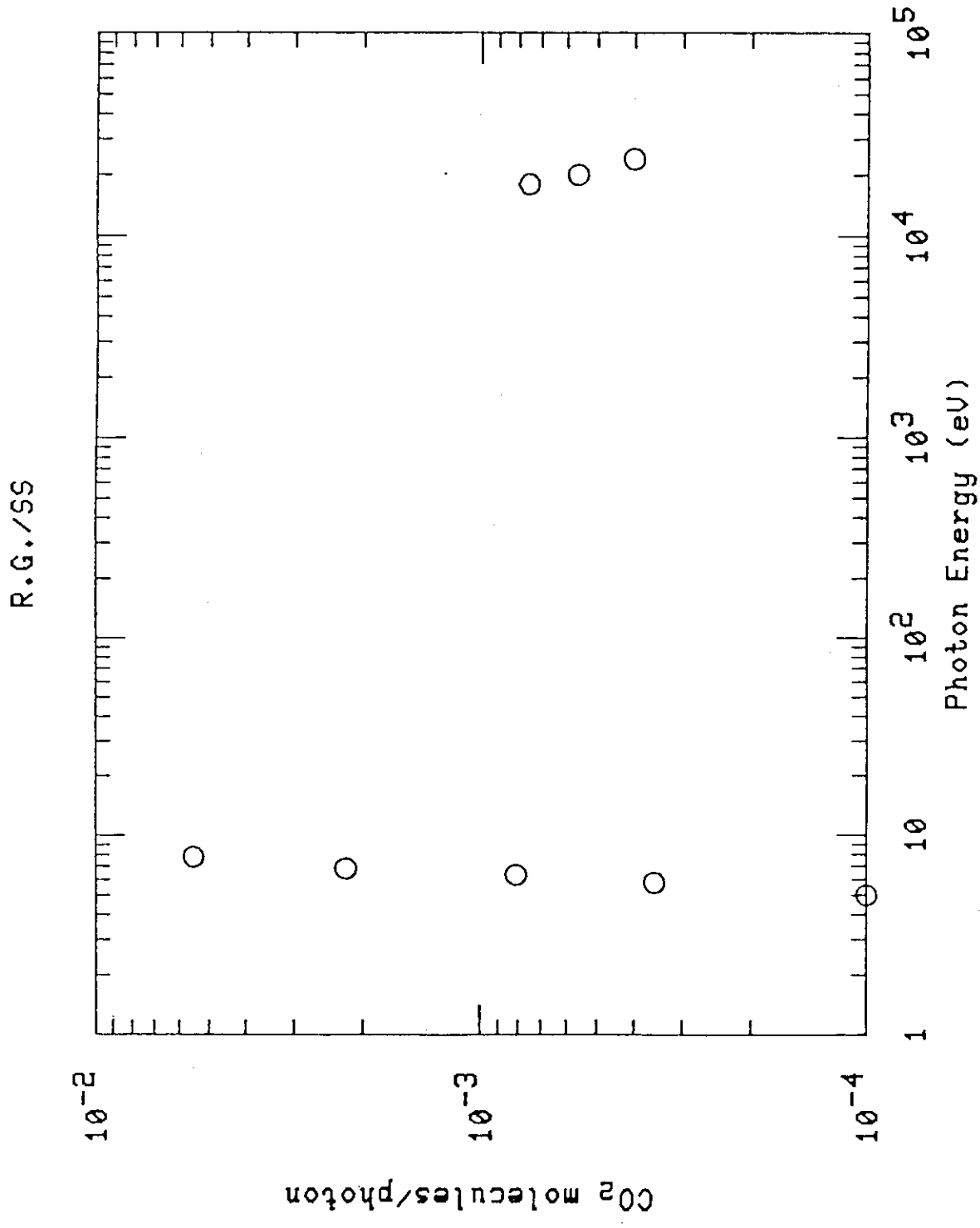

Fig.75 Desorption efficiency as a function of incident energy

DATA LIST

Substrate	Adsorbed gases	Incident photon energy (eV)	Desorbed species	Method	Molecules per photon	Ref.	Remark
SS 302	R.G.	0.497E+01	CO2	MS	0.100E-03	76Br01	*1)
SS 302	R.G.	0.576E+01	CO2	MS	0.354E-03	76Br01	*1)
SS 302	R.G.	0.630E+01	CO2	MS	0.806E-03	76Br01	*1)
SS 302	R.G.	0.675E+01	CO2	MS	0.220E-02	76Br01	*1)
SS 302	R.G.	0.776E+01	CO2	MS	0.547E-02	76Br01	*1)
SS 302	R.G.	0.180E+05	CO2	MS	0.751E-03	76Br01	*2)
SS 302	R.G.	0.200E+05	CO2	MS	0.559E-03	76Br01	*2)
SS 302	R.G.	0.240E+05	CO2	MS	0.401E-03	76Br01	*2)

*1) Monochromatic ultraviolet light
*2) W Bremsstrahlung spectrum

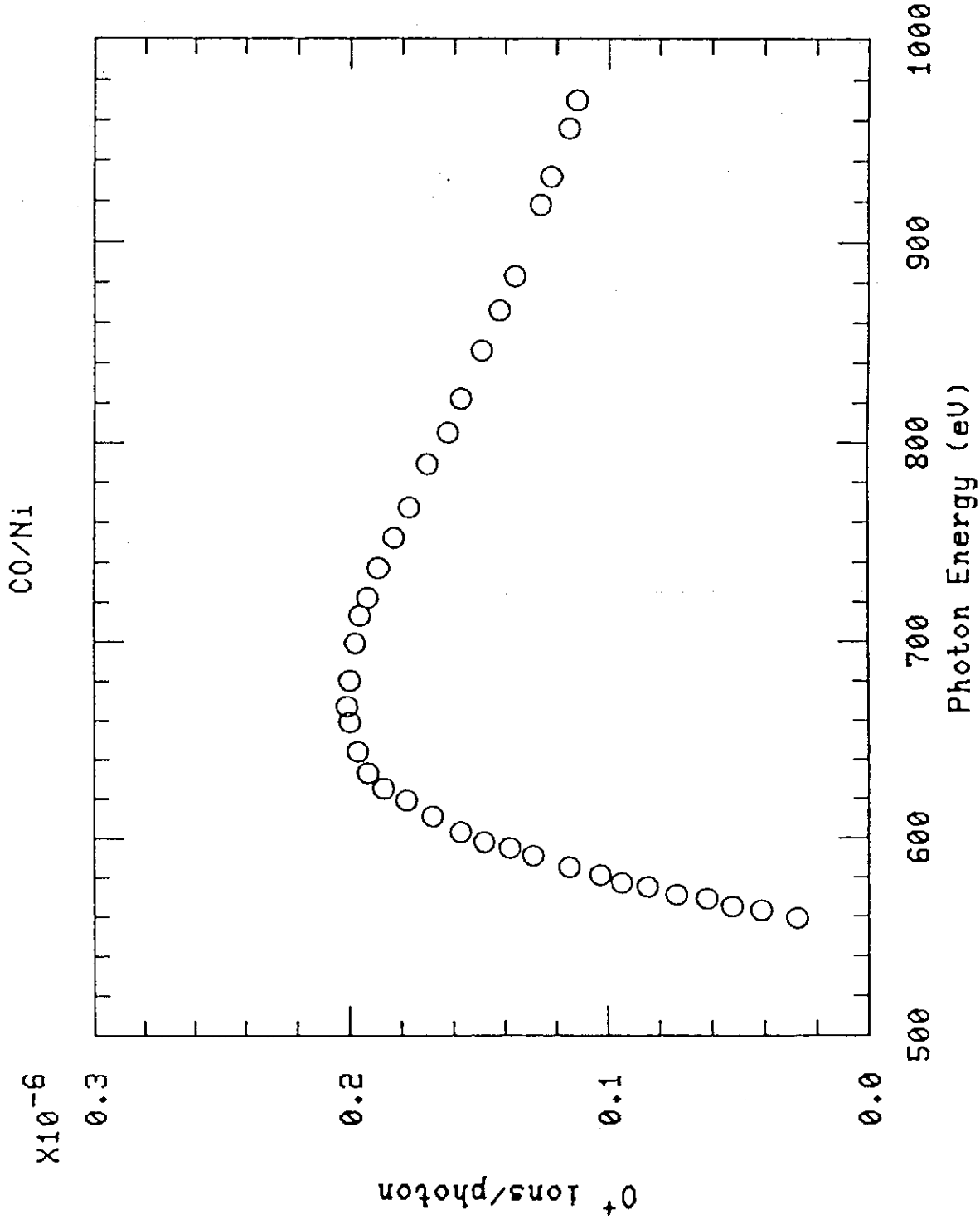

Fig.76 Desorption efficiency as a function of incident energy

DATA LIST

Substrate	Adsorbed gases	Incident photon energy (eV)	Desorbed species	Method	Ions per photon	Ref.
Ni(100)	CO	0.559E+03	O+	TOF	0.275E-07	82Ja04
Ni(100)	CO	0.563E+03	O+	TOF	0.412E-07	82Ja04
Ni(100)	CO	0.565E+03	O+	TOF	0.523E-07	82Ja04
Ni(100)	CO	0.569E+03	O+	TOF	0.619E-07	82Ja04
Ni(100)	CO	0.571E+03	O+	TOF	0.735E-07	82Ja04
Ni(100)	CO	0.575E+03	O+	TOF	0.846E-07	82Ja04
Ni(100)	CO	0.577E+03	O+	TOF	0.947E-07	82Ja04
Ni(100)	CO	0.581E+03	O+	TOF	0.103E-06	82Ja04
Ni(100)	CO	0.585E+03	O+	TOF	0.115E-06	82Ja04
Ni(100)	CO	0.591E+03	O+	TOF	0.129E-06	82Ja04
Ni(100)	CO	0.595E+03	O+	TOF	0.138E-06	82Ja04
Ni(100)	CO	0.598E+03	O+	TOF	0.148E-06	82Ja04
Ni(100)	CO	0.603E+03	O+	TOF	0.157E-06	82Ja04
Ni(100)	CO	0.611E+03	O+	TOF	0.168E-06	82Ja04
Ni(100)	CO	0.619E+03	O+	TOF	0.178E-06	82Ja04
Ni(100)	CO	0.625E+03	O+	TOF	0.187E-06	82Ja04
Ni(100)	CO	0.633E+03	O+	TOF	0.193E-06	82Ja04
Ni(100)	CO	0.644E+03	O+	TOF	0.197E-06	82Ja04
Ni(100)	CO	0.659E+03	O+	TOF	0.200E-06	82Ja04
Ni(100)	CO	0.667E+03	O+	TOF	0.201E-06	82Ja04
Ni(100)	CO	0.680E+03	O+	TOF	0.200E-06	82Ja04
Ni(100)	CO	0.699E+03	O+	TOF	0.198E-06	82Ja04
Ni(100)	CO	0.713E+03	O+	TOF	0.196E-06	82Ja04
Ni(100)	CO	0.722E+03	O+	TOF	0.193E-06	82Ja04
Ni(100)	CO	0.737E+03	O+	TOF	0.189E-06	82Ja04
Ni(100)	CO	0.752E+03	O+	TOF	0.183E-06	82Ja04
Ni(100)	CO	0.767E+03	O+	TOF	0.177E-06	82Ja04
Ni(100)	CO	0.789E+03	O+	TOF	0.170E-06	82Ja04
Ni(100)	CO	0.805E+03	O+	TOF	0.162E-06	82Ja04
Ni(100)	CO	0.822E+03	O+	TOF	0.157E-06	82Ja04
Ni(100)	CO	0.846E+03	O+	TOF	0.149E-06	82Ja04
Ni(100)	CO	0.866E+03	O+	TOF	0.142E-06	82Ja04
Ni(100)	CO	0.883E+03	O+	TOF	0.136E-06	82Ja04
Ni(100)	CO	0.918E+03	O+	TOF	0.126E-06	82Ja04
Ni(100)	CO	0.932E+03	O+	TOF	0.122E-06	82Ja04
Ni(100)	CO	0.956E+03	O+	TOF	0.115E-06	82Ja04
Ni(100)	CO	0.970E+03	O+	TOF	0.112E-06	82Ja04

CO+ ions were not detectable over the photon energy range.
CO exposure 20L

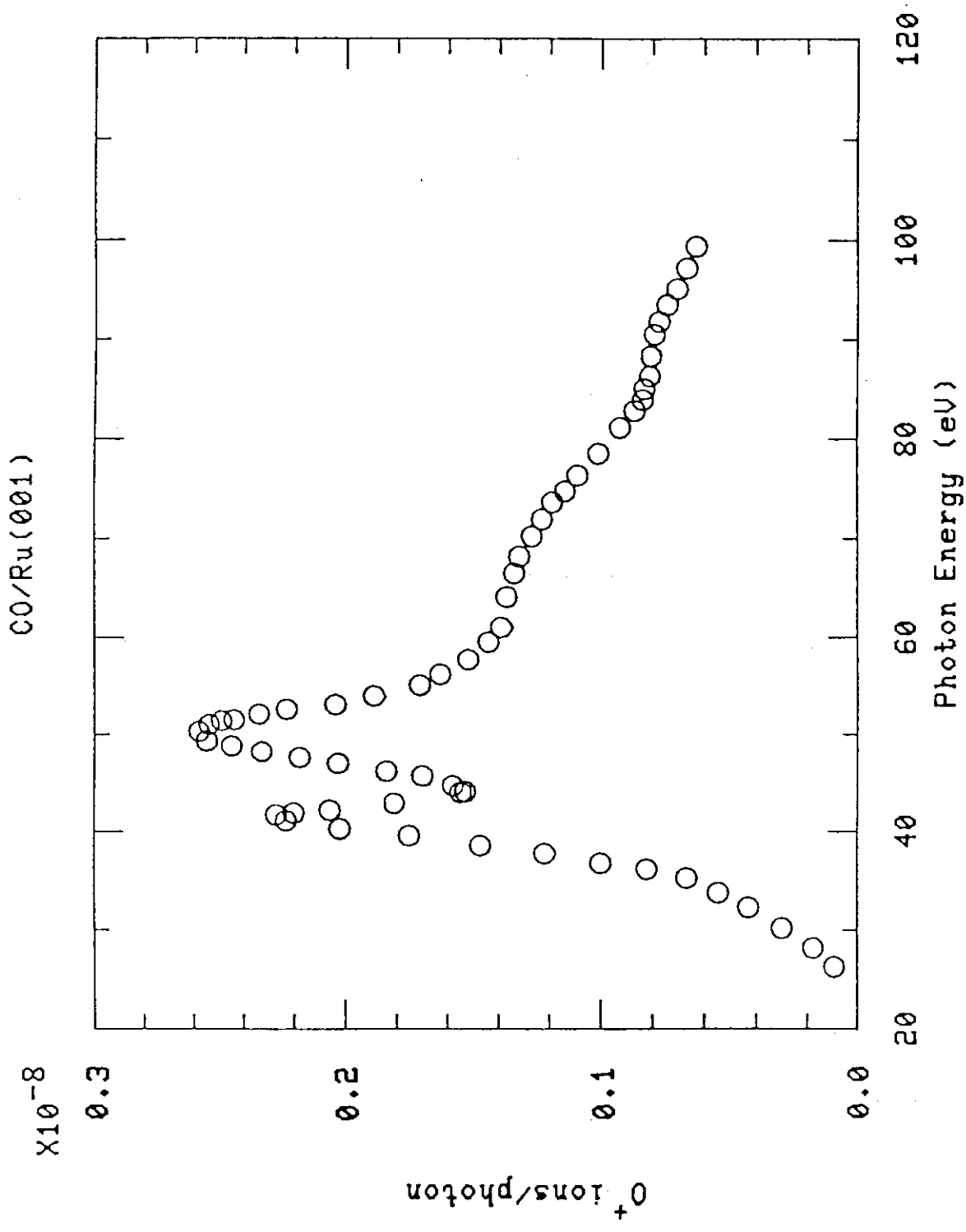

Fig.77 Desorption efficiency as a function of incident energy

DATA LIST

Substrate	Adsorbed gases	Incident photon energy (eV)	Desorbed species	Method	Ions per photon	Ref.
Ru(001)	CO	0.263E+02	O+	TOF	0.928E-10	81Ma02
Ru(001)	CO	0.282E+02	O+	TOF	0.178E-09	81Ma02
Ru(001)	CO	0.302E+02	O+	TOF	0.300E-09	81Ma02
Ru(001)	CO	0.323E+02	O+	TOF	0.429E-09	81Ma02
Ru(001)	CO	0.338E+02	O+	TOF	0.545E-09	81Ma02
Ru(001)	CO	0.353E+02	O+	TOF	0.667E-09	81Ma02
Ru(001)	CO	0.362E+02	O+	TOF	0.820E-09	81Ma02
Ru(001)	CO	0.368E+02	O+	TOF	0.100E-08	81Ma02
Ru(001)	CO	0.378E+02	O+	TOF	0.122E-08	81Ma02
Ru(001)	CO	0.386E+02	O+	TOF	0.147E-08	81Ma02
Ru(001)	CO	0.396E+02	O+	TOF	0.175E-08	81Ma02
Ru(001)	CO	0.403E+02	O+	TOF	0.202E-08	81Ma02
Ru(001)	CO	0.411E+02	O+	TOF	0.223E-08	81Ma02
Ru(001)	CO	0.417E+02	O+	TOF	0.227E-08	81Ma02
Ru(001)	CO	0.419E+02	O+	TOF	0.220E-08	81Ma02
Ru(001)	CO	0.422E+02	O+	TOF	0.206E-08	81Ma02
Ru(001)	CO	0.429E+02	O+	TOF	0.181E-08	81Ma02
Ru(001)	CO	0.440E+02	O+	TOF	0.155E-08	81Ma02
Ru(001)	CO	0.441E+02	O+	TOF	0.153E-08	81Ma02
Ru(001)	CO	0.447E+02	O+	TOF	0.158E-08	81Ma02
Ru(001)	CO	0.457E+02	O+	TOF	0.170E-08	81Ma02
Ru(001)	CO	0.462E+02	O+	TOF	0.184E-08	81Ma02
Ru(001)	CO	0.470E+02	O+	TOF	0.203E-08	81Ma02
Ru(001)	CO	0.476E+02	O+	TOF	0.218E-08	81Ma02
Ru(001)	CO	0.482E+02	O+	TOF	0.233E-08	81Ma02
Ru(001)	CO	0.488E+02	O+	TOF	0.245E-08	81Ma02
Ru(001)	CO	0.493E+02	O+	TOF	0.255E-08	81Ma02
Ru(001)	CO	0.503E+02	O+	TOF	0.258E-08	81Ma02
Ru(001)	CO	0.510E+02	O+	TOF	0.254E-08	81Ma02
Ru(001)	CO	0.514E+02	O+	TOF	0.249E-08	81Ma02
Ru(001)	CO	0.515E+02	O+	TOF	0.244E-08	81Ma02
Ru(001)	CO	0.521E+02	O+	TOF	0.234E-08	81Ma02
Ru(001)	CO	0.526E+02	O+	TOF	0.223E-08	81Ma02
Ru(001)	CO	0.531E+02	O+	TOF	0.204E-08	81Ma02
Ru(001)	CO	0.540E+02	O+	TOF	0.189E-08	81Ma02
Ru(001)	CO	0.551E+02	O+	TOF	0.171E-08	81Ma02
Ru(001)	CO	0.562E+02	O+	TOF	0.163E-08	81Ma02
Ru(001)	CO	0.577E+02	O+	TOF	0.152E-08	81Ma02
Ru(001)	CO	0.595E+02	O+	TOF	0.144E-08	81Ma02
Ru(001)	CO	0.610E+02	O+	TOF	0.139E-08	81Ma02
Ru(001)	CO	0.641E+02	O+	TOF	0.137E-08	81Ma02
Ru(001)	CO	0.665E+02	O+	TOF	0.134E-08	81Ma02
Ru(001)	CO	0.682E+02	O+	TOF	0.132E-08	81Ma02
Ru(001)	CO	0.702E+02	O+	TOF	0.127E-08	81Ma02
Ru(001)	CO	0.719E+02	O+	TOF	0.123E-08	81Ma02

•/••

Ru(001)	CO	0.736E+02	O+	TOF	0.119E-08	81Ma02
Ru(001)	CO	0.747E+02	O+	TOF	0.114E-08	81Ma02
Ru(001)	CO	0.763E+02	O+	TOF	0.109E-08	81Ma02
Ru(001)	CO	0.785E+02	O+	TOF	0.101E-08	81Ma02
Ru(001)	CO	0.811E+02	O+	TOF	0.926E-09	81Ma02
Ru(001)	CO	0.828E+02	O+	TOF	0.870E-09	81Ma02
Ru(001)	CO	0.839E+02	O+	TOF	0.839E-09	81Ma02
Ru(001)	CO	0.850E+02	O+	TOF	0.832E-09	81Ma02
Ru(001)	CO	0.863E+02	O+	TOF	0.813E-09	81Ma02
Ru(001)	CO	0.883E+02	O+	TOF	0.807E-09	81Ma02
Ru(001)	CO	0.905E+02	O+	TOF	0.793E-09	81Ma02
Ru(001)	CO	0.918E+02	O+	TOF	0.775E-09	81Ma02
Ru(001)	CO	0.935E+02	O+	TOF	0.743E-09	81Ma02
Ru(001)	CO	0.951E+02	O+	TOF	0.706E-09	81Ma02
Ru(001)	CO	0.972E+02	O+	TOF	0.668E-09	81Ma02
Ru(001)	CO	0.994E+02	O+	TOF	0.631E-09	81Ma02

Surface coverage 5.3E+14 molecules/cm**2

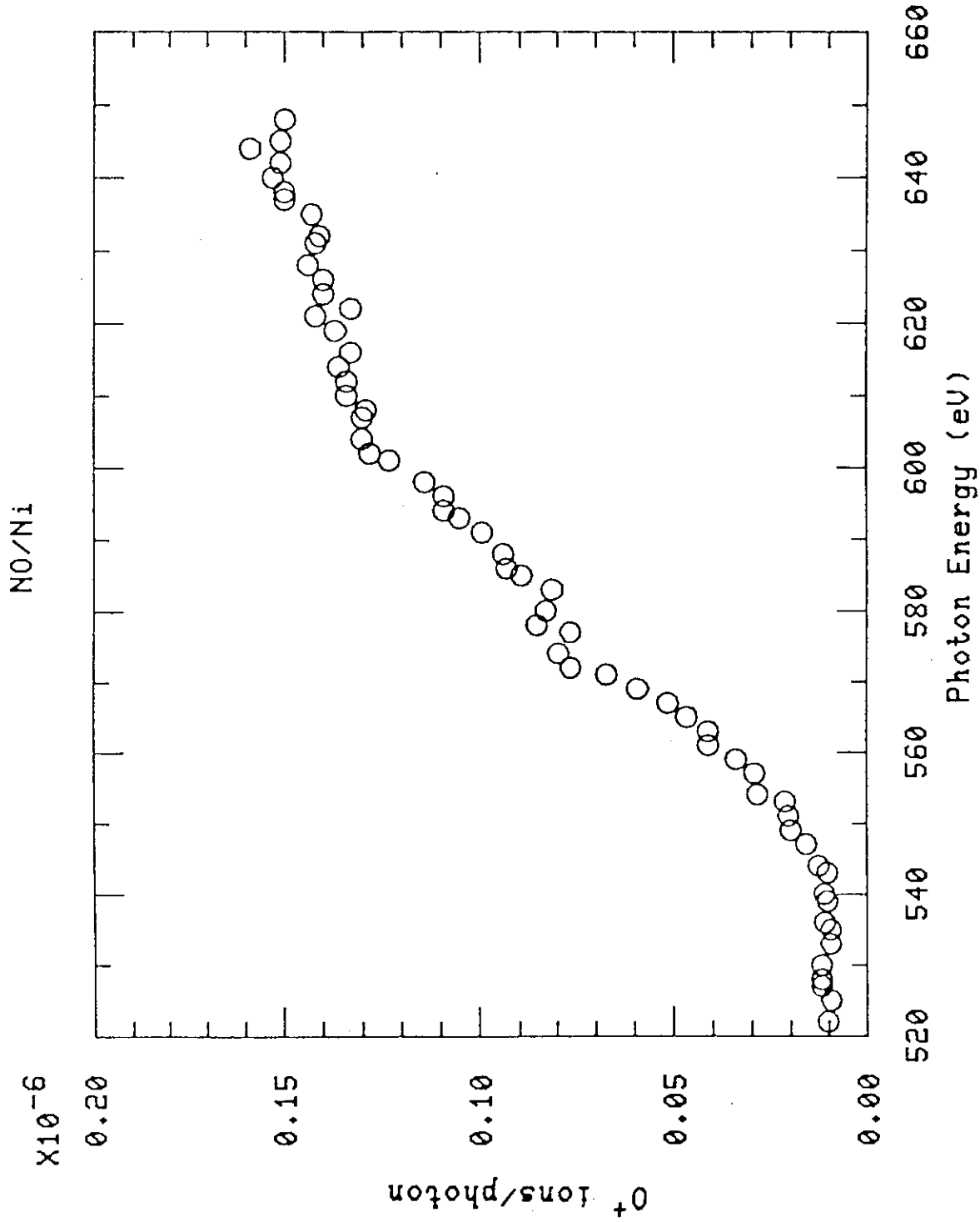

Fig.78 Desorption efficiency as a function of incident energy

DATA LIST

Substrate	Adsorbed gases	Incident photon energy (eV)	Desorbed species	Method	Ions per photon	Ref.
Ni(100)	NO	0.522E+03	O+	TOF	0.103E-07	82Ja04
Ni(100)	NO	0.525E+03	O+	TOF	0.950E-08	82Ja04
Ni(100)	NO	0.527E+03	O+	TOF	0.119E-07	82Ja04
Ni(100)	NO	0.528E+03	O+	TOF	0.119E-07	82Ja04
Ni(100)	NO	0.530E+03	O+	TOF	0.119E-07	82Ja04
Ni(100)	NO	0.533E+03	O+	TOF	0.954E-08	82Ja04
Ni(100)	NO	0.535E+03	O+	TOF	0.955E-08	82Ja04
Ni(100)	NO	0.536E+03	O+	TOF	0.111E-07	82Ja04
Ni(100)	NO	0.539E+03	O+	TOF	0.104E-07	82Ja04
Ni(100)	NO	0.540E+03	O+	TOF	0.112E-07	82Ja04
Ni(100)	NO	0.543E+03	O+	TOF	0.104E-07	82Ja04
Ni(100)	NO	0.544E+03	O+	TOF	0.127E-07	82Ja04
Ni(100)	NO	0.547E+03	O+	TOF	0.159E-07	82Ja04
Ni(100)	NO	0.549E+03	O+	TOF	0.199E-07	82Ja04
Ni(100)	NO	0.551E+03	O+	TOF	0.206E-07	82Ja04
Ni(100)	NO	0.553E+03	O+	TOF	0.214E-07	82Ja04
Ni(100)	NO	0.554E+03	O+	TOF	0.285E-07	82Ja04
Ni(100)	NO	0.557E+03	O+	TOF	0.293E-07	82Ja04
Ni(100)	NO	0.559E+03	O+	TOF	0.340E-07	82Ja04
Ni(100)	NO	0.561E+03	O+	TOF	0.411E-07	82Ja04
Ni(100)	NO	0.563E+03	O+	TOF	0.411E-07	82Ja04
Ni(100)	NO	0.565E+03	O+	TOF	0.466E-07	82Ja04
Ni(100)	NO	0.567E+03	O+	TOF	0.514E-07	82Ja04
Ni(100)	NO	0.569E+03	O+	TOF	0.592E-07	82Ja04
Ni(100)	NO	0.571E+03	O+	TOF	0.671E-07	82Ja04
Ni(100)	NO	0.572E+03	O+	TOF	0.765E-07	82Ja04
Ni(100)	NO	0.574E+03	O+	TOF	0.796E-07	82Ja04
Ni(100)	NO	0.577E+03	O+	TOF	0.765E-07	82Ja04
Ni(100)	NO	0.578E+03	O+	TOF	0.851E-07	82Ja04
Ni(100)	NO	0.580E+03	O+	TOF	0.828E-07	82Ja04
Ni(100)	NO	0.583E+03	O+	TOF	0.812E-07	82Ja04
Ni(100)	NO	0.585E+03	O+	TOF	0.890E-07	82Ja04
Ni(100)	NO	0.586E+03	O+	TOF	0.929E-07	82Ja04
Ni(100)	NO	0.588E+03	O+	TOF	0.937E-07	82Ja04
Ni(100)	NO	0.591E+03	O+	TOF	0.992E-07	82Ja04
Ni(100)	NO	0.593E+03	O+	TOF	0.105E-06	82Ja04
Ni(100)	NO	0.594E+03	O+	TOF	0.109E-06	82Ja04
Ni(100)	NO	0.596E+03	O+	TOF	0.109E-06	82Ja04
Ni(100)	NO	0.598E+03	O+	TOF	0.114E-06	82Ja04
Ni(100)	NO	0.601E+03	O+	TOF	0.123E-06	82Ja04
Ni(100)	NO	0.602E+03	O+	TOF	0.128E-06	82Ja04
Ni(100)	NO	0.604E+03	O+	TOF	0.130E-06	82Ja04
Ni(100)	NO	0.607E+03	O+	TOF	0.130E-06	82Ja04
Ni(100)	NO	0.608E+03	O+	TOF	0.129E-06	82Ja04
Ni(100)	NO	0.610E+03	O+	TOF	0.134E-06	82Ja04

·/··

Ni(100)	NO	0.612E+03	O+	TOF	0.134E-06	82Ja04
Ni(100)	NO	0.614E+03	O+	TOF	0.136E-06	82Ja04
Ni(100)	NO	0.616E+03	O+	TOF	0.133E-06	82Ja04
Ni(100)	NO	0.619E+03	O+	TOF	0.137E-06	82Ja04
Ni(100)	NO	0.621E+03	O+	TOF	0.142E-06	82Ja04
Ni(100)	NO	0.622E+03	O+	TOF	0.133E-06	82Ja04
Ni(100)	NO	0.624E+03	O+	TOF	0.140E-06	82Ja04
Ni(100)	NO	0.626E+03	O+	TOF	0.140E-06	82Ja04
Ni(100)	NO	0.628E+03	O+	TOF	0.144E-06	82Ja04
Ni(100)	NO	0.631E+03	O+	TOF	0.142E-06	82Ja04
Ni(100)	NO	0.632E+03	O+	TOF	0.141E-06	82Ja04
Ni(100)	NO	0.635E+03	O+	TOF	0.143E-06	82Ja04
Ni(100)	NO	0.637E+03	O+	TOF	0.150E-06	82Ja04
Ni(100)	NO	0.638E+03	O+	TOF	0.150E-06	82Ja04
Ni(100)	NO	0.640E+03	O+	TOF	0.153E-06	82Ja04
Ni(100)	NO	0.642E+03	O+	TOF	0.151E-06	82Ja04
Ni(100)	NO	0.644E+03	O+	TOF	0.159E-06	82Ja04
Ni(100)	NO	0.645E+03	O+	TOF	0.151E-06	82Ja04
Ni(100)	NO	0.648E+03	O+	TOF	0.150E-06	82Ja04

The measurements were carried out in the range of temperatures between 100K and 270K.
NO Exposure 20L
Adsorption temperature < 100K

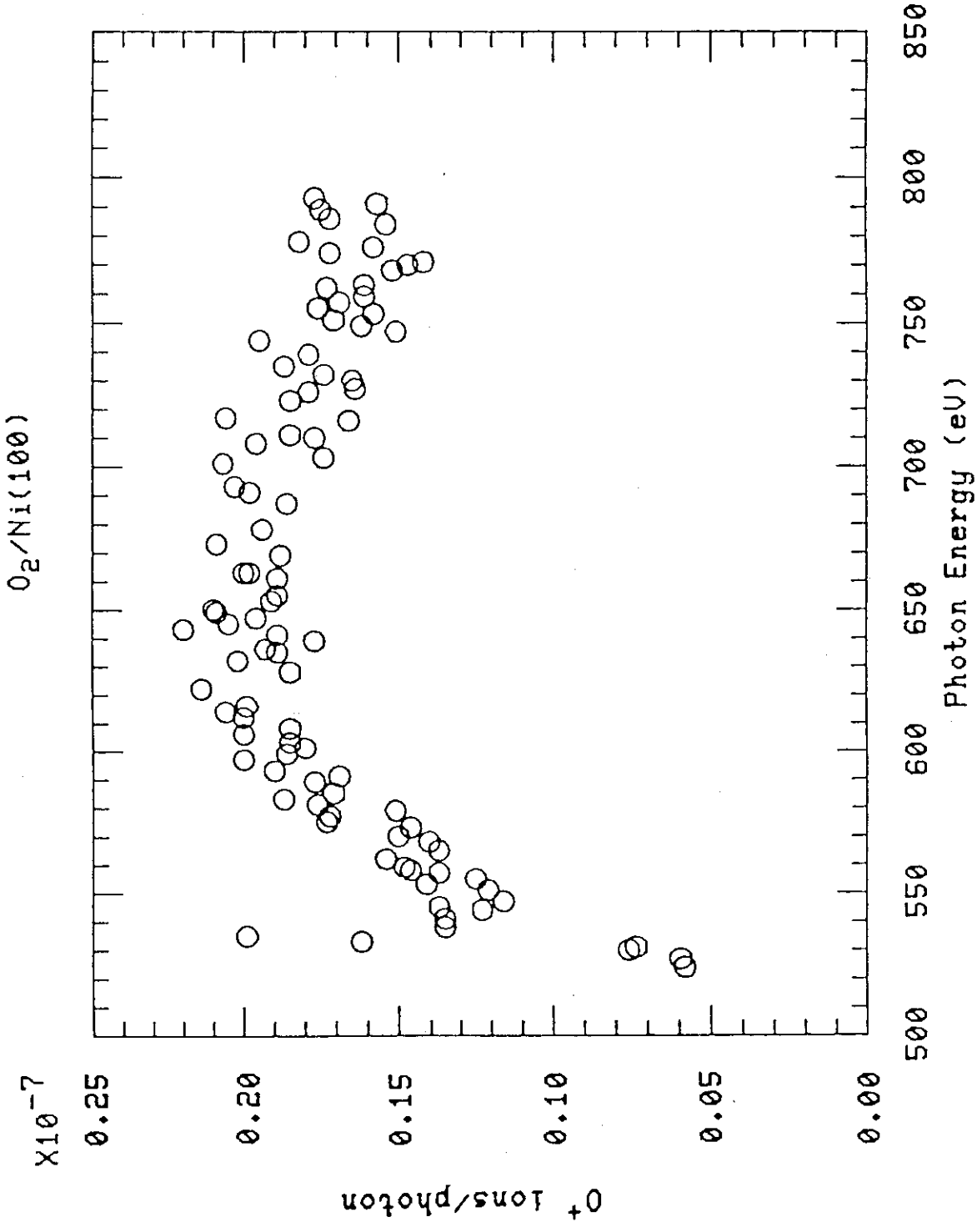

Fig.79 Desorption efficiency as a function of incident energy

DATA LIST

Substrate	Adsorbed gases	Incident photon energy (eV)	Desorbed species	Method	Ions per photon	Ref.
Ni(100)	O2	0.524E+03	O+	TOF	0.581E-08	81Ja02
Ni(100)	O2	0.527E+03	O+	TOF	0.596E-08	81Ja02
Ni(100)	O2	0.530E+03	O+	TOF	0.759E-08	81Ja02
Ni(100)	O2	0.531E+03	O+	TOF	0.737E-08	81Ja02
Ni(100)	O2	0.533E+03	O+	TOF	0.162E-07	81Ja02
Ni(100)	O2	0.535E+03	O+	TOF	0.199E-07	81Ja02
Ni(100)	O2	0.538E+03	O+	TOF	0.135E-07	81Ja02
Ni(100)	O2	0.541E+03	O+	TOF	0.135E-07	81Ja02
Ni(100)	O2	0.544E+03	O+	TOF	0.123E-07	81Ja02
Ni(100)	O2	0.545E+03	O+	TOF	0.137E-07	81Ja02
Ni(100)	O2	0.547E+03	O+	TOF	0.116E-07	81Ja02
Ni(100)	O2	0.551E+03	O+	TOF	0.121E-07	81Ja02
Ni(100)	O2	0.553E+03	O+	TOF	0.141E-07	81Ja02
Ni(100)	O2	0.555E+03	O+	TOF	0.125E-07	81Ja02
Ni(100)	O2	0.557E+03	O+	TOF	0.137E-07	81Ja02
Ni(100)	O2	0.558E+03	O+	TOF	0.146E-07	81Ja02
Ni(100)	O2	0.559E+03	O+	TOF	0.148E-07	81Ja02
Ni(100)	O2	0.562E+03	O+	TOF	0.154E-07	81Ja02
Ni(100)	O2	0.565E+03	O+	TOF	0.137E-07	81Ja02
Ni(100)	O2	0.568E+03	O+	TOF	0.140E-07	81Ja02
Ni(100)	O2	0.570E+03	O+	TOF	0.150E-07	81Ja02
Ni(100)	O2	0.573E+03	O+	TOF	0.146E-07	81Ja02
Ni(100)	O2	0.575E+03	O+	TOF	0.173E-07	81Ja02
Ni(100)	O2	0.577E+03	O+	TOF	0.172E-07	81Ja02
Ni(100)	O2	0.579E+03	O+	TOF	0.151E-07	81Ja02
Ni(100)	O2	0.581E+03	O+	TOF	0.176E-07	81Ja02
Ni(100)	O2	0.583E+03	O+	TOF	0.187E-07	81Ja02
Ni(100)	O2	0.585E+03	O+	TOF	0.171E-07	81Ja02
Ni(100)	O2	0.589E+03	O+	TOF	0.177E-07	81Ja02
Ni(100)	O2	0.591E+03	O+	TOF	0.169E-07	81Ja02
Ni(100)	O2	0.593E+03	O+	TOF	0.190E-07	81Ja02
Ni(100)	O2	0.597E+03	O+	TOF	0.200E-07	81Ja02
Ni(100)	O2	0.599E+03	O+	TOF	0.186E-07	81Ja02
Ni(100)	O2	0.601E+03	O+	TOF	0.180E-07	81Ja02
Ni(100)	O2	0.603E+03	O+	TOF	0.185E-07	81Ja02
Ni(100)	O2	0.606E+03	O+	TOF	0.200E-07	81Ja02
Ni(100)	O2	0.608E+03	O+	TOF	0.185E-07	81Ja02
Ni(100)	O2	0.612E+03	O+	TOF	0.200E-07	81Ja02
Ni(100)	O2	0.614E+03	O+	TOF	0.206E-07	81Ja02
Ni(100)	O2	0.616E+03	O+	TOF	0.199E-07	81Ja02
Ni(100)	O2	0.622E+03	O+	TOF	0.214E-07	81Ja02
Ni(100)	O2	0.632E+03	O+	TOF	0.202E-07	81Ja02
Ni(100)	O2	0.628E+03	O+	TOF	0.185E-07	81Ja02
Ni(100)	O2	0.635E+03	O+	TOF	0.189E-07	81Ja02
Ni(100)	O2	0.636E+03	O+	TOF	0.193E-07	81Ja02
Ni(100)	O2	0.639E+03	O+	TOF	0.177E-07	81Ja02
Ni(100)	O2	0.641E+03	O+	TOF	0.189E-07	81Ja02

·/··

Ni(100)	O2	0.643E+03	O+	TOF	0.220E-07	81Ja02
Ni(100)	O2	0.645E+03	O+	TOF	0.205E-07	81Ja02
Ni(100)	O2	0.647E+03	O+	TOF	0.196E-07	81Ja02
Ni(100)	O2	0.649E+03	O+	TOF	0.209E-07	81Ja02
Ni(100)	O2	0.650E+03	O+	TOF	0.210E-07	81Ja02
Ni(100)	O2	0.653E+03	O+	TOF	0.191E-07	81Ja02
Ni(100)	O2	0.655E+03	O+	TOF	0.189E-07	81Ja02
Ni(100)	O2	0.661E+03	O+	TOF	0.189E-07	81Ja02
Ni(100)	O2	0.663E+03	O+	TOF	0.198E-07	81Ja02
Ni(100)	O2	0.663E+03	O+	TOF	0.200E-07	81Ja02
Ni(100)	O2	0.669E+03	O+	TOF	0.188E-07	81Ja02
Ni(100)	O2	0.673E+03	O+	TOF	0.209E-07	81Ja02
Ni(100)	O2	0.678E+03	O+	TOF	0.194E-07	81Ja02
Ni(100)	O2	0.687E+03	O+	TOF	0.186E-07	81Ja02
Ni(100)	O2	0.691E+03	O+	TOF	0.198E-07	81Ja02
Ni(100)	O2	0.693E+03	O+	TOF	0.203E-07	81Ja02
Ni(100)	O2	0.701E+03	O+	TOF	0.207E-07	81Ja02
Ni(100)	O2	0.703E+03	O+	TOF	0.174E-07	81Ja02
Ni(100)	O2	0.708E+03	O+	TOF	0.196E-07	81Ja02
Ni(100)	O2	0.710E+03	O+	TOF	0.177E-07	81Ja02
Ni(100)	O2	0.711E+03	O+	TOF	0.185E-07	81Ja02
Ni(100)	O2	0.717E+03	O+	TOF	0.206E-07	81Ja02
Ni(100)	O2	0.716E+03	O+	TOF	0.166E-07	81Ja02
Ni(100)	O2	0.723E+03	O+	TOF	0.185E-07	81Ja02
Ni(100)	O2	0.726E+03	O+	TOF	0.179E-07	81Ja02
Ni(100)	O2	0.727E+03	O+	TOF	0.164E-07	81Ja02
Ni(100)	O2	0.730E+03	O+	TOF	0.165E-07	81Ja02
Ni(100)	O2	0.732E+03	O+	TOF	0.174E-07	81Ja02
Ni(100)	O2	0.735E+03	O+	TOF	0.187E-07	81Ja02
Ni(100)	O2	0.739E+03	O+	TOF	0.179E-07	81Ja02
Ni(100)	O2	0.744E+03	O+	TOF	0.195E-07	81Ja02
Ni(100)	O2	0.747E+03	O+	TOF	0.151E-07	81Ja02
Ni(100)	O2	0.749E+03	O+	TOF	0.162E-07	81Ja02
Ni(100)	O2	0.751E+03	O+	TOF	0.171E-07	81Ja02
Ni(100)	O2	0.753E+03	O+	TOF	0.158E-07	81Ja02
Ni(100)	O2	0.755E+03	O+	TOF	0.176E-07	81Ja02
Ni(100)	O2	0.757E+03	O+	TOF	0.169E-07	81Ja02
Ni(100)	O2	0.759E+03	O+	TOF	0.161E-07	81Ja02
Ni(100)	O2	0.762E+03	O+	TOF	0.173E-07	81Ja02
Ni(100)	O2	0.763E+03	O+	TOF	0.161E-07	81Ja02
Ni(100)	O2	0.768E+03	O+	TOF	0.152E-07	81Ja02
Ni(100)	O2	0.770E+03	O+	TOF	0.147E-07	81Ja02
Ni(100)	O2	0.771E+03	O+	TOF	0.142E-07	81Ja02
Ni(100)	O2	0.774E+03	O+	TOF	0.172E-07	81Ja02
Ni(100)	O2	0.776E+03	O+	TOF	0.158E-07	81Ja02
Ni(100)	O2	0.778E+03	O+	TOF	0.182E-07	81Ja02
Ni(100)	O2	0.784E+03	O+	TOF	0.154E-07	81Ja02
Ni(100)	O2	0.786E+03	O+	TOF	0.172E-07	81Ja02
Ni(100)	O2	0.789E+03	O+	TOF	0.175E-07	81Ja02
Ni(100)	O2	0.791E+03	O+	TOF	0.157E-07	81Ja02
Ni(100)	O2	0.793E+03	O+	TOF	0.177E-07	81Ja02

Oxygen exposure 180L
The incident angle of photon was 80 deg. from the normal of surface.

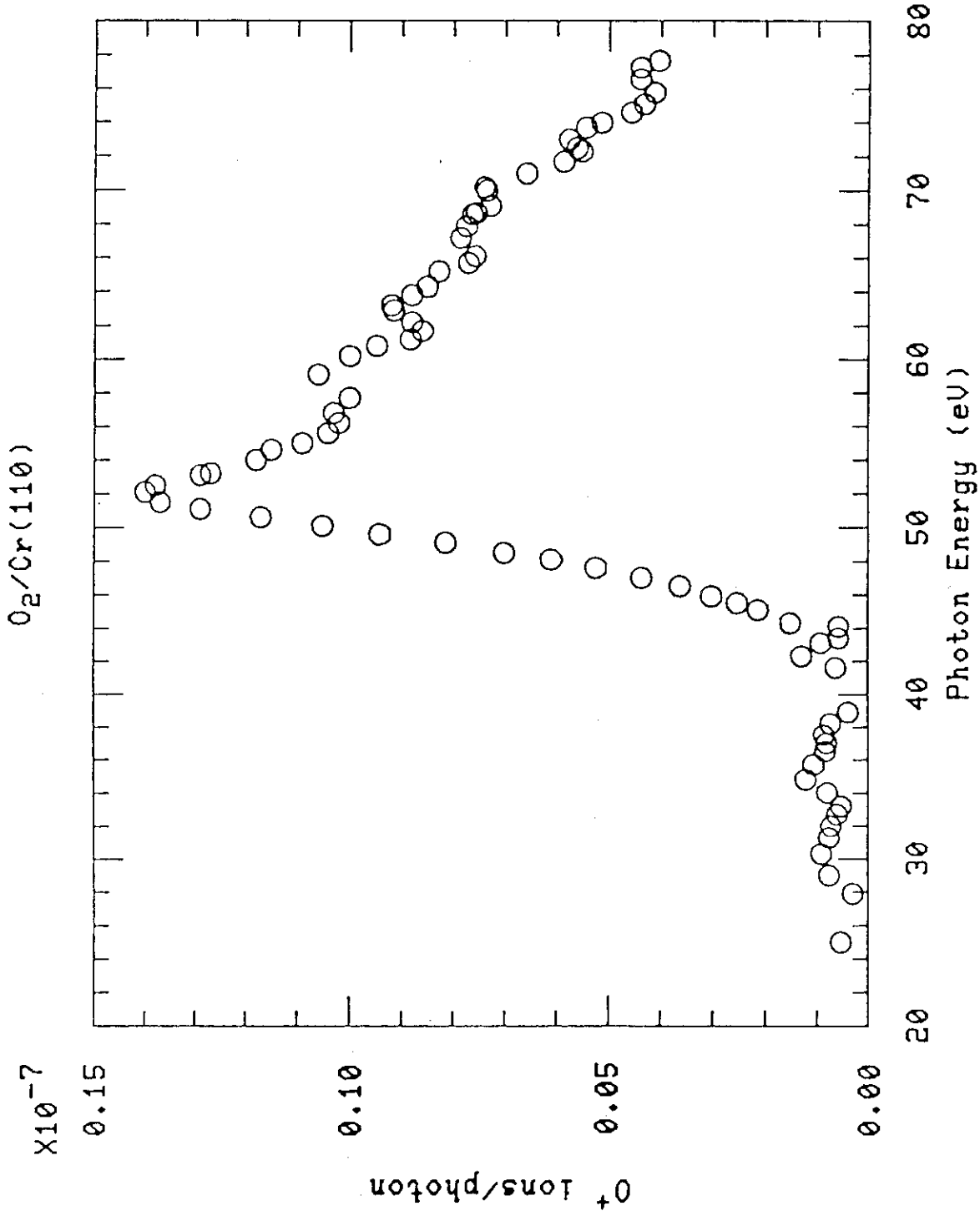

Fig.80 Desorption efficiency as a function of incident energy

DATA LIST

Substrate	Adsorbed gases	Incident photon energy (eV)	Desorbed species	Method	Ions per photon	Ref.
Cr(110)	O2	0.250E+02	O+	TOF	0.530E-09	84St02
Cr(110)	O2	0.279E+02	O+	TOF	0.299E-09	84St02
Cr(110)	O2	0.290E+02	O+	TOF	0.766E-09	84St02
Cr(110)	O2	0.303E+02	O+	TOF	0.911E-09	84St02
Cr(110)	O2	0.313E+02	O+	TOF	0.760E-09	84St02
Cr(110)	O2	0.320E+02	O+	TOF	0.733E-09	84St02
Cr(110)	O2	0.327E+02	O+	TOF	0.607E-09	84St02
Cr(110)	O2	0.332E+02	O+	TOF	0.531E-09	84St02
Cr(110)	O2	0.340E+02	O+	TOF	0.801E-09	84St02
Cr(110)	O2	0.348E+02	O+	TOF	0.122E-08	84St02
Cr(110)	O2	0.357E+02	O+	TOF	0.107E-08	84St02
Cr(110)	O2	0.365E+02	O+	TOF	0.844E-09	84St02
Cr(110)	O2	0.370E+02	O+	TOF	0.818E-09	84St02
Cr(110)	O2	0.375E+02	O+	TOF	0.866E-09	84St02
Cr(110)	O2	0.382E+02	O+	TOF	0.740E-09	84St02
Cr(110)	O2	0.389E+02	O+	TOF	0.391E-09	84St02
Cr(110)	O2	0.416E+02	O+	TOF	0.631E-09	84St02
Cr(110)	O2	0.423E+02	O+	TOF	0.130E-08	84St02
Cr(110)	O2	0.431E+02	O+	TOF	0.924E-09	84St02
Cr(110)	O2	0.434E+02	O+	TOF	0.576E-09	84St02
Cr(110)	O2	0.441E+02	O+	TOF	0.574E-09	84St02
Cr(110)	O2	0.443E+02	O+	TOF	0.152E-08	84St02
Cr(110)	O2	0.451E+02	O+	TOF	0.213E-08	84St02
Cr(110)	O2	0.455E+02	O+	TOF	0.253E-08	84St02
Cr(110)	O2	0.459E+02	O+	TOF	0.302E-08	84St02
Cr(110)	O2	0.465E+02	O+	TOF	0.362E-08	84St02
Cr(110)	O2	0.470E+02	O+	TOF	0.436E-08	84St02
Cr(110)	O2	0.476E+02	O+	TOF	0.525E-08	84St02
Cr(110)	O2	0.481E+02	O+	TOF	0.611E-08	84St02
Cr(110)	O2	0.485E+02	O+	TOF	0.701E-08	84St02
Cr(110)	O2	0.491E+02	O+	TOF	0.814E-08	84St02
Cr(110)	O2	0.496E+02	O+	TOF	0.941E-08	84St02
Cr(110)	O2	0.501E+02	O+	TOF	0.105E-07	84St02
Cr(110)	O2	0.506E+02	O+	TOF	0.117E-07	84St02
Cr(110)	O2	0.511E+02	O+	TOF	0.129E-07	84St02
Cr(110)	O2	0.515E+02	O+	TOF	0.137E-07	84St02
Cr(110)	O2	0.521E+02	O+	TOF	0.140E-07	84St02
Cr(110)	O2	0.525E+02	O+	TOF	0.138E-07	84St02
Cr(110)	O2	0.531E+02	O+	TOF	0.129E-07	84St02
Cr(110)	O2	0.532E+02	O+	TOF	0.127E-07	84St02
Cr(110)	O2	0.540E+02	O+	TOF	0.118E-07	84St02
Cr(110)	O2	0.546E+02	O+	TOF	0.115E-07	84St02
Cr(110)	O2	0.550E+02	O+	TOF	0.109E-07	84St02
Cr(110)	O2	0.556E+02	O+	TOF	0.104E-07	84St02
Cr(110)	O2	0.562E+02	O+	TOF	0.102E-07	84St02
Cr(110)	O2	0.568E+02	O+	TOF	0.103E-07	84St02
Cr(110)	O2	0.577E+02	O+	TOF	0.100E-07	84St02
Cr(110)	O2	0.591E+02	O+	TOF	0.106E-07	84St02
Cr(110)	O2	0.602E+02	O+	TOF	0.100E-07	84St02

Cr(110)	O2	0.608E+02	O+	TOF	0.948E-08	84St02
Cr(110)	O2	0.612E+02	O+	TOF	0.884E-08	84St02
Cr(110)	O2	0.617E+02	O+	TOF	0.861E-08	84St02
Cr(110)	O2	0.622E+02	O+	TOF	0.881E-08	84St02
Cr(110)	O2	0.629E+02	O+	TOF	0.916E-08	84St02
Cr(110)	O2	0.632E+02	O+	TOF	0.920E-08	84St02
Cr(110)	O2	0.638E+02	O+	TOF	0.881E-08	84St02
Cr(110)	O2	0.643E+02	O+	TOF	0.851E-08	84St02
Cr(110)	O2	0.652E+02	O+	TOF	0.828E-08	84St02
Cr(110)	O2	0.657E+02	O+	TOF	0.771E-08	84St02
Cr(110)	O2	0.661E+02	O+	TOF	0.758E-08	84St02
Cr(110)	O2	0.672E+02	O+	TOF	0.786E-08	84St02
Cr(110)	O2	0.679E+02	O+	TOF	0.775E-08	84St02
Cr(110)	O2	0.686E+02	O+	TOF	0.763E-08	84St02
Cr(110)	O2	0.687E+02	O+	TOF	0.755E-08	84St02
Cr(110)	O2	0.691E+02	O+	TOF	0.728E-08	84St02
Cr(110)	O2	0.700E+02	O+	TOF	0.735E-08	84St02
Cr(110)	O2	0.702E+02	O+	TOF	0.740E-08	84St02
Cr(110)	O2	0.710E+02	O+	TOF	0.658E-08	84St02
Cr(110)	O2	0.717E+02	O+	TOF	0.586E-08	84St02
Cr(110)	O2	0.723E+02	O+	TOF	0.551E-08	84St02
Cr(110)	O2	0.725E+02	O+	TOF	0.561E-08	84St02
Cr(110)	O2	0.730E+02	O+	TOF	0.576E-08	84St02
Cr(110)	O2	0.737E+02	O+	TOF	0.543E-08	84St02
Cr(110)	O2	0.740E+02	O+	TOF	0.513E-08	84St02
Cr(110)	O2	0.746E+02	O+	TOF	0.456E-08	84St02
Cr(110)	O2	0.751E+02	O+	TOF	0.431E-08	84St02
Cr(110)	O2	0.758E+02	O+	TOF	0.411E-08	84St02
Cr(110)	O2	0.766E+02	O+	TOF	0.438E-08	84St02
Cr(110)	O2	0.773E+02	O+	TOF	0.438E-08	84St02
Cr(110)	O2	0.777E+02	O+	TOF	0.403E-08	84St02

The dependence of O+ ion yields on photon energy was similar to that of this figure for the ranges of oxygen exposure below 50L and adsorption temperatures (80~700K).

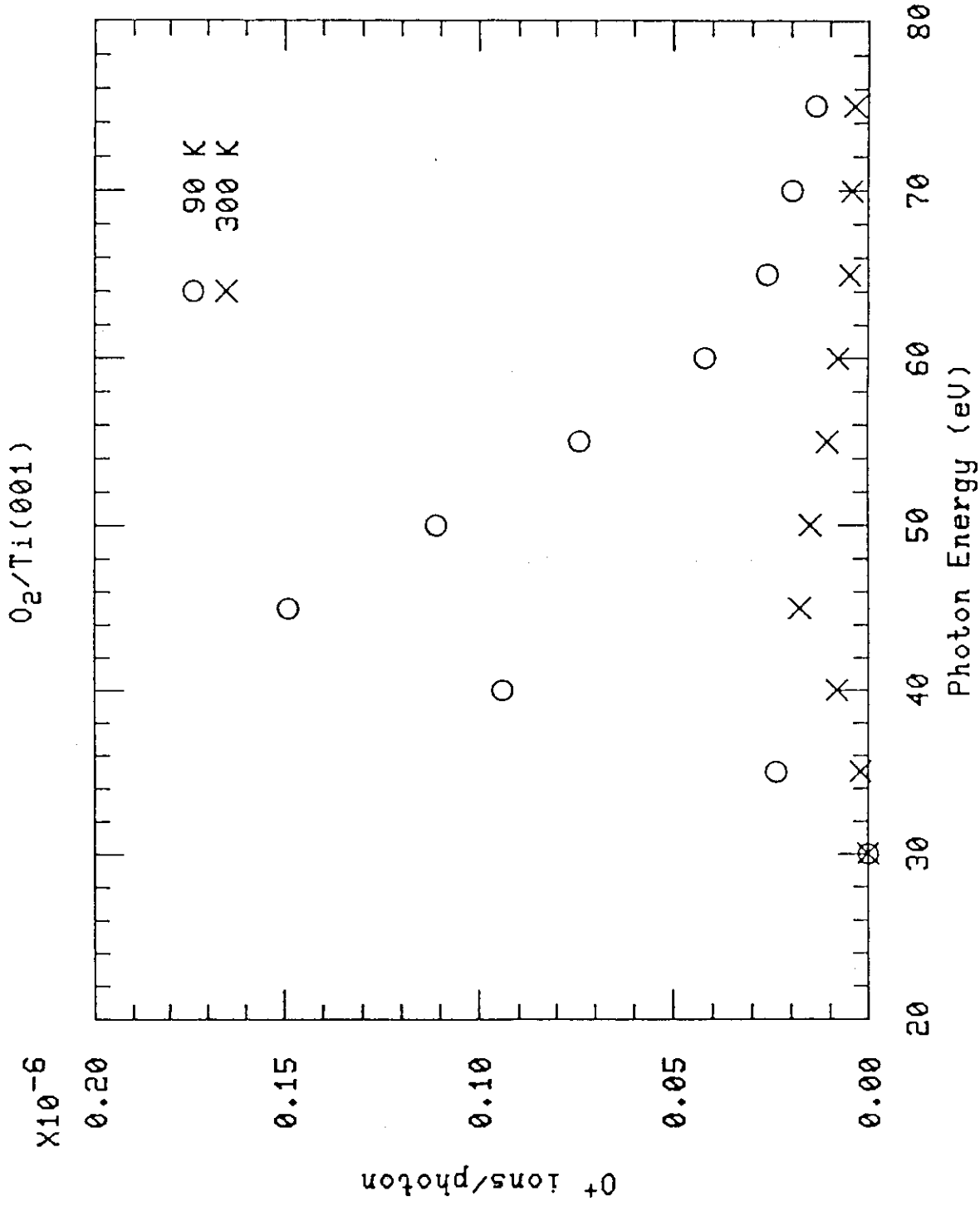

Fig.81 Desorption efficiency as a function of incident energy

DATA LIST

Substrate	Adsorbed gases	Incident energy (eV)	Desorbed species	Method	Ions per photon	Ref.	Remark
Ti(001)	O2	0.300E+02	O+	CMA	0.000E+00	81Ha01	*1)
Ti(001)	O2	0.350E+02	O+	CMA	0.239E-07	81Ha01	*1)
Ti(001)	O2	0.400E+02	O+	CMA	0.939E-07	81Ha01	*1)
Ti(001)	O2	0.450E+02	O+	CMA	0.149E-06	81Ha01	*1)
Ti(001)	O2	0.500E+02	O+	CMA	0.111E-06	81Ha01	*1)
Ti(001)	O2	0.550E+02	O+	CMA	0.739E-07	81Ha01	*1)
Ti(001)	O2	0.600E+02	O+	CMA	0.419E-07	81Ha01	*1)
Ti(001)	O2	0.650E+02	O+	CMA	0.263E-07	81Ha01	*1)
Ti(001)	O2	0.700E+02	O+	CMA	0.198E-07	81Ha01	*1)
Ti(001)	O2	0.750E+02	O+	CMA	0.137E-07	81Ha01	*1)
Ti(001)	O2	0.300E+02	O+	CMA	0.000E+00	81Ha01	*2)
Ti(001)	O2	0.350E+02	O+	CMA	0.198E-08	81Ha01	*2)
Ti(001)	O2	0.400E+02	O+	CMA	0.818E-08	81Ha01	*2)
Ti(001)	O2	0.450E+02	O+	CMA	0.178E-07	81Ha01	*2)
Ti(001)	O2	0.500E+02	O+	CMA	0.151E-07	81Ha01	*2)
Ti(001)	O2	0.550E+02	O+	CMA	0.106E-07	81Ha01	*2)
Ti(001)	O2	0.600E+02	O+	CMA	0.789E-08	81Ha01	*2)
Ti(001)	O2	0.650E+02	O+	CMA	0.488E-08	81Ha01	*2)
Ti(001)	O2	0.700E+02	O+	CMA	0.419E-08	81Ha01	*2)
Ti(001)	O2	0.750E+02	O+	CMA	0.363E-08	81Ha01	*2)

*1) Surface temperature 90K, O2 exposure 15L.
*2) Surface temperature 300K, O2 exposure 8L.
O+ ions desorbed perpendicular to the surface.

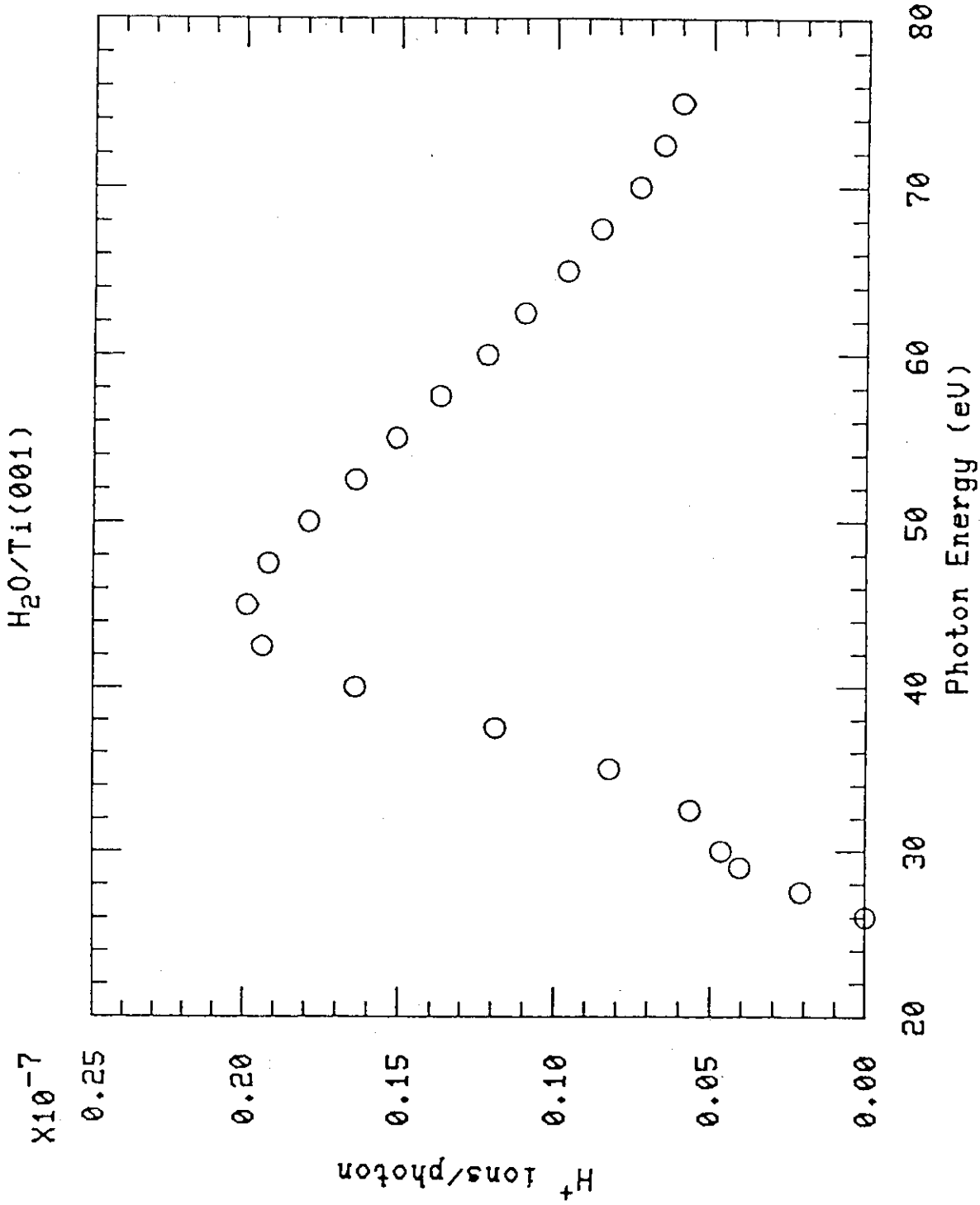

Fig.82 Desorption efficiency as a function of incident energy

DATA LIST

Substrate	Adsorbed gases	Incident energy (eV)	Desorbed species	Method	Ions per photon	Ref.
Ti(001)	H2O	0.260E+02	H+	CMA	0.000E+00	82St02
Ti(001)	H2O	0.275E+02	H+	CMA	0.213E-08	82St02
Ti(001)	H2O	0.290E+02	H+	CMA	0.406E-08	82St02
Ti(001)	H2O	0.300E+02	H+	CMA	0.466E-08	82St02
Ti(001)	H2O	0.325E+02	H+	CMA	0.565E-08	82St02
Ti(001)	H2O	0.350E+02	H+	CMA	0.824E-08	82St02
Ti(001)	H2O	0.375E+02	H+	CMA	0.119E-07	82St02
Ti(001)	H2O	0.400E+02	H+	CMA	0.164E-07	82St02
Ti(001)	H2O	0.425E+02	H+	CMA	0.194E-07	82St02
Ti(001)	H2O	0.450E+02	H+	CMA	0.199E-07	82St02
Ti(001)	H2O	0.475E+02	H+	CMA	0.192E-07	82St02
Ti(001)	H2O	0.500E+02	H+	CMA	0.179E-07	82St02
Ti(001)	H2O	0.525E+02	H+	CMA	0.164E-07	82St02
Ti(001)	H2O	0.550E+02	H+	CMA	0.151E-07	82St02
Ti(001)	H2O	0.575E+02	H+	CMA	0.137E-07	82St02
Ti(001)	H2O	0.600E+02	H+	CMA	0.122E-07	82St02
Ti(001)	H2O	0.625E+02	H+	CMA	0.110E-07	82St02
Ti(001)	H2O	0.650E+02	H+	CMA	0.963E-08	82St02
Ti(001)	H2O	0.675E+02	H+	CMA	0.854E-08	82St02
Ti(001)	H2O	0.700E+02	H+	CMA	0.730E-08	82St02
Ti(001)	H2O	0.725E+02	H+	CMA	0.655E-08	82St02
Ti(001)	H2O	0.750E+02	H+	CMA	0.599E-08	82St02

H2O exposure 0.5 L
Surface temperature 90K
The energy of desorbed H+ ions was 4eV.

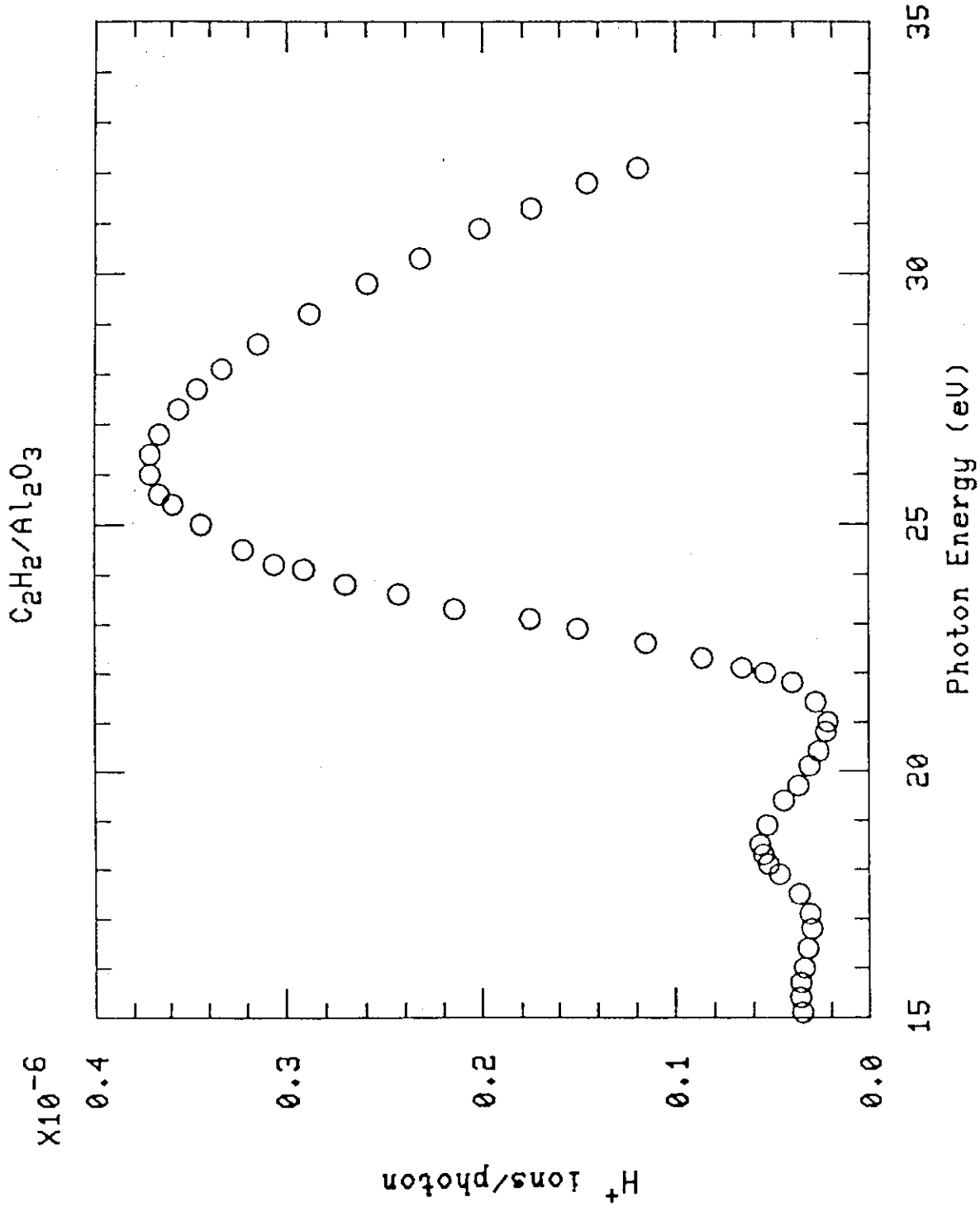

Fig.83 Desorption efficiency as a function of incident energy

DATA LIST

Substrate	Adsorbed gases	Incident photon energy (eV)	Desorbed species	Method	Ions per photon	Ref.
Al2O3	C2H2	0.151E+02	H+	TOF	0.352E-07	83Ro02
Al2O3	C2H2	0.154E+02	H+	TOF	0.361E-07	83Ro02
Al2O3	C2H2	0.157E+02	H+	TOF	0.360E-07	83Ro02
Al2O3	C2H2	0.160E+02	H+	TOF	0.341E-07	83Ro02
Al2O3	C2H2	0.164E+02	H+	TOF	0.321E-07	83Ro02
Al2O3	C2H2	0.168E+02	H+	TOF	0.301E-07	83Ro02
Al2O3	C2H2	0.171E+02	H+	TOF	0.310E-07	83Ro02
Al2O3	C2H2	0.175E+02	H+	TOF	0.365E-07	83Ro02
Al2O3	C2H2	0.179E+02	H+	TOF	0.466E-07	83Ro02
Al2O3	C2H2	0.181E+02	H+	TOF	0.521E-07	83Ro02
Al2O3	C2H2	0.183E+02	H+	TOF	0.548E-07	83Ro02
Al2O3	C2H2	0.185E+02	H+	TOF	0.566E-07	83Ro02
Al2O3	C2H2	0.189E+02	H+	TOF	0.528E-07	83Ro02
Al2O3	C2H2	0.194E+02	H+	TOF	0.443E-07	83Ro02
Al2O3	C2H2	0.197E+02	H+	TOF	0.368E-07	83Ro02
Al2O3	C2H2	0.201E+02	H+	TOF	0.311E-07	83Ro02
Al2O3	C2H2	0.204E+02	H+	TOF	0.264E-07	83Ro02
Al2O3	C2H2	0.208E+02	H+	TOF	0.226E-07	83Ro02
Al2O3	C2H2	0.210E+02	H+	TOF	0.216E-07	83Ro02
Al2O3	C2H2	0.214E+02	H+	TOF	0.280E-07	83Ro02
Al2O3	C2H2	0.218E+02	H+	TOF	0.400E-07	83Ro02
Al2O3	C2H2	0.220E+02	H+	TOF	0.539E-07	83Ro02
Al2O3	C2H2	0.221E+02	H+	TOF	0.659E-07	83Ro02
Al2O3	C2H2	0.223E+02	H+	TOF	0.863E-07	83Ro02
Al2O3	C2H2	0.226E+02	H+	TOF	0.115E-06	83Ro02
Al2O3	C2H2	0.229E+02	H+	TOF	0.150E-06	83Ro02
Al2O3	C2H2	0.231E+02	H+	TOF	0.175E-06	83Ro02
Al2O3	C2H2	0.233E+02	H+	TOF	0.214E-06	83Ro02
Al2O3	C2H2	0.236E+02	H+	TOF	0.243E-06	83Ro02
Al2O3	C2H2	0.238E+02	H+	TOF	0.270E-06	83Ro02
Al2O3	C2H2	0.241E+02	H+	TOF	0.291E-06	83Ro02
Al2O3	C2H2	0.242E+02	H+	TOF	0.306E-06	83Ro02
Al2O3	C2H2	0.245E+02	H+	TOF	0.322E-06	83Ro02
Al2O3	C2H2	0.250E+02	H+	TOF	0.344E-06	83Ro02
Al2O3	C2H2	0.254E+02	H+	TOF	0.359E-06	83Ro02
Al2O3	C2H2	0.256E+02	H+	TOF	0.366E-06	83Ro02
Al2O3	C2H2	0.260E+02	H+	TOF	0.371E-06	83Ro02
Al2O3	C2H2	0.264E+02	H+	TOF	0.371E-06	83Ro02
Al2O3	C2H2	0.268E+02	H+	TOF	0.366E-06	83Ro02
Al2O3	C2H2	0.273E+02	H+	TOF	0.356E-06	83Ro02
Al2O3	C2H2	0.277E+02	H+	TOF	0.346E-06	83Ro02
Al2O3	C2H2	0.281E+02	H+	TOF	0.333E-06	83Ro02
Al2O3	C2H2	0.286E+02	H+	TOF	0.314E-06	83Ro02
Al2O3	C2H2	0.292E+02	H+	TOF	0.288E-06	83Ro02
Al2O3	C2H2	0.298E+02	H+	TOF	0.259E-06	83Ro02
Al2O3	C2H2	0.303E+02	H+	TOF	0.232E-06	83Ro02
Al2O3	C2H2	0.309E+02	H+	TOF	0.201E-06	83Ro02
Al2O3	C2H2	0.313E+02	H+	TOF	0.174E-06	83Ro02
Al2O3	C2H2	0.318E+02	H+	TOF	0.145E-06	83Ro02
Al2O3	C2H2	0.321E+02	H+	TOF	0.119E-06	83Ro02

The signals of other positive ions were very weak.
Thickness 10nm

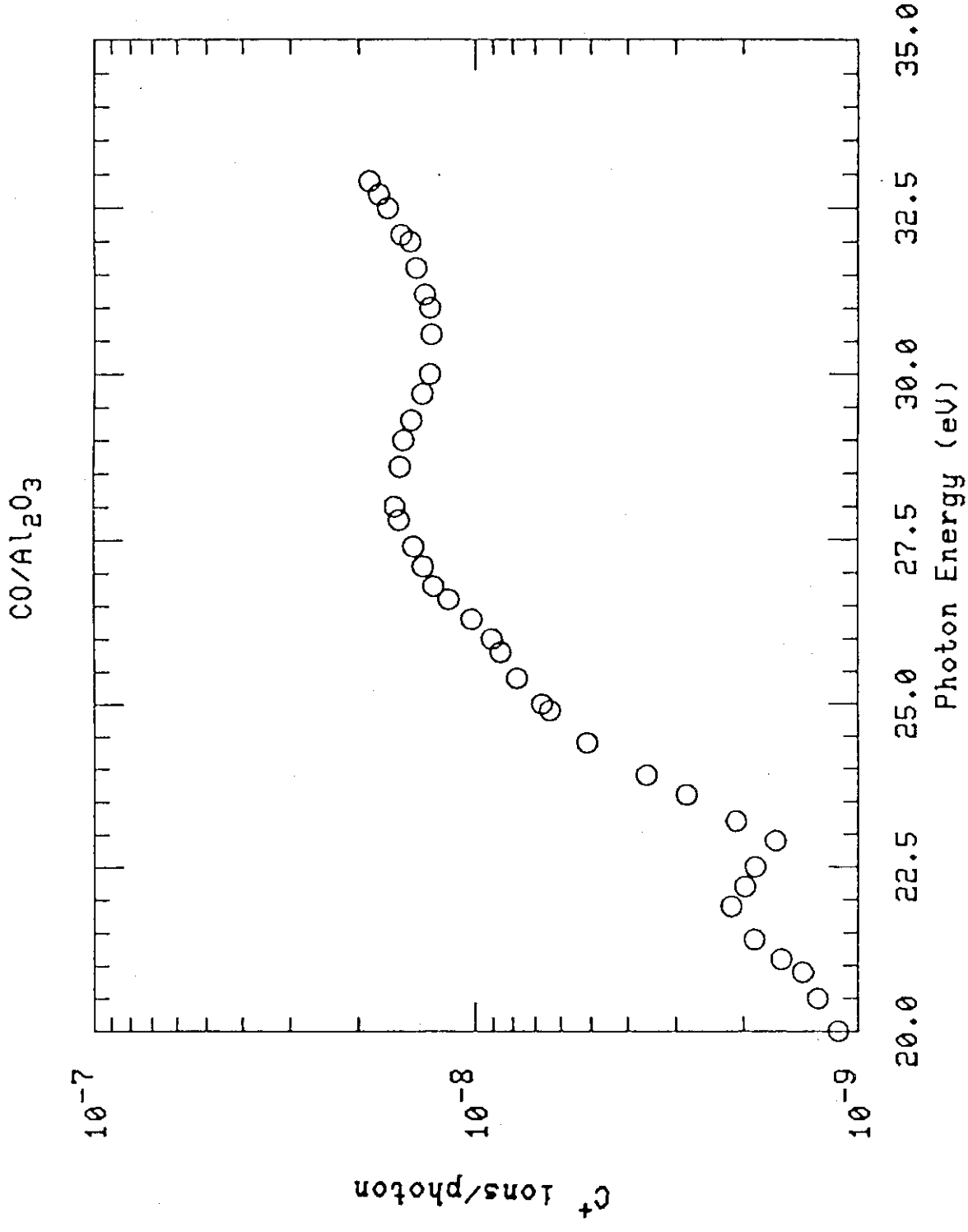

Fig.84 Desorption efficiency as a function of incident energy

DATA LIST

Substrate	Adsorbed gases	Incident photon energy (eV)	Desorbed species	Method	Ions per photon	Ref.
Al2O3	CO	0.200E+02	C+	TOF	0.113E-08	83Ro02
Al2O3	CO	0.205E+02	C+	TOF	0.128E-08	83Ro02
Al2O3	CO	0.209E+02	C+	TOF	0.140E-08	83Ro02
Al2O3	CO	0.211E+02	C+	TOF	0.159E-08	83Ro02
Al2O3	CO	0.214E+02	C+	TOF	0.187E-08	83Ro02
Al2O3	CO	0.219E+02	C+	TOF	0.215E-08	83Ro02
Al2O3	CO	0.222E+02	C+	TOF	0.198E-08	83Ro02
Al2O3	CO	0.225E+02	C+	TOF	0.186E-08	83Ro02
Al2O3	CO	0.229E+02	C+	TOF	0.165E-08	83Ro02
Al2O3	CO	0.232E+02	C+	TOF	0.209E-08	83Ro02
Al2O3	CO	0.236E+02	C+	TOF	0.281E-08	83Ro02
Al2O3	CO	0.239E+02	C+	TOF	0.357E-08	83Ro02
Al2O3	CO	0.244E+02	C+	TOF	0.510E-08	83Ro02
Al2O3	CO	0.249E+02	C+	TOF	0.638E-08	83Ro02
Al2O3	CO	0.250E+02	C+	TOF	0.670E-08	83Ro02
Al2O3	CO	0.254E+02	C+	TOF	0.779E-08	83Ro02
Al2O3	CO	0.258E+02	C+	TOF	0.859E-08	83Ro02
Al2O3	CO	0.260E+02	C+	TOF	0.904E-08	83Ro02
Al2O3	CO	0.263E+02	C+	TOF	0.102E-07	83Ro02
Al2O3	CO	0.266E+02	C+	TOF	0.117E-07	83Ro02
Al2O3	CO	0.268E+02	C+	TOF	0.128E-07	83Ro02
Al2O3	CO	0.271E+02	C+	TOF	0.136E-07	83Ro02
Al2O3	CO	0.274E+02	C+	TOF	0.144E-07	83Ro02
Al2O3	CO	0.278E+02	C+	TOF	0.157E-07	83Ro02
Al2O3	CO	0.280E+02	C+	TOF	0.161E-07	83Ro02
Al2O3	CO	0.286E+02	C+	TOF	0.156E-07	83Ro02
Al2O3	CO	0.290E+02	C+	TOF	0.153E-07	83Ro02
Al2O3	CO	0.293E+02	C+	TOF	0.146E-07	83Ro02
Al2O3	CO	0.297E+02	C+	TOF	0.137E-07	83Ro02
Al2O3	CO	0.300E+02	C+	TOF	0.131E-07	83Ro02
Al2O3	CO	0.306E+02	C+	TOF	0.130E-07	83Ro02
Al2O3	CO	0.310E+02	C+	TOF	0.131E-07	83Ro02
Al2O3	CO	0.312E+02	C+	TOF	0.135E-07	83Ro02
Al2O3	CO	0.316E+02	C+	TOF	0.142E-07	83Ro02
Al2O3	CO	0.320E+02	C+	TOF	0.147E-07	83Ro02
Al2O3	CO	0.321E+02	C+	TOF	0.155E-07	83Ro02
Al2O3	CO	0.325E+02	C+	TOF	0.168E-07	83Ro02
Al2O3	CO	0.327E+02	C+	TOF	0.177E-07	83Ro02
Al2O3	CO	0.329E+02	C+	TOF	0.187E-07	83Ro02

Thickness 10nm

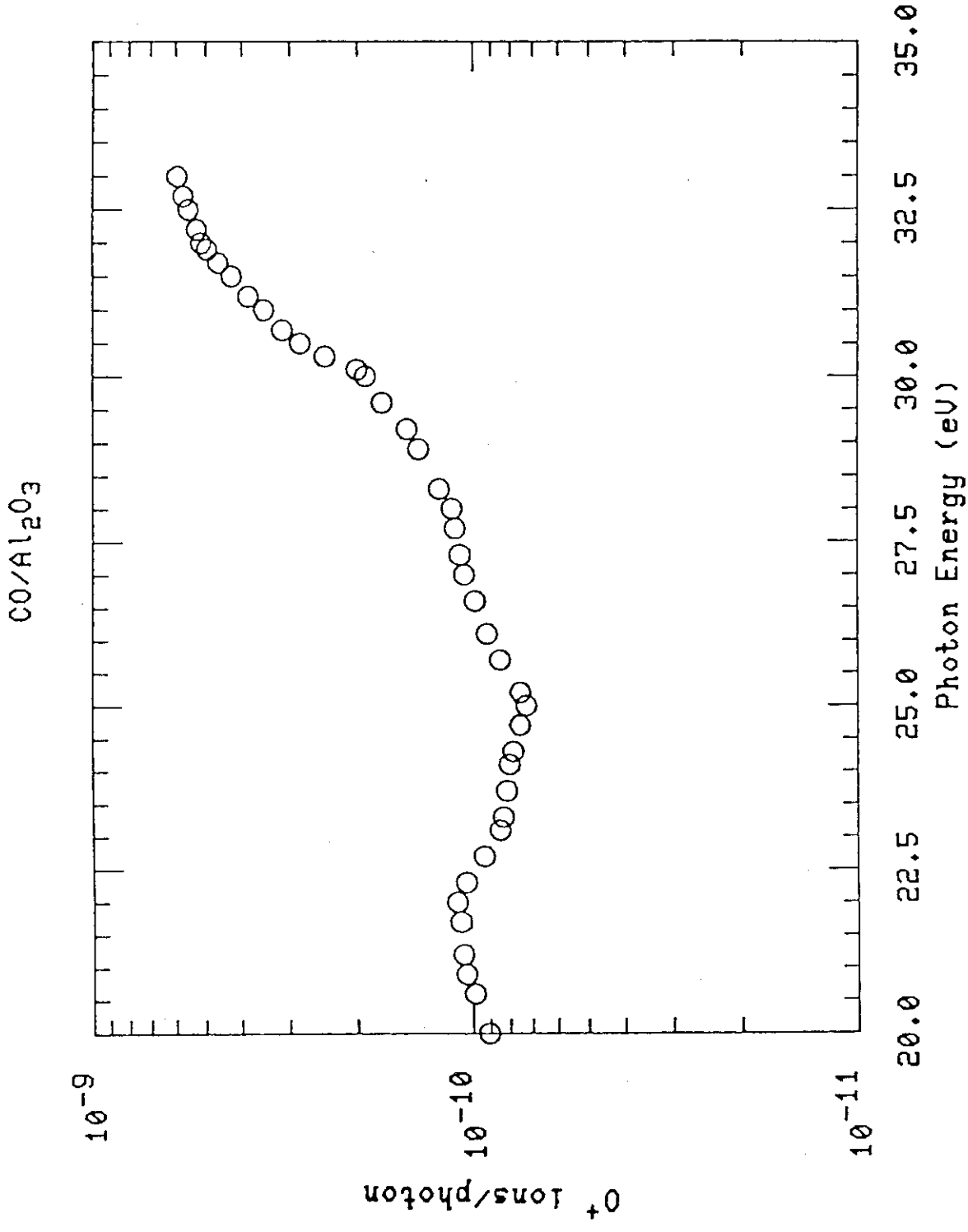

Fig.85 Desorption efficiency as a function of incident energy

DATA LIST

Substrate	Adsorbed gases	Incident photon energy (eV)	Desorbed species	Method	Ions per photon	Ref.
Al2O3	CO	0.200E+02	O+	TOF	0.908E-10	83Ro02
Al2O3	CO	0.206E+02	O+	TOF	0.990E-10	83Ro02
Al2O3	CO	0.209E+02	O+	TOF	0.104E-09	83Ro02
Al2O3	CO	0.212E+02	O+	TOF	0.106E-09	83Ro02
Al2O3	CO	0.217E+02	O+	TOF	0.108E-09	83Ro02
Al2O3	CO	0.220E+02	O+	TOF	0.110E-09	83Ro02
Al2O3	CO	0.223E+02	O+	TOF	0.104E-09	83Ro02
Al2O3	CO	0.227E+02	O+	TOF	0.935E-10	83Ro02
Al2O3	CO	0.231E+02	O+	TOF	0.848E-10	83Ro02
Al2O3	CO	0.233E+02	O+	TOF	0.832E-10	83Ro02
Al2O3	CO	0.237E+02	O+	TOF	0.816E-10	83Ro02
Al2O3	CO	0.241E+02	O+	TOF	0.800E-10	83Ro02
Al2O3	CO	0.243E+02	O+	TOF	0.784E-10	83Ro02
Al2O3	CO	0.247E+02	O+	TOF	0.753E-10	83Ro02
Al2O3	CO	0.250E+02	O+	TOF	0.723E-10	83Ro02
Al2O3	CO	0.252E+02	O+	TOF	0.750E-10	83Ro02
Al2O3	CO	0.252E+02	O+	TOF	0.751E-10	83Ro02
Al2O3	CO	0.257E+02	O+	TOF	0.847E-10	83Ro02
Al2O3	CO	0.261E+02	O+	TOF	0.916E-10	83Ro02
Al2O3	CO	0.266E+02	O+	TOF	0.984E-10	83Ro02
Al2O3	CO	0.270E+02	O+	TOF	0.105E-09	83Ro02
Al2O3	CO	0.273E+02	O+	TOF	0.108E-09	83Ro02
Al2O3	CO	0.277E+02	O+	TOF	0.111E-09	83Ro02
Al2O3	CO	0.280E+02	O+	TOF	0.113E-09	83Ro02
Al2O3	CO	0.283E+02	O+	TOF	0.122E-09	83Ro02
Al2O3	CO	0.289E+02	O+	TOF	0.138E-09	83Ro02
Al2O3	CO	0.292E+02	O+	TOF	0.148E-09	83Ro02
Al2O3	CO	0.296E+02	O+	TOF	0.172E-09	83Ro02
Al2O3	CO	0.300E+02	O+	TOF	0.190E-09	83Ro02
Al2O3	CO	0.301E+02	O+	TOF	0.200E-09	83Ro02
Al2O3	CO	0.303E+02	O+	TOF	0.242E-09	83Ro02
Al2O3	CO	0.305E+02	O+	TOF	0.281E-09	83Ro02
Al2O3	CO	0.307E+02	O+	TOF	0.313E-09	83Ro02
Al2O3	CO	0.310E+02	O+	TOF	0.350E-09	83Ro02
Al2O3	CO	0.312E+02	O+	TOF	0.385E-09	83Ro02
Al2O3	CO	0.315E+02	O+	TOF	0.426E-09	83Ro02
Al2O3	CO	0.317E+02	O+	TOF	0.463E-09	83Ro02
Al2O3	CO	0.319E+02	O+	TOF	0.495E-09	83Ro02
Al2O3	CO	0.320E+02	O+	TOF	0.514E-09	83Ro02
Al2O3	CO	0.322E+02	O+	TOF	0.528E-09	83Ro02
Al2O3	CO	0.325E+02	O+	TOF	0.556E-09	83Ro02
Al2O3	CO	0.327E+02	O+	TOF	0.574E-09	83Ro02
Al2O3	CO	0.330E+02	O+	TOF	0.597E-09	83Ro02

Thickness 10nm

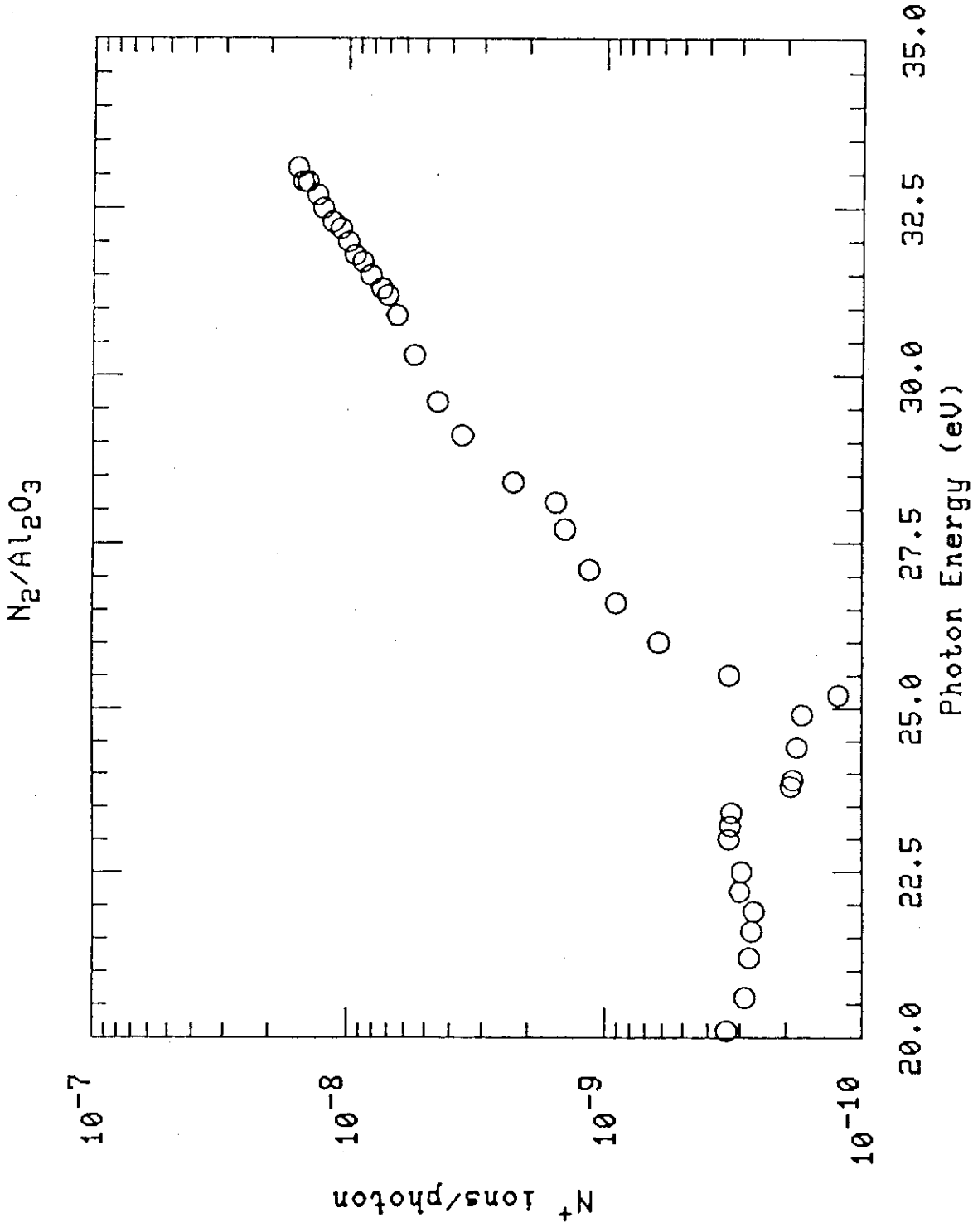

Fig.86 Desorption efficiency as a function of incident energy

DATA LIST

Substrate	Adsorbed gases	Incident photon energy (eV)	Desorbed species	Method	Ions per photon	Ref.
Al2O3	N2	0.201E+02	N+	TOF	0.337E-09	83Ro02
Al2O3	N2	0.206E+02	N+	TOF	0.287E-09	83Ro02
Al2O3	N2	0.212E+02	N+	TOF	0.276E-09	83Ro02
Al2O3	N2	0.216E+02	N+	TOF	0.270E-09	83Ro02
Al2O3	N2	0.219E+02	N+	TOF	0.265E-09	83Ro02
Al2O3	N2	0.222E+02	N+	TOF	0.301E-09	83Ro02
Al2O3	N2	0.225E+02	N+	TOF	0.296E-09	83Ro02
Al2O3	N2	0.230E+02	N+	TOF	0.330E-09	83Ro02
Al2O3	N2	0.232E+02	N+	TOF	0.327E-09	83Ro02
Al2O3	N2	0.234E+02	N+	TOF	0.323E-09	83Ro02
Al2O3	N2	0.238E+02	N+	TOF	0.190E-09	83Ro02
Al2O3	N2	0.239E+02	N+	TOF	0.187E-09	83Ro02
Al2O3	N2	0.244E+02	N+	TOF	0.180E-09	83Ro02
Al2O3	N2	0.249E+02	N+	TOF	0.172E-09	83Ro02
Al2O3	N2	0.252E+02	N+	TOF	0.124E-09	83Ro02
Al2O3	N2	0.255E+02	N+	TOF	0.330E-09	83Ro02
Al2O3	N2	0.260E+02	N+	TOF	0.618E-09	83Ro02
Al2O3	N2	0.266E+02	N+	TOF	0.903E-09	83Ro02
Al2O3	N2	0.271E+02	N+	TOF	0.115E-08	83Ro02
Al2O3	N2	0.277E+02	N+	TOF	0.143E-08	83Ro02
Al2O3	N2	0.281E+02	N+	TOF	0.155E-08	83Ro02
Al2O3	N2	0.284E+02	N+	TOF	0.227E-08	83Ro02
Al2O3	N2	0.291E+02	N+	TOF	0.360E-08	83Ro02
Al2O3	N2	0.296E+02	N+	TOF	0.448E-08	83Ro02
Al2O3	N2	0.303E+02	N+	TOF	0.553E-08	83Ro02
Al2O3	N2	0.309E+02	N+	TOF	0.649E-08	83Ro02
Al2O3	N2	0.312E+02	N+	TOF	0.703E-08	83Ro02
Al2O3	N2	0.313E+02	N+	TOF	0.741E-08	83Ro02
Al2O3	N2	0.315E+02	N+	TOF	0.816E-08	83Ro02
Al2O3	N2	0.317E+02	N+	TOF	0.875E-08	83Ro02
Al2O3	N2	0.318E+02	N+	TOF	0.938E-08	83Ro02
Al2O3	N2	0.320E+02	N+	TOF	0.992E-08	83Ro02
Al2O3	N2	0.322E+02	N+	TOF	0.106E-07	83Ro02
Al2O3	N2	0.323E+02	N+	TOF	0.114E-07	83Ro02
Al2O3	N2	0.325E+02	N+	TOF	0.124E-07	83Ro02
Al2O3	N2	0.327E+02	N+	TOF	0.131E-07	83Ro02
Al2O3	N2	0.329E+02	N+	TOF	0.143E-07	83Ro02
Al2O3	N2	0.329E+02	N+	TOF	0.149E-07	83Ro02
Al2O3	N2	0.331E+02	N+	TOF	0.156E-07	83Ro02

Thickness 10nm

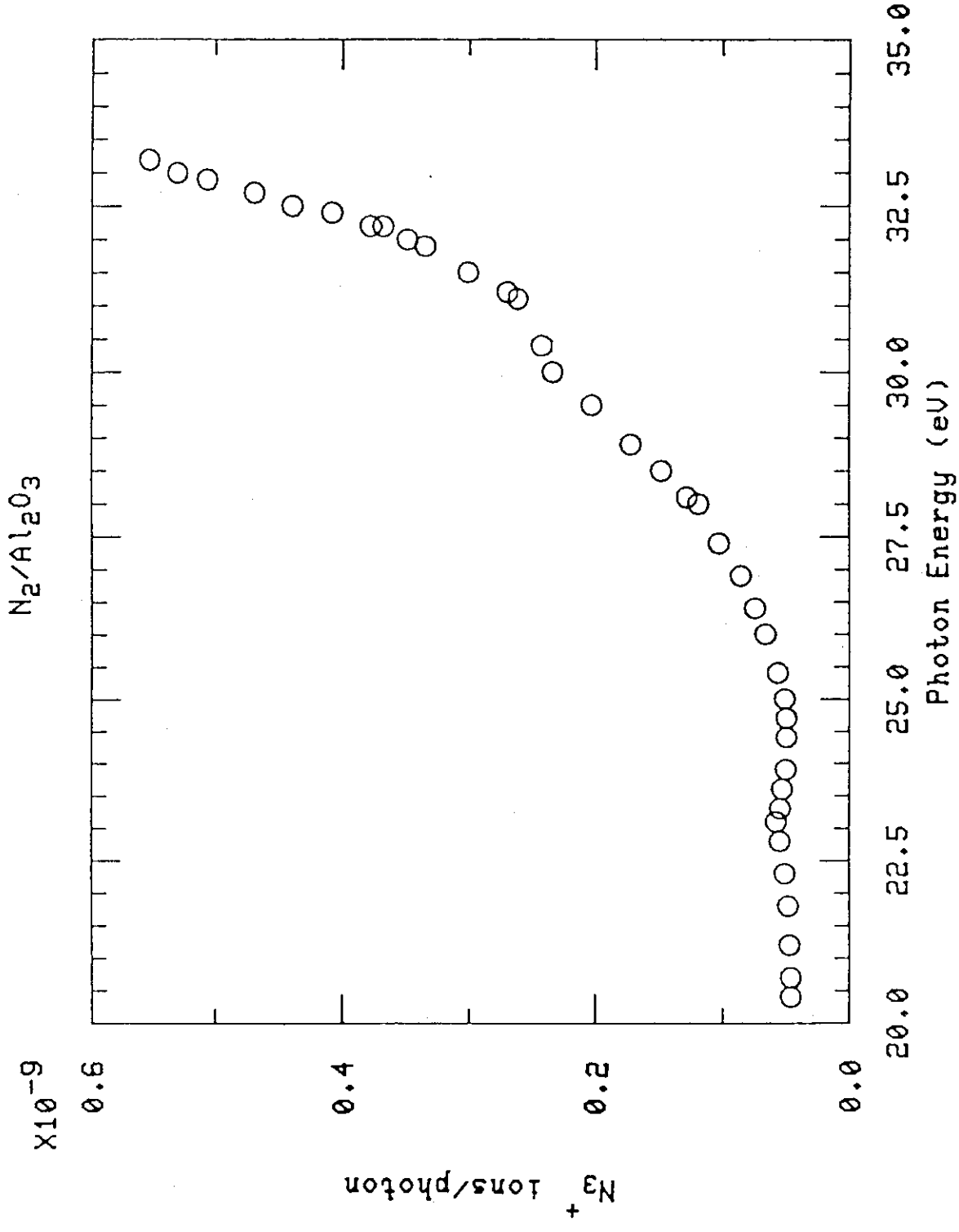

Fig.87 Desorption efficiency as a function of incident energy

DATA LIST

Substrate	Adsorbed gases	Incident photon energy (eV)	Desorbed species	Method	Ions per photon	Ref.
Al2O3	N2	0.204E+02	N3 +	TOF	0.468E-10	83Ro02
Al2O3	N2	0.207E+02	N3 +	TOF	0.466E-10	83Ro02
Al2O3	N2	0.212E+02	N3 +	TOF	0.478E-10	83Ro02
Al2O3	N2	0.218E+02	N3 +	TOF	0.489E-10	83Ro02
Al2O3	N2	0.223E+02	N3 +	TOF	0.514E-10	83Ro02
Al2O3	N2	0.228E+02	N3 +	TOF	0.554E-10	83Ro02
Al2O3	N2	0.231E+02	N3 +	TOF	0.581E-10	83Ro02
Al2O3	N2	0.233E+02	N3 +	TOF	0.551E-10	83Ro02
Al2O3	N2	0.236E+02	N3 +	TOF	0.536E-10	83Ro02
Al2O3	N2	0.239E+02	N3 +	TOF	0.505E-10	83Ro02
Al2O3	N2	0.244E+02	N3 +	TOF	0.502E-10	83Ro02
Al2O3	N2	0.247E+02	N3 +	TOF	0.501E-10	83Ro02
Al2O3	N2	0.250E+02	N3 +	TOF	0.513E-10	83Ro02
Al2O3	N2	0.254E+02	N3 +	TOF	0.568E-10	83Ro02
Al2O3	N2	0.260E+02	N3 +	TOF	0.664E-10	83Ro02
Al2O3	N2	0.264E+02	N3 +	TOF	0.747E-10	83Ro02
Al2O3	N2	0.269E+02	N3 +	TOF	0.859E-10	83Ro02
Al2O3	N2	0.274E+02	N3 +	TOF	0.103E-09	83Ro02
Al2O3	N2	0.280E+02	N3 +	TOF	0.119E-09	83Ro02
Al2O3	N2	0.281E+02	N3 +	TOF	0.128E-09	83Ro02
Al2O3	N2	0.285E+02	N3 +	TOF	0.148E-09	83Ro02
Al2O3	N2	0.289E+02	N3 +	TOF	0.172E-09	83Ro02
Al2O3	N2	0.295E+02	N3 +	TOF	0.203E-09	83Ro02
Al2O3	N2	0.300E+02	N3 +	TOF	0.234E-09	83Ro02
Al2O3	N2	0.304E+02	N3 +	TOF	0.243E-09	83Ro02
Al2O3	N2	0.311E+02	N3 +	TOF	0.262E-09	83Ro02
Al2O3	N2	0.312E+02	N3 +	TOF	0.270E-09	83Ro02
Al2O3	N2	0.315E+02	N3 +	TOF	0.301E-09	83Ro02
Al2O3	N2	0.319E+02	N3 +	TOF	0.335E-09	83Ro02
Al2O3	N2	0.320E+02	N3 +	TOF	0.349E-09	83Ro02
Al2O3	N2	0.322E+02	N3 +	TOF	0.368E-09	83Ro02
Al2O3	N2	0.322E+02	N3 +	TOF	0.378E-09	83Ro02
Al2O3	N2	0.324E+02	N3 +	TOF	0.408E-09	83Ro02
Al2O3	N2	0.325E+02	N3 +	TOF	0.439E-09	83Ro02
Al2O3	N2	0.327E+02	N3 +	TOF	0.469E-09	83Ro02
Al2O3	N2	0.329E+02	N3 +	TOF	0.507E-09	83Ro02
Al2O3	N2	0.330E+02	N3 +	TOF	0.531E-09	83Ro02
Al2O3	N2	0.332E+02	N3 +	TOF	0.554E-09	83Ro02

Thickness 10nm

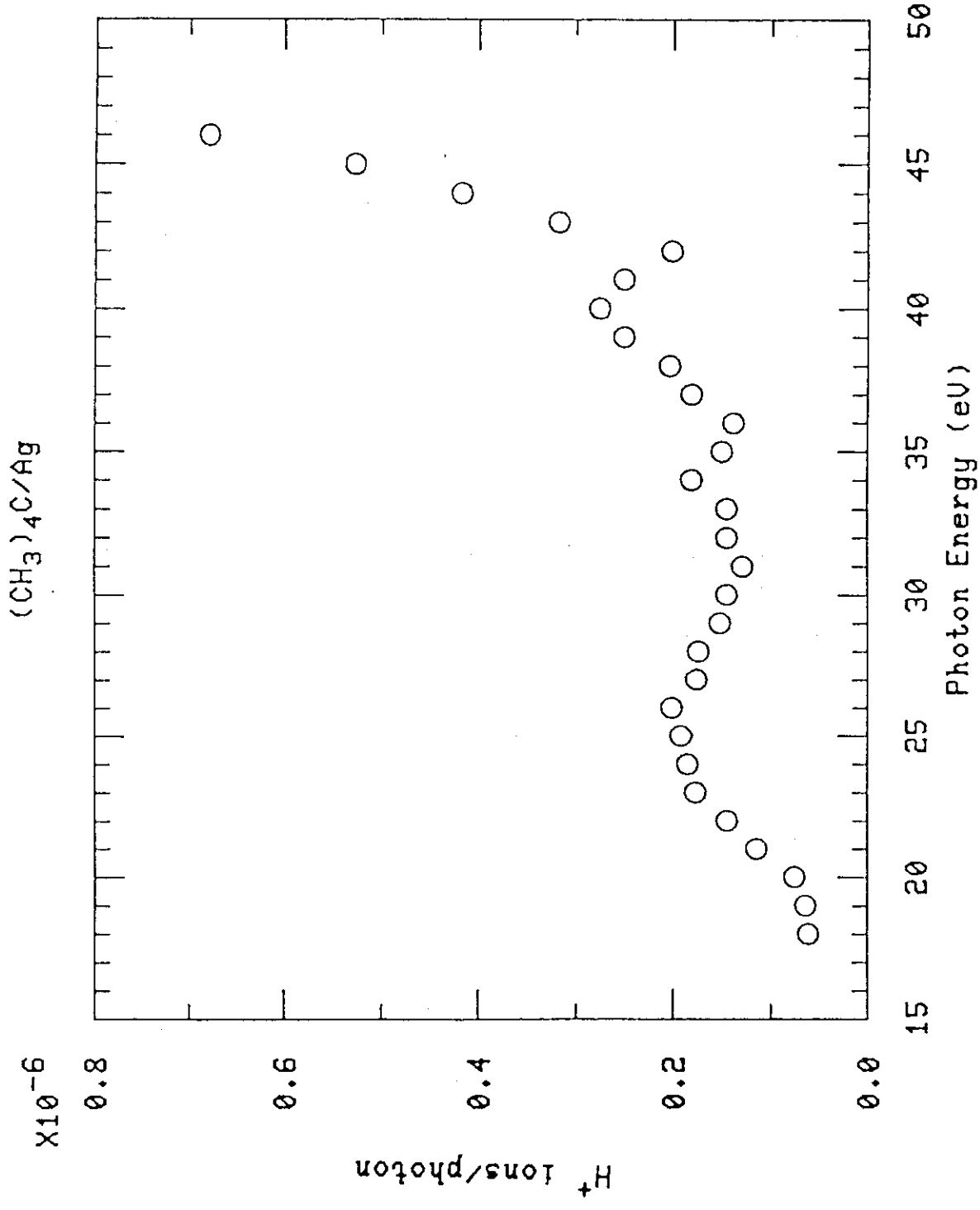

Fig.88 Desorption efficiency as a function of incident energy

DATA LIST

Substrate	Adsorbed gases	Incident energy (eV)	Desorbed species	Method	Ions per photon	Ref.
Ag	(CH3)4C	0.180E+02	H+	MS	0.617E-07	84Ke01
Ag	(CH3)4C	0.190E+02	H+	MS	0.647E-07	84Ke01
Ag	(CH3)4C	0.200E+02	H+	MS	0.761E-07	84Ke01
Ag	(CH3)4C	0.210E+02	H+	MS	0.115E-06	84Ke01
Ag	(CH3)4C	0.220E+02	H+	MS	0.145E-06	84Ke01
Ag	(CH3)4C	0.230E+02	H+	MS	0.177E-06	84Ke01
Ag	(CH3)4C	0.240E+02	H+	MS	0.185E-06	84Ke01
Ag	(CH3)4C	0.250E+02	H+	MS	0.192E-06	84Ke01
Ag	(CH3)4C	0.260E+02	H+	MS	0.201E-06	84Ke01
Ag	(CH3)4C	0.270E+02	H+	MS	0.176E-06	84Ke01
Ag	(CH3)4C	0.280E+02	H+	MS	0.174E-06	84Ke01
Ag	(CH3)4C	0.290E+02	H+	MS	0.152E-06	84Ke01
Ag	(CH3)4C	0.300E+02	H+	MS	0.145E-06	84Ke01
Ag	(CH3)4C	0.310E+02	H+	MS	0.129E-06	84Ke01
Ag	(CH3)4C	0.320E+02	H+	MS	0.145E-06	84Ke01
Ag	(CH3)4C	0.330E+02	H+	MS	0.145E-06	84Ke01
Ag	(CH3)4C	0.340E+02	H+	MS	0.181E-06	84Ke01
Ag	(CH3)4C	0.350E+02	H+	MS	0.150E-06	84Ke01
Ag	(CH3)4C	0.360E+02	H+	MS	0.138E-06	84Ke01
Ag	(CH3)4C	0.370E+02	H+	MS	0.181E-06	84Ke01
Ag	(CH3)4C	0.380E+02	H+	MS	0.203E-06	84Ke01
Ag	(CH3)4C	0.390E+02	H+	MS	0.250E-06	84Ke01
Ag	(CH3)4C	0.400E+02	H+	MS	0.275E-06	84Ke01
Ag	(CH3)4C	0.410E+02	H+	MS	0.250E-06	84Ke01
Ag	(CH3)4C	0.420E+02	H+	MS	0.201E-06	84Ke01
Ag	(CH3)4C	0.430E+02	H+	MS	0.317E-06	84Ke01
Ag	(CH3)4C	0.440E+02	H+	MS	0.417E-06	84Ke01
Ag	(CH3)4C	0.450E+02	H+	MS	0.527E-06	84Ke01
Ag	(CH3)4C	0.460E+02	H+	MS	0.679E-06	84Ke01

Solid neopentane

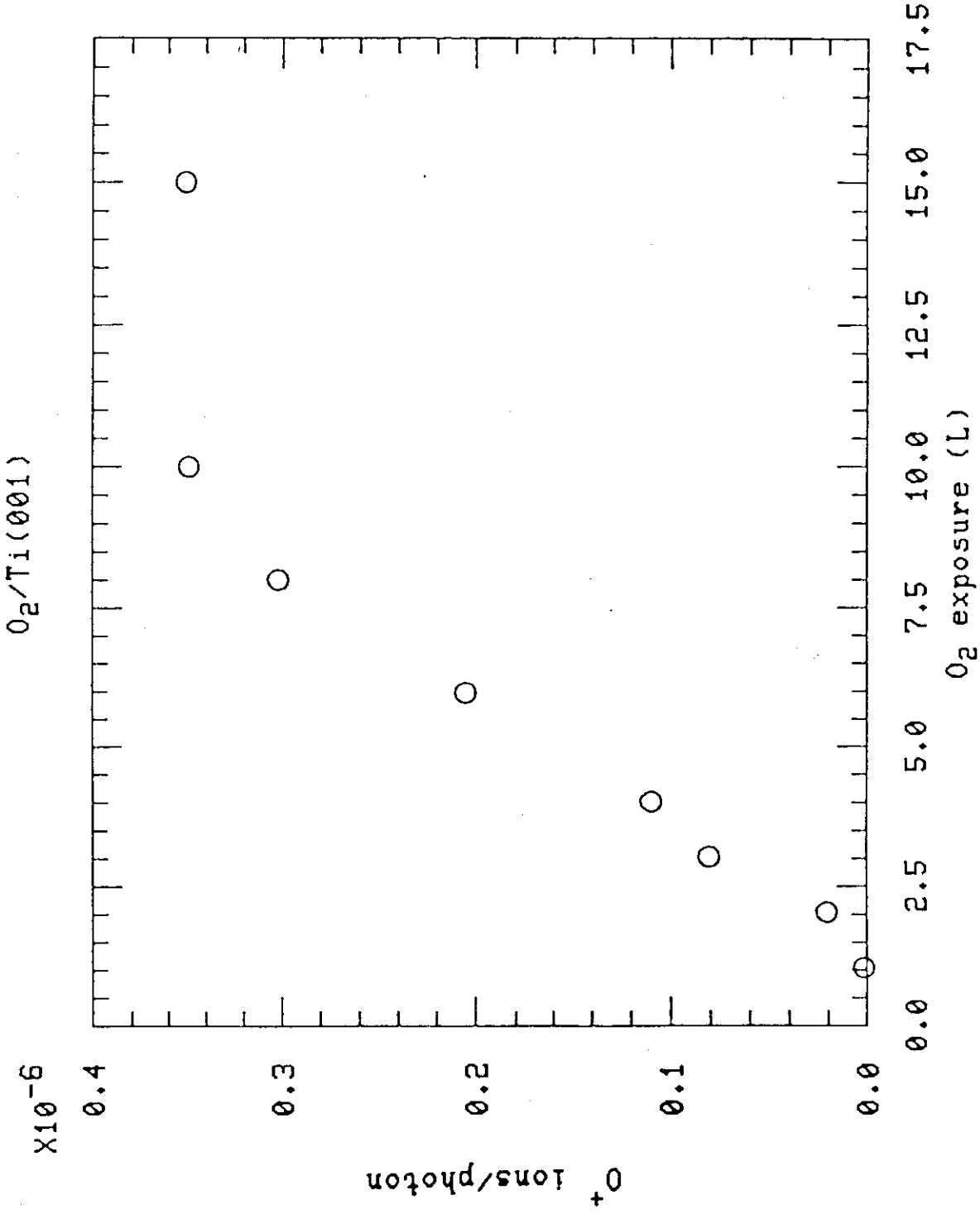

Fig.89 Desorption efficiency as a function of exposure

DATA LIST

Substrate	Adsorbed gases	Exposure (L)	Desorbed spaces	Method	Ions per photon	Ref.
Ti(001)	O2	0.103E+01	O+	TOF	0.156E-08	81Ha01
Ti(001)	O2	0.203E+01	O+	TOF	0.211E-07	81Ha01
Ti(001)	O2	0.302E+01	O+	TOF	0.809E-07	81Ha01
Ti(001)	O2	0.400E+01	O+	TOF	0.110E-06	81Ha01
Ti(001)	O2	0.597E+01	O+	TOF	0.205E-06	81Ha01
Ti(001)	O2	0.800E+01	O+	TOF	0.302E-06	81Ha01
Ti(001)	O2	0.999E+01	O+	TOF	0.349E-06	81Ha01
Ti(001)	O2	0.150E+02	O+	TOF	0.351E-06	81Ha01

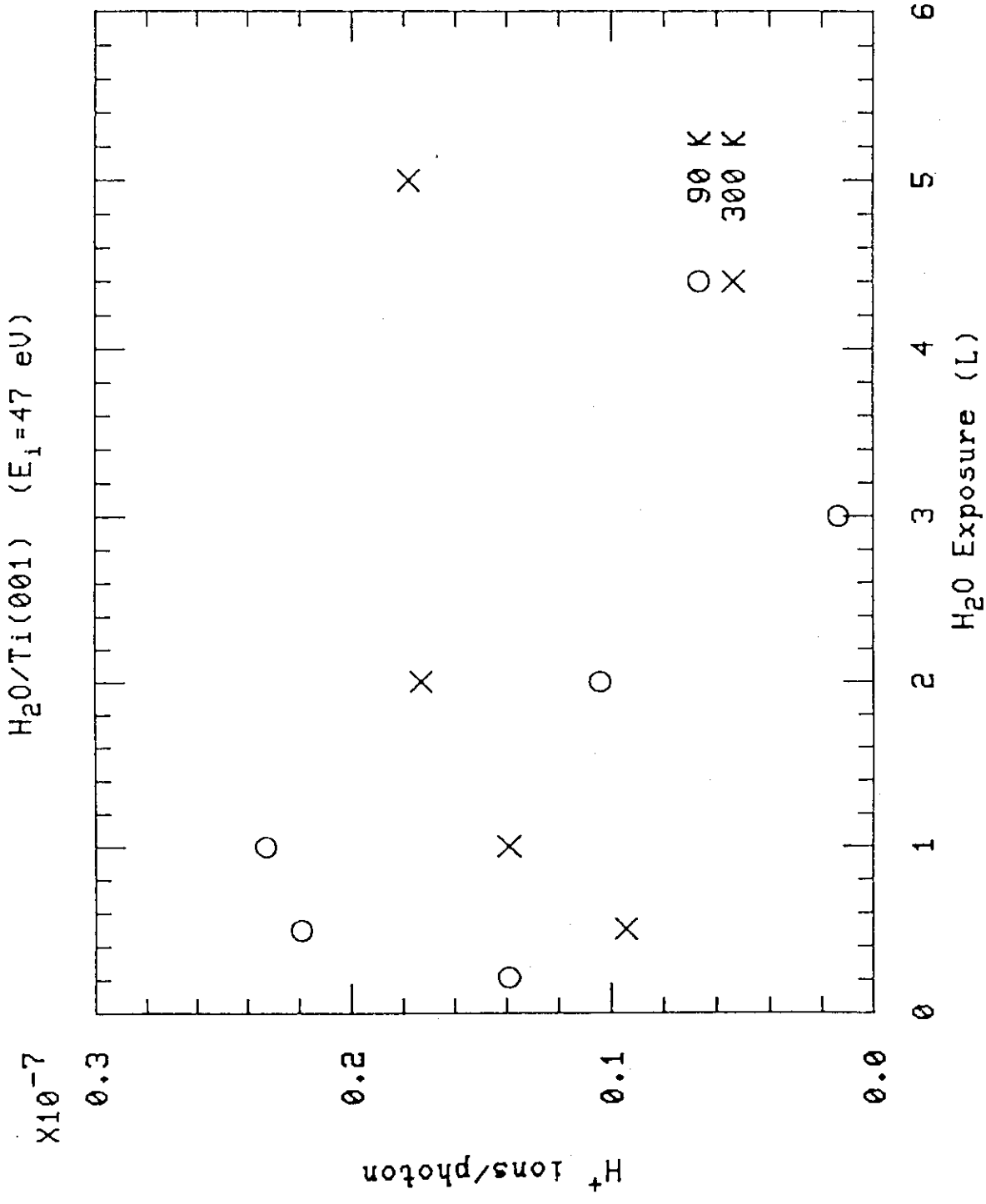

Fig.90 Desorption efficiency as a function of exposure

DATA LIST

Substrate	Adsorbed gases	Exposure (L)	Desorbed species	Method	Ions per photon	Ref.	Remark
Ti(001)	H2O	0.215E+00	H+	CMA	0.139E-07	82St02	*1)
Ti(001)	H2O	0.500E+00	H+	CMA	0.219E-07	82St02	*1)
Ti(001)	H2O	0.100E+01	H+	CMA	0.233E-07	82St02	*1)
Ti(001)	H2O	0.200E+01	H+	CMA	0.104E-07	82St02	*1)
Ti(001)	H2O	0.300E+01	H+	CMA	0.137E-08	82St02	*1)
Ti(001)	H2O	0.500E+00	H+	CMA	0.942E-08	82St02	*2)
Ti(001)	H2O	0.100E+01	H+	CMA	0.139E-07	82St02	*2)
Ti(001)	H2O	0.200E+01	H+	CMA	0.173E-07	82St02	*2)
Ti(001)	H2O	0.500E+01	H+	CMA	0.178E-07	82St02	*2)

*1) Surface temperature 90K
*2) Surface temperature 300K
Photon energy 47eV

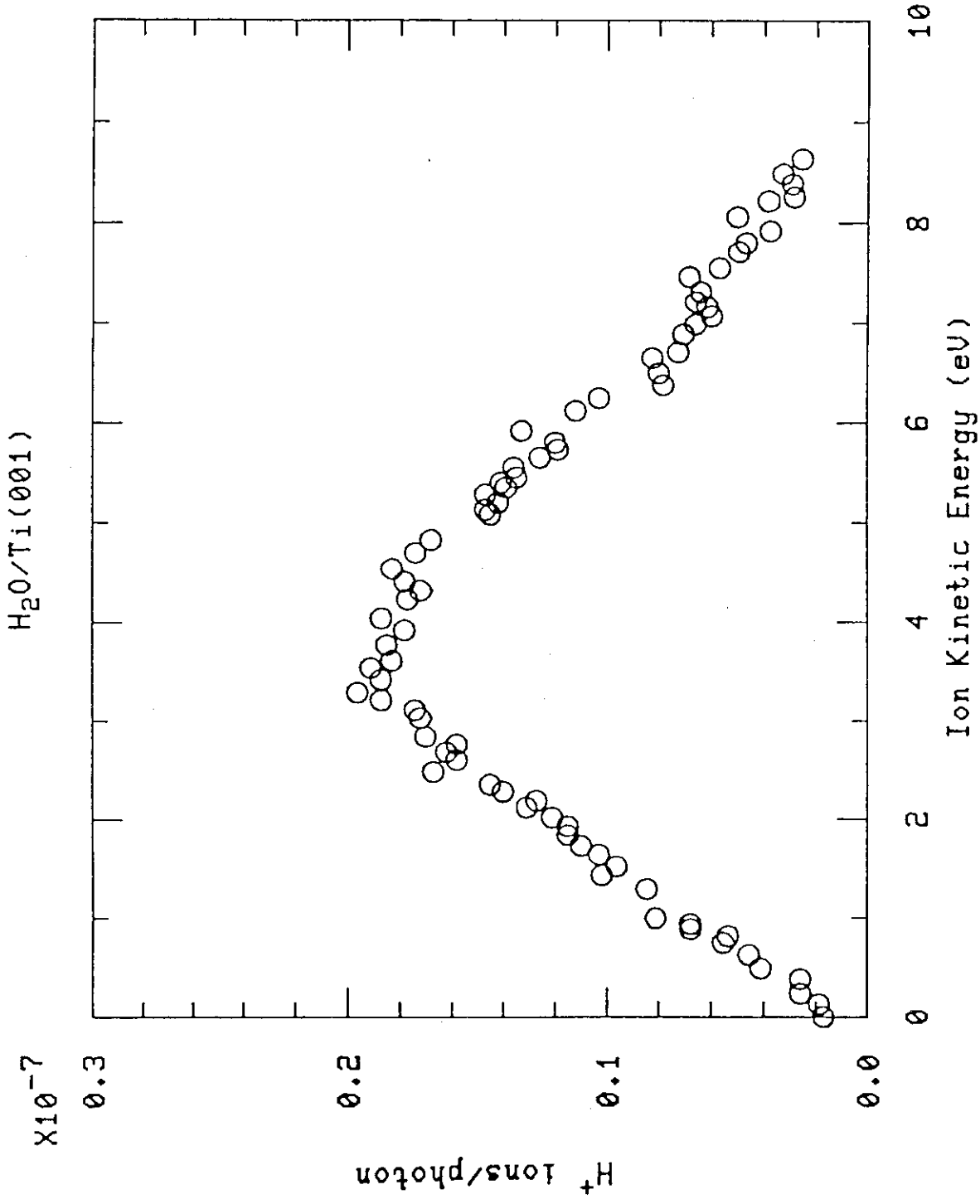

Fig.91 Desorption efficiency as a function of kinetic energy of desorbed ion

DATA LIST

Substrate	Adsorbed gases	H+ ion kinetic energy (eV)	Desorbed species	Method	Ions per photon	Ref.
Ti(001)	H2O	0.000E+00	H+	CMA	0.171E-08	82St02
Ti(001)	H2O	0.125E+00	H+	CMA	0.188E-08	82St02
Ti(001)	H2O	0.233E+00	H+	CMA	0.260E-08	82St02
Ti(001)	H2O	0.381E+00	H+	CMA	0.259E-08	82St02
Ti(001)	H2O	0.491E+00	H+	CMA	0.411E-08	82St02
Ti(001)	H2O	0.626E+00	H+	CMA	0.455E-08	82St02
Ti(001)	H2O	0.749E+00	H+	CMA	0.553E-08	82St02
Ti(001)	H2O	0.816E+00	H+	CMA	0.535E-08	82St02
Ti(001)	H2O	0.886E+00	H+	CMA	0.678E-08	82St02
Ti(001)	H2O	0.940E+00	H+	CMA	0.678E-08	82St02
Ti(001)	H2O	0.996E+00	H+	CMA	0.812E-08	82St02
Ti(001)	H2O	0.129E+01	H+	CMA	0.846E-08	82St02
Ti(001)	H2O	0.143E+01	H+	CMA	0.102E-07	82St02
Ti(001)	H2O	0.152E+01	H+	CMA	0.962E-08	82St02
Ti(001)	H2O	0.164E+01	H+	CMA	0.103E-07	82St02
Ti(001)	H2O	0.173E+01	H+	CMA	0.110E-07	82St02
Ti(001)	H2O	0.184E+01	H+	CMA	0.115E-07	82St02
Ti(001)	H2O	0.193E+01	H+	CMA	0.115E-07	82St02
Ti(001)	H2O	0.202E+01	H+	CMA	0.121E-07	82St02
Ti(001)	H2O	0.212E+01	H+	CMA	0.131E-07	82St02
Ti(001)	H2O	0.219E+01	H+	CMA	0.127E-07	82St02
Ti(001)	H2O	0.228E+01	H+	CMA	0.140E-07	82St02
Ti(001)	H2O	0.235E+01	H+	CMA	0.145E-07	82St02
Ti(001)	H2O	0.248E+01	H+	CMA	0.167E-07	82St02
Ti(001)	H2O	0.260E+01	H+	CMA	0.158E-07	82St02
Ti(001)	H2O	0.268E+01	H+	CMA	0.162E-07	82St02
Ti(001)	H2O	0.276E+01	H+	CMA	0.158E-07	82St02
Ti(001)	H2O	0.284E+01	H+	CMA	0.170E-07	82St02
Ti(001)	H2O	0.303E+01	H+	CMA	0.172E-07	82St02
Ti(001)	H2O	0.311E+01	H+	CMA	0.174E-07	82St02
Ti(001)	H2O	0.321E+01	H+	CMA	0.187E-07	82St02
Ti(001)	H2O	0.329E+01	H+	CMA	0.196E-07	82St02
Ti(001)	H2O	0.342E+01	H+	CMA	0.187E-07	82St02
Ti(001)	H2O	0.354E+01	H+	CMA	0.191E-07	82St02
Ti(001)	H2O	0.361E+01	H+	CMA	0.183E-07	82St02
Ti(001)	H2O	0.377E+01	H+	CMA	0.185E-07	82St02
Ti(001)	H2O	0.392E+01	H+	CMA	0.178E-07	82St02
Ti(001)	H2O	0.404E+01	H+	CMA	0.187E-07	82St02
Ti(001)	H2O	0.423E+01	H+	CMA	0.177E-07	82St02
Ti(001)	H2O	0.432E+01	H+	CMA	0.172E-07	82St02
Ti(001)	H2O	0.441E+01	H+	CMA	0.178E-07	82St02
Ti(001)	H2O	0.454E+01	H+	CMA	0.183E-07	82St02
Ti(001)	H2O	0.470E+01	H+	CMA	0.174E-07	82St02
Ti(001)	H2O	0.483E+01	H+	CMA	0.168E-07	82St02

./..

Ti(001)	H2O	0.508E+01	H+	CMA	0.145E-07	82St02
Ti(001)	H2O	0.513E+01	H+	CMA	0.147E-07	82St02
Ti(001)	H2O	0.520E+01	H+	CMA	0.142E-07	82St02
Ti(001)	H2O	0.528E+01	H+	CMA	0.147E-07	82St02
Ti(001)	H2O	0.535E+01	H+	CMA	0.139E-07	82St02
Ti(001)	H2O	0.540E+01	H+	CMA	0.141E-07	82St02
Ti(001)	H2O	0.545E+01	H+	CMA	0.135E-07	82St02
Ti(001)	H2O	0.555E+01	H+	CMA	0.136E-07	82St02
Ti(001)	H2O	0.565E+01	H+	CMA	0.126E-07	82St02
Ti(001)	H2O	0.573E+01	H+	CMA	0.119E-07	82St02
Ti(001)	H2O	0.580E+01	H+	CMA	0.120E-07	82St02
Ti(001)	H2O	0.592E+01	H+	CMA	0.133E-07	82St02
Ti(001)	H2O	0.612E+01	H+	CMA	0.112E-07	82St02
Ti(001)	H2O	0.625E+01	H+	CMA	0.103E-07	82St02
Ti(001)	H2O	0.638E+01	H+	CMA	0.782E-08	82St02
Ti(001)	H2O	0.650E+01	H+	CMA	0.799E-08	82St02
Ti(001)	H2O	0.665E+01	H+	CMA	0.825E-08	82St02
Ti(001)	H2O	0.671E+01	H+	CMA	0.725E-08	82St02
Ti(001)	H2O	0.689E+01	H+	CMA	0.706E-08	82St02
Ti(001)	H2O	0.699E+01	H+	CMA	0.660E-08	82St02
Ti(001)	H2O	0.707E+01	H+	CMA	0.597E-08	82St02
Ti(001)	H2O	0.716E+01	H+	CMA	0.614E-08	82St02
Ti(001)	H2O	0.721E+01	H+	CMA	0.659E-08	82St02
Ti(001)	H2O	0.731E+01	H+	CMA	0.640E-08	82St02
Ti(001)	H2O	0.746E+01	H+	CMA	0.684E-08	82St02
Ti(001)	H2O	0.755E+01	H+	CMA	0.567E-08	82St02
Ti(001)	H2O	0.771E+01	H+	CMA	0.494E-08	82St02
Ti(001)	H2O	0.780E+01	H+	CMA	0.466E-08	82St02
Ti(001)	H2O	0.792E+01	H+	CMA	0.375E-08	82St02
Ti(001)	H2O	0.806E+01	H+	CMA	0.500E-08	82St02
Ti(001)	H2O	0.822E+01	H+	CMA	0.382E-08	82St02
Ti(001)	H2O	0.826E+01	H+	CMA	0.283E-08	82St02
Ti(001)	H2O	0.839E+01	H+	CMA	0.291E-08	82St02
Ti(001)	H2O	0.849E+01	H+	CMA	0.327E-08	82St02
Ti(001)	H2O	0.864E+01	H+	CMA	0.254E-08	82St02

Photon energy 47eV
H2O exposure 5 L
Surface temperature 300K

5.2.4 List for Miscellaneous Data of PSD

DATA LIST FOR PSD 1 --DESORPTION CROSS SECTION--

Substrate	Adsorbate	Incident photon energy	Photon source	Desorbed species	Method	Desorption cross section (cm^2)	Ref.	Remark
W	R.G.	200 (nm)	SOR	H_2, CO, CO_2	MS	7.8×10^{-21}	71Pe01	*1)
Metals	R.G.		UV	CO_2	QMS	$\sim 1.0 \times 10^{-23}$	76Li03	*2)
ZnO Powder	R.G.	365 (nm)	Hg lamp	CO_2	MS	4.0×10^{-19}	75Sh01	
ZnO Powder	R.G.	365 (nm)	Hg lamp	O	MS	2.0×10^{-17}	75Sh01	
ZnO	R.G.	365 (nm)	Hg lamp	CO_2	*3)	$\sim 1.0 \times 10^{-17}$	77Sh03	
ZnO	R.G.	365 (nm)			QMS	$\sim 1.0 \times 10^{-17}$	76Li03	*4)
Ti_2O powder	R.G.	365 (nm)	Hg lamp	CO_2	MS	3.0×10^{-20}	76Co01	*5)
Semicon.	R.G.		UV	CO_2	QMS	$\sim 1.0 \times 10^{-17}$	76Li03	*2)
W(001)	O_2 (β)	21.2 (eV)	He I	O^+	MS	$< 1.0 \times 10^{-22}$	80Ca01	
Ni	CO	230 (nm)	?	CO	*6)	$\sim 1.0 \times 10^{-23}$	72Pa01	

Ni tilm	CO	270 (nm)	Hg lamp	CO		4.0×10^{-21}	65Ad01	*7)
Ni(100)	CO	650 (nm)	SOR	O^+	TOF	1.0×10^{-22}	81Ja02	*8)
W	CO	350 (nm)	Hg lamp	CO	MS	$\sim 1.0 \times 10^{-22}$	65La02	*9)
W poly	CO (α)	250 (nm)	?	CO	MS	5.0×10^{-21}	72Kr01	
NaCl film	CH_3F	975.9 (cm^{-1})	CO_2 laser	CH_3F^+	TOF	2.0×10^{-19}	82He01	*10)

*1) Electron storage ring

*2) Ultraviolet photo-induced desorption, Semicon. :semiconductor

*3) Surface-conductivity change

*4) Refer to 77Fa01

*5) PSD begins at 406 nm

*6) A pulsed photon beam and lock-in detection method

*7) Surface coverage 5.0×10^{-14} molecules/cm^2

*8) The desorption cross section was almost constant in the energy range of 650 ∿ 700 (eV)

*9) Surface coverage 1.0×10^{14} molecules/cm^2

*10) Resonant laser-induced desorption

DATA LIST FOR PSD 2 --IONS PER PHOTON--

Substrate	Adsorbate	Incident photon energy	Photon source	Desorbed species	Method	Ions per photon	Ref.	Remark
W	O_2	1 ∿ 12(KeV)	X-rays	O^+	QMS	1×10^{-7}	77Fr01	*1)
W(111)	O_2	55(eV)	SOR	O^+	TOF	3×10^{-8}	80Ma01	*2)
W(111)	O_2	500(eV)	SOR	O^+	TOF	1×10^{-6}	80Ma01	*2)
W(001)	O_2 (β)	40.8(eV)	He II	O^+	MS	1×10^{-8}	80Ca01	
W(110)	O_2/CO	1 ∿ 12(KeV)	X-rays	O^+	QMS	1×10^{-7}	77Fr01	*1)
W(110)	H_2/CO	1 ∿ 12(KeV)	X-rays	H^+	QMS	1×10^{-7}	77Fr01	*1)
TiO_2	H_2O	18 ∿ 38(eV)	SOR	H^+, OH^+, F^+	TOF	$>1 \times 10^{-6}$	79Kn01	*3)
W poly	R.G.	1 ∿ 12(KeV)	X-rays	H^+	QMS	1×10^{-7}	77Fr01	*1)
W(110)	R.G.	1 ∿ 12(KeV)	X-rays	H^+, O^+, CO^+	QMS	1×10^{-7}	77Fr01	*1)
SS	R.G.	1 ∿ 12(KeV)	X-rays	K^+, Na^+	QMS	$10^{-3} \sim 10^{-5}$	77Fr01	*1)
Nacl film	CH_3F	975.9(cm^{-2})	CO_2 laser	CH_3F^+	TOF	1×10^{-2}	82He01	*4)

*1) The spectrum of the photon source consisted of about 90% AlKα with the rest Bremsstrahlung. (Electron voltage 12kV)
*2) NBS Tantalus II storage ring
*3) Stanford Synchrotron-Radiation Laboratory
*4) Resonent laser-induced desorption

DATA LIST FOR PSD 3 --MOLECULES PER PHOTON--

Substrate	Adsorbate	Incident photon energy	Photon source	Desorbed species	Method	Molecules per photon	Ref.	Remark
Ni poly	CO	300 ∿ 700(nm)	Hg lamp	CO	MS	$10^{-8} \sim 10^{-9}$	73Mc01	
Ni	CO	265(nm)	Hg lamp	CO	*1)	5×10^{-9}	72Pa01	
Mo	CO	200 ∿ 600(nm)	Hg lamp			∿ 0.0	65Ad01	*2)
W ribbon	CO	230 ∿ 320(nm)	Hg lamp	CO	MS	2×10^{-8}	65La02	
W ribbon	CO	375(nm)	Hg lamp	CO	MS	1×10^{-9}	65La02	
W	CO	200 ∿ 600(nm)	Hg lamp			∿ 0.0	65Ad01	*2)
Metals	CO	300(nm)				$\sim 1 \times 10^{-8}$	79Mc02	*3)

*1) Differential amplification method
*2) Photodesorption of CO was not observed
*3) Refer to 68Re01

DATA LIST FOR PSD 3 --CONTINUED

Substrate	Adsorbate	Incident photon energy	Photon source	Desorbed species	Method	Molecules per photon	Ref.	Remark
Metals	R.G.			CO_2	QMS	1×10^{-9}	76Li03	*1)
Semicon.	R.G.			CO_2	QMS	1×10^{-2}	76Li03	*2)
SS 302	R.G.	10 ∿ 50(KeV)	X-rays	CO	QMS	2×10^{-4}	76Br01	*3)
SS 302	R.G.	10 ∿ 50(KeV)	X-rays	CO	QMS	$< 6 \times 10^{-5}$	76Br01	*3)
Al_2O_3 poly	R.G.	10 ∿ 50(KeV)	X-rays	CO	QMS	1×10^{-4}	76Br01	*3)
Al_2O_3 poly	R.G.	10 ∿ 50(KeV)	X-rays	CO	QMS	$< 6 \times 10^{-5}$	76Br01	*3)
SS 302	R.G.	10 ∿ 50(KeV)	X-rays	O_2	QMS	9×10^{-4}	76Br01	*3)
SS 302	R.G.	10 ∿ 50(KeV)	X-rays	O_2	QMS	5×10^{-4}	76Br01	*3)
Al_2O_3 poly	R.G.	10 ∿ 50(KeV)	X-rays	O_2	QMS	1×10^{-4}	76Br01	*3)
Al_2O_3 poly	R.G.	10 ∿ 50(KeV)	X-rays	O_2	QMS	$< 3 \times 10^{-5}$	76Br01	*3)
SS 302	R.G.	10 ∿ 50(KeV)	X-rays	CO_2	QMS	4×10^{-4}	76Br01	*3)
SS 302	R.G.	10 ∿ 50(KeV)	X-rays	CO_2	QMS	2×10^{-4}	76Br01	*3)
Al_2O_3 poly	R.G.	10 ∿ 50(KeV)	X-rays	CO_2	QMS	2×10^{-3}	76Br01	*3)
Al_2O_3 poly	R.G.	10 ∿ 50(KeV)	X-rays	CO_2	QMS	8×10^{-5}	76Br01	*3)
SS degreased	R.G.	10 ∿ 30(KeV)	X-rays	CO_2	QMS	4×10^{-4}	76Br02	*4)

Al-alloy	R.G.	?	γ -rays	H_2	*5)	$< 4.7 \times 10^{-3}$	68Ba01 *5)

*1) Refer to 72Pa01 and 79Mc02
*2) Refer to 73Fa01, Semicon. :semiconductor
*3) The tungsten bremsstrahlumg spectrum (electron voltage 50 KV)
No major impurities except for carbon was observed prior to irradiation.
SS: Stainless steel
*4) Mean photon energy 18 KeV
*5) Measurement of total pressure change

DATA LIST FOR PSD 4 --GAS DESORPTION FROM AL ALLOY USING SYNCHROTRON RADIATION--

Surface preparation	Desorbed species	Molecules per photon	Ref.	Remark
Cleaning in perchlorethylene vapour (Al-alloy chamber)	H_2	~ 1.0	82Ko02	*1)
	CO	$\sim 1.0 \times 10^{-1}$	82Ko02	*1)
	CO_2	$\sim 8.0 \times 10^{-1}$	82Ko02	*1)
	CH_4	$\sim 9.0 \times 10^{-2}$	82Ko02	*1)
Cleaning in toluene and drying (Al-alloy speciemen)	H_2	$2.2 \times 10^{-2} \sim 8.0 \times 10^{-5}$	84Mo02	*2)
	CO	$4.6 \times 10^{-3} \sim 2.2 \times 10^{-7}$	84Mo02	*2)
	CO_2	$2.8 \times 10^{-3} \sim 5.0 \times 10^{-7}$	84Mo02	*2)
A venting to air followed by pumpdown for about 1 week. (Al-alloy chamber)	H_2	$4.0 \times 10^{-1} \sim 1.0 \times 10^{-2}$	83Gr01	*3)
	CO	$2.7 \times 10^{-3} \sim 4.0 \times 10^{-4}$	83Gr01	*3)
	CO_2	$1.8 \times 10^{-2} \sim 4.0 \times 10^{-4}$	83Gr01	*3)
	CH_4	$1.2 \times 10^{-3} \sim 5.0 \times 10^{-6}$	83Gr01	*3)
After pumpdown from atmospheric pressure a chamber previously baked at 150°C for 20h. (Al-alloy chamber)	H_2	$5.0 \times 10^{-1} \sim 1.8 \times 10^{-2}$	83Gr01	*3)
	CO	$\sim 3.0 \times 10^{-2} \sim 1.3 \times 10^{-3}$	83Gr01	*3)
	CO_2	$7.0 \times 10^{-2} \sim 3.0 \times 10^{-3}$	83Gr01	*3)
	CH_4	$\sim 8.0 \times 10^{-3} \sim 1.8 \times 10^{-2}$	83Gr01	*3)
After venting a chamber to air followd by a 12h bakeout at 150°C	H_2	$2.0 \times 10^{-1} \sim 1.0 \times 10^{-2}$	83Gr01	*3)
	CO	$3.0 \times 10^{-2} \sim 1.8 \times 10^{-3}$	83Gr01	*3)
	CO_2	$3.5 \times 10^{-3} \sim 4.0 \times 10^{-4}$	83Gr01	*3)
	CH_4	$5.0 \times 10^{-4} \sim 1.0 \times 10^{-5}$	83Gr01	*3)

A 24h bakeout at 150°C	H_2	$\sim 5.0 \times 10^{-1}$	84Ko02	*1)
	CO	3.0×10^{-2}	84Ko02	*1)
	CO_2	$\sim 1.0 \times 10^{-1}$	84Ko02	*1)
	CH_4	1.0×10^{-4}	84Ko02	*1)
A Ar-gas discharge at 150°C	H_2	$\sim 1.0 \times 10^{-1}$	84Ko02	*1)
	CO	1.8×10^{-3}	84Ko02	*1)
	CO_2	$\sim 7.0 \times 10^{-3}$	84Ko02	*1)
	CH_4	1.0×10^{-3}	84Ko02	*1)
	Ar	$\sim 5.0 \times 10^{-4}$	84Ko02	*1)
A Ar-gas discharge at RT	H_2	1.0×10^{-3}	84Ko02	*1)
	CO	3.0×10^{-4}	84Ko02	*1)
	CO_2	1.5×10^{-4}	84Ko02	*1)
	CH_4	1.0×10^{-4}	84Ko02	*1)
	Ar	1.5×10^{-4}	84Ko02	*1)

*1) These measurements were performed at Large Electron and Positron Storage Ring(LEP) in CERN and these results were reported at the IX Intern.Conf.Solid Surfaces(1983 Madrid).

*2) Desorption yields depend on photon dose ($10^{17} \sim 10^{20}$ photons/cm^2).

*3) These measurements were performed at electron storage ring(DCI) in Orsay. Desorption yields depend on accumulated photons ($10^{17} \sim 10^{22}$ photon/meter).

6. Conclusions

Experimental data on IID and PSD were compiled and stored in a computer, from which graphs and tables are obtained at any time. They are by no means sufficient to respond to the request from practical use. For instance, there is a great lack of the data on desorption using hydrogen as projectile. Especially, the data on H - H or H - D desorption processes are needed. They are very important in fuel recycling as well as impurity influx. It is known that the impurities with higher atomic number will be in a variety of ionized or excited states and will lose energy by line and recombination radiations etc. Therefore, there is an increasing interest in the use of low-Z materials for first wall or for surface coatings. For lower Z materials, less data are available.

The functional dependences of IID on the various parameters have been discussed up to date. If these dependences are explained quantitaively, the importance of the desorption can be assessed in special situations such as controlled thermonuclear fusion reactors. In ESD and PSD, the primary photon and electron energy is the decisive parameter for a given adsorbate-substrate system. On the other hand, there are many important parameters in IID. They are divided into three groups. The first group is concerned with incident ions, i.e. incident energy, atomic mass and incident angle. The second and third are concerned with the substrate and the adsorbate, respectively. Many investigations have been carried out on the dependences on the parameters concerning incident ions. However, it is difficult to say that these dependences are satisfactorily understood. For instance, the energy dependence near the threshold energies is not clear because experiments at the lowest possible energies are very few for the adsorbate-substrate systems ever studied. Furthermore, we have little information about desorbed particles, i.e. charge or molecular states of desorbed particles, emission angle of desorbed particles etc. In other words, there is a great lack of measurements to shed insight into the correlation between the desorption processes and the surface structures of adsorbates.

Recent works on photon-stimulated desorption have provided an increased understanding of the desorption mechanisms and showed the technique to be a great potential to probe the electronic and atomic structures of surfaces. It is due to the simplicity of the excitation processes in PSD relative to ESD. In the present situation, many works on PSD are carried out in an attempt to understand the nature of the surface bonds. However, there are limitations on the type of chemical state which can be studied with desorption, since there are many chemical configurations which do not yield desorption.

Although there are many difficulties, futher measurements of desorption cross sections and yields are necessary for understanding the contributions to impurity production and recycling effects in thermonuclear fusion reactors.

Appendix

Judging from the compiled data, the energy dependence of desorption cross sections seems to have a common feature regardless of the incident ion species, i.e., the desorption cross section increases to a maximum beyond the threshold energy and falls off very slowly with increasing energy. It is assumed that the desorption cross section σ is given by

$$\sigma (E) = a F(x) \quad , \qquad \text{(i)}$$

where E is the incident energy, a a fitting parameter, and x a dimensionless parameter. The parameter x is equal to $(E - \delta)/c$, where δ shows a threshold energy and c is also a fitting parameter. For F(x), we have chosen the following function which has normalized maximum at x=b;

$$F (x) = (x/b)^b \exp(-x + b) \quad . \qquad \text{(ii)}$$

It follows that the desorption cross section has a maximum value a at $E= bc + \delta$.

In general, the threshold energies for desorption are much lower than the usual sputtering thresholds. They are equal to or at most a few times the surface binding energies of the adsorbate. In addition, the energy considered is much larger than the threshold energy. Therefore δ is assumed to be 0. Substituting eq. (ii) into eq. (i), the desorption cross section becomes

$$\sigma (E) = a (E/c)^b \; b^{-b} \exp(-E/c + b) \quad . \qquad \text{(iii)}$$

The paramerters, a, b and c, can be determined from the following procedure, i.e., the least - square method.

We have the compiled data in the form of N pairs of values (E_1 , σ_1), (E_2 , σ_2), ..., (E_n , σ_n). The differences between σ_i and $\sigma (E_i)$ squared are summed up, namely

$$\chi^2 = \sum_i^N (\sigma_i - \sigma(E_i))^2 \qquad \text{(iv)}$$

The search for the value a,b,c which give the minimum for χ^2 has been carried out by using the a CERN library program called MINUIT. The obtained parameters are shown in the subsequent Table A. The curves fitted with the experimental data are shown in Figs. (A) - (E). In Fig. (E), the value of 2.65×10^{-14} cm^2 at 900 eV is excluded from the least - square method.

Table A

adsorbate /solid	incident ion	a ($\times 10^{-14}$)	b	c
O_2/Cu(110)	Ar^+	7.096×10^{-1}	2.272	1.442×10^3
O_2/Ni(110)	Ar^+	2.349	1.056	1.096×10^4
	Ne^+	4.223×10^{-1}	1.938	3.728×10^3
	He^+	7.084×10^{-3}	3.741	2.180×10^2
CO/Ni(110)	He^+	7.065	1.141	9.753×10^3
N_2/Mo(100)	Xe^+	1.472×10^{-1}	7.091×10^{-1}	6.194×10^3
	Ar^+	7.655×10^{-2}	1.602×10^{-1}	2.033×10^4
S/Ni(110)	Ar^+	9.563	3.162	1.920×10^3
	He^+	3.032×10^{-1}	5.309×10^{-1}	5.168×10^4

The desorption cross section also varies with angle of incidence θ with respect to the normal to the surface. All the data avialable are found to have a maximum at about 65 ^{o}. To fit also those data, we used the following function:

$$\sigma (\theta) = d \ R(\cos\theta) + g \ S(\cos\theta) , \qquad (v)$$

where R(x) is a step function smoothed containing two parameters e and f denoting the position and the steepness of the rise. Function S(x) is a derivative of R(x). The explicit forms of these functions are,

$$R(x) = (1 + \exp((e-x)/f))^{-1} \qquad (vi)$$

$$S(x) = 4 \exp((e-x)/f) (1 + \exp((e-x)/f))^{-1} . \qquad (vii)$$

The parameters e and f are to be varied together with d and g in eq. (v) to fit the data. We have gone through the same procedure described above for the fitting. The obtained parameters are listed in Table B. The curves fitted together with experimental data shown in Figs. (F) - (I)

Table B

adsorbate /solid	incident ion and energy	d ($\times 10^{-14}$)	e ($\times 10^{-1}$)	f ($\times 10^{-1}$)	g ($\times 10^{-14}$)
O_2/Si(111)	He^+ (1 KeV)	1.007×10^{-2}	3.891	1.601	2.646×10^{-2}
S/Ni(111)	Ne^+ (1 KeV)	3.825×10^{-4}	4.975	2.229	2.995×10^{-1}

Table B continued

CO/Ni(111)	Ne^+ (0.7 KeV)	5.815×10^{-1}	3.602	5.016×10^{-1}	8.158×10^{-1}
D_2/SS 316	H_3^+ (1 KeV)	9.323×10^{-3}	2.879	7.318×10^{-1}	5.030×10^{-2}

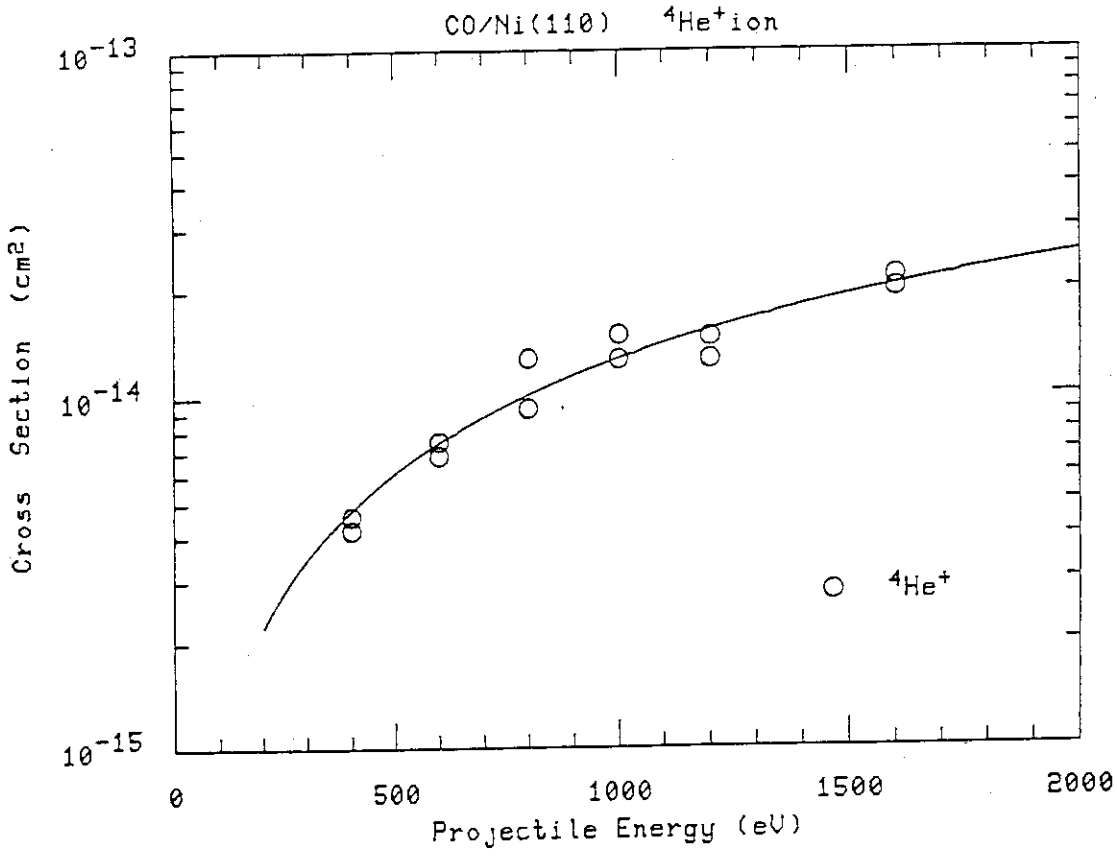

Fig. A Desorption cross section as a function of incident energy

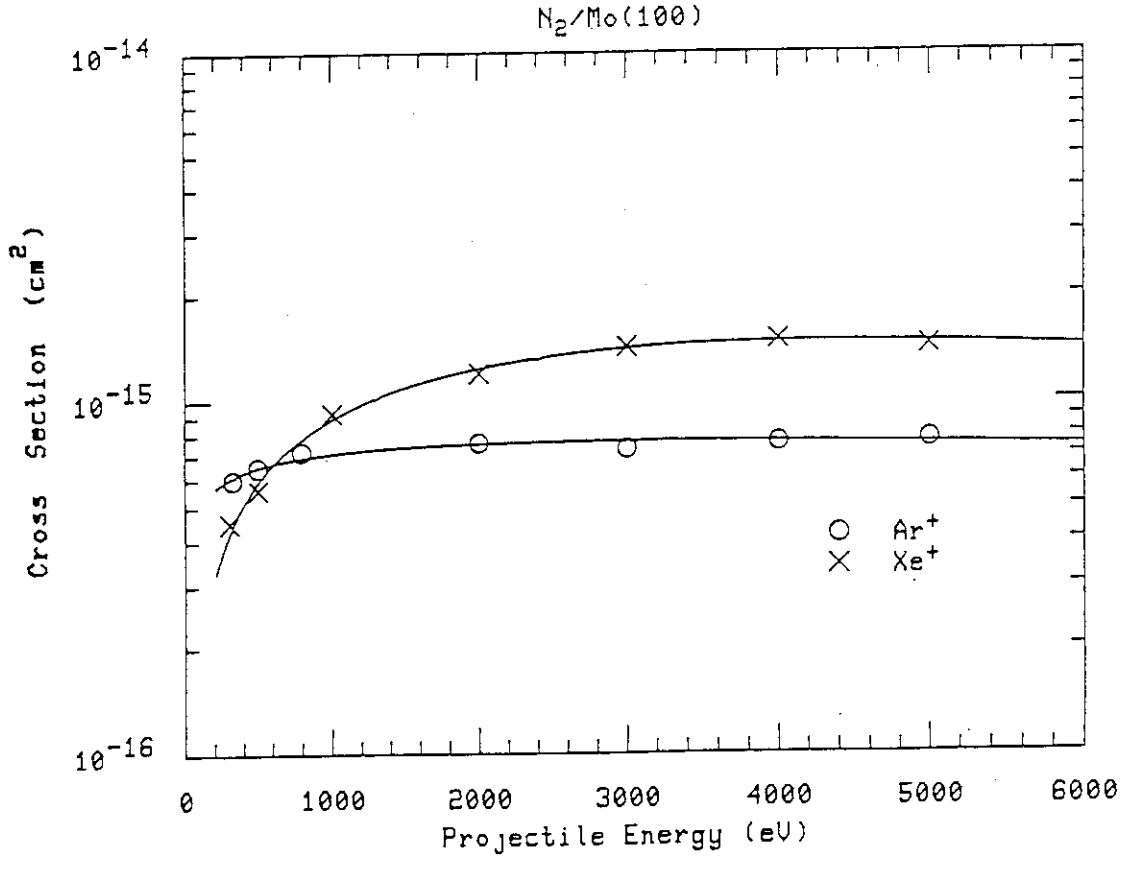

Fig. B Desorption cross section as a function of incident energy

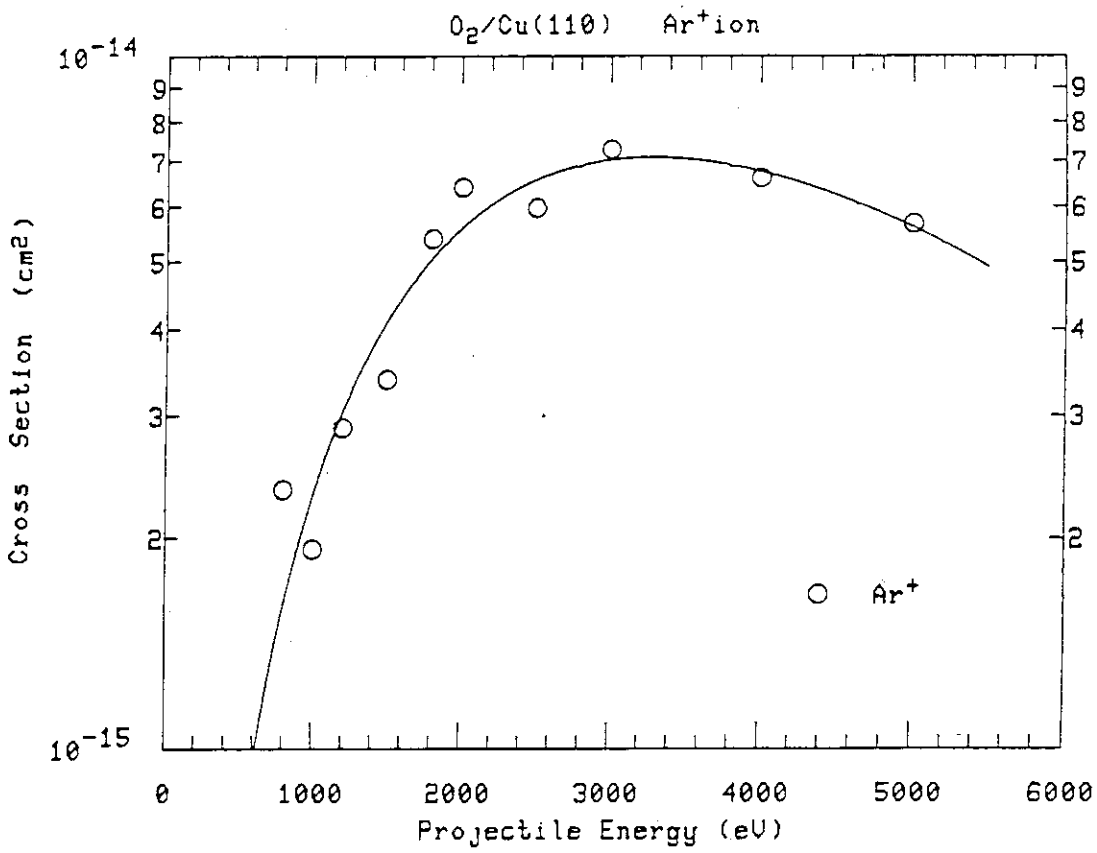

Fig. C Desorption cross section as a function of incident energy

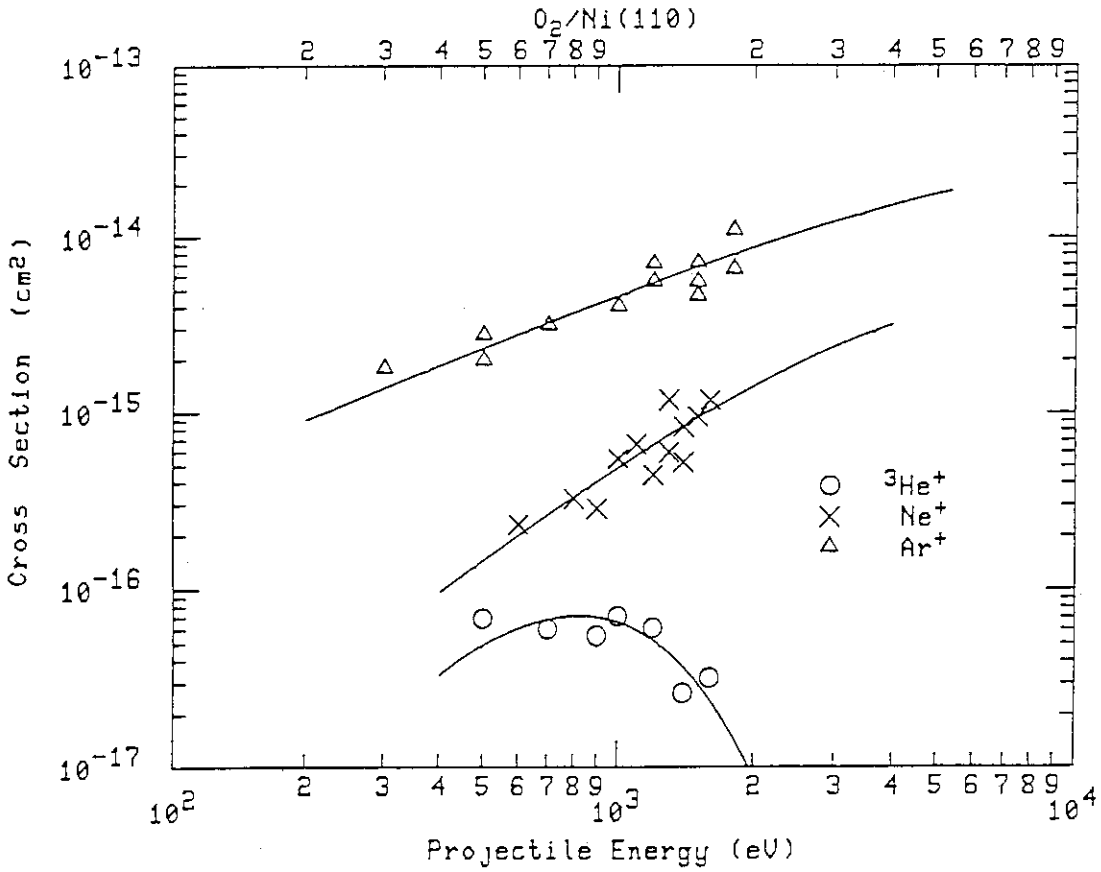

Fig. D Desorption cross section as a function of incident energy

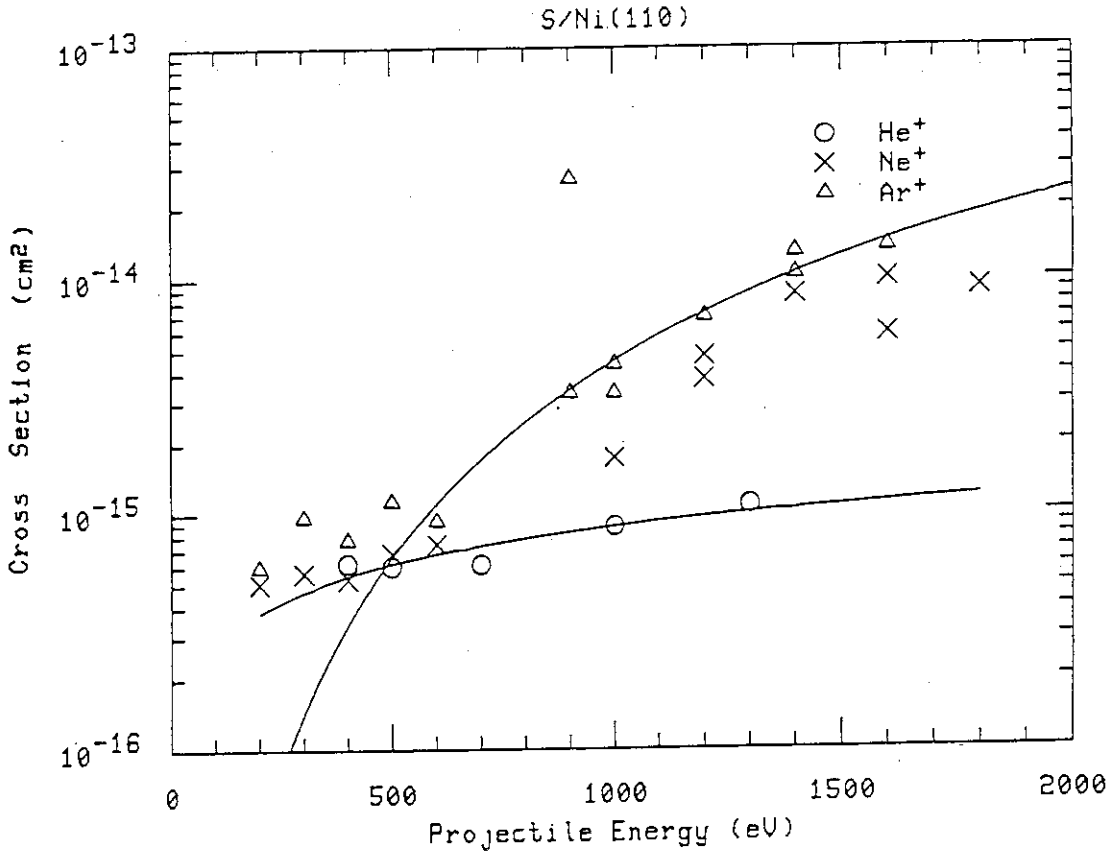

Fig. E Desorption cross section as a function of incident energy

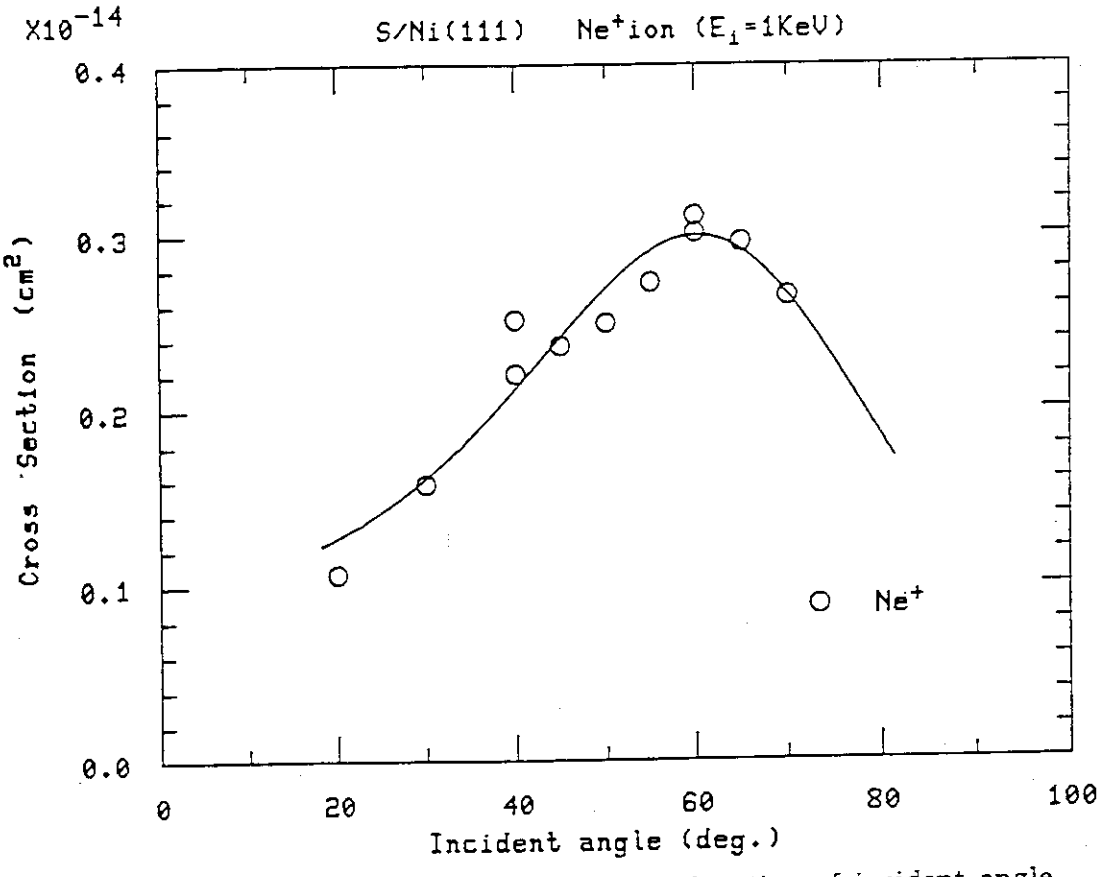

Fig. F Desorption cross section as a function of incident angle

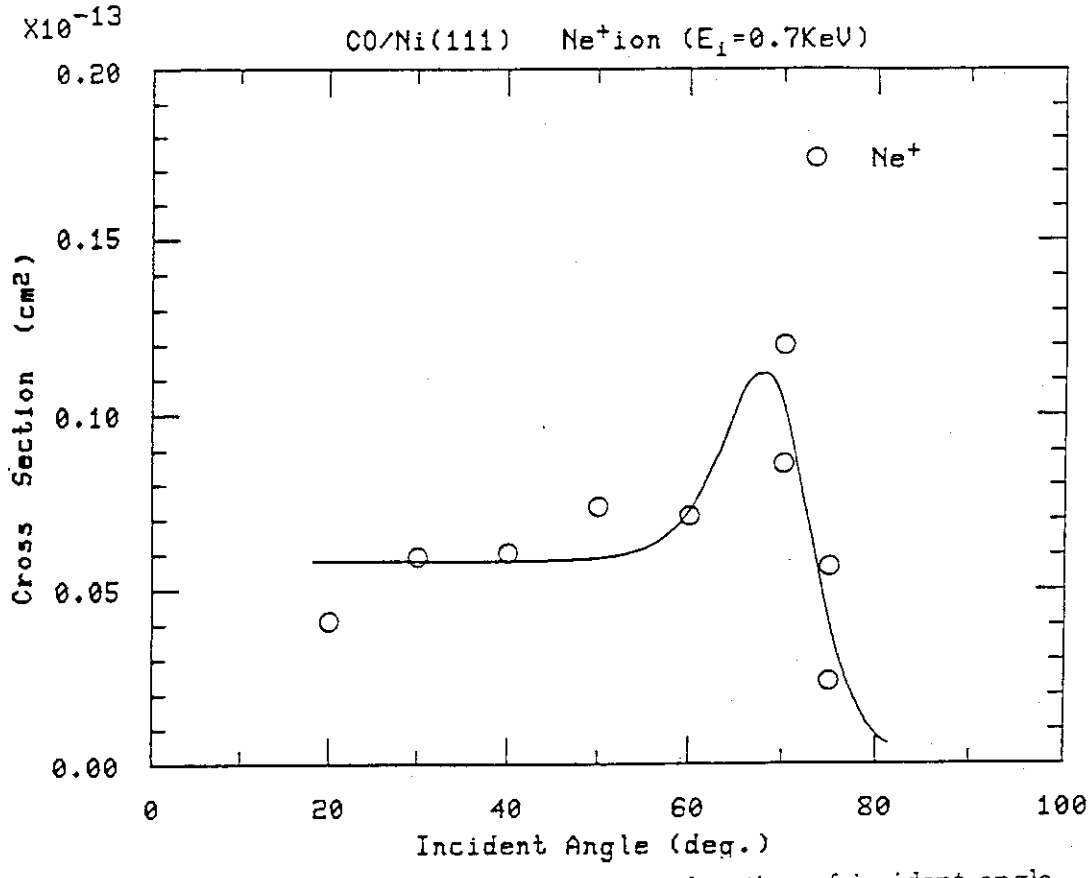

Fig. G Desorption cross section as a function of incident angle

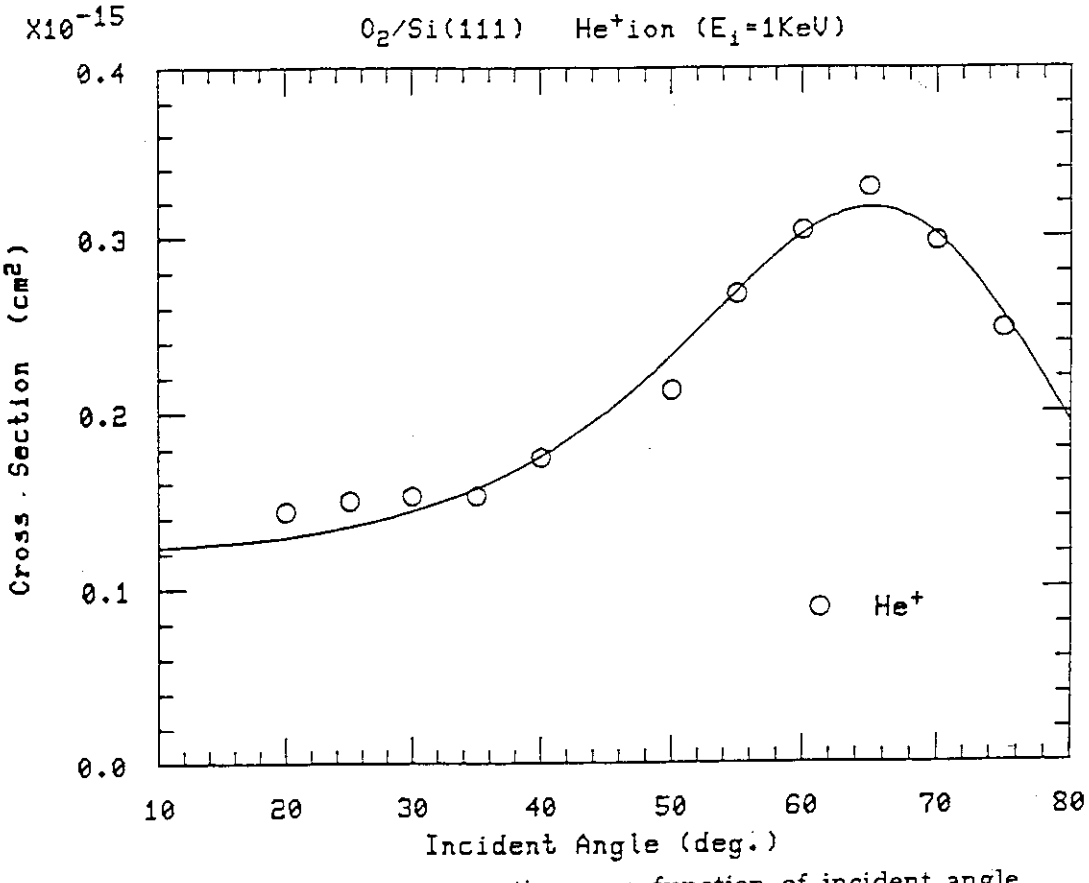

Fig. H Desorption cross section as a function of incident angle

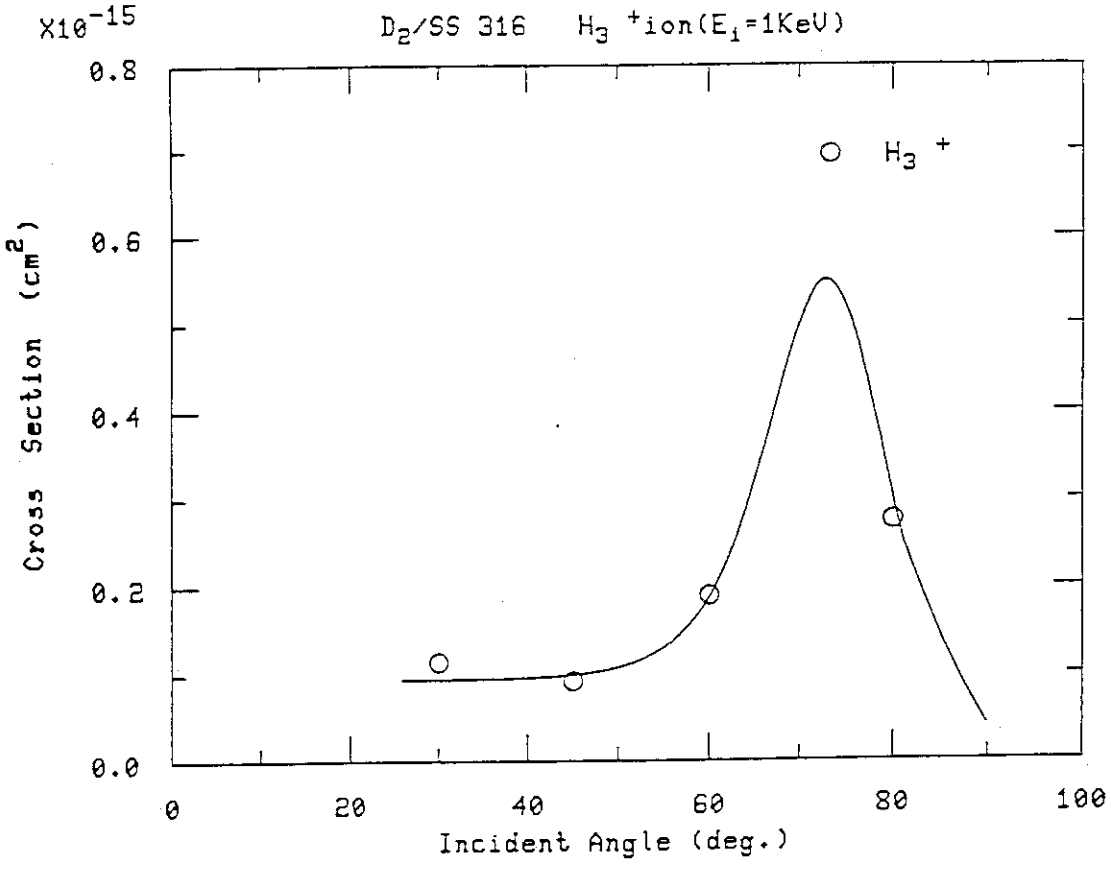

Fig. I Desorption cross section as a function of incident angle

1. Bibliography of Ion Impact Desorption

(A)

79Ac01 M. H. Achard, R. Calder and A. Mathewson, Vacuum 29, 53-65 (1979).
"The Effect of Bakeout Temperature on the Electron and Ion Induced Gases Desorption Coefficients of Some Technological Materials"

78Ak01 K. Akaishi, A. Miyahara and A. Sagara, J. Nucl. Mater. 76/77, 378-379 (1978).
"Low-enetgy Ion Scattering Study of Adsorbed Layers on Molybdenum Surface"

(B)

78Ba01 W. Bauer, J. Nucl. Mater. 76/77, 3-15 (1978).
"Surface Processes in Plasma Wall Interactions"

80Ba02 R. J. Bastasz, J. Nucl. Mater. 93/94, 830-833 (1980).
"Hydrogen Ion Impact Desorption of Sulfur from Stainless Steel"

81Ba03 R. J. Bastasz and L. G. Haggmark, J. Nucl. Mater. 103/104, 499-502 (1981).
"Ion Impact Desorption and Hydrogen Release"

82Ba04 R. J. Bastasz and L. G. Haggmark, J. Nucl. Matter. 111/112, 805-808 (1982).
"Hydrogen Ion Impact Desorption of Adsorbed Deuterium from Stainless Steel"

84Ba05 R. J. Bastasz, J. Vac. Sci. Technol. A 2, 638 (1984).

"Summary Abstract: Ion Impact Desorption Mechanisms-the Role of the Substrate"

75Be01 A. Benninghoven, Surf. Sci. 53, 596-625 (1975).
"Developments in Secondary Ion Mass Spectroscopy and Applications to Surface Studies"

78Be02 A. Benninghoven, K. H. Müller, M. Schemmer and P. Beckmann, Appl. Phys. 16, 367-373 (1978).
"SIMS and Flash Desorption Studies of Nickel Oxygen Interaction"

79Be03 A. Benninghoven, P. Beckmann, K. H. Müller and M. Schemmer, Surf. Sci. 89, 701-709 (1979).
"Investigation of Multi-Component Surface Reactions by SIMS: The Interaction between Hydrogen and Oxygen on Polycrystalline Nickel"

81Be04 A. Benninghoven, P. Beckmann, D. Greifendorf, K. H. Müller and M. Schemmer, Surf. Sci. 107, 148-164 (1981).
"Hydrogen Detection by Secondary Ion Mass Spectroscopy: Hydrogen on Polycrystalline Nickel"

82Bo01 S. Bourgeois and M. Perdereau, Surf. Sci. 117, 165-168 (1982).
"SIMS Study of the Interaction of Ni-O Surfaces with H_2 and H_2O"

82Br01 A. Brown and J. C. Vickerman, Surf. Sci. 117, 154-164 (1982).
"SIMS Studies of Adsorbate Structure. I. CO Adsorption on Ru(001), Ni(111) and Ni(100)"

(C)

74Ca01 R. Calder, Vacuum 24, 437-443 (1974).
"Ion Induced Gas Desorption Problems in the ISR"

82Cr01 J. H. Craing, Jr., Surf. Sci. 120, L412-416 (1982).
"Ion Induced Desorption of Oxygen from Platinum"

82Cr02 J. R. Creighton and J. M. White, Surf. Sci. 122, L648-652 (1982).
"SIMS and TDS Study of the Reaction of Water and Oxygen on Pt(111)"

84Cr03 J. H. Craig, Jr., Surf. Sci. 141, L291-294 (1984).
"Adsorption of Hydrogen and Carbon Monoxide on Nickel"

(D)

79De01 A. G. J. De Wit, R. P. N. Bronckers, Th. M. Hupkens and J. M. Fluit, Surf. Sci. 90, 676-687 (1979).
"Investigation of Oxygen Adsorption on Cu(110) by Low-Energy Ion Bombardment"

80Dy01 H. F. Dylla, J. Nucl. Mater. 93/94, 61-74 (1980).
"A Review of the Wall Problems and Conditioning Techniques for Tokamaks"

(E)

73Er01 S. K. Erents and G. M. McCracken, J. Appl. Phys. 44, 3139-3145 (1973).
"Desorption of Solid Hydrogen by Energetic Protons, Deuterons, and Electrons"

75Er02 S. K. Erents and G. H. McCracken, in The Atomic Collisions in Solids Vol.2, edited by S. Datz et al. (Plenum Press, New York, 1975), P625-634.
"Sputtering of Condensed Gases by Proton Bombardment"

(F)

80Fa01 G. Farrell and B. D. Eghawary, J. Nucl. Mater. 93/94, 834-838 (1980).
"Bombardment-Induced Desorption of CO Adsorbed on 304 Stainless Steel by Low Energy (75-100 eV) Light Active and Inert Gas Ions"

82Fo01 K. E. Foley and N. Winograd, Surf. Sci. 116, 1-12 (1982).
"A Static SIMS Study of the Chemisorption of CO on Ni(111)"

82Fo02 K. E. Foley and N. Winograd, Surf. Sci. 122, 541-555 (1982).
"Primary Beam Energy Effects on Secondary Ion Emission from Ni(001)c(2x2)-CO: Classical Dynamics Calculations and SIMS"

(H)

82Ha01 P. Hakansson, I. Kamensky and B. Sundquvist, Surf. Sci. 116, 302-312 (1982).
"Biomolecular Desorption Yields as a Function of the Angle of Incidence of Fast Heavy Ions"

78He01 W. Heiland, W. Englert and E. Taglauer, J. Vac. Sci. Technol. 15, 419-422 (1978).
"A Study of the Sorption of CO on W and Ni Single Crystal Surfaces by Ion Scattering"

78He02 W. Heliand and W. Taglauer, Symp. on Atomic and Surface Physics, Tirol (1978) 9-16.
"Surface Studies by Low Energy Ions"

77Hi01 N. Hilleret and R. Calder, in Proc. 7th Int. Vacuum Congr. and 3rd Int. Conf. Solid Surfaces 1977, edited by R. Dobrozemsky et al. (F. Berger & Söhne, Vienna, 1977), P227-230.
"Ion Desorption of Condensed Gases"

(L)

81Le01 K. O. Legg, R. Whaley and E. W. Thomas, Surf. Sci. 109, 11-19 (1981).
"An Inelastic Mechanism for Ion Induced Desorption of Oxygen from Titanium and Iron"

(M)

76Ma01 A. G. Mathewson, CERN Internal Report, CERN-ISR-VA/76-5 (1976).

77Ma02 A. G. Mathewson and M. H. Achard, in Proc. 7th Int. Vacuum Congr. and 3rd Int. Conf. Solid Sunfaces 1977, edited by R. Dobrozemsky et al. (F. Berger & Söhne, Vienna, 1977), P1217-1220.
"The Temperature Dependence of the Surface Composition and Electron and Ion Induced Gas Desorption Coefficients of Inconel 718 and 316L+N Stainless Steel"

78Ma03 A. G. Mathewson, Proc. 2nd Meeting on Ultra-High Vacuum

Techniques for Accelerators and Storage Rings, Tsukuba, March 27-28(1978) P89-132.
"Vacuum Problems of Storage Rings and Surface Treatment of Technological Materials"

78Ma04 R. J. MacDonald, W. Heiland and E. Taglauer, Appl. Phys. Lett. 33, 576-578 (1978).
"A Comparison of Surface Analysis Using Ion Scattering, Ion Produced Photons, and Secondary Ion Emission"

80Ma05 R. J. MacDonald, E. Taglauer and W. Heiland, Appl. Surf. Sci. 5, 197-211 (1980).
"The Effect of CO Adsorption on Ion and Photon Yields from Ion Bombarded Metal Surfaces"

74Mc01 G. M. McCracken, Vacuum 24, 463-467 (1974).
"Desorption of Adsorbed and Condensed Gases on Metals by Deuterons"

79Mc02 G. M. McCracken and P. E. Stott, Nucl. Fusion 19, 889-981 (1979).
"Plasma-Surface Interactions in Tokamaks"

83Mö01 J. Möller, M. Neumann and W. Heiland, Physica Scripta T6, 104-105 (1983).
"Electron Stimulated Desorption by Low Energy Ion Impact"

(N)

84Ne01 B. Nees, E. Nieschler, N. Bischof, H. Fröhlich, K. Riemer W. Tiereth and H. Voit, Surf. Sci. 145, 197-206 (1984).
"Fast Heavy Ion Induced Desorption : Dependence of the Yield on the Primary Ion Energy"

84Ni01 E. Nieschler, B. Ness, N. Bischof, H. Fröhlich, W. Tiereth and H. Voit, Surf. Sci. 145, 294-300 (1984).
"Fast Heavy Ion Induced Desorption : Dependance of the Yield on the Angle of Incidence of the Primary Ions"

(O)

80On01 J. Onsgaard, W. Heiland and E. Taglauer, Surf. Sci. 99, 112-120 (1980).
"Adsorption and Desorption of Oxygen and Carbon Monoxide on the Si(111) Surface Studied by Ion Scattering Spectroscopy"

77Or01 L. Oren and R. J. Taylor, Nucl. Fusion 17, 1143-1151 (1977).
"Trapping and Removal of Oxygen in Tokamaks"

(P)

81Pe01 J. L. Pena, Surf. Sci. 109, L550-554 (1981).
"Auger Electron Spectroscopy (AES) Studies of Argon Ion Induced Desorption of Carbon from Tantalum"

81Pe02 J. L. Pena, J. W. Dieball and D. Lichtman, J. Vac. Sci. Technol. 18, 566-569 (1981).
"Argon Ion Impact Desorption Cross Sections of Chlorine and Carbon from Nickel"

(R)

77Ra01 E. O. Rausch, M. W. Murray, H. Inouye and E. W. Thomas, J. Appl. Phys. 48, 4347-4352 (1977).
"The Influence of Oxygen on Backscattering of Excited H when

H_1^+, H_2^+ and H_3^+ ions at 4-30 KeV Energy are Incident on Molybdenum"

78Ra02 E. O. Rausch and E. W. Thomas, Nucl. Instr. Meth. 149, 511-515 (1978).
"Backscattering of Excited Hydrogen from Mo in the Presence of Oxygen"

(S)

79Sa01 A. Sagara, K. Akaishi and A. Miyahara, J. Nucl. Mater. 85/86, 1173-1177 (1979).
"ISS observations of Molybdenum Samples as Limiter and First Wall Materials after Various Preparation Methods"

80Sa02 A. Sagara, K. Akaishi, K. Kamada and A. Miyahara, J. Nucl. Mater. 93/94, 847-852 (1980).
"ISS Observations of Ti Film on Mo Substrate"

81Sa03 A. Sagara, K. Akaishi, K. Kamada and A. Miyahara, J. Nucl. Mater. 103/104, 357-362 (1981).
"ISS studies on Sputtering of Chemisorbed Gases by Low-Energy Ions"

82Sa04 A. Sagara and K. Kamada, J. Nucl. Mater. 111/112, 812-815 (1982).
"Compilation and Evaluation of Ion Impact Desorption Cross-Section"

84Su01 S. Sukenobu and Y. Gomay, J. Nucl. Mater. 128/129, 775-778 (1984).
"Ion Impact Desorption of Oxygen Adsorbed on TiC Coating"

(T)

75Ta01 E. Taglauer, W. Melchior, F. Schuster and W. Heiland, J. Phys. E 8, 768-772 (1975).
"SORBAS : Eine Apparature Zur Untersuchung der Oberflächenstreuung Von Ionen in Energiebereich 100-2000 ev" (In German)

76Ta02 E. Taglauer, W. Beitat, G. Marin and W. Heiland, J. Nucl. Mater. 63, 193-198 (1976).
"Sputtering of Adsorbed Layers by Ion Bombardment"

77Ta03 E. Taglauer, G. Marin and W. Heilalnd, Proc. Intern. Symp. on Plasma Wall Interaction, Jülich 1976 (Pergamon Press, Oxford, 1977), P301-307.
"Desorption of Surface Contaminants by Low Energy Particle Impact"

77Ta04 E. Taglauer, G. Marin and W. Heiland, Appl. Phys. 13, 47-49 (1977).
"Desorption by Ion Scattering"

77Ta05 E. Taglauer, G. Marin, W. Heiland and W. Beitat, Surf. Sci. 63, 507-513 (1977).
"Study of the Sputtering of Adsorbates by Low Energy Ions (O on Ni)"

78Ta06 E. Taglauer, W. Beitat and W. Heiland, Nucl. Instr. Meth. 149, 605-608 (1978).
"Investigation of Ion Impact Desorption of Atoms and Molecules by Low Energy Ion Scattering (ISS)"

78Ta07 E. Taglauer and W. Heiland, J. Nucl. Mater. 76/77, 328-311 (1978).

"Ion Impact Desorption Cross Sections of Hydrogen and Oxygen from Metals by Light Ion Bombardment"

79Ta08 E. Taglauer, W. Heiland and W. Beitat, Surf. Sci. 89, 710-717 (1979).
"The Influence of Adsorption Energies on Ion Impact Desorption of Surface Layers"

79Ta09 E. Taglauer, W. Heiland and R. J. MacDonald, Surf. Sci. 90, 661-675 (1979).
"The Study of Sputtering Effects in Oxides and Metal-Adsorbed-Gas Systems Using Combined Analytical Techniques"

80Ta10 E. Taglauer and W. Heilalnd, J. Nucl. Mater. 93/94, 823-829 (1980).
"Ion-Induced Desorption of Adsorption Layers on Annealed and Prebombarded Surfaces"

80Ta11 E. Taglauer, W. Heiland and J. Onsgaard, Nucl. Instr. Meth. 168, 571-575 (1980).
"Ion Beam Induced Desorption of Surface Layers"

84Ta12 E. Taglauer, Nucl. Fusion, Special Issue, "Data Compendium for Plasma-Surface Interactions" edited by R.A. Langley et al. (IAEA, Vienna 1984), P43-54.
"Desorption"

80Ts01 H. Tsuchidate, K. Akaishi and A. Miyahara, IPP Nagoya Univ. Annual Rev. (1980), P132-133.
"Ion Impact Desorption of Oxygen from Molybdenum Surface"

(U)

82Un01 S. E. Unger, R. G. Cooks, R. J. Steinmetz and W. N. Deglas, Surf. Sci. 116, L211-217 (1982).
"Molecular SIMS at Surfaces : Thiophene on Silver"

(V)

77Va01 J. A. Van den Berg, D. C. Armour and L. K. Verheij, The Intern. Conf. on Low-energy Ion Beams, Univ. of Salford (The Institute of Physics, Bristol and London, 1977), P298-304.
"A 2-100 KeV UHV Ion Impact Spectrometer for Ion Solid Interaction Studies"

(W)

71Wi01 H. F. Winters, J. Vac. Sci. Technol. 8, 17-21 (1971).
"Sputtering of Chemisorbed Nitrogen with Ar^+"

74Wi02 H. F. Winters and P. Sigmund, J. Appl. Phys. 45, 4760-4766 (1974).
"Sputtering of Chemisorbed Gas (Nitrogen on Tungsten) by Low Enedrgy Ions"

78Wi03 H. Windawi and J. R. Katzer, Surf. Sci. 75, L76-765 (1978).
"H^+ Ion Induced Desorption of Sulfur Adsorbed on Polycrystalline Ni Surface"

81Wi04 K. L. Wilson, J. Nucl. Mater. 103/104, 453-464 (1981).
"Hydrogen Recycling Properties of Stainless Steels"

82Wi05 H. F. Winters, J. Vac. Sci. Techonl. 20, 493-497 (1982).
"Mass Effect in the Physical Sputtering of Multi Component Materials"

2. Bibliography of Photon Stimulated Desorption

(A)

65Ad01 R. O. Adams and E. E. Donaldson, J. Chem. Phys. 42, 770-774 (1965).
"Photodesorption"

80An01 P. R. Antoniewicz, Phys. Rev. B 21, 3811-3815 (1980).
"Model for Electron and Photon-Stimulated Desorption"

(B)

68Ba01 E. Baltacis, R. Dobrozemsky and W. Kubischta, Proc. Int. Vac. Congr. (1968) P767.

71Ba02 S. Baidyaroy, W. R. Bottoms and P. Mark, Surf. Sci. 28, 517-524 (1971).
"Photodesorption from CdS"

80Bi01 A. Bianconi, Appl. Surf. Sci. 6, 392-418 (1980).
"Surface X-ray Absorption Spectroscopy: Surface EXAFS and Surface XANES"

76Br01 S. Brumback and M. Kaminsky, J. Appl. Phys. 47, 2844-2849 (1976).
"Gas Release from Al_2O_3 and Stainless-Steel Surfaces under X-ray Irradiation"

76Br02 S. Brumbach and M. Kaminsky, Adv. Chem. Ser. 158, 183-199 (1976).
"Gas Release from Surfaces under X-ray Impact : Photodesorption, Photocatalysis"

(C)

80Ca01 J. C. Campuzano and D. A. King, J. Phys. C 13, L565-569 (1980).
"Photon and Electron Stimulated Desorption Ion Energy and Angular Distribution for O^+ from W(001)"

80Ce01 F. G. Celii, M. P. Casassa and K. C. Janda, Surf. Sci. 141, 169-190 (1980).
"Photodesorption of Weakly Bound Molecules"

82Ch01 T. J. Chuang and H. Seki, Phys. Rev. Lett. 49, 382-386 (1982).
"Resonanthy Stimulated Desorption of Phyridine from Silver Surfaces by Polarized Infrared Laser Radiation"

82Ch02 T. J. Chuang, J. Chem. Phys. 76, 3829-3829 (1982).
"Infrared Laser Stimulated Desorption of Pyridine from KCl Surfaces"

76Co01 S. M. Cox and D. Lichtman, Surf. Sci. 54, 675-678 (1976).
"Photodesorption from TiO_2"

(D)

73De01 Y. De Ribaupierre, Surf. Sci. 34, 732-738 (1973).
"Thermodésorption et Photodesorption du Potassium Adsorbé sur du Cuivre"
(In French)

74Do01 R. Dobrozemsky, Nucl. Instr. Meth. 118, 1-37 (1974).
"Production of A Clean Neutron Gas for Decay and Scattering Experiments"

76Dr01 M. J. Drinkwine, Y. Shapira and D. Lichtman, Adv. Chem.

Ser. 158, 171-182 (1976).
"Electron- and Photon-Induced Desorption"

(F)

73Fa01 G. W. Fabel, S. M. Cox and D. Lichtman, Surf. Sci. 40, 571-582 (1973).
"Photodesorption from 304 Stainless Steel"

65Fi01 G. E. Fischer and R. A. Mack, J. Vac. Sci. Technol. 2, 123-130 (1965).
"Vacuum Design Problems of High Current Electron Storage Rings"

77Fr01 D. Franchy and D. Menzel, in Proc. 7th Int. Vacuum Congr. and 3rd Int. Conf. Solid Surfaces 1977, edited by R. Dobrozemsky et al. (F. Berger & Söhne, Vienna, 1977), P1217-1220.
"Photodesorption at High Photon Energies"

79Fr02 R. Franchy and D. Menzel, Phys. Rev. Lett. 43, 865-867 (1979).
"Adsorbate Core Ionization as Primary Process in Electron- and Photon-Stimulated Desorption from Metal Surfaces"

(G)

77Ga01 P. Gauthier, M. Babout and C. Guittard, in Proc. 7th Int. Vacuum Congr, and 3rd Int. Corf. Solid Surfaces 1977, edited by R. Dobrozemsky et al. (F. Berger & Söhne, Vienna, 1977), P1213-1215.
"Laser Desorption of Surfaces in Ultrahighvacuum"

78Ga02 P. Gauthier, M. Babout and C. Guittard, Phys. Stat. Sol.

(a) 48, 459-464 (1978).
"Laser Induced Desorption Studied with Mirror Electron Microscopy"

71Ge01 P. Genequand, Surf. Sci. 25, 643-646 (1971).
"Photodesorption"

75Ge02 J. I. Gersten, R. Janow and N. Tzoar, Phys. Rev. B 11, 1267-1272 (1975).
"Theory of Photodesorption"

83Gr01 O. Gröbner, A. G. Mathewson, H. Störi, P. Strubin and R. Souchet, Vacuum 33, 397-406 (1983).
"Studies of Photon Induceed Gas Desorption Using Synchrotron Radiation"

(H)

81Ha01 D. M. Hanson, R. Stockbauer and T. E. Madey, Phys. Rev. B 24, 5513-5521 (1981).
"Photo-Stimulated Desorption and Other Spectroscopic Studies of the Interaction of Oxygen with a Titanium (001) Surface"

82He01 J. Heibeberg, H. Stein and E. Riehl, Phys. Rev. Lett. 49, 666-669 (1982).
"Resonance Rate and Quantum Yield of Infrared-Laser-Induced Desorption by Multiquantum Vibrational Excitation of the Adsorbate CH_3F on NaCl"

83He02 J. Heidberg, H. Stein and E. Riehl, Surf. Sci. 126, 183-191 (1983).
"Infrared-Laser-Induced Desorption by Resonant Multiphoton Excitation of Adsorbate Vibration in CH_3F-NaCl at Different Coverages"

(J)

81Ja01 R. Jaeger, J. Feldhaus, J. Haase, J. Stöhr, Z. Haussain, D. Menzel and D. Norman, Phys. Rev. Lett. 45, 1870-1873 (1980).
"Surface Extended-X-Ray-Adsorption Fine Structure by Means of Photn-Stimulated Ion Desorption: O on Mo(100)"

81Ja02 R. Jaeger, J. Stöhr, R. Treichler and K. Baberschke, Phys. Rev. Lett. 47, 1300-1304 (1981).
"Photo-Stimulated Desorption due to Multielectron Excitations in Chemisorbed Moleueles: CO on Ni(100)"

81Ja03 R. Jager, J. Stöhr, J. Feldhaus, S. Brennan and D. Menzel, Phys. Rev. B 23, 2102-2110 (1981).
"Photon-Stimulated Desorption Following Deep Core-Level Excitation: O on Mo(100)"

82Ja04 R. Jaeger, R. Treichler and J. Stöhr, Surf. Sci. 117, 533-548 (1982).
"Evidence for Multi-Electron Excitations in Photon Stimulated Ion Desorption: CO and NO on Ni(100)"

83Ja05 R. Jaeger, J. Stöhr and T. Kendelewicz, Phys. Rev. B 28, 1145-1147 (1983).
"Ion Desorption from Surfaces Following Photon Excitation of Core Electrons in the Bulk"

83Je01 D. R. Jennison and D. Emin, J. Vac. Sci. Technol. A 1, 1154-1156 (1983).
"Localization of Surface Excitations and Stimulated Desorption"

(K)

84Ka01 H. Kanzaki and T. Mori, Phys. Rev. B 29, 3573-3585 (1984).

"Photon-Stimulated Desorption of Neutrals from Silver and Alkali Halides"

84Ke01 J. A. Kelber, R. R. Daniels, M. Turowski, G. Morgaritondo N. H. Tolk and J. S. Kraus, Phys. Rev. B 30, 4748-4752 (1984).
"Photon-Stimulated Desorption of Solid Neopentane"

79Kn01 M. L. Knotek, V. O. Jones and V. Rehn, Phys. Rev. Lett. 43, 300-303 (1979).
"Photon-Stimulated Desorption of Ions"

81Kn02 M. L. Knotek, V. O. Jones and V. Rehn, Surf. Sci. 102, 566-577 (1981).
"Photon-Stimulated Desorption by Core Level Excitation: Density of States and Extended Fine Structure"

82Kn03 M. L. Knotek, G. M. Loubriel, R. H. Stulen, C. E. Parks, B. E. Koel and Z. Hussain, Phys. Rev. B 26, 2292-2295 (1982).
"Hydrogen Surface Segregation on Si(111) by Photon-Stimulated Desorption at the Si K Edge"

83Kn04 M. L. Knotek, Physica Scripta T6, 94-103 (1983).
"Surface Chemical Information from Electron-and Photon-Stimulated Desorption"

83Kn05 M. L. Knotek, R. H. Stulen, G. M. Loubriel, V. Rehn and R. A. Rosenberg, Surf. Sci. 133, 291-304 (1983).
"Photon-Stimulated Desorption of H^+ and F^+ from BeO, Al_2O_3 and SiO_2: Comparison of Near Edge Structure to Photoelectron Yield"

82Ko01 B. E. Koel, G. M. Lonbriel, M. L. Knotek, R. H. Stulen, R. A. Rosenberg and C. C. Parks, Phys. Rev. B 25, 5551-5554

(1982).
"Resonant Photon-Stimulated Desorption of Ions from Oxidized Cerium"

84Ko02 M. Kobayashi, J. Vac. Soc. Japan 27, 255-266 (1984).
"Photon Stimulated Desorption and it Related Phenomena"
(In Japanese)

72Kr01 P. Kronauer and D. Menzel, in The Adsorption-Desorption Phenomena, edited by F. Ricca (Academic Press, London, 1972), P313.
"Photodesorption of Carbon Monoxide from W"

81Kr02 H. J. Kreuzer and D. N. Lowy, Chem. Phys. Lett. 78, 50-53 (1981).
"Photodesorption of Diatomic Molecules by Laser Molecular Vibrational Coupling"

(L)

61La01 W. J. Lange and H. Riemersma, Trans. Am. Vacuum Symp. 8, 167 (1961). (Trans. Am. Vacuum Soc. Pergamon Press (1962) P167)
"Desorption of Gases by Photons"

65La02 W. J. Lange, J. Vac. Sci. Technol. 2, 74-79 (1965).
"Photodesorption of Carbon Monoxide"

69Li01 A. A. Lisachenko and F. I. Vilesov, Zh. Tekh. Fiz. 39, 590-592 (1969) (Sov. Phys. Tech. Phys. 14, 442-444 (1969)).
"Photodesorption of OH Radicals from a ZnO Surface Containing Adsorbed Water"

74Li02 D. Lichtman, J. Nucl. Mater. 53, 285-288 (1974).

"Electron-and Photon-Induced Desorption"

76Li03 D. Lichtman and Y. Shapira, J. Nucl. Mater. 63, 184-187 (1976).
"The Role of Carbon in Photodesorption"

77Li04 D. Lichtman and T. Lin, in The Proc. 7th Int. Vacuum Congr. and 3rd Int. Conf. Solid Surfaces 1977, edited by R. Dobrozemsky et al. (F. Berger & Söhne, Vienna, 1977), P1277-1280.
"Photodesorption from Niobium Surfaces"

78Li05 D. Lichtman and Y. Shapira, CRC Crit. Rev. Solid State Mater. Sci. 8, 93-118 (1978).
"Photodesorption"

79Li06 D. Lichtman, Surf. Sci. 90, 579-587 (1979).
"Mechanisms of Desorption due to Electrons or Photons"

83Lo01 G. Loubriel, M. L. Knotek, R. H. Stuler, B. E. Koel and C. C. Parks, J. Vac. Sci. Technol. A 1, 1145-1148 (1983).
"Photon-and Electron-Stimulated Desorption from Rare Earth Oxides"

(M)

80Ma01 T. E. Madey, R. Stockbauer, J. F. van der Veen and D. E. Eastman, Phys. Rev. Lett. 45, 187-190 (1980).
"Angle-Resolved Photon-Stimulated Desorption of Oxygen Ions from a W(111) Surface"

81Ma02 T. E. Madey, R. Stockbauer, S. A. Flodström, J. F. van der Veen, F. J. Himpsel and D. E. Eastman, Phys. Rev. B 23, 6847-6850 (1981).

"Photon-Stimulated Desorption from Covalently Bonded Species: CO Adsorbed on Ru(001)"

73Mc01 J. W. McAllister and J. M. White, J. Chem. Phys. 58, 1496-1504 (1973).
"Photodesorption of Carbon Monoxide from Polycrystalline Nickel"

79Mc02 G. M. McCracken and P. E. Stott, Nucl. Fusion 19, 889-981 (1979).
"Plasma-Surface Interactions in Tokamaks"

58Me01 D. B. Medved, J. Chem. Phys. 28, 870-873 (1958).
"Photodesorption in Zinc Oxide Semiconductor"

75Me02 D. Menzel, Interactions on Metal Surfaces, (Springer-Verlag Berlin 1975) P102-142.
"Desorption Phenomena"

82Me03 D. Menzel, J. Vac. Sci. Technol. 20, 538-543 (1982).
"Recent Developments in Electron and Photon Stimulated Desorption"

82Me04 C. F. Melius, R. H. Stulen and J. O. Noell, Phys. Rev. Lett. 48, 1429-1432 (1982).
"Mechanism of Near-Threshold Stimulated Desorption of Protons from Transition-Metal Surfaces"

64Mo01 H. Moesta, Surf. Sci. 2, 267-276 (1964).
"Photo-Generation of Ions from Atoms in the Adsorbed State"

84Mo02 T. Momose, O. Gröbner, G. Horikoshi, H. Ishimaru, K. Kanazawa, M. Kobayashi, H. Mizuno, K. Narushima and H. Watanabe, J. Vac. Soc. Japan 27, 452-456 (1984).

"Gas Desorption from an Aluminium Alloy Exposed to Synchrotron Radiation" (In Japanese)

(N)

82Ma01 T. Nakayama, H. Ichikawa and N. Itoh, Surf. Sci. 123, L693-697 (1982).
"Non-Linear Photo-Induced Desorption of GaP"

(P)

72Pa01 J. Paigne, J. Chim. Phys. (France) 69, 1-8 (1972).
"Photodesorption of CO Adsorbed on a Ni(110) Monocrystal" (In French)

71Pe01 J. Peavey and D. Lichtman, Surf. Sci. 27, 649-652 (1971).
"Photon Indeed Desorption Using Synchrotron Radiation"

(R)

82Ra01 D. E. Ramaker, C. T. White and J. S. Murday, Phys Lett. 89A, 211-214 (1982).
"On Auger Induced Decomposition/Desorption of Covalent and Ionic Systems"

83Ra02 D. E. Ramaker, J. Vac. Sci. Technol. A 1, 1137-1144 (1983).
"Covalent Interaction Effects in Electron/Photon Stimulated Desorption"

83Ra03 D. E. Ramaker, J. Chem. Phys. 78, 2998-3013 (1983).
"Comparison of Photon Stimulated Dissociation of Gas Phase and Chemisorbed CO"

68Re01 P. A. Redhead, J. P. Hobson and E. V. Kornelson, The

Physical Basis of Ultra-High Vacuum (Chapman and Hall, London, 1968), P170.

81Ro01 R. A. Rosenberg, V. Rehn, V. O. Jones, A. K. Green, C. C. Parks, G. Loubriel and R. H. Stulen, Chem. Phys. Lett. 80, 488-494 (1981).
"The Photodissociative Ionization of Amorphous Ice"

83Ro02 R. A. Rosemberg, V. Rehn, A. K. Green, P. R. LaRoe and C. C. Parks, Phys. Rev. Lett. 51, 915-918 (1983).
"Electron Correlation and Hole Localization in Photon-Stimulated Ion Desorption"

73Ry01 V. K. Ryabuchuck, L. L. Basov, A. A. Lisachenko and F. I. Vilesov, Zh. Tekh. Fiz. 43, 2148-2152 (1973) (Sov. Phys. Tech. Phys., 18, 1349-1351 (1974)).
"Time of Flight Determination of the Kinetic Energy of Photodesorption Products (the NO/Al_2O_3 system)"

(S)

84Sa01 H. Sambe, M. Yousif and D. E. Ramaker, J. Vac. Sci. Technol. A 2, 1011-1012 (1984).
"Summary Abstract : Photon-Stimulated Ion Desorption from Condensed CO and N_2"

82Se01 H. Seki and T. J. Chuang, Solid State Commun. 44, 473-475 (1982).
"The Detection by SERS of Resonantly Excited Desorption of Pyridine from Silver Island Films by Laser Absorption"

75Sh01 Y. Shapira, S. M. Cox and D. Lichtman, Surf. Sci. 50, 503-514 (1975).
"Photodesorption from Powdered Zinc Oxide"

76Sh02 Y. Shapira, S. M. Cox and D. Lichtman, Surf. Sci. 54, 43-59 (1976).
"Chemisorption, Photodesorption and Conductivity Measurements on ZnO Surfaces"

77Sh03 Y. Shapira, R. B. McQuisten and D. Lichtman, Phys. Rev. B 15, 2163-2169 (1977).
"Relationship between Photodesorption and Surfaces Conductivity in ZnO"

82St01 R. H. Stulen, T. E. Felter, R. A. Rosenberg, M. L. Knotek, G. Loubriel and C. C. Parks, Phys. Rev. B 25, 6530-6533 (1982).
"Direct Correlation between Angle-Resolved Photoemission and Photon-Stimulated Desorption : Hydrogen on Pd(100)"

82St02 R. Stockbauer, D. M. Hanson, S. A. Flodströn and T. E. Madey, Phys. Rev. B 26, 1885-1892 (1982).
"Photon-Stimulated Desorption and Ultraviolent Photoemission Spectroscopic Study of the Interaction of H_2O with a Ti(001) Surface"

84St03 R. Stockbauer, D. E. Ramaker, E. Bertel, R. L. Kurtz and T. E. Madey, J. Vac. Sci. Techonol. A 2, 1053-1054 (1984).
"Summary Abstract : Mechanisms for Photon Stimulated Desorption of O^+ from Cr(110)"

(V)

80Va01 J. F. Van der Veen, F. J. Himpsel, D. E. Eastman and P. Heimann, Solid State Commun. 36, 99-104 (1980).
"Angular Dependent Photon-Stimulated Desorption of Ions from a V_2O_5(010) Surface"

81Va02 N. Van Hieu and D. Lichtman, Surf. Sci. 103, 535-541 (1981).
"Bandgap Radiation Induced Photodesorption from Titanium Oxides Surfaces"

(W)

82We01 G. Weder and H. Ruhmann, Surf. Sci. 121, 464-486 (1982).
"Laser Induced Thermal Desorption of Carbon Monoxide from Fe(110) Surfaces"

80Wo01 D. P. Woodruff, M. M. Traum, H. H. Farrell, N. V. Smith, P. D. Johnson, D. A. King, R. L. Benbow and Z. Hurych, Phys. Rev. B 21, 5642-5645 (1980).
"Photon-and Electron-Stimulated Desorption from a Metal Surface"

81Wo02 D. P. Woodruff, P. D. Johnson, M. M. Traum, H. H. Farrell, N. V. Smith, R. L. Benbow and Z. Hurych, Surf. Sci. 104, 282-299 (1981).
"Photon and Electron Stimulated Desorption of Adsorbates from W(100)"